

**Bangor University**

## **DOCTOR OF PHILOSOPHY**

### **Electrochemical and spectroelectrochemical studies on polythiophene derivatives**

Anjos, Tania

*Award date:*  
2006

*Awarding institution:*  
Bangor University

[Link to publication](#)

#### **General rights**

Copyright and moral rights for the publications made accessible in the public portal are retained by the authors and/or other copyright owners and it is a condition of accessing publications that users recognise and abide by the legal requirements associated with these rights.

- Users may download and print one copy of any publication from the public portal for the purpose of private study or research.
- You may not further distribute the material or use it for any profit-making activity or commercial gain
- You may freely distribute the URL identifying the publication in the public portal ?

#### **Take down policy**

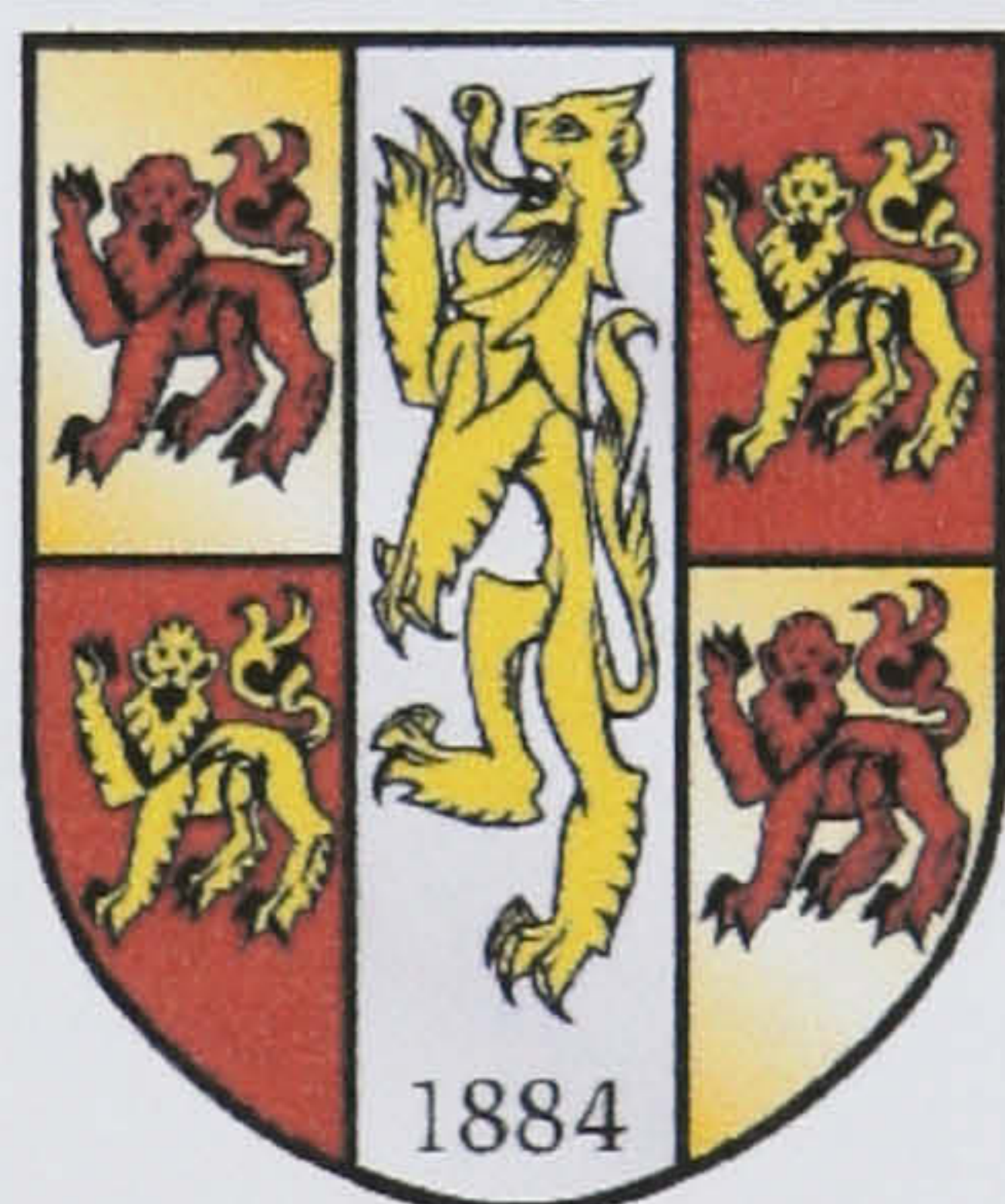
If you believe that this document breaches copyright please contact us providing details, and we will remove access to the work immediately and investigate your claim.



# Electrochemical and Spectroelectrochemical Studies on Polythiophene Derivatives

A Thesis submitted by Tânia Gomes Anjos for the degree of  
Doctor of Philosophy of the University of Wales

• PRIFYSGOL CYMRU •  
UNIVERSITY OF WALES  
**BANGOR**



Department of Chemistry, University of Wales, Bangor  
Gwynedd, LL57 2UW

July 2006





# Acknowledgments

Firstly, I would like to acknowledge Professor Maher Kalaji, the PhD supervisor, for all the support and proficient guidance throughout the project.

I am also extremely grateful to Dr. Patrick Murphy, PhD supervisor, who provided his expertise and orientation in the area of organic chemistry.

Thanks to my research committee, Professor Stuart Irvine and Professor Mark Baird. For their technical assistance I am indebted to the staff of the Chemistry Department and in particular to Denis Williams, Glyn Connolly, Gwynfor Davies, John Charles, Kevin Spencer, Mike Lewis and Steve Jones.

I also express all my gratitude to the many friends that I have come across in the electrochemistry group, Ben Jones, Chris Gwenin, Duarte Tito, Eric Lascombe, Phil Adams, and Siân Masson. I would like to thank the 'Chemistry Football Club' and the members of the squash ladder who gave me the opportunity to enjoy a sporty life in Bangor. For their friendship and all the brilliant moments that we have spent together I specially thank to Alfonso, Jokin, Quique, Julia, Gorka, Cristina, Itxaso and Andrés.

I am also grateful to the University of Wales for the provided financial support.

Pelo imenso apoio recebido gostaria de agradecer à minha família e amigos. Um obrigado muito especial para a minha mãe que sempre esteve a meu lado ao longo destes muitos anos de estudo. Estou também eternamente agradecida ao meu pai e à minha maninha pelo constante ânimo e incentivo dado.



*Porque o seu incessante apoio e carinho foi fundamental para a realização deste trabalho, esta tese de doutoramento é dedicada ao Alfonso, aos meus pais, Manuel e Helena, e à minha irmã, Eunice.*



## Abstract

The polymerisation of dithienylethylenes (*cis* and *trans* 1,2-di(3-thienyl) ethylene, **DTE-cis** and **DTE-trans**), thiophene dithiolenes (4,5-dithiophen-3-yl-[1,3] dithiol-2-one, **Th-3,3**, 4,5-di-thiophen-2-yl-[1,3]dithiol-2-one, **Th-2,2**, 4-thiophen-3-yl-5-thiophen-2-yl-[1,3]dithiol-2-one, **Th-2,3** and 4,5-di-(5-methyl-thiophen-3-yl)-[1,3]dithiol-2-one, **Th-3,3Me**), and nickel dithiolenes (bis[1,2-di(3-thienyl)-1,2-ethenedithiolene] nickel tetrafluoroborate, **Ni(Th-3,3)<sub>2</sub>** and bis[1,2-di(2-thienyl)-1,2-ethenedithiolene] nickel tetrafluoroborate, **Ni(Th-2,2)<sub>2</sub>**) was carried out and the resultant polymers were analysed by electrochemical and spectroelectrochemical methods.

The voltammetric behaviour of the electropolymerised **PDTE-cis** and **PDTE-trans** suggested that polarons and bipolarons were produced upon oxidation. Nevertheless, the formation of a conducting state was not observed in the SNIFTIRS measurements. Upon I<sub>2</sub> chemical doping, **PDTE-cis** and **PDTE-trans** showed increased stability in the doped state and the SNIFTIRS response of **PDTE-trans**, revealed similar IR characteristics to those of conductive polymers.

The voltammetric and IR behaviour of the dithiolenes, **PTh-3,3**, **PTh-2,2** and **PTh-2,3** was similar to that of many conducting polymers. From the UV-Visible spectra of the neutral films it was determined that **PTh-3,3**, **PTh-2,2** and **PTh-2,3** have a bandgap of 2.04, 2.30 and 2.18 eV, respectively. The electrochemical and SNIFTIRS results for **PTh-3,3Me** were noticeably different from the other dithiolene polymers revealing a poorly conductive polymer. The solid-state modification of **PTh-3,3** to produce a new TTF derivatised polythiophene was carried out. The inclusion of TTF into the **PTh-3,3** film was confirmed by voltammetry and IR data that also suggested that only partial modification of the polymer had occurred.

The voltammetry of **polyNi(Th-3,3)<sub>2</sub>** and **polyNi(Th-2,2)<sub>2</sub>** showed a redox couple attributed to the electrochemistry of the nickel dithiolene centre, confirming the incorporation of the metal complex into the polymer. Whilst the SNIFTIR spectra of **polyNi(Th-3,3)<sub>2</sub>** showed the characteristic features of metal dithiolenes, the IR behaviour of **polyNi(Th-2,2)<sub>2</sub>** was more comparable to that of conducting polythiophenes. This result indicates that charge delocalisation in **polyNi(Th-2,2)<sub>2</sub>** occurs through the Ni dithiolene sites disrupting the typical electroactivity of the dithiolene unit. For the **polyNi(Th-3,3)<sub>2</sub>** films, the nickel dithiolene sites seem to be electronically isolated, preserving the aromaticity of the dithiolene system.



# Table of Contents

<b>Chapter 1 – Introduction .....</b>	<b>1</b>
1.1 Area of Study .....	2
1.2 Background Literature .....	7
1.2.1 <i>Conducting Polymers</i> .....	7
1.2.2 <i>Synthesis of Conducting Polymers</i> .....	10
1.2.3 <i>Mechanism of Conduction</i> .....	11
1.2.4 <i>Polythiophenes</i> .....	17
1.2.5 <i>Solid-State Modification – Wittig reaction</i> .....	19
1.2.6 <i>Nickel Dithiolenes</i> .....	24
1.3 Aims of the Project .....	29
1.4 References .....	31
<b>Chapter 2 – Experimental .....</b>	<b>37</b>
2.1 Experimental Techniques .....	38
2.1.1 <i>Cyclic Voltammetry (CV)</i> .....	38
2.1.2 <i>SNIFTIRS - Subtractively Normalised Interfacial Fourier Transform Infrared Spectroscopy.....</i>	41
2.1.3 <i>UV-Visible Spectroscopy</i> .....	46
2.2 Chemical Synthesis .....	49
2.2.1 <i>Synthesis of trans-1,2-di(3-thienyl)ethylene and cis-1,2-di(3-thienyl) ethylene (DTE-trans/DTE-cis) .....</i>	49
2.2.2 <i>Synthesis of 4,5-di-thiophen-3-yl-[1,3]dithiol-2-one (Th-3,3) ...</i>	51
2.2.3 <i>Synthesis of 4,5-di-thiophen-2-yl-[1,3]dithiol-2-one (Th-2,2) ...</i>	54
2.2.4 <i>Solid-state modification of electrochemically synthesised poly-4,5-di-thiophen-3-yl-[1,3]dithiol-2-one (PTh-3,3) .....</i>	56
2.3 General Experimental .....	59
2.3.1 <i>Chemicals and Solvents</i> .....	59
2.3.2 <i>Characterisation Techniques</i> .....	59
2.4 References .....	60



<b>Chapter 3 – Studies on Dithienylethylenes .....</b>	<b>62</b>
3.1 Introduction .....	63
3.2 Experimental .....	64
3.3 Results and Discussion .....	65
3.3.1 <i>Studies on trans-dithienylethylene DTE-trans</i> .....	65
3.3.2 <i>Studies on cis-dithienylethylene DTE-cis</i> .....	78
3.4 Conclusions .....	85
3.5 References .....	87
<b>Chapter 4 – Studies on Thiophene Dithiolenes .....</b>	<b>91</b>
4.1 Introduction .....	92
4.2 Experimental .....	94
4.3 Results and Discussion .....	95
4.3.1 <i>Studies on Thiophene Dithiolenes Th-3,3</i> .....	95
4.3.2 <i>Studies on Thiophene Dithiolenes Th-2,2</i> .....	105
4.3.3 <i>Studies on Thiophene Dithiolenes Th-2,3</i> .....	112
4.3.4 <i>Studies on Thiophene Dithiolenes Th-3,3Me</i> .....	119
4.3.5 <i>Chemical in situ modification of Thiophene Dithiolenes</i> .....	122
4.4 Conclusions .....	126
4.5 References .....	129
<b>Chapter 5 – Studies on Nickel Dithiolenes .....</b>	<b>133</b>
5.1 Introduction .....	134
5.2 Experimental .....	136
5.3 Results and Discussion .....	137
5.3.1 <i>Studies on Nickel Dithiolenes Ni(Th-3,3)<sub>2</sub></i> .....	137
5.3.2 <i>Studies on Nickel Dithiolenes Ni(Th-2,2)<sub>2</sub></i> .....	144
5.4 Conclusions .....	151
5.5 References .....	153
<b>Chapter 6 – Conclusions and Further Work .....</b>	<b>156</b>



# **Chapter 1**

## **Introduction**



## 1.1 Area of Study

Polymers are of major importance in everyday life. They are frequently used as insulators in electrical and electronic applications mainly because of their intrinsic property of covalent bonding.<sup>1</sup> They are also extensively employed due to particular characteristics such as mechanical strength, high resistance to corrosion, low densities, stability and low cost.<sup>2</sup> Polymers were thought of as electrical insulators until the discovery that, when exposed to iodine vapour, polyacetylene (PA) exhibited an increase in electrical conductivity by several orders of magnitude.<sup>3</sup> Polyacetylene, the simplest conjugated polymer, fascinated chemists, physicists, and material scientists, because it was the first organic polymer to have the electrical and electronic properties of a metal. This finding was published by Shirakawa, Heeger and MacDiarmid<sup>3</sup> in 1977 and as a result of their pioneering research they received the Nobel Prize in Chemistry in 2000.

Since this discovery, an active interest has been taken in the search for these new conducting organic materials, also called conducting polymers (CPs) or synthetic metals and, as a result, other CPs such as polyaniline (PANI), polypyrrole (PPy), polythiophene (PT) and polyfuran (PFu), have been synthesised and analysed.<sup>4,5,6</sup> It has become apparent, from this vast research work, that extensive delocalisation of electrons along the polymer backbone is necessary for a polymer to behave as an electrical conductor.<sup>2</sup> In addition, molecular orbitals must be partially filled so that there is a free movement of electrons throughout the lattice.<sup>7</sup> These conjugated polymers are generally insulators or semi-conductors but can be converted into electrically conductive forms when subjected to a doping process achieved either by oxidation or reduction of the polymeric chains.<sup>8</sup>

The development of this new class of polymeric materials, that combines the electrical and optical properties of metals and semiconductors retaining the attractive mechanical properties and processing advantages of polymers, offers of a wide range of novel applications.<sup>9,10</sup> The prospect of using conducting polymers in biosensors<sup>11</sup>, molecular electronics<sup>8</sup>, electrochromic displays<sup>12</sup>, solar cells<sup>7</sup>, or electrochemical storage systems<sup>13</sup>, among other possibilities, has increased the interest of researchers in this important field.<sup>14</sup> Apart from the preparation and study of new polymers, a



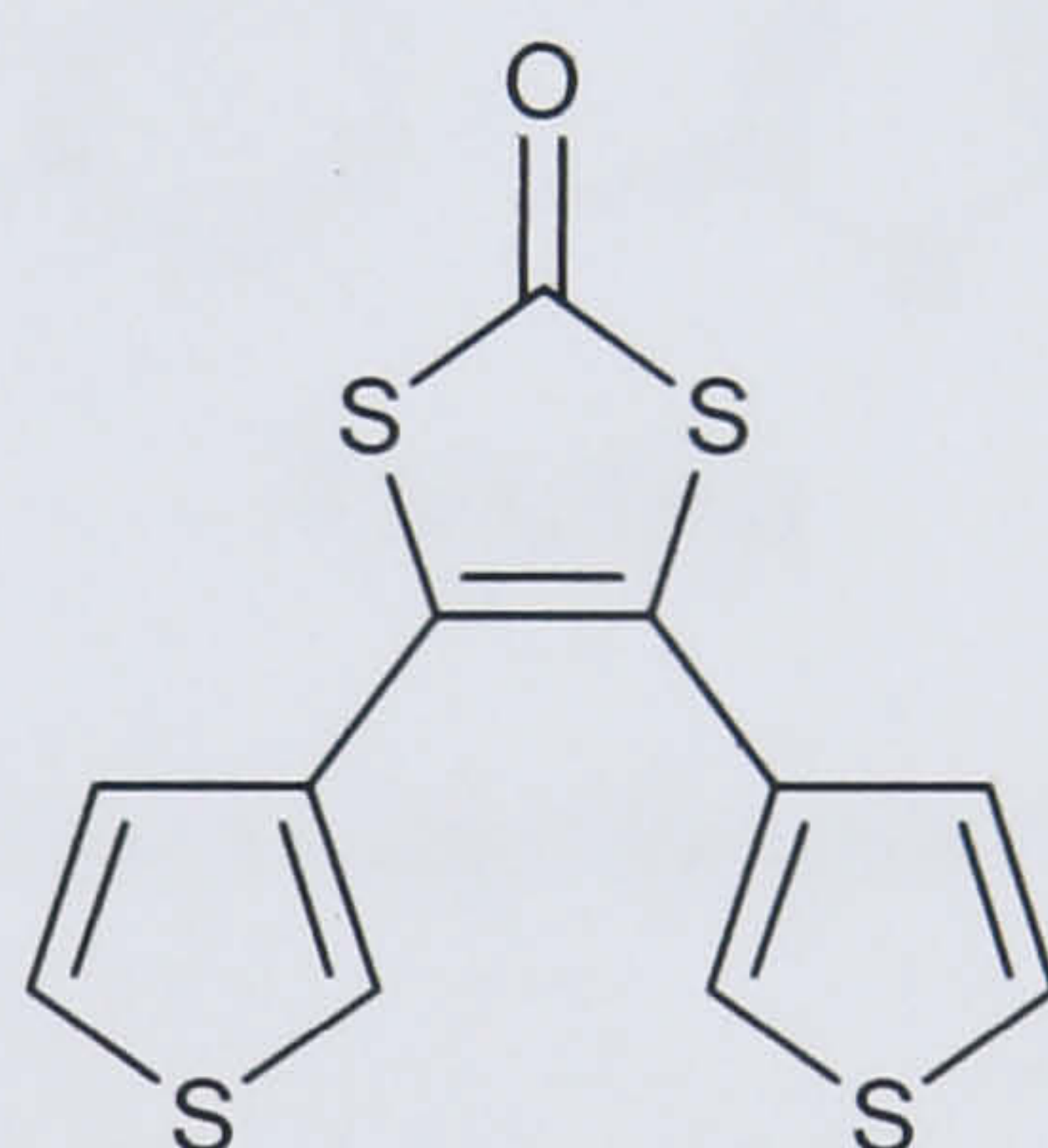




These polymers can be viewed as a combination of the structures of acetylene and thiophene.<sup>22,23</sup> Compared to polythiophene, the presence of the central ethylene linkage between thiophene rings leads to a rigid polymeric structure with lower aromatic character.<sup>24,25</sup>

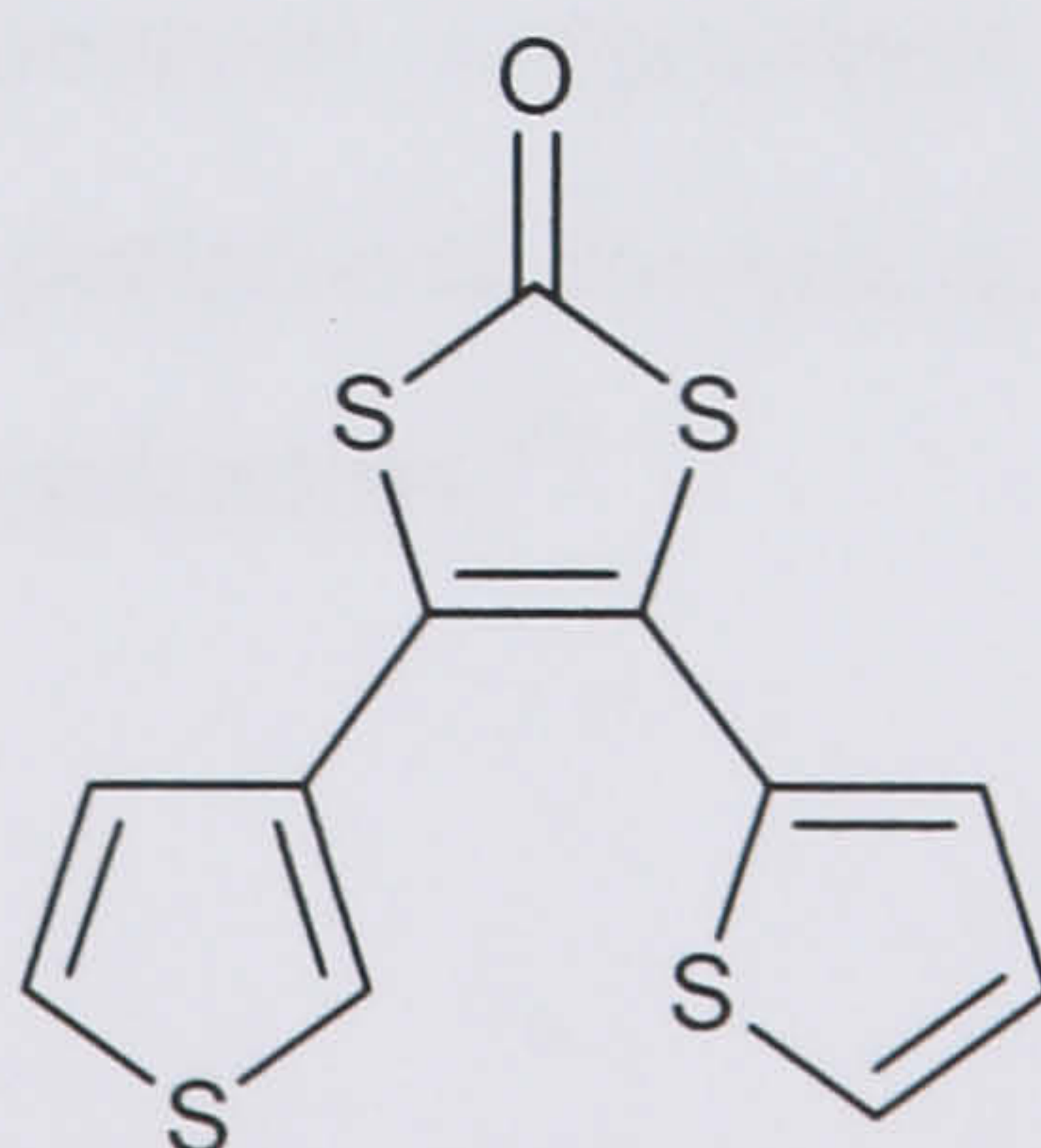
The chemical structures of the four thiophene dithiolenes studied are shown in Figures 1.02 - 1.05. Except for compound **Th-3,3Me**, which has two methyl groups, the only difference between them is the substitution pattern of the thiophene rings. Following electropolymerisation, the *in situ* solid-state modification of the resultant polythiophene dithiolenes was attempted. This could give access to a class of polymers that cannot be directly obtained by electrochemical methods.<sup>16</sup> The chemical modification was carried out under Wittig conditions with the aim of incorporating tetrathiafulvalene (TTF) into the polymer backbone. A detailed description of the solid-state modification is given in section 1.2.5 of this Chapter.

- Thiophene dithiolenes



**Th-3,3**

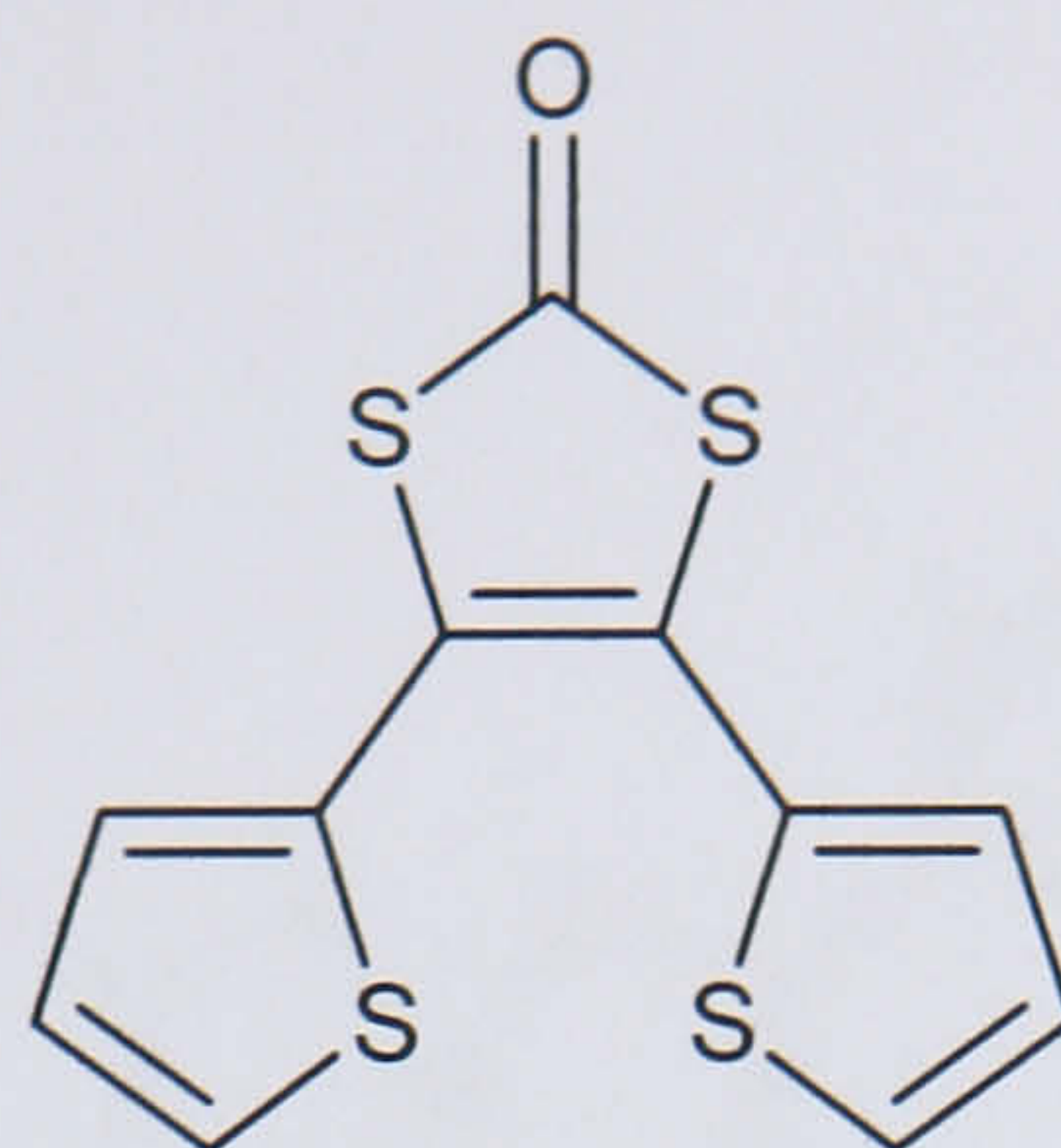
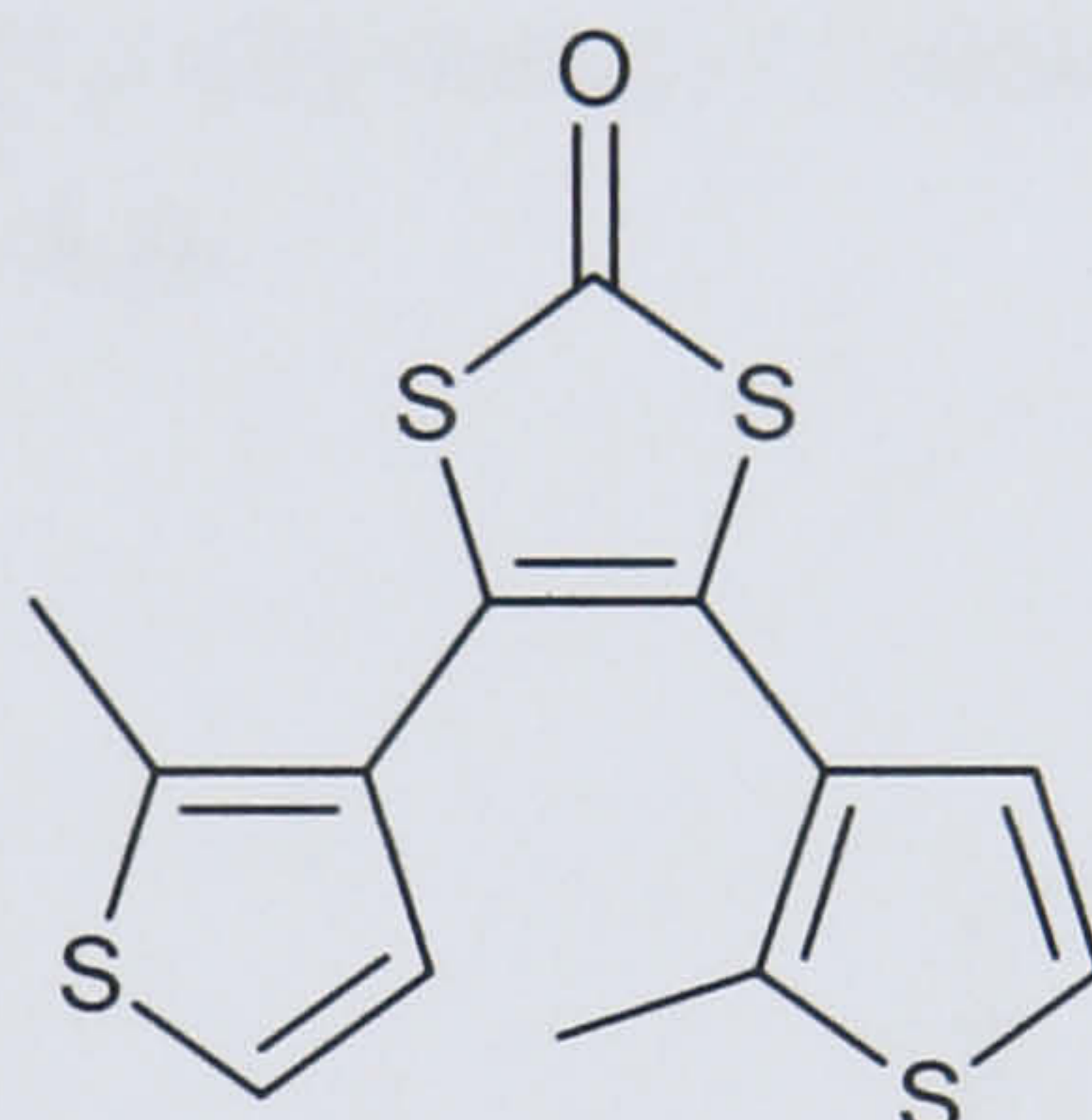
**Figure 1.02** - Structure of 4,5-di-thiophen-3-yl-[1,3]dithiol-2-one **Th-3,3**.



**Th-2,3**

**Figure 1.03** - Structure of 4-thiophen-3-yl-5-thiophen-2-yl-[1,3]dithiol-2-one **Th-2,3**.



**Th-2,2****Figure 1.04** - Structure of 4,5-di-thiophen-2-yl-[1,3]dithiol-2-one **Th-2,2**.**Th-3,3Me****Figure 1.05** - Structure of 4,5-di-(5-methyl-thiophen-3-yl)-[1,3]dithiol-2-one **Th-3,3Me**.

The electrochemical properties of some related nickel dithiolenes (Figures 1.06 - 1.07) were also investigated in this project. The incorporation of transition metal complexes into conjugated organic polymers has attracted considerable attention since it offers the prospect of new advanced conducting,<sup>26</sup> magnetic,<sup>27</sup> and catalytic materials.<sup>28</sup> The extensive conjugation of nickel dithiolenes and the electron donating effect of the peripheral thiophenes make them important units in the development of molecular conductors.<sup>29</sup>



- Nickel Dithiolenes

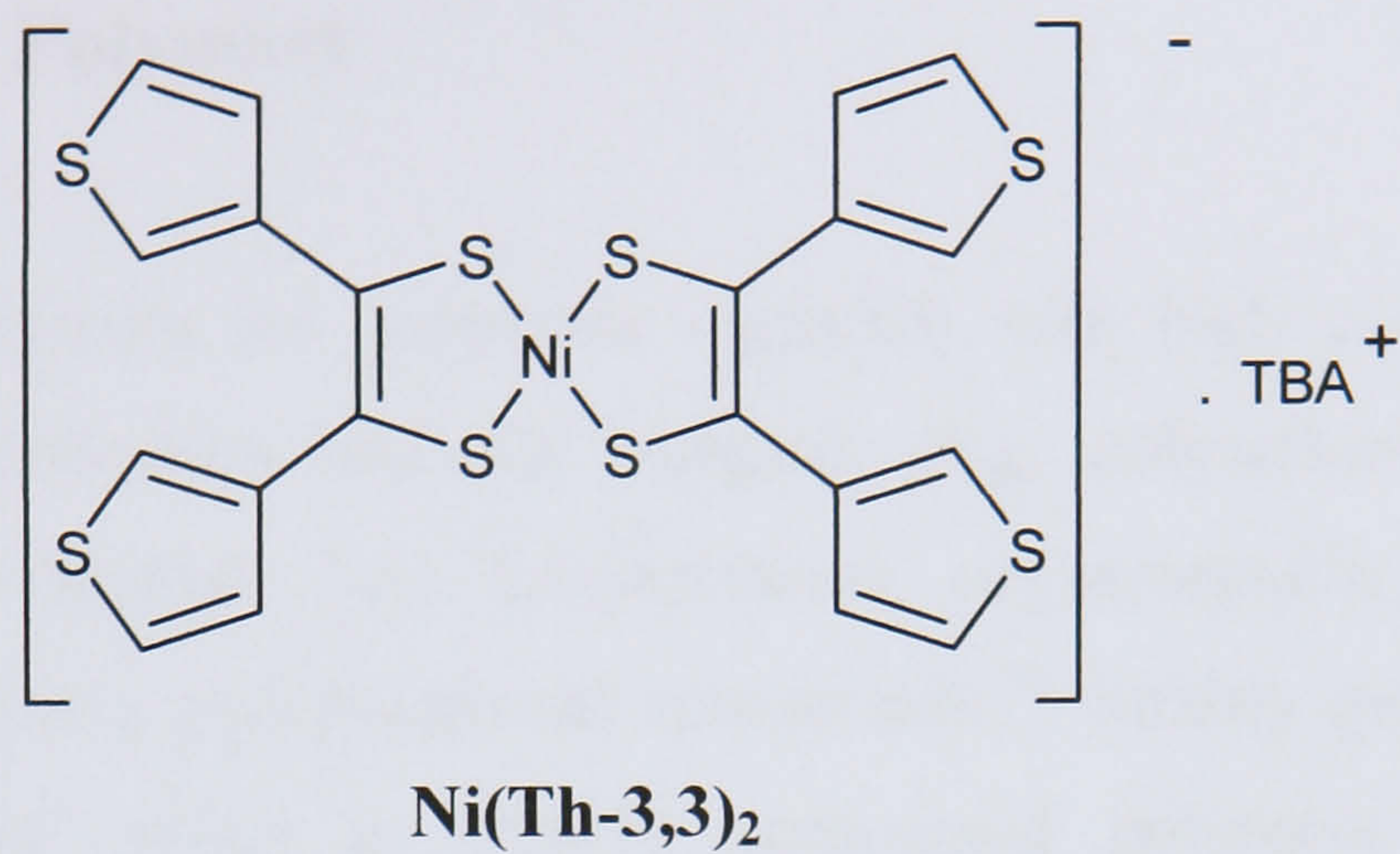


**Figure 1.06** - Structure of bis[1,2-di(3-thienyl)-1,2-ethenedithiolene] nickel tetrafluoroborate **Ni(Th-3,3)<sub>2</sub>**.

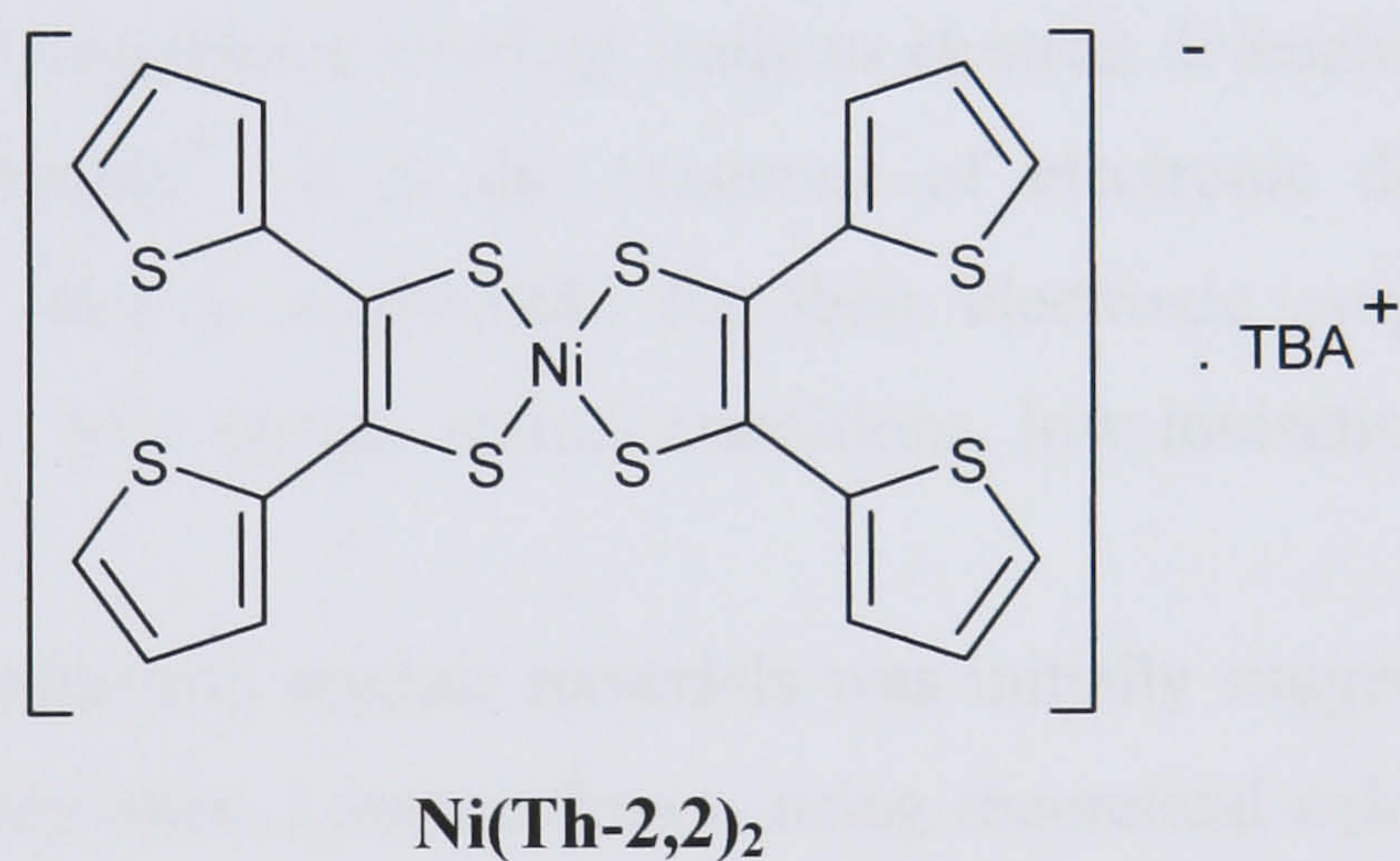


**Figure 1.07** - Structure of bis[1,2-di(2-thienyl)-1,2-ethenedithiolene] nickel tetrafluoroborate **Ni(Th-2,2)<sub>2</sub>**.



## 1.2 Background Literature

### 1.2.1 Conducting Polymers

Conducting polymers are polymeric materials with high ionic or electrical conductivity. This definition includes inorganic (e.g. polysulfonitrile, which is superconductive at extremely low temperatures), organometallic (e.g. phthalocyanines) and organic (e.g. polythiophene) compounds.<sup>30</sup> Strictly speaking, the term “conducting polymers” refers to organic conjugated polymers in which the monomeric units are covalently linked.<sup>31</sup> In conjugated polymers, the bonds between the carbon atoms are alternately single ( $\sigma$ -bonds) and double ( $\pi$ -bonds) leading to one unpaired electron (the  $\pi$ -electron) per carbon atom. In addition,  $\pi$ -bonding, with carbon orbitals in the  $sp^2p_z$  configuration and in which the orbitals of successive carbon atoms along the backbone overlap, leads to electron delocalisation along the backbone of the polymer.<sup>9</sup> It is the existence of electronic delocalisation in conjugated polymers that is responsible for their electronic properties such as electrical conductivity, low energy optical transitions, low ionisation potential and high electron affinity.<sup>7</sup>

The idea of conducting organic materials was initially suggested in 1931 by Hückel.<sup>31</sup> A few years later, Lennard Jones, using theoretical calculations on the electronic states of  $sp^2$  carbon, predicted that polyacetylene should have metallic behaviour.<sup>32</sup> Nevertheless, it was only in 1977, that Shirakawa *et al.*<sup>3</sup> reported an increase in the conductivity of PA by more than 10 orders of magnitude, which corresponds to a change from an insulator to a metal.<sup>33</sup> This discovery, although accidental at that time, was a significant breakthrough in the field of organic conductors and encouraged a series of investigations in this area.<sup>2</sup> Following the case of polyacetylene, other polymers such as polypyrrole<sup>34</sup>, polythiophene<sup>35</sup>, polyaniline<sup>36</sup>, poly(*p*-phenylene)<sup>37</sup>, poly(*p*-phenylenevinylene)<sup>38</sup>, and poly-(2,5-thienylene-vinylene)<sup>39</sup> were reported as conducting materials. Their molecular structures can be seen in Figure 1.08.



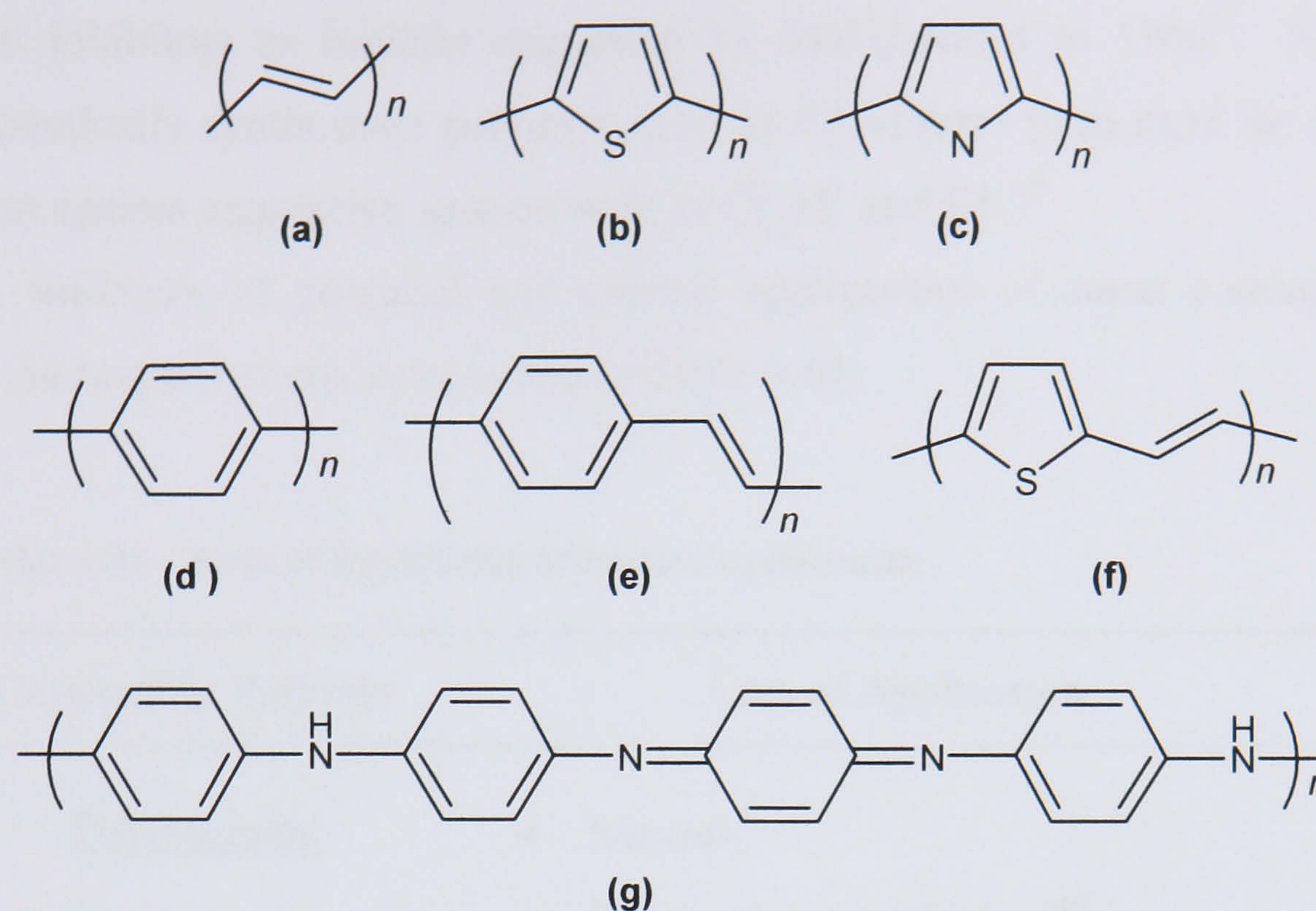


**Figure 1.08** - Structure of conjugated polymers: (a) *trans*-polyacetylene; (b) polythiophene; (c) polypyrrole, (d) poly(*p*-phenylene); (e) poly(*p*-phenylenevinylene); (f) poly(2,5-thienylenevinylene); (g) polyaniline.

These polymers generally exhibit semiconductive to insulating levels of conductivity ( $10^{-10}$  -  $10^{-5}$  S/cm) in their pristine state but can be made conductive ( $\sim 1-10^4$  S/cm) by doping.<sup>4,40</sup> The term doping is derived by analogy with the insertion of electrons or holes in 3D inorganic semiconductors.<sup>31</sup> However, for a conducting polymer it refers to the oxidation (p-doping) or reduction (n-doping) of the extended  $\pi$ -electronic system.<sup>41</sup> The introduction of deficiency or excess of  $\pi$ -electrons in the polyconjugated chain alters the electrical and optical properties of the polymers, and by controlling the redox process, it is possible to regulate these properties.<sup>42</sup>

Research in the area of conducting polymers has led to the development of this class of polymeric materials offering a wide range of novel applications.<sup>43,44</sup> For instance, gas-sensing devices made with polythiophene films have been investigated.<sup>20</sup> These are based on the fact that the conductivity of the polymeric film decreases on exposure to reducing gases like  $\text{H}_2\text{S}$  or  $\text{NH}_3$  whereas  $\text{NO}$  or  $\text{NO}_2$  have the opposite effect.<sup>31</sup> Their ability to store charge reversibly indicates they can also be used in rechargeable batteries.<sup>45,46</sup> The change in colour observed in conjugated polymers upon their oxidation or reduction has led to the development of electrochromic devices.<sup>47</sup> Furthermore, polymer coatings can be employed as



corrosion inhibitors as initially suggested by MacDiarmid in 1985<sup>8</sup>. Since then electrochemically synthesised polymers such as PANI have been used for mild steel protection against aggressive species such as O<sub>2</sub>, H<sup>+</sup> and Cl<sup>-</sup>.<sup>48</sup>

A summary of potential and current applications of some conducting and semiconducting polymers is presented in Table 1.01:

**Table 1.01** - Areas of applications of conducting polymers.

Conducting Polymer	Area of Application
<u>Polypyrroles</u>	<ul style="list-style-type: none"> <li>• Sensors<sup>7</sup></li> <li>• Electrochromic displays<sup>45</sup></li> <li>• Solar energy cells<sup>49</sup></li> <li>• Light weight battery<sup>13</sup></li> </ul>
<u>Polythiophenes</u>	<ul style="list-style-type: none"> <li>• Electrochromic materials<sup>17</sup></li> <li>• Electroluminescence<sup>5,50</sup></li> <li>• Cathode materials for batteries<sup>51</sup></li> <li>• Chemical and biological sensors<sup>52,53</sup></li> <li>• Solar cells<sup>54</sup></li> <li>• Corrosion protection<sup>48</sup></li> </ul>
<u>Polyanilines</u>	<ul style="list-style-type: none"> <li>• Electrochromic displays<sup>45</sup></li> <li>• Rechargeable batteries<sup>13</sup></li> <li>• Biosensors<sup>7,11</sup></li> <li>• Corrosion protection<sup>45</sup></li> </ul>
<u>Poly(phenylenes)</u>	<ul style="list-style-type: none"> <li>• Solar energy cells<sup>55</sup></li> <li>• Electroluminescence<sup>45,56</sup></li> <li>• Corrosion protection<sup>44</sup></li> <li>• Laser materials<sup>57</sup></li> </ul>



## 1.2.2 Synthesis of Conducting Polymers

Conducting polymers can be produced by chemical and electrochemical methods.<sup>58</sup> Due to its simplicity and reproducibility, electrochemical synthesis is usually the preferred technique to prepare electrically conducting polymers.<sup>7</sup> It also presents clear advantages over chemical methods as it is a relatively cheap process that can be performed at a small scale, does not require catalysts and can be carried out at room temperature.<sup>4,59</sup> Furthermore, the thickness of the polymer films can be controlled by adjusting the applied electrochemical potential.<sup>60</sup>

The electrochemical synthesis of conducting polymers can be performed by anodic oxidation of the monomers to generate radical cations, followed by coupling to form radical di-cations.<sup>7</sup> These species undergo further coupling reactions producing the polymer chain. The oxidation of monomer units is done either at constant potential, constant current or by potential cycling.<sup>4</sup> Since this reaction proceeds *via* radical cation intermediates, the nature of the surrounding solvent and electrolyte plays quite an important role.<sup>61</sup> It is vital to avoid solvent interaction with the cation intermediates and this can be achieved by using poor nucleophiles and aprotic solvents such as acetonitrile or benzonitrile.<sup>62</sup> The choice of supporting electrolyte depends upon the solubility, degree of dissociation and nucleophilicity criteria. The most frequently used are the tetra-alkyl ammonium salts, which are highly dissociated and soluble in aprotic solvents.<sup>5</sup> Other experimental variables such as monomer concentration, temperature, electrode material and applied electrical conditions can also influence the electropolymerisation process.<sup>31</sup>

Despite the considerable amount of work that has already been carried out on the synthesis of conducting polymers, there is still a need for routes to new materials. One approach that is receiving increasing attention is functionalisation after polymerisation.<sup>15,63</sup> This process can give access to polymers that could not be obtained directly by electropolymerisation of the corresponding monomers, either because substituent groups were sensitive to the oxidative conditions of film growth, or because they inhibited the polymerisation process.<sup>64</sup>



### 1.2.3 Mechanism of Conduction

Conjugated polymers are organic semiconductors that, with respect to electronic energy levels, hardly differ from inorganic semiconductors.<sup>65</sup> Both have their electrons organised in bands rather than in discrete levels and both have their ground state energy bands either completely filled or completely empty.<sup>66</sup> In conjugated polymers the band structure is created from the interaction of the  $\pi$ -orbitals of the repeating units throughout the chain. This is exemplified for polythiophene in Figure 1.09. The addition of every new thiophene unit causes hybridization of the energy levels yielding more levels until a point is reached at which there are bands rather than discrete levels.<sup>65</sup>

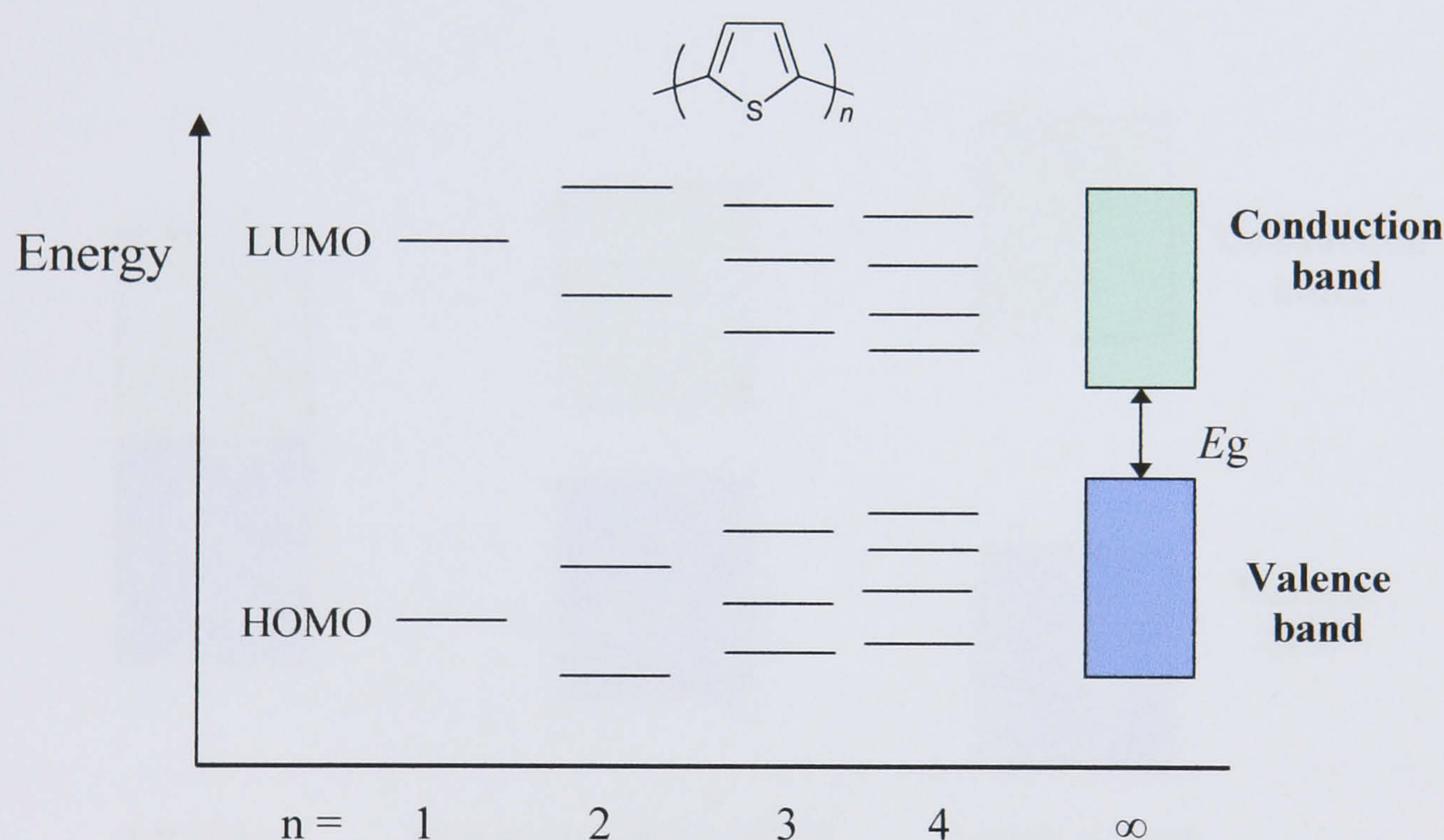


**Figure 1.09** - Schematic formation of a band structure in polythiophene. LUMO and HOMO are, respectively, the lowest unoccupied molecular orbital and highest occupied molecular orbital, of the thiophene unit;  $E_g$  – energy gap.

A band can then be considered as being composed of different energy states, separated by infinitesimal energy differences. The highest occupied electronic levels constitute the valence band (VB) and the lowest unoccupied levels, the conduction band (CB).<sup>30</sup> The difference in energy  $E_g$  between these levels is called the band gap.<sup>6</sup>



The nature of the electrical properties of a conjugated polymer is determined by the extent of occupation of the energy bands and the magnitude of the gap between them. According to the band theory, a material must have a partly filled valence band in order to have metallic conduction. For this to happen, the band gap between the valence and conduction bands must be considerably narrow.<sup>32,66</sup> The transition generally occurs if there is thermal excitation of the valence band electrons.

In the metallic state, there is no gap between the valence and conduction band which allows electrons to move freely (see Figure 1.10). For a semiconductor the band gap is small enough so that electrons may be thermally excited across it.<sup>67</sup> In insulators, the electrons in the valence band are separated by a large gap from the conduction band, and hence, thermal excitation of carriers is not possible.<sup>66</sup>

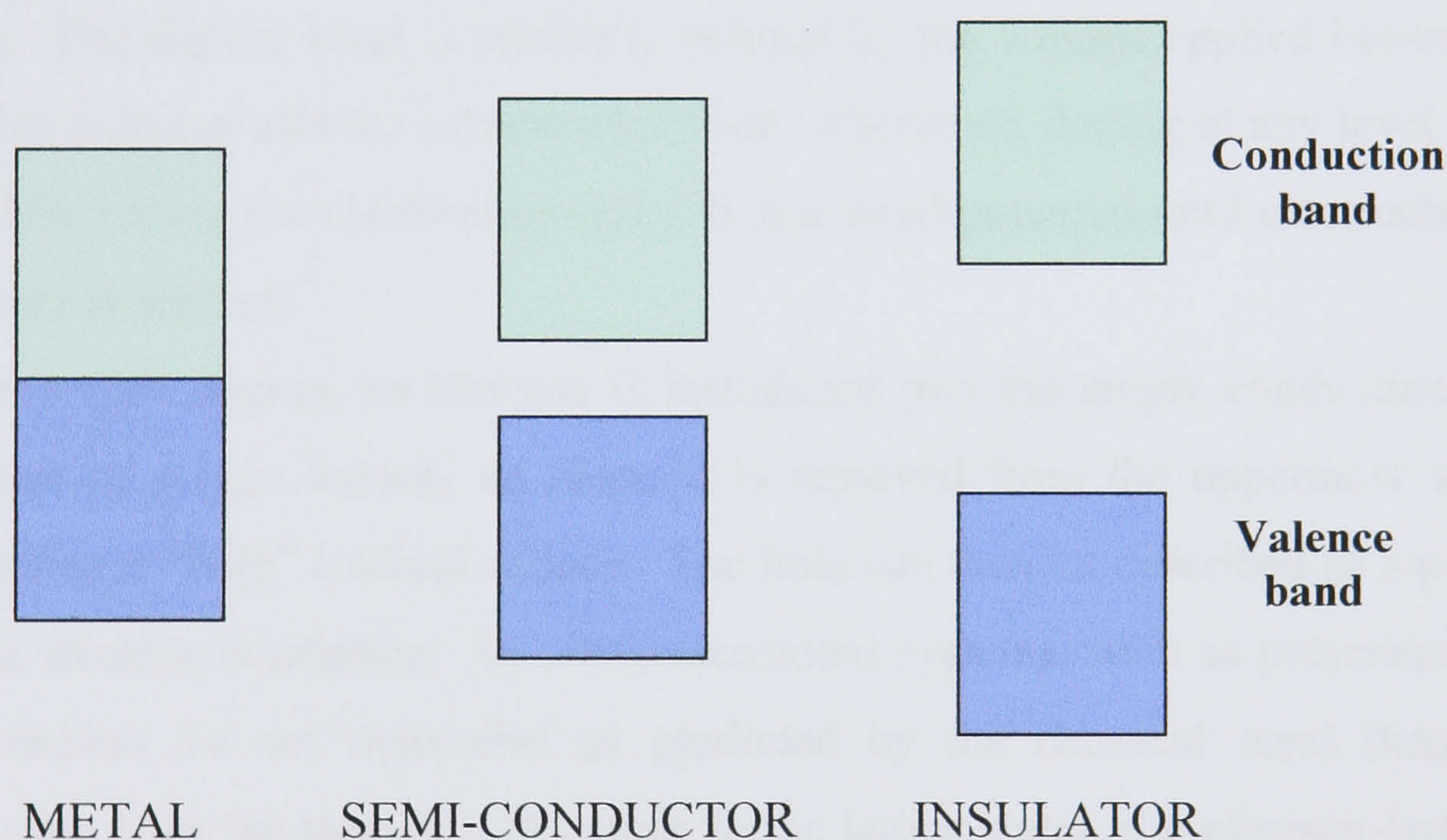


**Figure 1.10** - Representation of Band Theory in solids.

Conjugated polymers are semiconductors in their neutral or pristine state but can be made conductive by chemical or electrochemical doping reaction. This can be achieved by removing electrons (oxidation or p-doping) or by the addition of electrons to the polymer backbone (reduction or n-doping).<sup>8</sup>

Chemical doping is performed by exposing a polymer to an electron acceptor (e.g. iodine,  $\text{AsF}_5$ ) or an electron donor (e.g. alkali metals). The main process of



doping is a redox reaction between polymer chains and acceptors or donors. In acceptor doping (p-doping), an ionic complex consisting of positively charged polymer chains and counter anions ( $I_3^-$ ,  $AsF_6^-$ ), formed by reduction of acceptors, is produced. Upon donor doping (n-doping), an ionic complex consisting of negatively charged polymeric chains and counter cations ( $Na^+$ ,  $K^+$ , etc.), generated by oxidation of donors, is created.<sup>33</sup> Chemical doping is an efficient and straightforward process where the conductivity of the polymer can be controlled by its content of dopant. The disadvantage of this method is that frequently, attempts to obtain intermediate doping levels result in inhomogeneous doping.<sup>9</sup>

In electrochemical doping, the electrode supplies the redox charge to the conducting polymer, while electrolyte ions diffuse into (or out of) the polymer structure in order to ensure electroneutrality. This process repeats itself until all electroactive sites are oxidised, and is accompanied by a volume expansion of the polymer. The doping level is precisely defined by the voltage applied between the conducting polymer and the counter-electrode. Therefore, doping at any level can be achieved by setting the electrochemical cell at a fixed potential until electrochemical equilibrium is reached.<sup>9</sup>

In n-type doping, an electron is introduced into the empty conduction band. In the case of p-type doping, an electron is removed from the uppermost valence band creating a "hole" (radical cation). The hole can then be described as a position where an electron is missing. In one-dimensional systems, such as polymers, these charge carriers do not delocalise as predicted by the classical band theory.<sup>31,68</sup> Instead, they have the tendency to couple to the lattice states, the electron-lattice (or hole-lattice) interaction, leading to important geometry relaxations and electronic modifications in the polymer backbone.<sup>47,69</sup> The charge carrier and its associated lattice distortion can then be seen as constituting a single entity termed as soliton, polaron or bipolaron.<sup>70</sup> In chemical terminology, the soliton is an ion, a polaron is a radical ion (spin  $1/2$ ) and a bipolaron is a di-ion (spinless and doubly charged), formed by the union of two polarons.<sup>30,69</sup> As a consequence of the rearrangement of single and double bonds, solitons, polarons and bipolarons act as charge carriers by moving along the polymer. Except for the metallic state, these are the entities through which charge transport is accomplished in conducting polymers.<sup>55</sup>



Solitons are the dominant charge carriers for polymers with degenerate ground states.<sup>58</sup> The prototype of a degenerate polymer is *trans*-polyacetylene (*trans*-PA), which has two energetically equivalent resonance forms (A and B in Figure 1.11). The two structures differ from one another by the exchange of the carbon-carbon single and double bonds.<sup>30,69</sup> A soliton is a domain boundary between the two possible ground-state configurations in *trans*-PA (A and B), as shown in the following figure.<sup>9</sup>

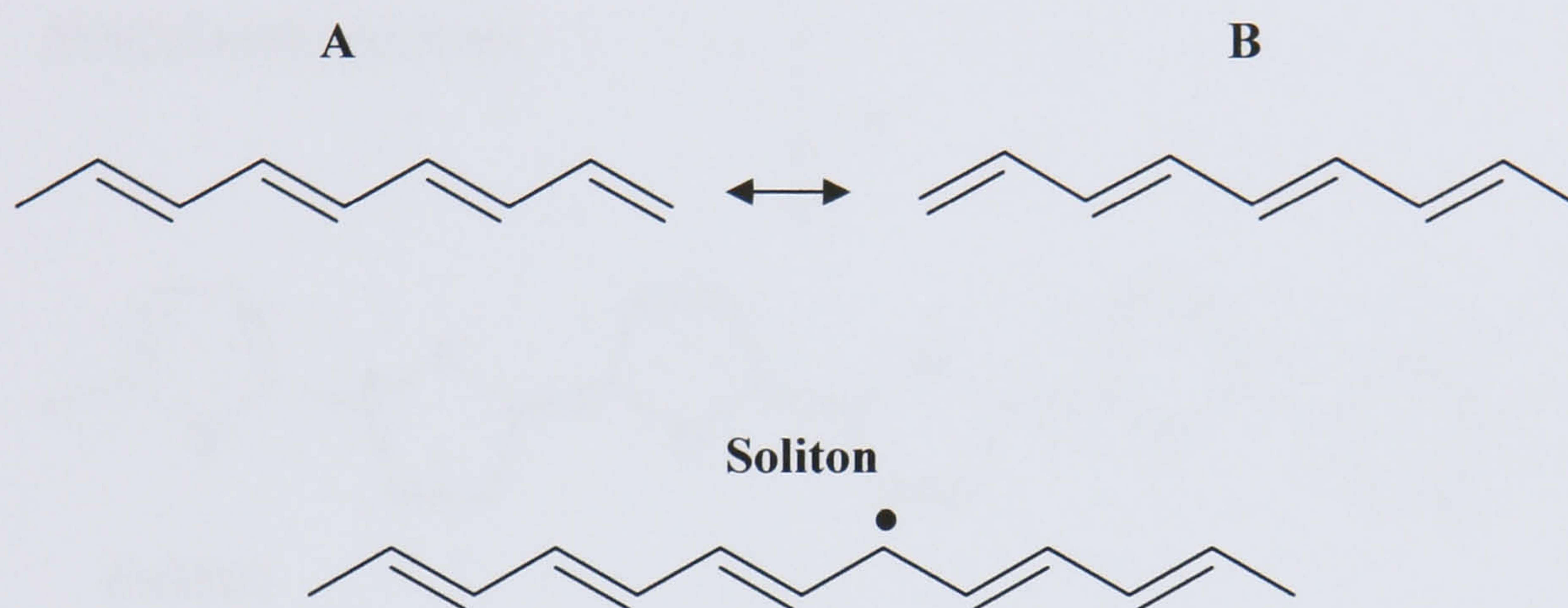


**Figure 1.11** - The two ground-state degenerate structures (A and B) and soliton in *trans*-(CH)<sub>x</sub>.

Unlike *trans*-PA, polyaromatic polymers such as polypyrrole (PPy), or polythiophene (PT) are non-degenerate given that the ground state has a single geometric structure which, in their case, is aromatic-like. A quinoid-like resonance structure could be expected but it has a higher total energy.<sup>30</sup>

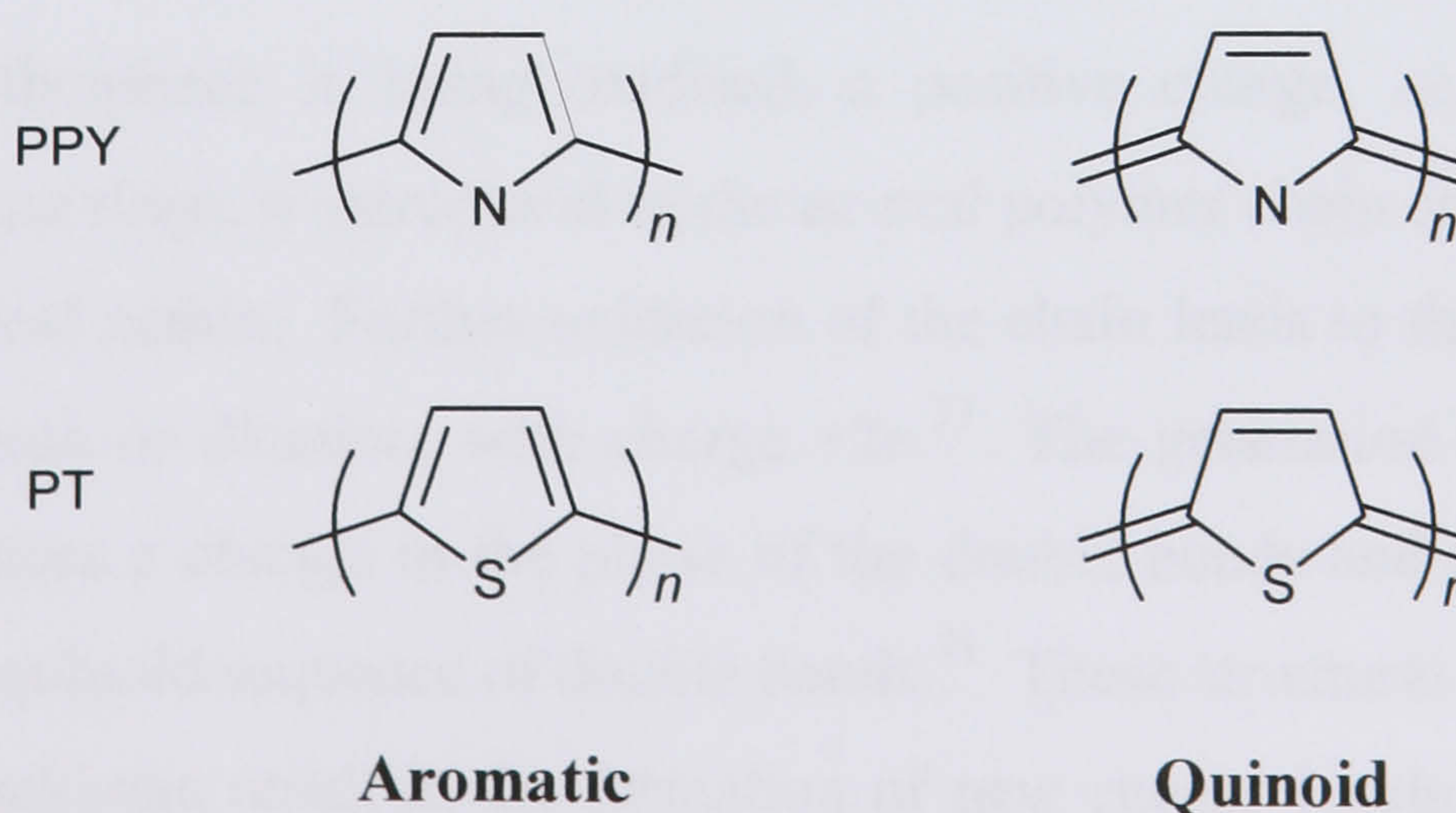


**Figure 1.12** - Aromatic (ground-state) and quinoid-like geometric structures for polypyrrole and polythiophene.



In conjugated polymers with a non-degenerate ground state, the charge introduced upon doping is stored in the form of polarons and bipolarons.<sup>71</sup> Taking polythiophene as an example, the formation of charge carriers in a non-degenerate polymer is shown in Figure 1.13.

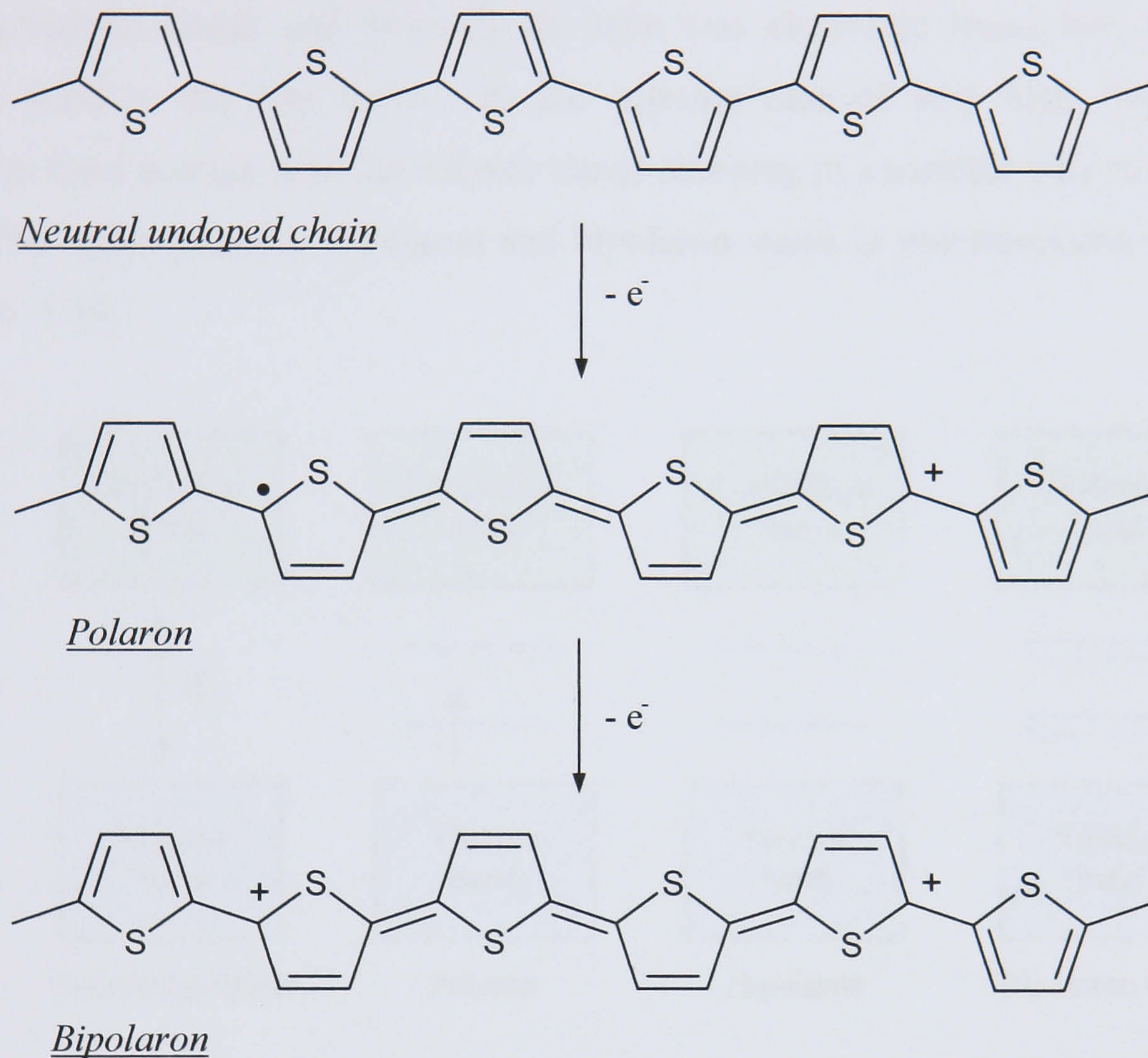


**Figure 1.13** - Schematic structures of a polaron and bipolaron in polythiophene.

As polythiophene is being oxidised, a positive charge,  $+e$ , localised over several thiophene rings, is introduced in the neutral polymer chain creating a positive polaron or radical cation. Further oxidation of the chain leads to the formation of a positive bipolaron or dication, with charge  $+2e$ .<sup>33</sup> The generation of polarons and bipolarons induces a change in the phase of the double bonds and the creation of a domain with a quinoid sequence of double bonds.<sup>71</sup> These structural modifications in the polymer backbone result in the formation of new energy levels within the band gap (Figure 1.14).<sup>62</sup> A positive polaron has two electronic states in the band gap, symmetrically localised with respect to the gap centre, with the lower energy state



being occupied by a positive charge.<sup>72,73</sup> Due to the new energy levels, polarons are expected to have three intragap transitions (two from the valence band to the gap states and an additional subgap transition between two localised energy levels).<sup>72</sup>

Upon further oxidation, a positive bipolaron, lower in energy than two distinct polarons, is formed. A bipolaron gives rise to two empty levels between the valence and conduction bands and is likely to have two electronic transitions from the valence band to the gap states. In the extreme case of very high doping, the bipolaron band merges with the valence bands resulting in a metallic-like structure.<sup>73</sup>

The representation of polaron and bipolaron states in polythiophene is shown in Figure 1.14.

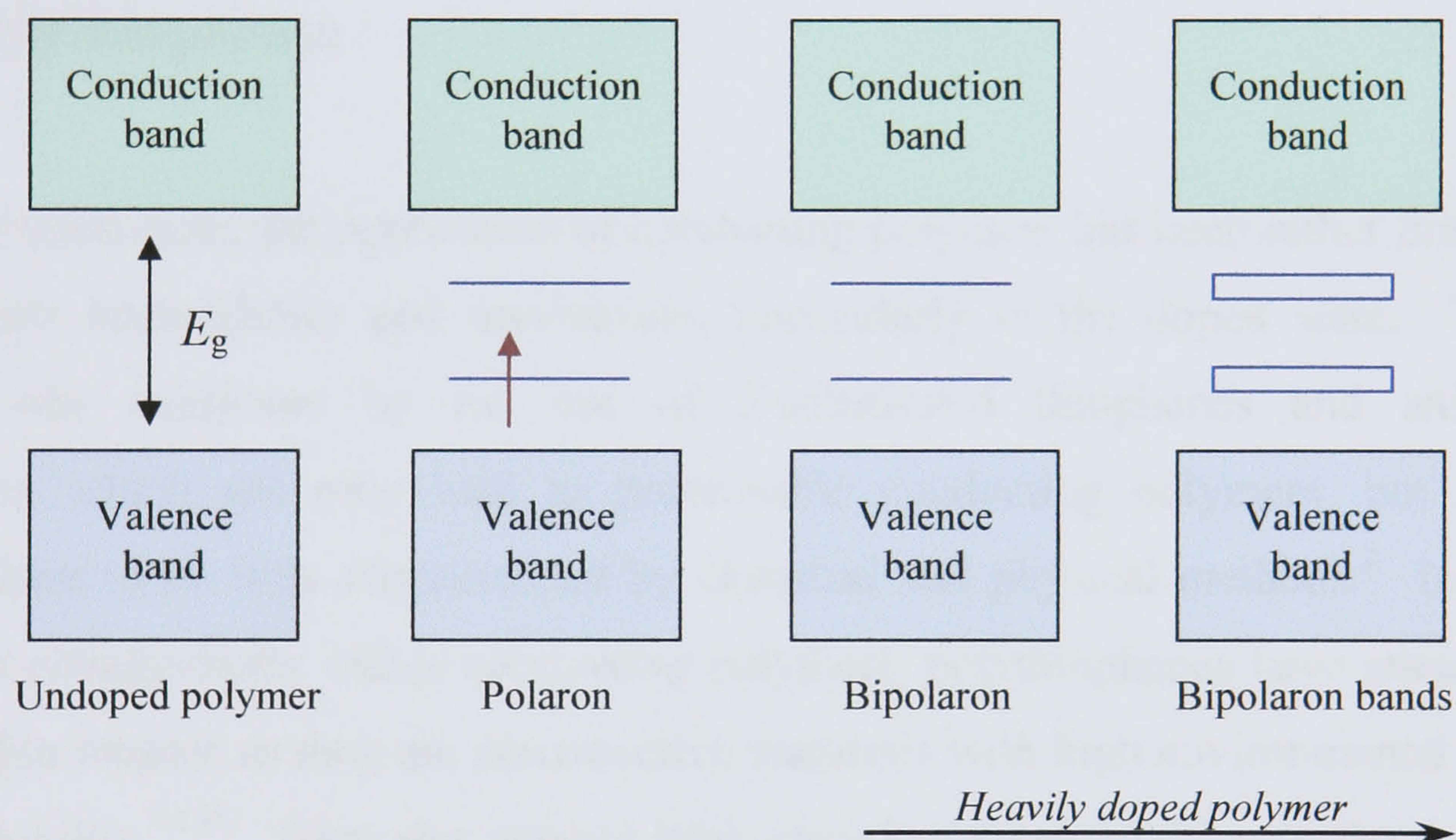


**Figure 1.14** - Schematic electronic structures of a neutral polymer chain, positive polaron and positive bipolaron.<sup>74</sup>

The band gap of a conjugated polymer determines its optical and electrical properties. The introduction, with the doping process, of new states in the band gap alters these properties and by adjusting the doping level it is possible to control them. Since  $\pi$ -conjugated polymers allow virtually endless manipulation of their chemical structure, control of the band gap of these semiconductors is a research issue of ongoing interest. This “band gap engineering” (e.g., introduction of electron donating substituents) may give the polymer the required electrical and optical properties, and reduction of the band gap to approximately zero is expected to afford an intrinsically conducting polymer.<sup>2,65</sup>



Several methods have been used to study optical and electrical properties of doped conjugated polymers. For example, upon doping, the new absorptions associated with charged excitations (polarons or bipolarons) can be detected by electronic absorption, vibrational, and electron-spin-resonance spectroscopies. In particular, vibrational (Raman and infrared) spectroscopy gives useful information about the structures of conjugated polymers in the doped states as well as in the neutral states.<sup>33</sup> The experimental data collected from the various characterisation methods has played a crucial role, not only in delineating the novel properties of conducting polymers, but also in setting up their future applications.<sup>4</sup>

### 1.2.4 Polythiophenes

For some time, the application of conducting polymers has been rather limited due to their intractability and insolubility, particularly in the doped state. This problem was overcome by the use of 3-substituted thiophenes and aniline derivatives, which not only lead to processable conducting polymers, but also allowed them to be fully characterised by chemical and physical methods.<sup>2</sup> In the search for commercially viable conducting polymers, polythiophenes have attracted considerable interest as they are electroactive materials with high environmental and thermal stability.<sup>31,75</sup> They also present high electrical conductivities in the doped state, which results from the highly conjugated, structurally regular nature of the polymer backbone.<sup>16,76</sup> The vast research done on polythiophenes has led to their many applications, e.g., in electrochromic devices,<sup>17,77,78</sup> polymer light emitting diodes,<sup>50,79</sup> sensors<sup>20</sup> and batteries<sup>13</sup>.

Polythiophene (PT) can be easily synthesised by electrochemical and chemical techniques.<sup>4</sup> The electrochemical synthesis of PT was first reported by Diaz *et al.*<sup>35</sup> in 1981. Since then, many studies have been made on the electropolymerisation of polythiophene and it is expected that most thiophene derivatives polymerise in a similar manner.<sup>71,80</sup> The first step in the mechanism of electropolymerisation consists in the oxidation of thiophene, adsorbed on the electrode surface or in solution, to its radical cation.<sup>81,82</sup> The oxidation of thiophene is irreversible, which



implies that the radical cation formed in the first step is extremely reactive. The second step involves the coupling of two radical cations to produce a dihydrodimer dication which forms a dimer after loss of two protons and rearomatisation.<sup>31</sup> Further oxidation leads to the formation of a polymer chain as illustrated in Figure 1.15. When the chain length reaches the solubility limit, the polymer precipitates onto the electrode surface.<sup>83</sup>

Electropolymerisation mechanism of polythiophene

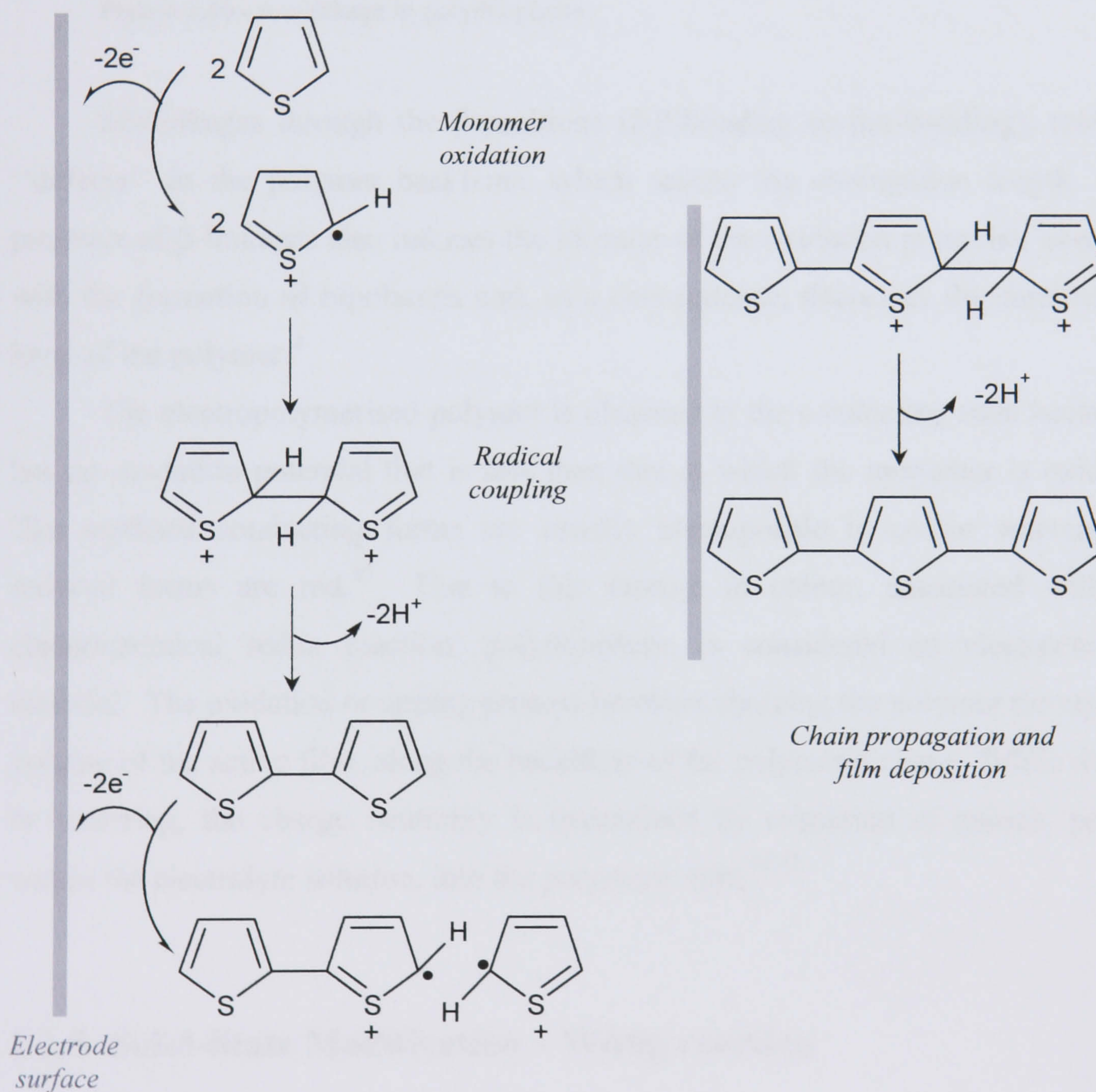
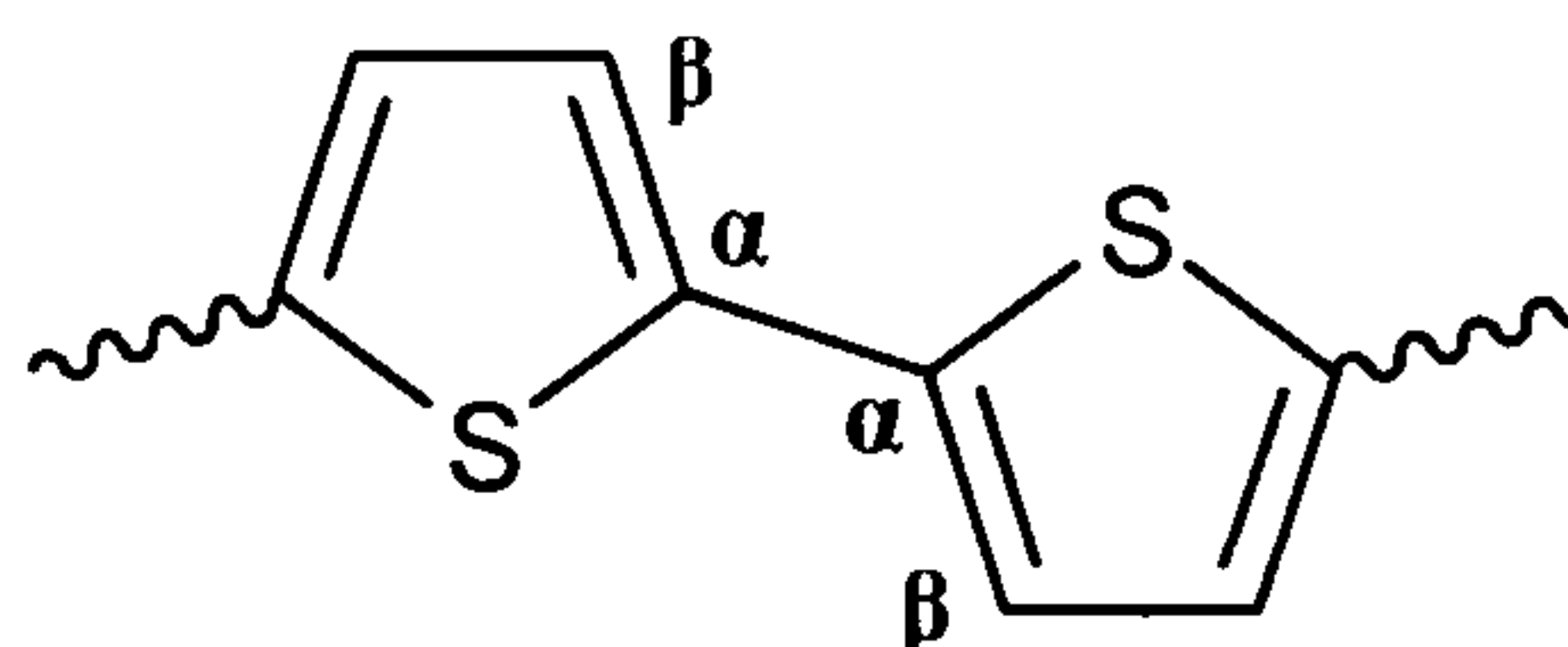


Figure 1.15 - Mechanism of electropolymerisation of polythiophene.<sup>81</sup>



The electrochemical polymerisation of thiophene occurs *via* a two-electron process followed by monomer coupling with the loss of two protons. Since the intermediate radical cation formed in the  $\alpha$ -position of the thiophene ring is more stable than the one formed in the  $\beta$ -position, the coupling between thiophene units is expected to proceed mainly through  $\alpha,\alpha$ -bondings.<sup>67,84-86</sup>



**Figure 1.16** -  $\alpha,\alpha$ -linkage in polythiophene.

Mislinkages through the  $\beta$ -positions ( $\beta,\beta$ -bonding or  $\beta,\alpha$ -bonding), result in “defects” in the polymer backbone, which reduce the conjugation length. The presence of  $\beta$ -linkages also induces the increase of the oxidation potential, interferes with the formation of bipolarons and, as a consequence, decreases the conductivity level of the polymer.<sup>2</sup>

The electropolymerised polymer is obtained in the conducting state because it has an oxidation potential that is less than that at which the monomer is oxidised. The oxidised conducting forms are usually black-purple in colour whereas the reduced forms are red.<sup>87</sup> Due to this change in colour, associated with the electrochemical redox reaction, polythiophene is considered an electrochromic material. The oxidation or doping process involves charging the polymer through the volume of the active film, along the backbone of the polymeric chain. While doping is occurring, the charge neutrality is maintained by migration of anions, present within the electrolyte solution, into the polymeric film.<sup>47,88</sup>

### 1.2.5 Solid-State Modification – Wittig reaction

An important aspect that has been responsible for the widespread research in the area of electronically conducting polymers such as polythiophenes is the diversity of properties that can be obtained by using different substituted monomers. The “tailoring” of these properties can provide remarkable opportunities to produce



polymeric materials with novel applications.<sup>15</sup> Despite the vast number of studies carried out on the synthesis of substituted polythiophenes, there is still a need for routes to produce new materials. An approach that is receiving increasing attention is functionalisation after polymerisation, e.g., the incorporation of groups, such as tetrathiafulvalene (TTF) into the polymer backbone.<sup>89</sup> This can give access to polymers that are difficult to produce by electropolymerisation, either because substituent groups are sensitive to the growth conditions, or because they inhibit the polymerisation process.<sup>90</sup> The incorporation of TTF, an extensively studied redox active molecule, opens the possibility of enhanced electrical conductivities in the resultant polymers. The concept of combining the ordered, large molecular weight polymers based on thiophene with the high conductivities observed in doped TTFs into a single framework is an attractive ambition from the perspective of obtaining conducting, yet mechanically processable, polymeric systems.<sup>16,91</sup>

The preparation of tetrathiafulvalene was first reported by Wudl *et al.*<sup>92</sup> in 1970. Since then, many studies have been made on TTF and its derivatives, well known for their unusual conducting and magnetic properties.<sup>93,94</sup> This research, moved primarily by the quest for new organic metals and organic superconductors, turned TTF into one of the strongest  $\pi$ -electron donating systems widely used for the elaboration of conducting and superconducting materials.<sup>95,96</sup> The ability of TTF and its derivatives to behave as reversible electron donors, forming stable radical cations, also makes them ideal components in charge transfer complexes.<sup>62,97</sup> The oxidation of a TTF unit from the neutral form to a radical cation and from there to the dication form is shown in Figure 1.17.

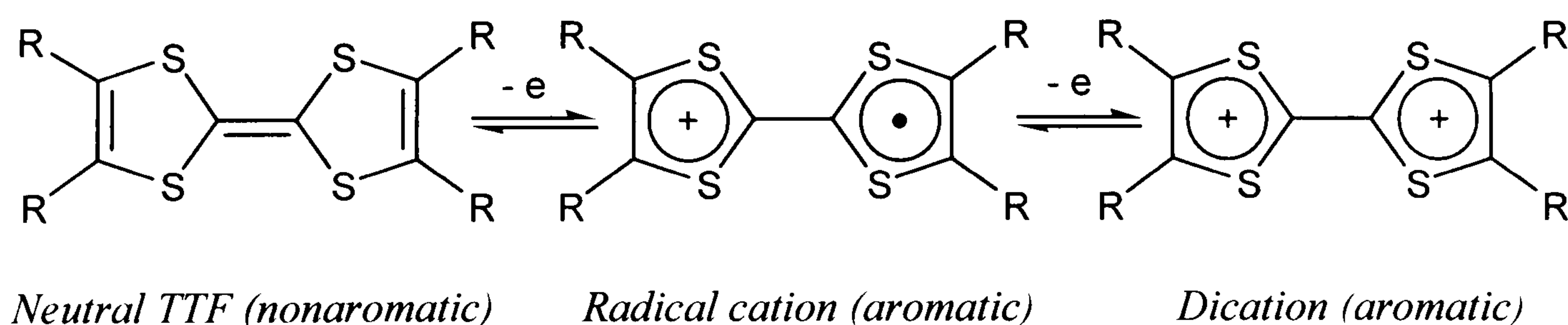


**Figure 1.17** - Electron donating nature of the TTF unit.<sup>98</sup>



Despite their inherent electronic advantages, charge transfer complexes and radical cation salts of TTF are fragile and unprocessable materials, which represent a major obstacle to practical applications.<sup>99</sup> This problem can be overcome by the inclusion of TTF into polymers.<sup>100</sup> Whereas the incorporation of TTF in polymeric matrices seeking to improve the processability of TTF-based conductors has been investigated for some years, the association of TTF with linear  $\pi$ -conjugated structures is a relatively recent concept.<sup>101</sup>

The first report of an electropolymerised TTF-derivatised polythiophene was published in 1991 by Bryce and co-workers<sup>102</sup>, describing the formation of a polymer film based on a thiophene unit linked to the TTF redox active centre via an ester group linkage (Figure 1.18).

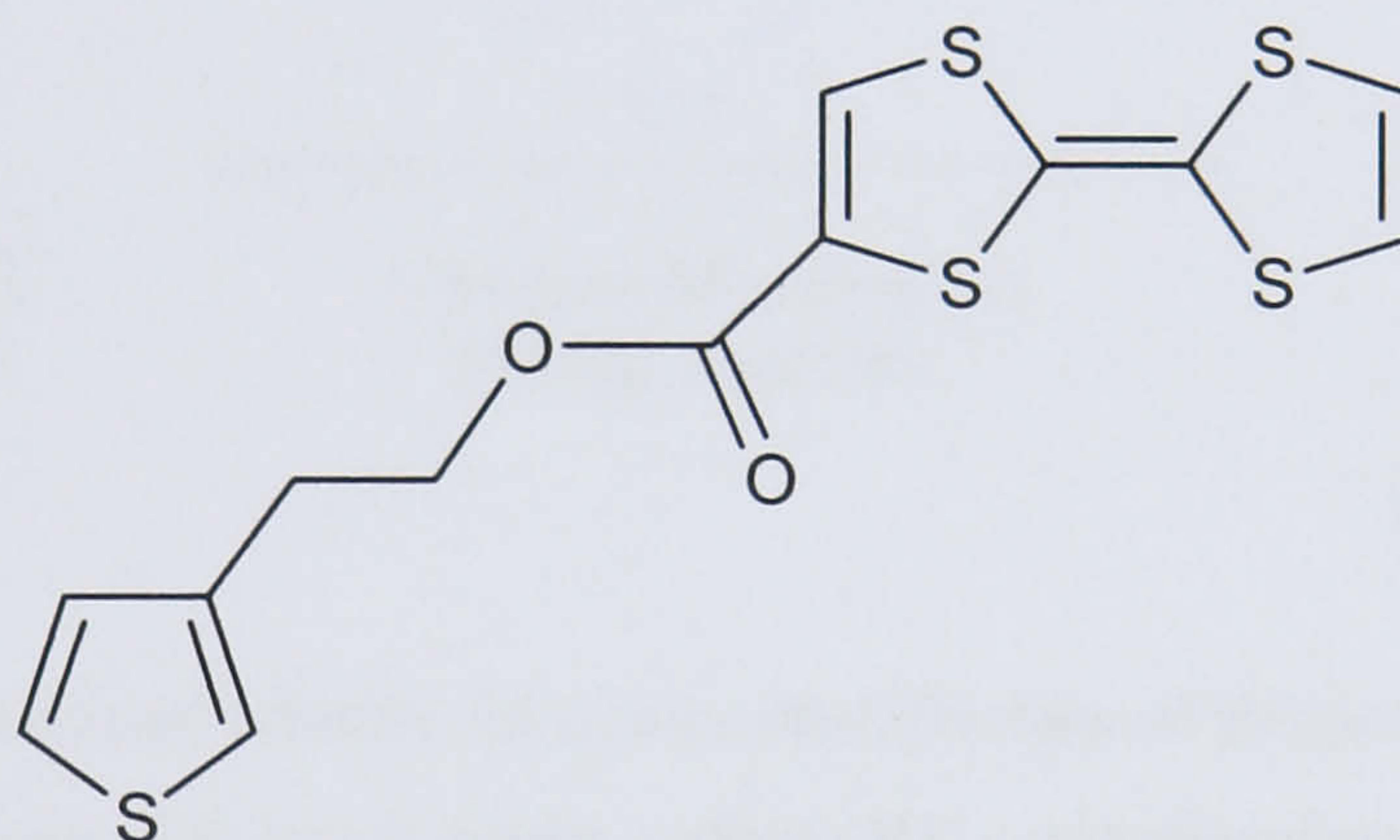


**Figure 1.18** - Structure of a TTF-derivatised thiophene monomer.

Nevertheless, this polymer presented a rather short conjugation length probably caused by a distortion in the PT backbone produced by steric interactions between TTF groups linked to the thiophene ring by a too short spacer group.<sup>103</sup>

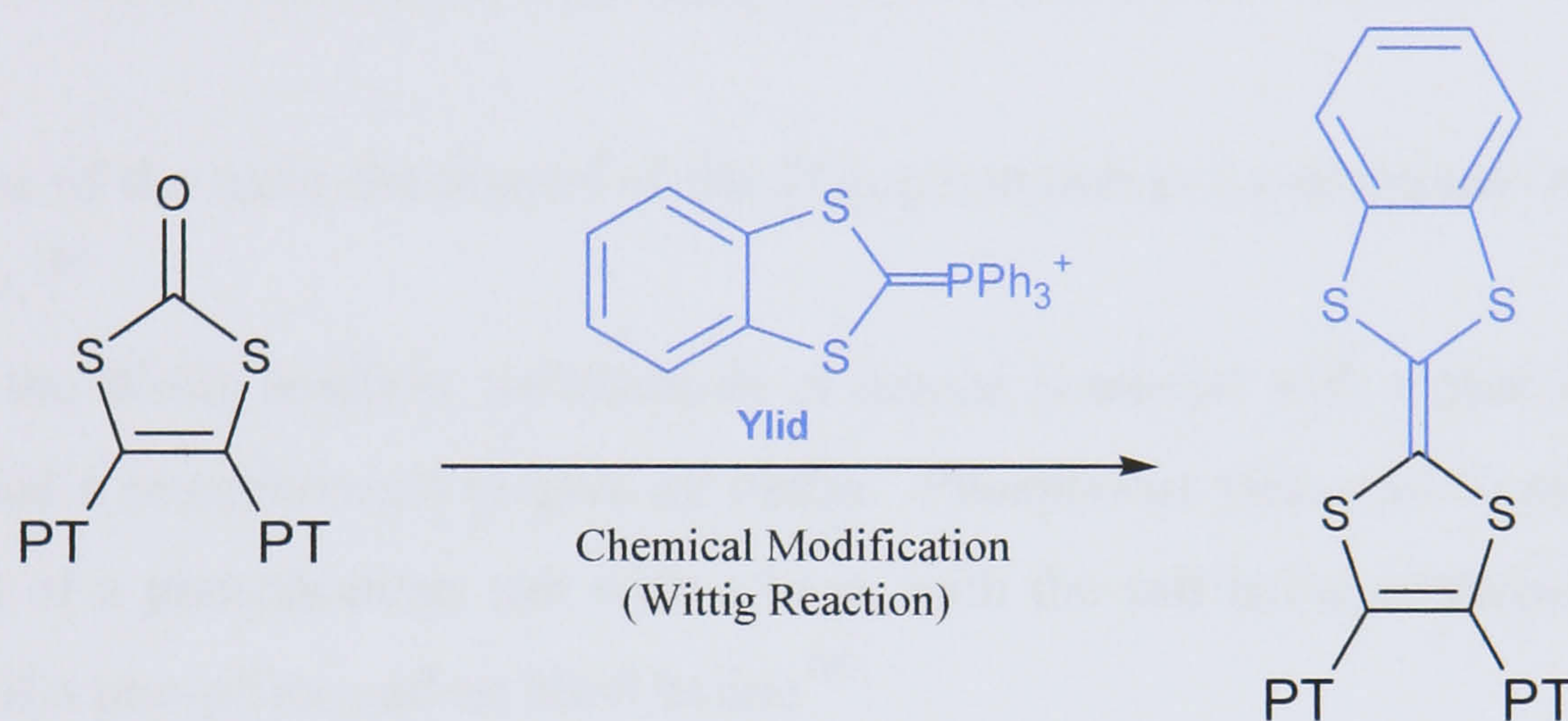
Following this work, a wide variety of polythiophenes linked to TTF units *via* saturated spacer groups have been synthesised.<sup>103,104</sup> Even though such linkages do provide the spatial proximity of the redox centers, they cannot ensure a well-defined orientation of the TTF groups relative to one another because the torsion around the bridging bonds allows a great number of different conformations. Thus, these polymers are deficient both in the order of the TTF subunits and in the dimensionality of the conduction process in the doped state.

The electropolymerisation of TTF–thiophene monomers, in which these two redox-active moieties are directly bonded to each other, is still seen as a rather



difficult process.<sup>105</sup> For instance, Charlton *et al.*<sup>16,106</sup> produced a series of new thiophene-functionalised TTF derivatives that could not be polymerised due to disruption in the aromaticity of the dicationic TTF core, generated in solution prior to the oxidation of the thiophene units.

To avoid the problematic polymerisation of TTF-derivatised thiophene monomers, the *in situ* solid-state modification of the electropolymerised polythiophene derivatives shown in Figures 1.02 - 1.04 was undertaken in this project. This reaction was carried out as shown in Scheme 1.01.



**Scheme 1.01** - Reactional scheme for *in situ* modification of the polythiophene dithiolenes, deposited at an electrode surface; PT – polythiophene chain.

As presented in Scheme 1.01, TTF units are incorporated into the polythiophene derivatives, under Wittig conditions, with an intermediate ylid reacting with the carbonyl groups present in polymeric film deposited on the electrode surface.

The Wittig reaction, also called Wittig carbonyl olefination reaction consists in the condensation of a carbonyl compound with an alkylidenetriphenyl phosphorane to give an olefin and triphenylphosphine oxide<sup>107</sup>:



**Scheme 1.02** - The Wittig Reaction: alkylidene-de-oxo-bisubstitution.

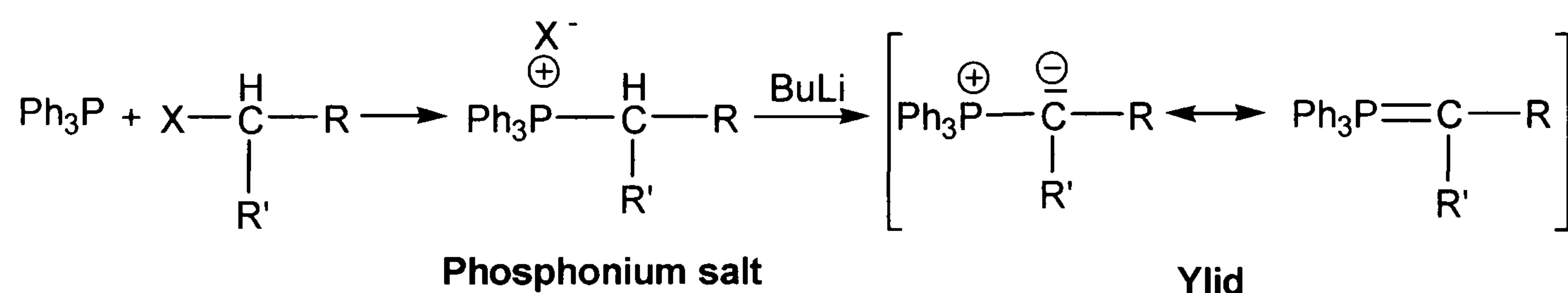


This reaction has become one of the preferred methods of olefin synthesis showing several advantages, such as:

- specificity: as a rule, no double bond isomerisation occurs under the reaction conditions, i.e. the new C=C double bond appears exclusively at the site of the former CO function.
- good reaction yields.
- the starting materials, aldehydes or ketones and phosphonium salts derived from alkyl halides and triphenylphosphine, are readily available.<sup>108</sup>

One of the main drawbacks of the Wittig reaction is its susceptibility to steric hindrance.<sup>109</sup>

In the Wittig reaction, an aldehyde or ketone is treated with a phosphorus ylid (also called a phosphorane) to give an olefin. Phosphorus ylids can be prepared by treatment of a phosphonium salt with a base, with the salt being obtained from the reaction of a phosphine and an alkyl halide<sup>107</sup>:

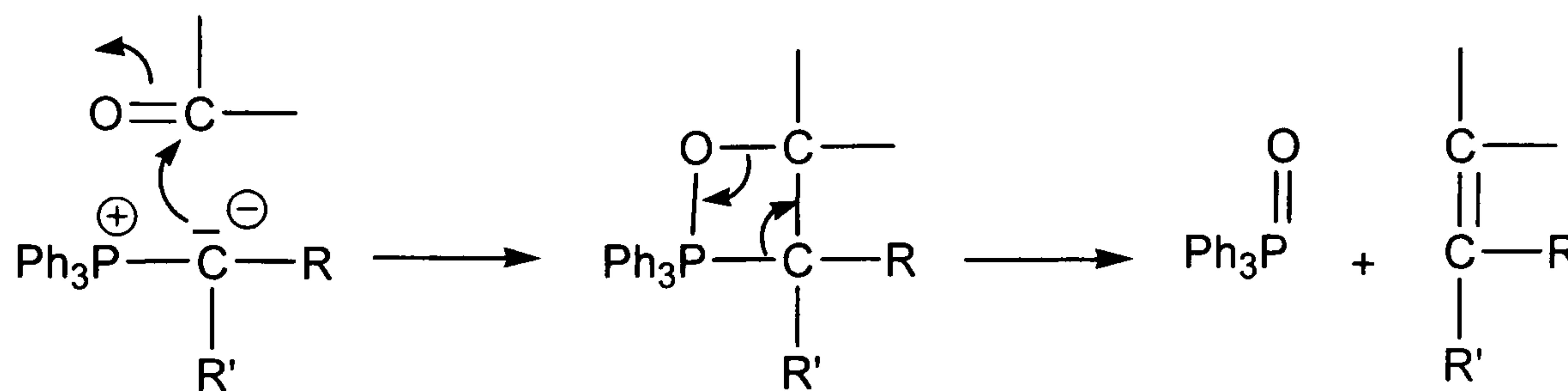


**Scheme 1.03** - The Wittig Reaction: formations of the phosphonium salt and the ylid.

The overall sequence of three steps or occasionally, only the final step, are called the Wittig reaction. This reaction is considered very general: the aldehyde or ketone may be aliphatic or aromatic; it may contain double or triple bonds; it also may contain various functional groups, such as OH, OR, NR<sub>2</sub>, aromatic nitro or halo, acetal, or even ester groups.



The mechanism of the key step of the Wittig reaction is as follows<sup>107</sup>:



Scheme 1.04 - The Wittig Reaction: mechanism of the key step.

## 1.2.6 Nickel Dithiolenes

In the search for new molecular materials with unusual electronic and magnetic properties, transition metal complexes of 1,2-dithiolenes have been intensively studied.<sup>67</sup> Metal 1,2-dithiolenes seem to have many of the physical properties required for advanced technological applications in areas related to conducting and magnetic materials<sup>26</sup>, catalysis<sup>110</sup>, dyes<sup>111</sup>, and so on. These applications arise due to a combination of functional properties, specific geometries and intermolecular interactions.<sup>26</sup> The general structure of this class of compounds is shown in Figure 1.19.

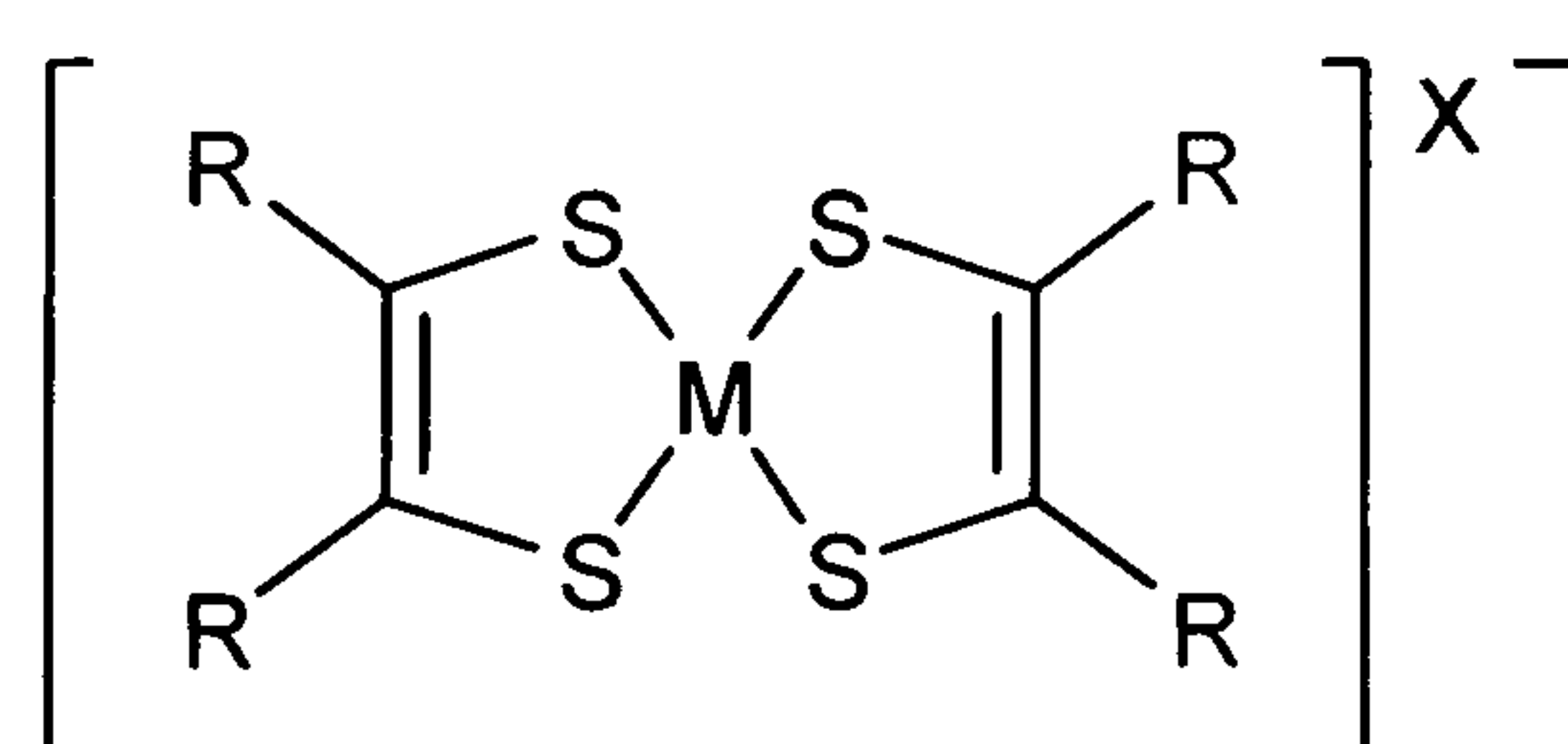


Figure 1.19 - General structure of a metal 1,2-dithiolenyl complex  $[M(\text{dithiolenyl})_2]^{X^-}$ .

Metal dithiolenes were initially synthesised in the 1960s and since then extensive research has been made on bisdithiolenyl metal complexes.<sup>110,112,113</sup> This interest was driven by the discovery of phenomena such as superconductivity and ferromagnetism in metal dithiolenyl salts and has resulted in the search for new analogues with better properties.<sup>26</sup>



The first observation of metallic behaviour in the dithiolene complexes occurred in 1981 for  $[\text{Pt}(\text{S}_2\text{C}_4\text{N}_2)_2]^{n-}$  (or  $\text{Pt}(\text{mnt})_2$  with  $\text{mnt}$  – maleonitriledithiolate).<sup>114</sup> In 1983, Valade *et al.*<sup>115</sup> reported the first conducting  $\text{M}(\text{dmit})_2$  salt ( $\text{dmit}$  – 1,3-dithiole-2-thione-4,5-dithiolate). This discovery was followed by the synthesis in 1985 of a  $(\text{dddt})_2$ -based complex with the formula  $[\text{NEt}_4][\text{Ni}(\text{dddt})_2]$ .<sup>116</sup> The  $\text{M}(\text{dddt})_2$  molecule ( $\text{dddt}$  – 5,6-dihydro-1,4-dithiin-2,3-dithiolate) was seen as a metal complex analogue of the well known organic donor bis(ethylenedithio) tetrathiafulvalene, BEDT-TTF, where the central  $\text{C}=\text{C}$  bond of BEDT-TTF is substituted by a transition metal (Figure 1.20).

A few years later, the first superconductor, based on a metal dithiolene complex was discovered. The  $(\text{TTF})[\text{Ni}(\text{dmit})_2]_2$  complex undergoes a superconducting transition at 1.62 K under 7 kbar.<sup>117</sup>

The structures of some important classes of metal dithiolenes and of the organic donor BEDT-TTF are shown in Figure 1.20:

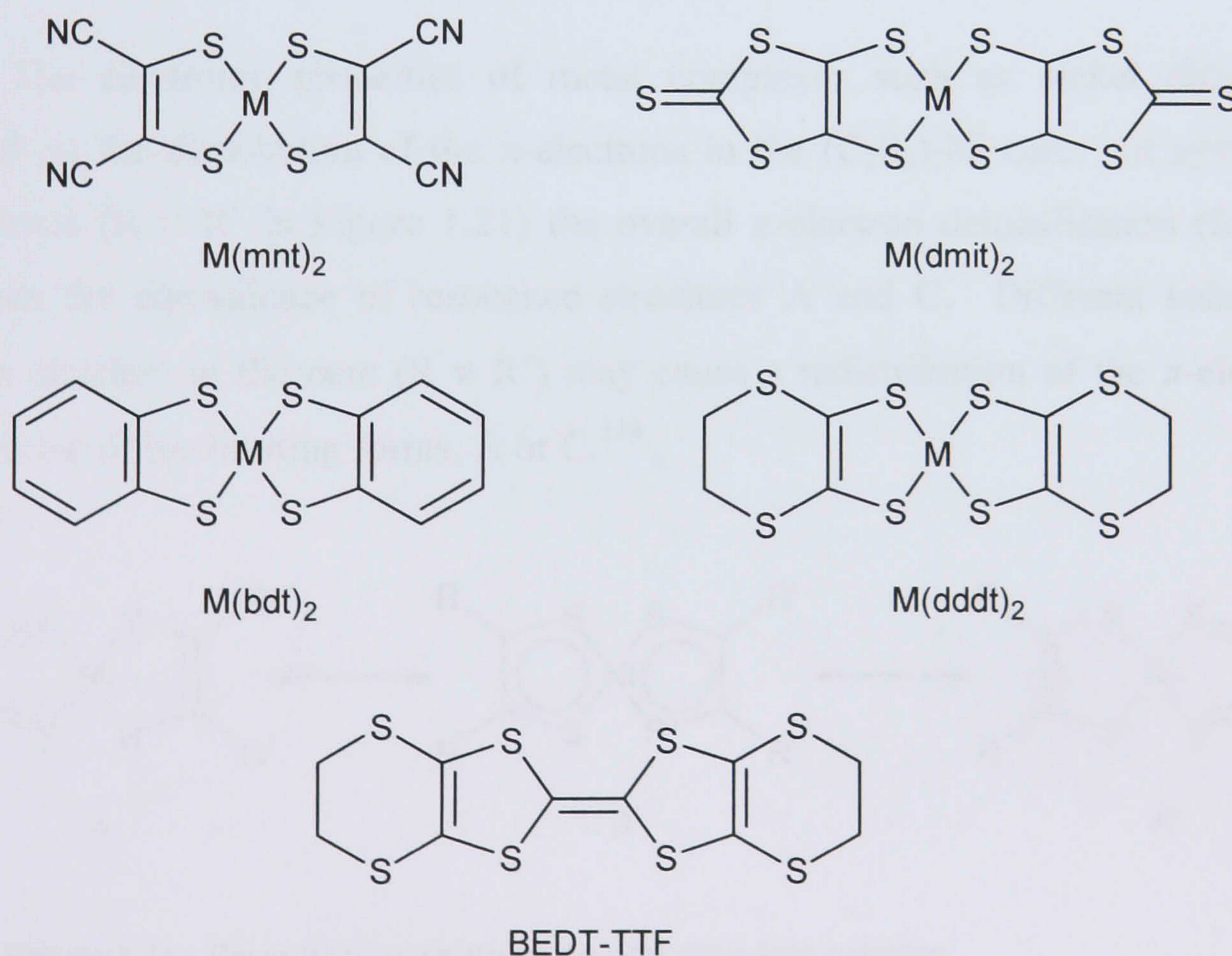


**Figure 1.20** - Structure of  $\text{M}(\text{mnt})_2$  – maleonitriledithiolate;  $\text{M}(\text{dmit})_2$  - 1,3-dithiole-2-thione-4,5-dithiolate;  $\text{M}(\text{bdt})_2$  - benzene-1,2-dithiolate;  $\text{M}(\text{dddt})_2$  - 5,6-dihydro-1,4-dithiin-2,3-dithiolate; BEDT-TTF - bis(ethylenedithio) tetrathiafulvalene.



Metal-bis-1,2-dithiolene complexes have a delocalised electron system with a planar central core containing the central metal, four sulphurs and the C=C units.<sup>118</sup> In many cases, the delocalisation can be further extended by the choice of appropriate substituent groups (R in Figure 1.19). This electronic delocalisation is responsible for a number of important properties such as:

- (i) electrochemical performance usually with one or more reversible redox processes;
- (ii) low energy absorption assigned to a  $\pi \rightarrow \pi^*$  transition between the HOMO and the LUMO, in the visible or near IR region;
- (iii) the frontier orbitals are dispersed over much, or all, of the molecule;
- (iv) in general, a planar arrangement of the complex with a variety of central metals like Ni, Au, Pt, Pd, Co, Fe, and Cu;
- (v) the large sulphur atoms are part of the delocalised core and therefore, can participate in intermolecular interactions.<sup>26</sup>

The electronic properties of metal complexes such as nickel dithiolenes depend on the distribution of the  $\pi$ -electrons in the  $(C_2S_2)_2Ni$  core. In symmetric complexes ( $R = R'$  in Figure 1.21) the overall  $\pi$ -electron delocalisation (form B) involves the equivalence of resonance structures A and C. Different substituent groups attached to the core ( $R \neq R'$ ) may cause a redistribution of the  $\pi$ -electrons toward one of the limiting forms, A or C.<sup>119</sup>

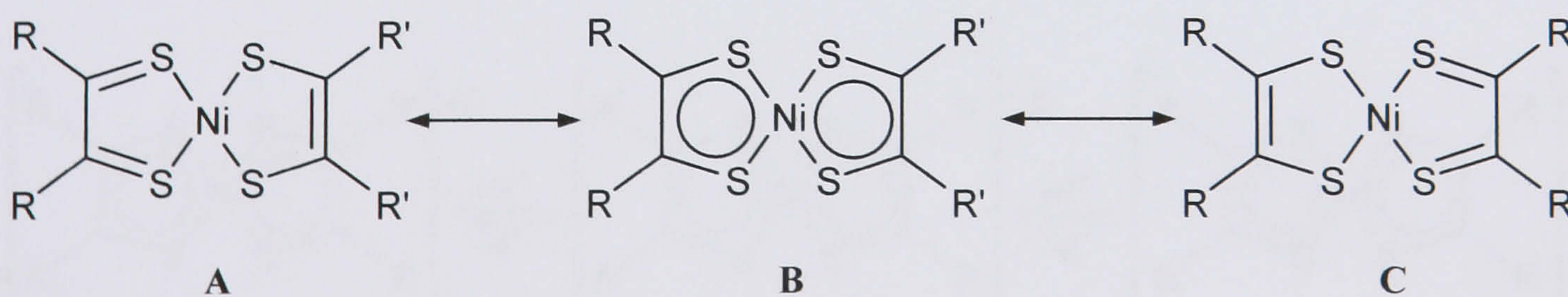


**Figure 1.21** - Resonance structures of a nickel dithiolene complex.



Since the electronic charge in metal dithiolenes is delocalised over the entire molecule, the assignment of formal oxidation states to the central metal and ligand has often been considered ambiguous.<sup>120,121</sup> The dithiolene is a “non-innocent” ligand that can either be neutral or dianionic as shown in Figure 1.22.<sup>122,123</sup> This “non-innocent” character is due to a strong mixing between ligand and metal orbitals making the assignment of the oxidation state of the metal or ligand components rather difficult.<sup>124</sup>

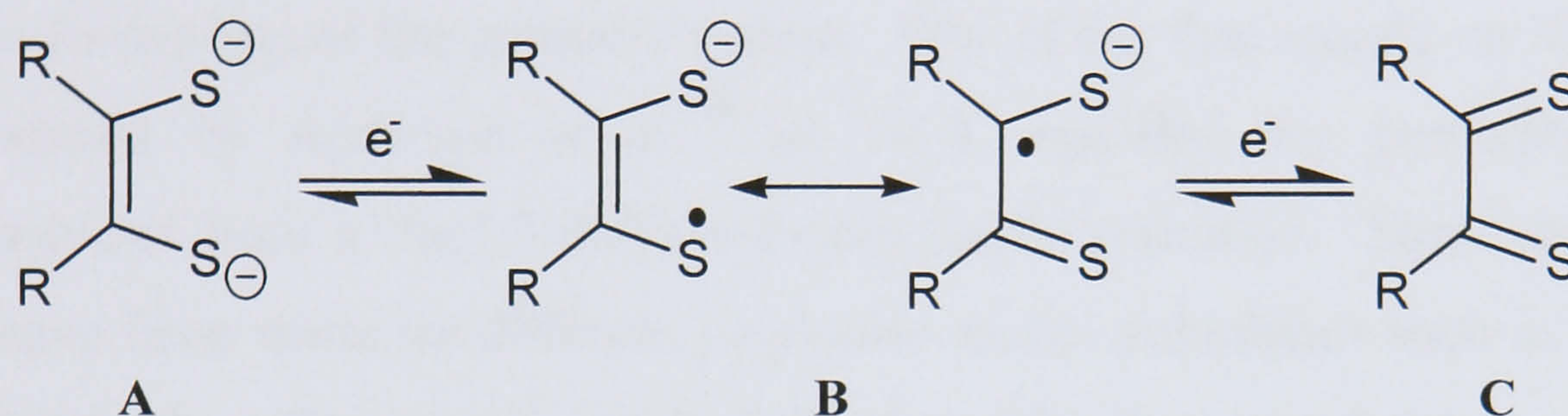


**Figure 1.22** - Resonance structures of the A - dinegative dithiolate (-2), B – radical (-1), and C - neutral dithioketone forms.

The neutral dithioketone and the dinegative dithiolate forms differ in the number of  $\pi$ -electrons: the neutral form has four  $\pi$ -electrons and the dianionic possesses six.<sup>125</sup>

By virtue of the extended delocalised nature of these complexes, nickel dithiolenes have the ability to exist in a number of well defined, but interconvertible oxidation states (Figure 1.23). Interchange between neutral, mono- and dianionic species, can be achieved by either chemical or electrochemical methods.<sup>67,126</sup>

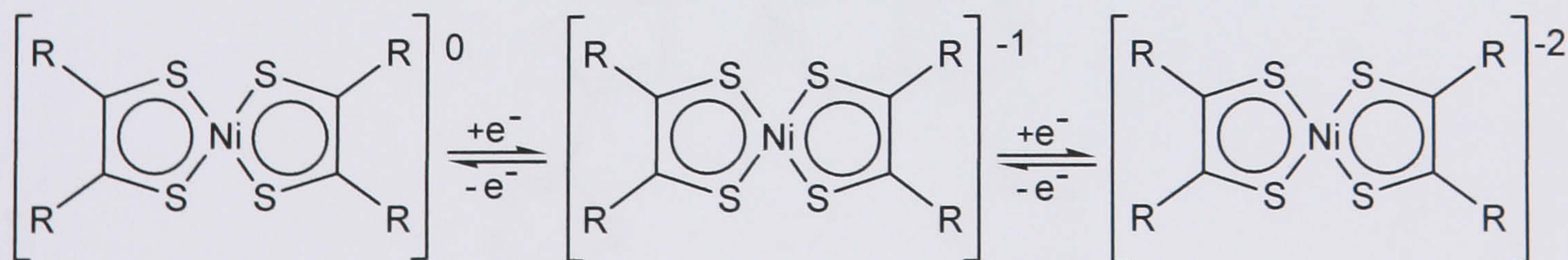


**Figure 1.23** - The interconvertible oxidation states of metal dithiolenes.

The reduction of the neutral species to the mono- or dianions is usually accompanied by an increase in the infra-red frequency (blue shift) associated with



the C=C bonds, and a decrease in the frequency (red shift) associated with the C-S bonds.<sup>111</sup> This reflects the fact that the reduction of metal dithiolenes causes the increase in dithiolate character (Figure 1.22 A) of the ligand, which is consistent with dithiolene complexes possessing both a dithioketone and dithiolate behaviour<sup>67,127</sup>

One area that has been under investigation is the incorporation of transition metal complexes into conjugated organic polymers, which offers the possibility of developing new advanced electronic materials.<sup>128</sup> Dithiolene complexes are attractive building blocks for such systems due to their aromaticity, and the ease of reduction (n-doping) of the aromatic system. One of the first reports on this matter was produced by Anderson *et al.*<sup>129</sup> in 1978 regarding the preparation of a metallopolymer from a bis(1,3-dithiole-2-one) ligand precursor. Since then, many studies have been made on different polymeric nickel dithiolenes such as the ones obtained from the polymerisation of the following dithiolene complexes.

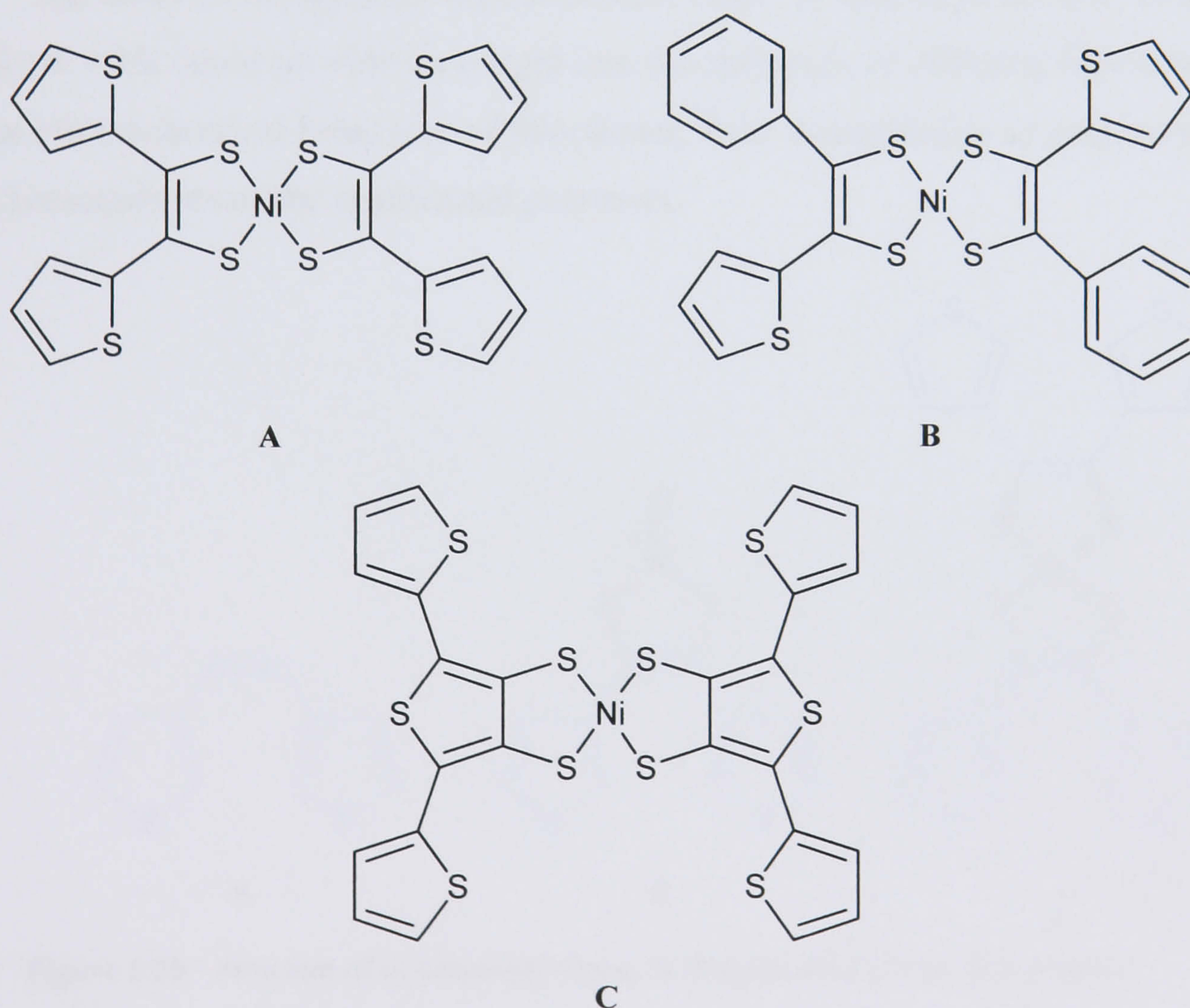


**Figure 1.24** - Structures of nickel dithiolene complexes investigated by Kean *et al.*<sup>29</sup> (A and B) and Pozo-Gonzalo *et al.*<sup>130</sup> (C).



The polymerisation of the nickel dithiolenes shown in Figures 1.06 - 1.07 has been attempted in this research work. The incorporation of nickel dithiolene complexes may prove to be advantageous in the control of the electronic properties of the final polymer, by providing an alternative pathway for conduction and/or improving its structural regularity.

### 1.3 Aims of the Project

Bearing in mind the important role of polythiophenes in the area of conducting polymers, an electrochemical and spectroelectrochemical study of new thiophene derivatives was proposed in this project. The main objective was to attempt the electropolymerisation of these compounds and investigate the electrochemical and spectroscopic properties of the resultant polymers.

The study of compounds with structures based on dithienylethylene, as shown in Figure 1.25, could provide an insight into the influence of different functionalities on the electrochemical behaviour of thiophenes, their susceptibility to polymerisation and characteristics of the synthesised polymers.

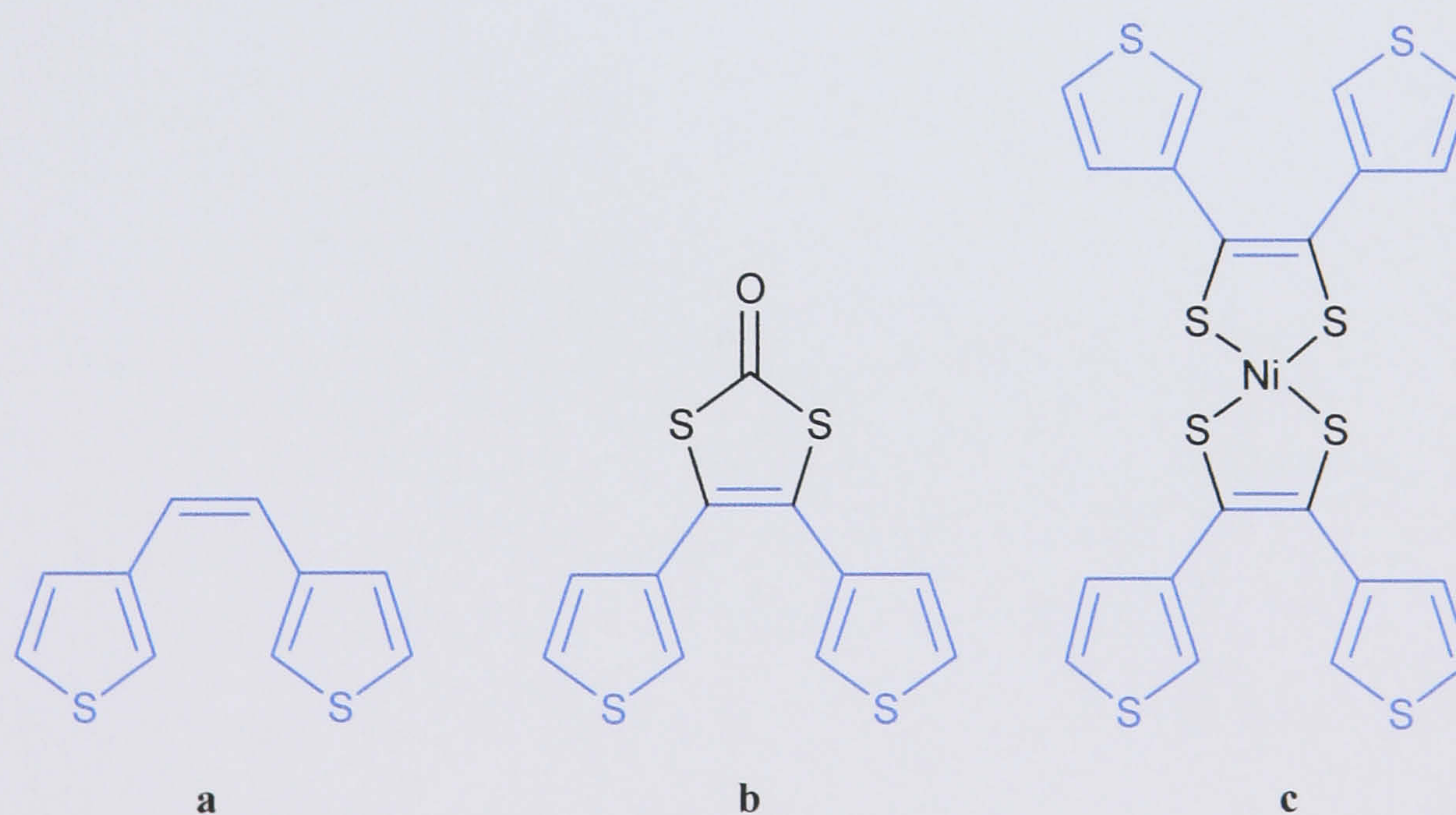


**Figure 1.25** - Structure of a) dithienylethylene, b) thiophene dithiolene and c) nickel dithiolene.

In view of the fact that the electron donor TTF is known to have the ability to form conducting and superconducting materials, it was of interest to prepare and



study novel polymers featuring TTF moieties attached to thiophene units. The *in situ* solid state Wittig reaction on electrosynthesised polythiophene dithiolenes would give access to new a class of polymers that cannot be easily obtained by electrochemical polymerisation.

With the aim of incorporating transition metal complexes into conjugated organic polymers, the polymerisation of nickel dithiolenes has been attempted. The extensive conjugation exhibited by nickel dithiolenes complexes and the electron donating effect of the peripheral thiophenes makes them important units in the research towards the development of molecular conductors.



## 1.4 References

1. V.N. Prigodin and A.J. Epstein, *Synth. Met.*, 125 (2001) 43.
2. H. S. O. Chan and S. C. Ng, *Progr. Poly. Sci.*, 23 (1998) 1167.
3. H. Shirakawa, E.J. Louis, A.G. MacDiarmid, C.K. Chiang and A.J. Heeger, *J. Chem. Soc., Chem. Commun.*, (1977) 578.
4. V. Saxena and B.D. Malhotra, *Curr. Appl. Phys.*, 3 (2003) 293.
5. K. Gurunathan, A.V. Murugan, R. Marimuthu, U.P. Mulik and D.P. Amalnerkar, *Mat. Chem. Phys.*, 61 (1999) 173.
6. S. Yang, P. Olishovski and M. Kertesz, *Synth. Met.*, 141 (2004) 171.
7. M. Gerard, A. Chaubey and B.D. Malhotra, *Biosens. Bioelec.*, 17 (2002) 345.
8. P. Zarras, N. Anderson, C. Webber, D.J. Irvin, J.A. Irvin, A. Guenther and J.D. Stenger-Smith, *Radiat. Phys. Chem.*, 68 (2003) 387.
9. A.J. Heeger, *Synth. Met.*, 125 (2002) 23.
10. G.O. Williams, Ph.D. thesis, University of Wales, Bangor (1999).
11. F. Davis and S.P.J. Higson, *Biosens. Bioelec.*, 21 (2005) 1.
12. G. Sonmez, P. Schottland, K. Zong and J.R. Reynolds, *J. Mater. Chem.*, 11 (2001) 289.
13. P. Novak, K. Muller, K.S.V. Santhanam and O. Haas, *Chem. Rev.*, 97 (1997) 207.
14. D. Kumar, *Synth. Met.*, 114 (2000) 369.
15. Z. Qi, N. G. Rees and P. G. Pickup, *Chem. Mater*, 8 (1996) 701.
16. A. Charlton, A. Underhill, G. W. M. Kalaji, P. J. Murphy, K. M. A. Malik and M. B. Hursthouse, *J. Org. Chem.*, 62 (1997) 3098.
17. R.J. Mortimer, *Electrochim. Acta*, 44 (1999) 2971.
18. J. Bobacka, A. Ivaska and M. Grzeszczuk, *Synth. Met.*, 44 (1991) 9.
19. S.R. Kim, S.A. Choi, J.D. Kim, K.J. Kim, C. Lee and S.B. Rhee, *Synth. Met.*, 71 (1995) 2027.
20. B. Adhikari and S. Majumdar, *Prog. Polym. Sci.*, 29 (2004) 699.
21. R. Galarini, A. Musco, R. Pontellini, A. Bolognesi, S. Destri, M. Catellani, M. Mascherpa and G. Zhuo, *J. Chem. Soc., Chem. Commun.*, 6 (1991) 364.



22. M. Onoda, S. Iwasa, H. Nakayama, K. Yoshino and M. Laguna, *J. Chem. Phys.*, 95 (1991) 8584.
23. A. Berlin and G. Zotti, *Synth. Met.*, 106 (1999) 197.
24. J. Roncali, *Chem. Rev.*, 97 (1997) 173.
25. H. Brisset, P. Blanchard, B. Illien, A. Riou and J. Roncali, *Chem. Commun.*, (1997) 569.
26. N. Robertson and L. Cronin, *Coord. Chem. Rev.*, 227 (2002) 93.
27. P.I. Clemenson, *Coord. Chem. Rev.*, 106 (1990) 171.
28. R.M. Olk, B. Olk, W. Dietzsch, R. Kirmse and E. Hoyer, *Coord. Chem. Rev.*, 117 (1992) 99.
29. C.L. Kean, D.O. Miller and P.G. Pickup, *J. Mater. Chem.*, 12 (2002) 2949.
30. J.L. Bredas and G.B. Street, *Acc. Chem. Res.*, 18 (1985) 309.
31. H. S. Nalwa, ed., "Handbook of organic conductive molecules and polymers - Conductive polymers: Synthesis and electrical properties", Vol. 2, J. Wiley & Sons Ltd., UK, (1997).
32. V. W. Jones, Ph.D. thesis, University of Wales, Bangor (1995).
33. Y. Furukawa, *J. Phys. Chem.*, 100 (1996) 15644.
34. A.F. Diaz, K.K. Kanazawa and G.P. Gardini, *J. Chem. Soc., Chem. Commun.*, (1979) 635.
35. A.F. Diaz, J. Crowley, J. Bargon, G.P. Gardini and J.B. Torrance, *J. Electroanal. Chem.*, 121 (1981) 355.
36. A.F. Diaz and J.A. Logan, *Electroanal. Chem.*, 111 (1980) 111.
37. D.M. Ivory, G.G. Miller and J.M. Sowa, *J. Chem. Phys.*, 71 (1979) 1506.
38. G.E. Wnek, J.C.W. Chien, F.E. Karasz and C.P. Lilly, *Polymer*, 20 (1979) 1441.
39. M. Bragadin, P. Cescon, A. Berlin and F. Sanniccolo, *Makromol. Chem.*, 188 (1987) 1425.
40. A.G. MacDiarmid, *Synth. Met.*, 125 (2001) 11.
41. D.T. McQuade, A.E. Pullen and T.M. Swager, *Chem. Rev.*, 100 (2000) 2537.
42. W. Hayes, F.L. Pratt, K.S. Wong, K. Kaneto and K. Yoshino, *J. Phys. C: Solid State Phys.*, 18 (1985) 555.
43. C. Xia, X. Fan, M. Park and R.C. Advincula, *Langmuir*, 17 (2001) 7893.



44. G. Inzelt, M. Pineri, J.W. Schultze and M.A. Vorotyntsev, *Electrochim. Acta*, 45 (2000) 2403.
45. J.D. Stenger-Smith, *Prog. Polym. Sci.*, 23 (1998) 57.
46. G. Tourillon and F. Garnier, *J. Electrochem. Soc.*, 130 (1983) 2042.
47. T.A. Skotheim, ed., "Handbook of Conducting Polymers", Vol. 1, Marcel Dekker Inc., New York, (1986).
48. T. Tuken, B. Yazici and M. Erbil, *Progress in Organic Coatings*, 51 (2004) 205.
49. P. Audebert and G. Bidan, *Electroanal. Chem.*, 190 (1985) 129.
50. L. Akcelrud, *Prog. Polym. Sci.*, 28 (2003) 875.
51. M. Biserni, A. Marinangeli and M. Mastragostino, *J. Electrochem. Soc.*, 132 (1985) 1597.
52. K.B. Crawford, M.B. Goldfinger and T.M. Swager, *J. Am. Chem. Soc.*, 129 (1998) 5274.
53. P. Bauerle and A. Emge, *Adv. Matter*, 3 (1998) 324.
54. H. Neugebauer, *J. Electroanal. Chem.*, 563 (2004) 153.
55. H.S. Nalwa, ed., "Handbook of organic conductive molecules and polymers – Conductive polymers: Transport, Photophysics and Applications", Vol. 4, J. Wiley & Sons Ltd., UK, (1997).
56. T. Ahn, B. Choi, S.H. Ahn, S.H. Han and H. Lee, *Synth. Met.*, 117 (2001) 219.
57. M.R. Fernandes, J.R. Garcia, M.S. Schultz and F.C. Nart, *Thin Solid Films*, 474 (2005) 279.
58. A. Patil, A.J. Heeger and F. Wudl, *Chem. Rev.*, 88 (1988) 183.
59. P.J. Skabara, D.M. Roberts, I.M. Serebryakov and C. Pozo-Gonzalo, *Chem. Commu.*, (2000) 1005.
60. P.A. Christensen, A. Hamnett and A.R. Hillman, *J. Electroanal. Chem.*, 242 (1988) 47.
61. M.A. Valle, P. Cury and R. Schrebler, *Electrochim. Acta*, 48 (2002) 397.
62. G.O. Williams, Ph.D. Thesis, University of Wales, Bangor (1999).
63. J.-W. Lee, F. Serna, J. Nickels and C. E. Schmidt, *Biomacromolecules Commu.*, 7 (2006) 1692.



64. M. S. Passos, M. A. Queiros, T. Le Gall, S. K. Ibrahim and C. J. Pickett, *J. Electroanal. Chem.*, 435 (1997) 189.
65. H.A.M. van Mullekom, J.A.J.M. Vekemans, E.E. Havinga and E.W. Meijer, *Mat. Sci. Eng. R* 32 (2001) 1.
66. T.A. Skotheim, ed., "Handbook of Conducting Polymers", Vol. 2, Marcel Dekker Inc., New York, (1986).
67. A. Charlton, Ph.D. thesis, University of Wales, Bangor (1994).
68. J. Przulski, in "Conducting Polymers - Electrochemistry", Sci-Tech Publications, Liechtenstein, (1991).
69. S. Stafstrom and J.L. Bredas, *J. Molec. Struct.: THEOC.*, 188 (1989) 393.
70. P.A. Christensen and A. Hamnett, *Electrochim. Acta*, 39 (1994) 187.
71. H.S. Nalwa, ed., "Handbook of organic conductive molecules and polymers – Conductive polymers: Spectroscopy and Physical Properties", Vol. 3, J. Wiley & Sons Ltd., UK, (1997).
72. M.J. Nowak, D. Spiegel, S. Hotta, A.J. Heeger and P.A. Pincus, *Macromolecules*, 22 (1989) 2917.
73. Y. Furukawa, *Synth. Met.*, 69 (1995) 629.
74. P.R. Somani and S. Radhakrishnan, *Mat. Chem. Phys.*, 77 (2003) 117.
75. P. Camurlu, A. Cirpan and L. Toppare, *Mat. Chem. Phys.*, 92 (2005) 413.
76. C.J. Walsh and T. Sooksimuang, *Macromolecules*, 32 (1999) 2397.
77. F. Garnier, G. Tourillon, M. Gazard and J.C. Dubios, *J. Electroanal. Chem.*, 148 (1983) 299.
78. U. Bulut and A. Cirpan, *Synth. Met.*, 148 (2005) 65.
79. M.R. Andersson, M. Berggren, G. Gustafson, T. Hjertberg, O. Inganas and O. Wennerstrom, *Synth. Met.*, 71 (1995) 2183.
80. G. Tourillon and F. Garnier, *J. Phys. Chem.*, 87 (1983) 2289.
81. R. Schrebler, P. Grez, P. Cury, C. Veas, M. Merino, H. Gomez, R. Cordova and M.A. del Valle, *J. Electroanal. Chem.*, 430 (1997) 77.
82. M. Kabasakaloglu, T. Kiyak, H. Toprak and M. L. Aksu, *App. Surf. Sci.*, 152 (1999) 115.
83. B. Ballarin, F. Costanzo, F. Mori, A. Mucci, L. Pigani, L. Schenetti, R. Seeber, D. Tonelli and C. Zanardi, *Electrochim. Acta*, 46 (2001) 881.



84. Y. Wei, C. Chan, J. Tian, G. Jang and K. Hsueh, *Chem. Mater.*, 3 (1991) 888.
85. R.J. Wattman, J. Bargon and A.F. Diaz, *J. Phys. Chem.*, 87 (1983) 1459.
86. J. R. Smith, P. A. Cox, S. A. Campbell and N. M. Ratcliffe, *J. Chem. Soc. Faraday Trans.*, 91 (1995) 2331.
87. S. J. Edge, Ph.D. Thesis, University of Wales, Bangor (1990).
88. G. Tourillon and F. Garnier, *J. Electroanal. Chem.*, 161 (1984) 51.
89. M. Besbes, G. Trippé, E. Levillain, M. Mazari, F. Le Derf, I. F. Perepichka, A. Derdour, A. Gorgues, M. Sallé, J. Roncali, *Adv. Mat.*, 13 (2001) 1249.
90. M. S. Passos, M. A. Queiros, T. Le Gall, S. K. Ibrahim and C. J. Pickett, *J. Electroanal. Chem.*, 435 (1997) 189.
91. L. Huchet, S. Akoudad, J. Roncali and E. Levillain, *Synth. Met.*, 101 (1999) 37.
92. F. Wudl, G. M. Smith and J. Hufnagel, *Chem. Commu.*, 1453 (1970).
93. M. R. Bryce, P. J. Skabara, A. J. Moore, A. S. Batsanov, J. A. K. Howard and V. J. Hoy, *Tetrahedron*, 53 (1997) 17781.
94. I. Perez, S. Liu, N. Martin and L. Echegoyen, *J. Org. Chem.*, 65 (2000) 3796.
95. A. Charlton, A. Underhill, G. Williams, M. Kalaji, P.J. Murphy, D.E. Hibbs, M.B. Hursthouse and K.M.A. Malik, *Chem. Commu.*, (1996) 2423.
96. P. Leriche, M. Turbez, V. Monroche, P. Frere, P. Blanchard, P. J. Skabara and J. Roncali, *Tetrahedron Lett.*, 44 (2003) 649.
97. T. Khan and P. J. Skabara, *Synth. Met.*, 120 (2001) 881.
98. D.L. Coffen, J.Q. Chambers and N.D. Canfield, *J Am. Chem. Soc.*, 93 (1971).
99. J. Roncali, *J. Mater. Chem.*, 7 (1997) 2307.
100. H. Tamura, T. Watanabe, K. Imanishi and M. Sawada, *Synth. Met.*, 107 (1999)
101. L. Huchet, S. Akoudad, E. Levillain, J. Roncali, A. Emge and P. Bäuerle, *J. Phys. Chem.*, 102 (1998) 7776.
102. M.R. Bryce, A.D. Chissel, J. Gopal, P. Kathirgamanathan and D. Parker, *Synth. Met.*, 39 (1991) 397.
103. C. Thobie-Gautier, A. Gorgues, M. Jubault and J. Roncali, *Macromolecules*, 16 (1993) 4094.
104. L. Huchet, S. Akoudad and J. Roncali, *Adv. Mater.*, 10 (1998) 541.
105. P.J. Skabara, R. Berridge, E.J.L. McInnes, D.P. West, S.J. Coles, M.B. Hursthouse and K. Mullen, *J. Mater. Chem.*, 14 (2004) 1964.



106. A. Charlton, M. Kalaji, P.J. Murphy, S. Salmaso, A.E. Underhill, G. Williams, M.B. Hursthouse and K.M. Abdul Malik, *Synth. Met.*, 95 (1998) 75.
107. J. March, in "Advanced Organic Chemistry - Reactions Mechanisms and Structure", John Wiley & Sons (1992).
108. M. C. Henry and G. Wittig, *J. Am. Chem. Soc.*, 82 (1960) 563.
109. K. B. Becker, *Tetrahedron*, 36 (1980) 1717.
110. C. Lauterbach and J. Fabian, *J. Inorg. Chem.*, (1999) 1995.
111. J. Fabian, H. Nakazumi and M. Matsuoka, *Chem. Rev.*, 92 (1992) 1197.
112. G.N. Schrauzer and V.P. Mayweg, *J. Am. Chem. Soc.*, 87 (1965) 3585.
113. G.N. Schrauzer and V.P. Mayweg, *J. Am. Chem. Soc.*, 85 (1962) 3221.
114. A.E. Underhill and M.M. Ahmad, *J. Chem. Soc., Chem. Commun.*, 3 (1981) 67.
115. L. Valade, M. Bousseau, A. Gleizes and P. Cassoux, *J. Chem. Soc., Chem. Commun.*, 3 (1983) 110.
116. C.T. Vance, R.D. Bereman, J. Bordner, W.E. Hatfield and J.H. Helms, *Inorg. Chem.*, 24 (1985) 2905.
117. L. Brossard, M. Ribault, L. Valade and P. Cassoux, *Physica B+C*, 143 (1986) 378.
118. R. Kato, *Chem. Rev.*, 104 (2004) 5319.
119. S. Curreli, P. Deplano, C. Faulmann, A. Ienco, C. Mealli, M. L. Mercuri, L. Pilia, G. Pintus, A. Serpe, and E. F. Trogu, *Inorg. Chem.*, 43 (2004) 5069.
120. P.I. Clemenson, *Coord. Chem. Rev.*, 106 (1990) 171.
121. N. Greenwood, in "Chemistry of the Elements", Pergamon Press Ltd. (1986).
122. B.S. Lim, D.V. Fomitchev and R.H. Holm, *Inorg. Chem.*, 40 (2001) 4257.
123. M. Fourmigue, *Acc. Chem. Res.*, 37 (2004) 179.
124. M.D. Ward and J.A. McCleverty, *J. Chem. Soc., Dalton Trans.*, 3 (2002) 275.
125. S. Alvarez, R. Vicente and R. Hoffmann, *J. Am. Chem. Soc.*, 107 (1985) 6253.
126. J.A. McCleverty, *Prog. Inorg. Chem.*, 20 (1968) 49.
127. G.N. Schrauzer, *Acc. Chem. Res.*, 2 (1968) 72.
128. C. L. Kean and P.G. Pickup, *Chem. Commu.*, (2001) 815.
129. J.R. Andersen, V.V. Patel and E.M. Engler, *Tetrahedron Lett.*, 19 (1978) 239.
130. C. Pozo-Gonzalo, R. Berridge, P. J. Skabara, E. Cerrada, M. Laguna, S. J. Coles and M.B. Hursthouse, *Chem. Commu.*, (2002) 2408.



## **Chapter 2**

# **Experimental**



## 2.1 Experimental Techniques

### 2.1.1 Cyclic Voltammetry (CV)

Cyclic voltammetry is one of the most versatile electroanalytical techniques for the study of electroactive species. This method enables a wide potential range to be scanned rapidly, uses a variable time scale and has a good sensitivity. All of these factors, combined with ease of measurement, have resulted in extensive use of CV in the fields of electrochemistry, inorganic chemistry, organic chemistry and biochemistry.<sup>1</sup>

This technique has become very popular for preliminary electroanalytical studies of new systems.<sup>2,3</sup> It is also commonly used for the synthesis of electrically conducting polymers due to its simplicity and reproducibility.<sup>4</sup> The electrochemical synthesis of conducting polymers is achieved by oxidation of monomer units.<sup>5</sup> This method offers several benefits over the chemical synthesis such as ease of preparation or absence of catalyst. Besides, it has the advantage of producing polymeric material deposits on an electrode surface, which can subsequently be used for further experiments by electrochemical and/or spectroscopic techniques.<sup>6</sup>

In cyclic voltammetry the electrode potential is cycled, at a known sweep rate, between the limits  $E_1$  and  $E_2$  and the cell current is recorded as a function of the applied potential (Figure 2.01).<sup>7</sup>

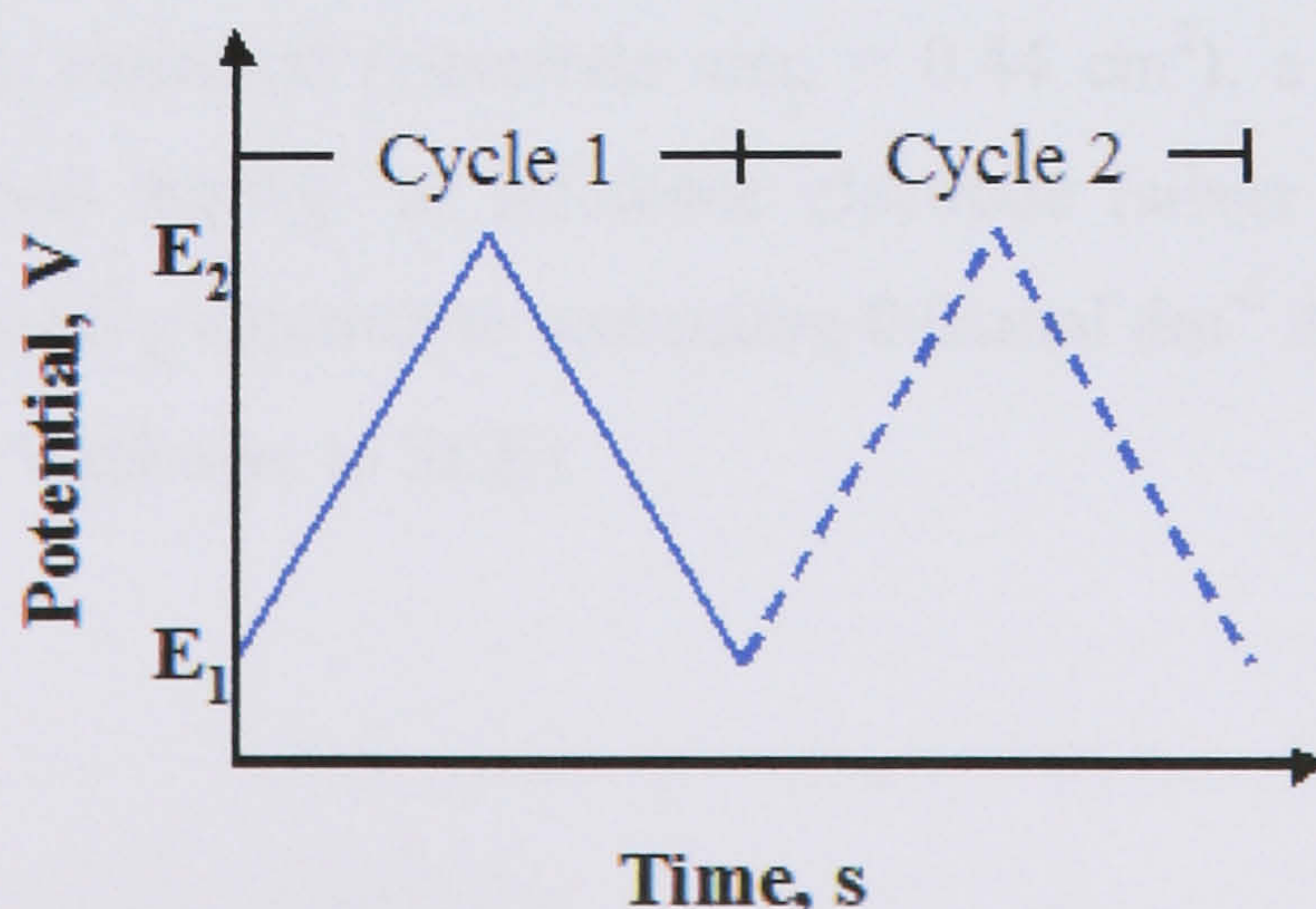


Figure 2.01 - Triangular waveform of a linear potential scan.



The obtained voltammogram is a representation of current (vertical axis) *versus* potential (horizontal axis) with current peaks due to oxidative and reductive electrochemical reactions. Since the potential varies linearly with time, the horizontal axis can also be regarded as a time axis.<sup>1</sup>

The instrumentation needed to carry out voltammetric measurements consist of a waveform generator to produce the excitation signal, a potentiostat to apply this signal to an electrochemical cell, a current-to-voltage converter to measure the resulting current, and an XY recorder to display the voltammogram.<sup>1</sup>

The potentiostat applies a chosen potential between the working electrode (WE) and the reference electrode (RE). The working electrode is the electrode at which the reaction of interest occurs and is composed of a chemically inert material, such as lead, vitreous carbon, gold or platinum.<sup>3,8</sup> The reference electrode (e.g. a saturated calomel electrode (SCE)) provides a stable and reproducible potential against which the potential of the working electrode is compared.<sup>7</sup>

A third electrode – counter or secondary electrode (CE) – is used to complete the electrical circuit and to transport the current required to sustain the electrolysis at the working electrode. The CE is usually made of an inert conducting material such as platinum wire or graphite rod.<sup>7,8</sup>

### **Experimental Procedure**

An electrochemical study of several thiophene derivatives was attempted. The experiments were performed in a three-electrode cell (Figure 2.02) using a platinum disc as the working electrode (electrode area = 0.44 cm<sup>2</sup>), a platinum foil as the counter electrode, and Ag/Ag<sup>+</sup> as reference electrode (silver wire immersed in a solution of the supporting electrolyte containing 0.01 mol dm<sup>-3</sup> AgNO<sub>3</sub>; this reference electrode lies +0.32 V relative to SCE).



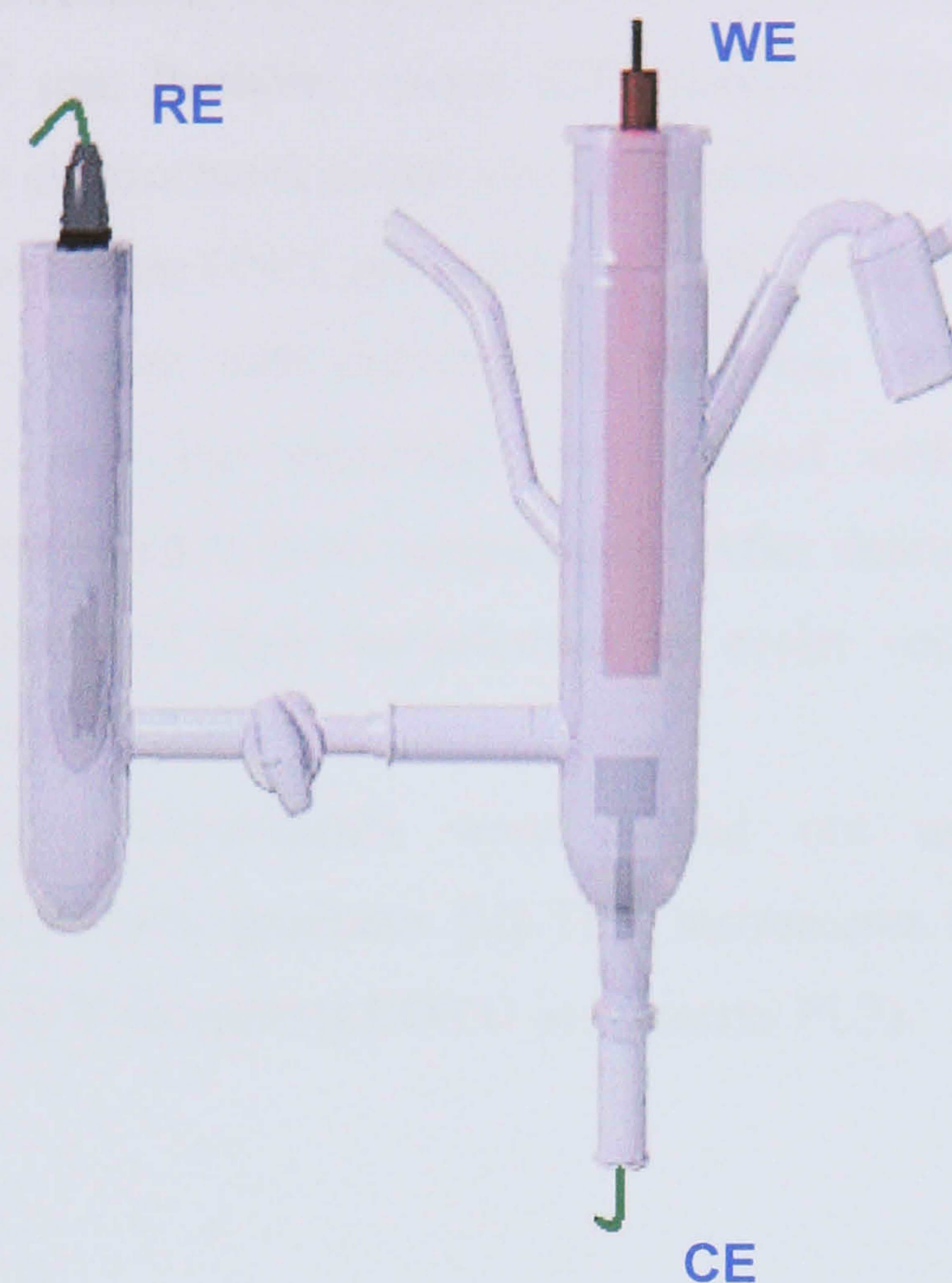


**Figure 2.02** - Schematic diagram of the electrochemical cell used in this work.

RE - reference electrode, WE - working electrode, CE - counter electrode.

Attempts to grow the polymeric films were carried out potentiodynamically by cycling the electrode potential in an electrolyte solution containing the monomer units. The electrolyte was made up of tetra-*n*-butyl ammonium hexafluorophosphate (TBAPF<sub>6</sub> purity > 98%, AVOCADO Research Chemicals Ltd; 0.1 mol dm<sup>-3</sup>) or tetra-*n*-butyl ammonium tetrafluoroborate (TBABF<sub>4</sub> purity > 98%, AVOCADO Research Chemicals Ltd; 0.1 mol dm<sup>-3</sup>) in acetonitrile (CH<sub>3</sub>CN - purity > 99.9%, Riedel-de H  en; stored over molecular sieves). TBAPF<sub>6</sub> and TBABF<sub>4</sub> were employed as supporting electrolytes aiming to decrease the resistance of the solution, eliminate electromigration effects, and maintain a constant ionic strength.<sup>7</sup>

Throughout the electrochemical experiments, nitrogen was used to degas the cell but, and in agreement with Tourillon *et al.*<sup>9</sup>, it was found that the polymerisation of most polythiophene derivatives was not affected by oxygen and therefore, the purging procedure was not employed in those cases.



Between measurements, the working electrode was subsequently polished with  $\text{Al}_2\text{O}_3$  (0.1 and 0.05  $\mu\text{m}$ , Buehler), rinsed with distilled water and cleaned in an ultrasonic bath. The electrochemical cell was left overnight in an acid bath (mixture 1:1 v:v of concentrated nitric  $\text{HNO}_3$  and sulphuric  $\text{H}_2\text{SO}_4$  acid), washed with distilled water, steamed in a vapour bath and dried in the oven. Prior to use, both the electrochemical cell and the electrodes were rinsed with acetonitrile. All experiments were performed at room temperature. After deposition, the films were rinsed with acetonitrile and then characterised by cyclic voltammetry in a fresh monomer-free electrolyte solution.

All voltammetry experiments were carried out using a home-made potentiostat, and a waveform generator (HI-TEK instruments PP R1). The output was plotted using an X-Y recorder (LLOYD instruments PL3).

### **2.1.2 SNIFTIRS - Subtractively Normalised Interfacial Fourier Transform Infrared Spectroscopy**

In spectroelectrochemical studies, changes induced by electrochemical processes occurring at the electrode surface are recorded. Spectroelectrochemistry consists of the combination of spectroscopic (e.g. FTIR) and electrochemical techniques such as cyclic voltammetry. This method has been widely used in the study of adsorbed species (reactants, intermediates, products) and to examine species in solution.<sup>2</sup>

In spectroelectrochemical investigations, spectroscopic changes are correlated with the oxidation/reduction level, which is varied by changing the potential of a working electrode.<sup>10</sup> Species are probed at the electrode surface and in a thin zone of solution near the surface. The infrared radiation passes through a transparent IR window and a thin layer of solution, reflects off the electrode surface, and it is detected (Figure 2.03). The solution layer between the window and the electrode must be thin (1 to 100  $\mu\text{m}$ ) as most solvents are good absorbers of IR radiation.<sup>2</sup>



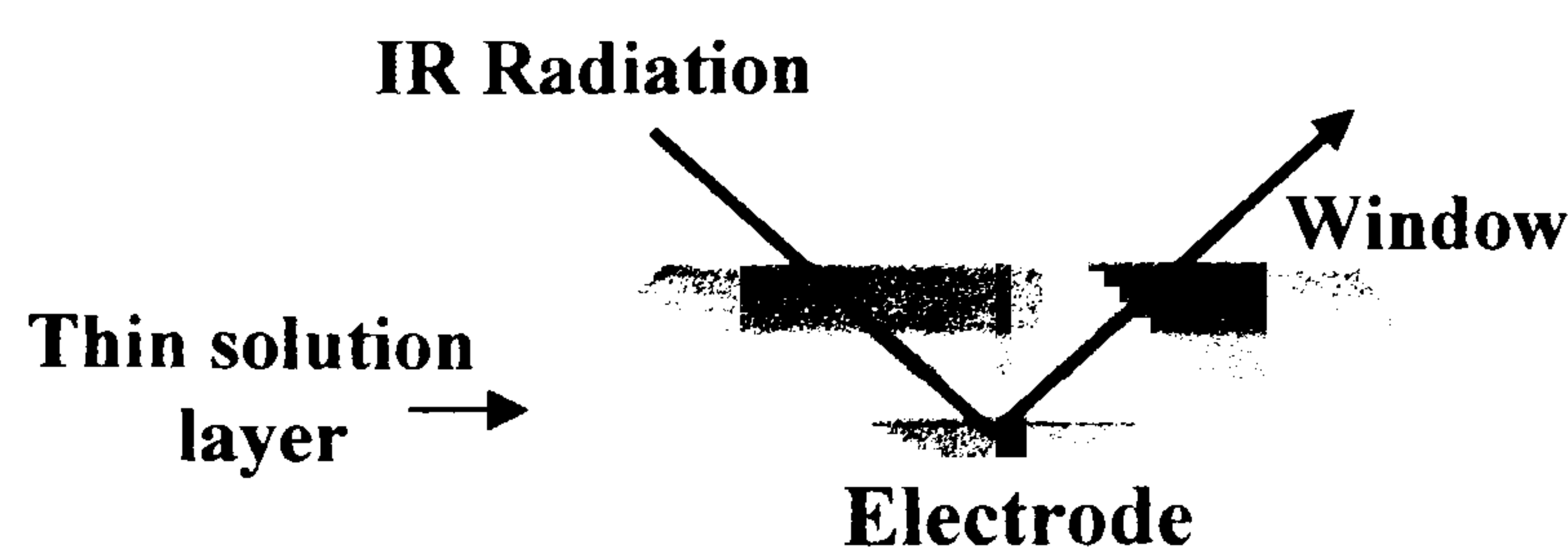


Figure 2.03 - Diagram of the external reflectance configuration.

As mentioned in Chapter One, the electrochemical oxidation or doping of a conducting polymer with a non-degenerate ground state (e.g. polythiophene) leads to the formation of polaron/bipolaron charge carriers in the polymer chains.<sup>11</sup> As a consequence, subgap energy states are formed and new electronic transitions become possible. The transition of electrons from their ground state (valence band) to the new electronic state in the bandgap appears in the IR region as a strong electronic absorption around  $4000\text{ cm}^{-1}$ .<sup>11,12,13</sup> In addition, as a conjugated polymer is doped, new and very intense infrared active vibrations (IRAV) bands appear in the infrared spectra between  $1000$  and  $1600\text{ cm}^{-1}$ .<sup>14</sup> These bands are due to the coupling of electronic excitations (polarons/bipolarons) to the lattice vibrations of the polymer leading to a reduction of the aromatic character and formation of a quinoid state.<sup>15,16</sup>

As the bond structure of a polymer is modified, the position of the IR bands frequency will change. These shifts are not easily identified by conventional spectroscopy on electrode surfaces. However, they can be detected using a more sensitive technique - Subtractively Normalised Interfacial Fourier Transform Infrared Spectroscopy (SNIFTIRS) that allows the detection of small changes.<sup>17</sup> This method has also been established as a suitable method for the *in situ* detection of either electrogenerated intermediates in the double layer or species adsorbed at the electrode surface.<sup>18</sup> By using *in situ* SNIFTIRS, researchers have achieved a better understanding of the structural changes that occur during the redox switching of conducting polymers.

In SNIFTIRS, infrared light is emitted from a source and directed into an interferometer, which modulates the light. After the interferometer, the infrared radiation is reflected at the electrode surface and the signal is then focused onto the detector. The measured signal is called the interferogram and represents the detected



intensity as a function of mirror position in the interferometer. The general apparatus for this experiment is shown in Figure 2.04.

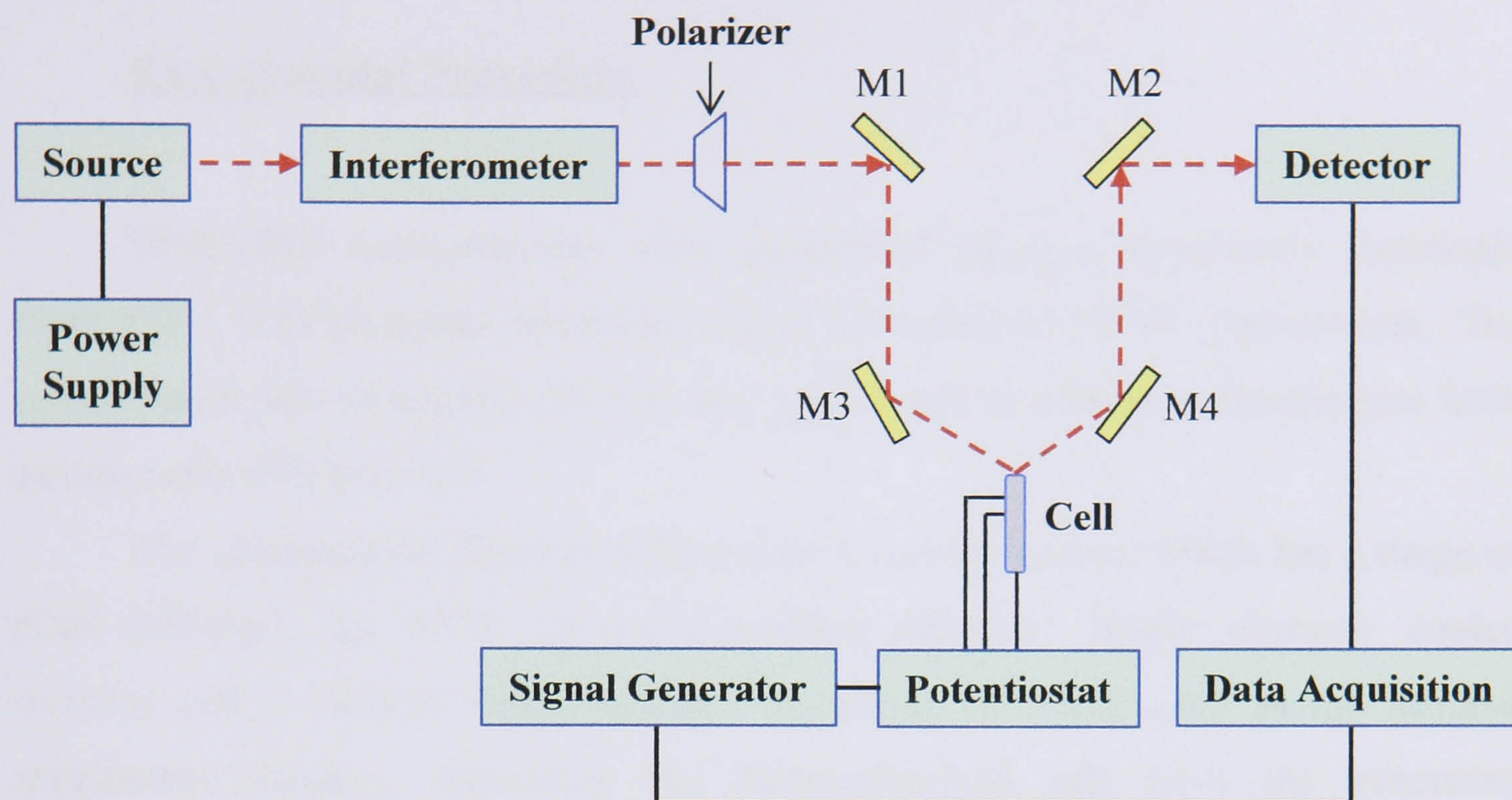


Figure 2.04 - Diagram for a SNIFTIRS equipment.<sup>2</sup>

The SNIFTIRS technique consists of collecting successive series of spectra at each of two potential limits,  $E_1$  and  $E_2$ , chosen according to the electrochemical behaviour of the system under study.  $E_1$  is the reference potential and  $E_2$  a potential of interest at which an electrochemical process occurs. The step between  $E_1$  and  $E_2$  is repeated until the desired signal-to-noise ratio is obtained. Usually it is necessary to take an average of 100 scans at each potential. Considering  $R_1$  and  $R_2$  as the reflectivity measured at  $E_1$  and  $E_2$ , it is simple to determine the relative change of reflectivity  $\Delta R/R$  by using the following expression.<sup>18,19</sup>

$$\frac{\Delta R}{R} = \frac{R_2 - R_1}{R_1} = \frac{R_2}{R_1} - 1 \quad \text{Equation 2.01}$$

The resulting difference spectrum provides information about the change in the spectral absorbance of the polymer over a selected potential range. In such a spectrum, positive and negative bands (extending upward and downward,



respectively) can be observed. Positive bands correspond to decreased absorbance at  $E_2$  whereas negative bands indicate enhanced infrared absorption at  $E_2$ .

### **Experimental Procedure**

SNIFTIRS measurements were performed using a completely evacuated Bruker IFS 113v computer controlled (Opus 2.0 software) FT-IR spectrometer. The optics bench was evacuated prior to any experiment to eliminate interference from atmospheric  $\text{CO}_2$  and  $\text{H}_2\text{O}$ .

The spectrometer operates with a silicon carbide source, which has a range of  $6000 - 100 \text{ cm}^{-1}$ , an MCT (mercury-cadmium-telluride) liquid nitrogen cooled detector and a Ge/KBr beam splitter. A silicon disc was used as the infrared transparent window, separating the electrochemical cell from the evacuated spectrometer. The instrument was setup to allow external reflection by focusing the IR beam onto the working electrode. A schematic diagram of a spectro-electrochemical cell used in the SNIFTIRS experiments is shown in Figure 2.05.



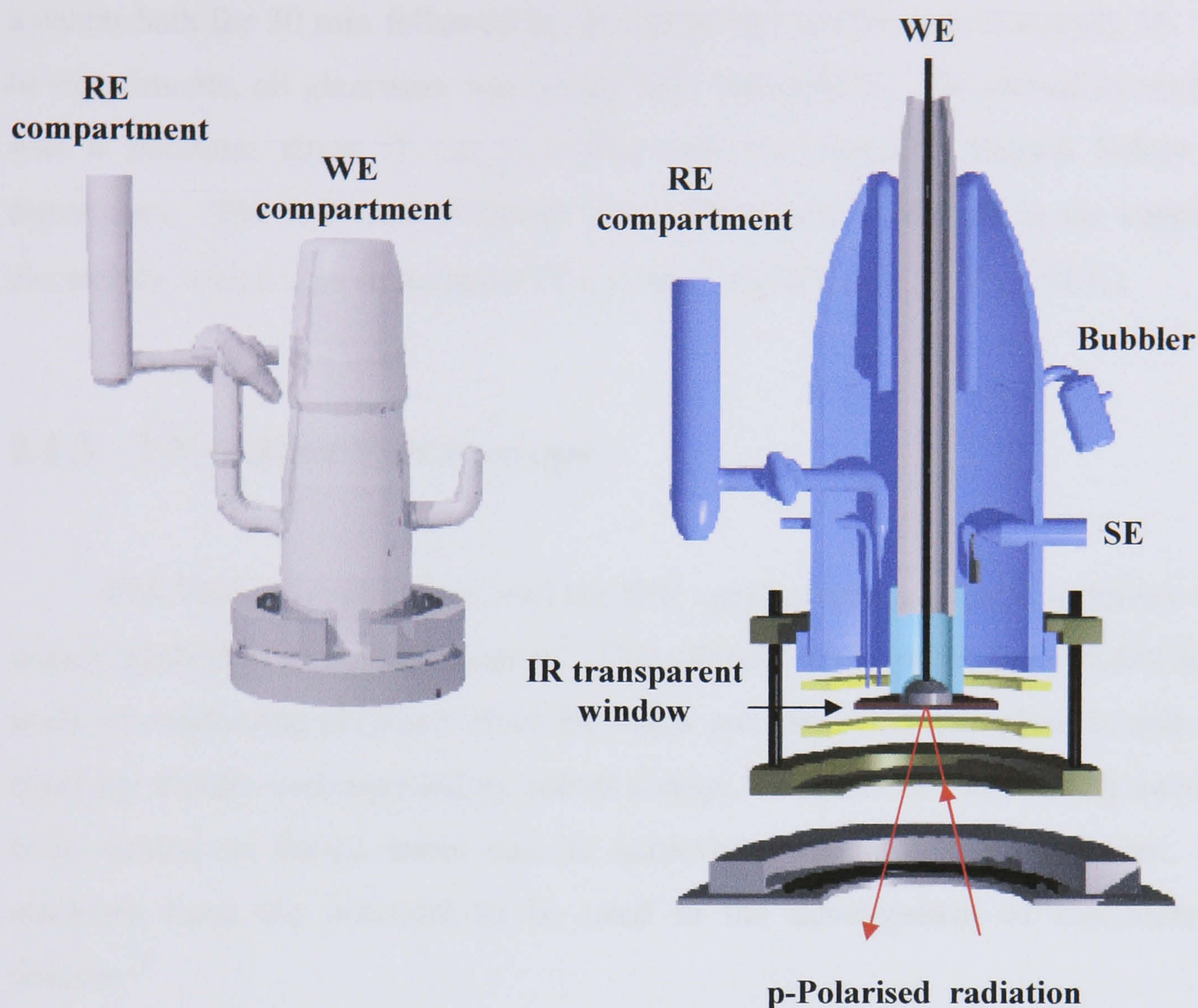


**Figure 2.05** - FTIR three-electrode glass cell and cross-section of the main compartment.

RE – reference electrode; WE – working electrode; SE – secondary electrode.<sup>20</sup>

In this cell, the working electrode was pressed against a silicon window forming a thin layer of electrolyte (1-10  $\mu\text{m}$ ) which ensures minimum absorbance from the solvent. The IR beam was then aligned onto the working electrode by adjusting the position of the electrode and the two focusing mirrors within the optics bench until a strong signal was obtained from the interferogram.

The potential was applied to the working electrode using a potentiostat, HI TEK type DT2101, connected to a waveform generator (HI-TEK instruments PP R1). The electrode potential was then allowed to stabilise before collecting the IR data. At each potential 100 spectra were taken, co-added and averaged. The resulting spectrum was then normalised according to equation 2.01.

All experiments were performed under nitrogen atmosphere in a three-electrode cell, which was cleaned in an acid bath (1:1 conc.  $\text{HNO}_3$  and conc.  $\text{H}_2\text{SO}_4$ )



overnight. Glassware was subsequently rinsed with distilled water and transferred to a steam bath for 30 min followed by drying in an oven for approximately 1h. Prior to experiments, all glassware was rinsed with acetonitrile. The secondary electrode was a platinum sheet (1 cm x 1 cm) and was carefully flamed before each experiment. The reference electrode was a silver wire immersed in the supporting electrolyte, which also contained  $0.01 \text{ mol dm}^{-3} \text{ AgNO}_3$  (+ 0.32 V vs. SCE).

### 2.1.3 UV-Visible Spectroscopy

UV-Visible spectroscopy was the first spectroelectrochemical technique to be widely applied in scientific research.<sup>7</sup> This method can be particularly useful for the study of conducting polymers since the redox processes that take place in polymeric films are usually accompanied by colour change.<sup>21</sup> Given that repetitively switching from neutral to doped states can be achieved with high colour contrast, these materials have the potential to be used in the development of electrochromic devices.<sup>19</sup>

The change in colour with the oxidation state can be explained by the existence of a spatially extended  $\pi$ -bonding system in conjugated polymers that gives rise to electronic transitions in the uv-vis-nir region of the spectrum.<sup>10,22</sup> In the neutral state, the colour is determined by the bandgap of the polymer, the  $\pi$ - $\pi^*$  absorption peak wavelength. Upon doping (removal or addition of electrons), new electronic states can be formed in the bandgap, giving rise to optical absorption energies lower than the original bandgap.<sup>23</sup>

In the polythiophene family of compounds, the maximum of the  $\pi$ - $\pi^*$  transition peak is dependent of the type of substituents and the length of the polymeric chain. In this category of conducting polymers, with a non-degenerate ground state, the charge introduced using doping can be stored in the form of polarons and bipolarons. The creation of these two states results in a substantial change of the electronic spectrum of the polymer which involves bleaching of the  $\pi$ - $\pi^*$  transition peak with simultaneous growth of bands in the lower energy part of the spectrum associated with polarons and/or bipolarons.<sup>23,24</sup> The allowed electronic



transitions for polaronic (three transitions) and bipolaronic (two transitions) states are indicated in the following figure.<sup>6,25</sup>

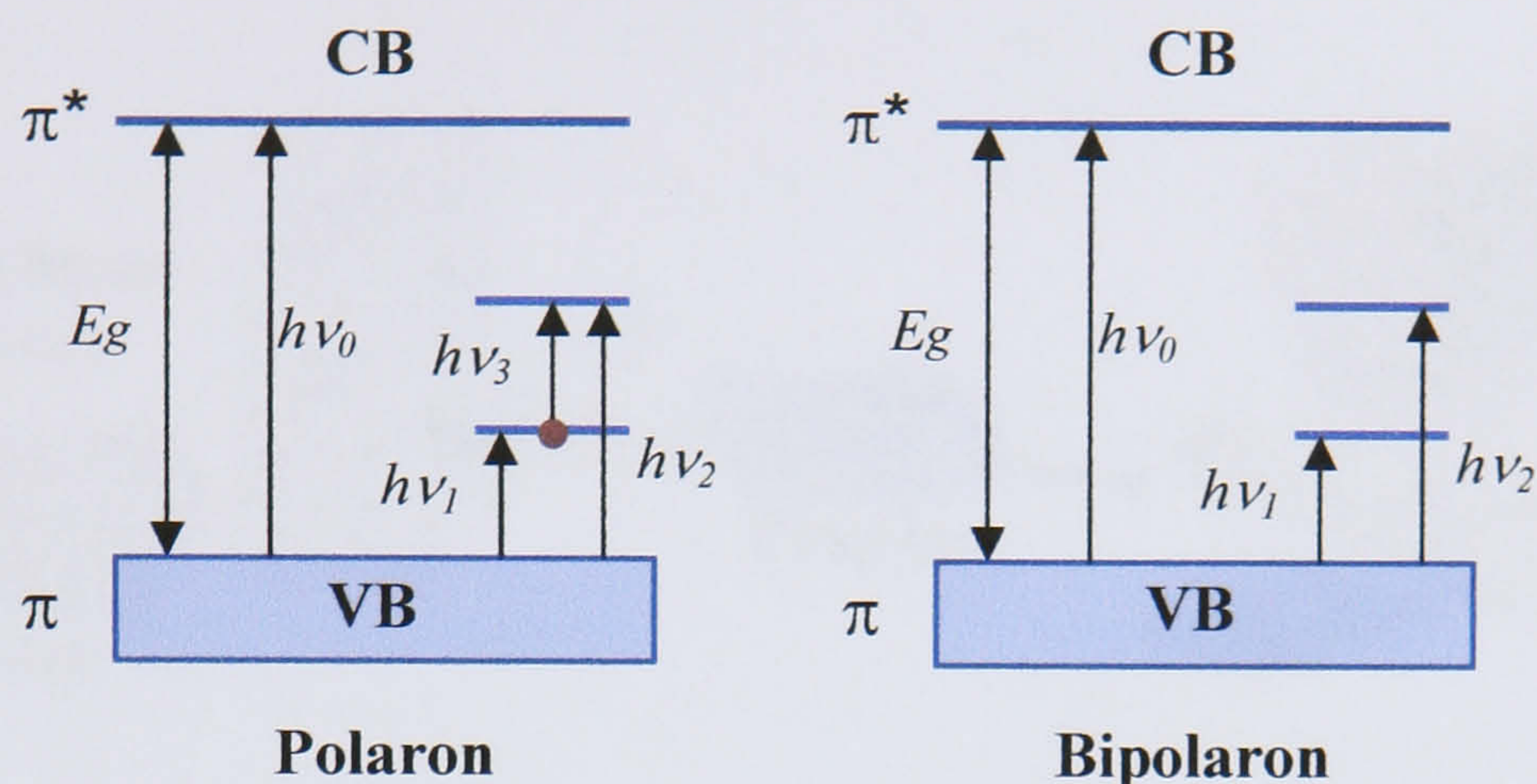


**Figure 2.06** - Band diagram showing the gap state and allowed transitions; CB – conduction band, VB – valence band.

In Figure 2.06,  $h\nu_1$  and  $h\nu_2$  correspond to transitions from the HOMO to the subgap levels and  $h\nu_3$  to the transitions from the lower to the higher subgap level. In the case of the bipolarons, this transition is forbidden, since the lower subgap level is not occupied.<sup>24,26</sup>

### Experimental Procedure

*In situ* UV-Visible spectroelectrochemical measurements were performed on polymeric films previously grown on an indium-tin oxide (ITO) coated glass electrode. A conventional three-electrode electrochemical quartz cell was used to carry out these studies. Prior to each experiment, the UV-vis spectrum of an uncoated ITO electrode immersed in the electrolyte solution was taken and used as reference. Subtracting the reference spectrum from the spectrum of the polymer coated electrode allowed the electrolyte absorbance to be accounted for.

The light beam was focused on the electrode using a lens attached to the end of an optical fibre. The transmitted beam was collected using another optical fibre which carried the light to a spectrograph (Oriel MS125 1/8) fitted with a grating (600 lines per mm) and a photodiode array detector.



A diagram of the UV-Visible set-up used to perform spectroelectrochemical measurements can be seen in Figure 2.07.

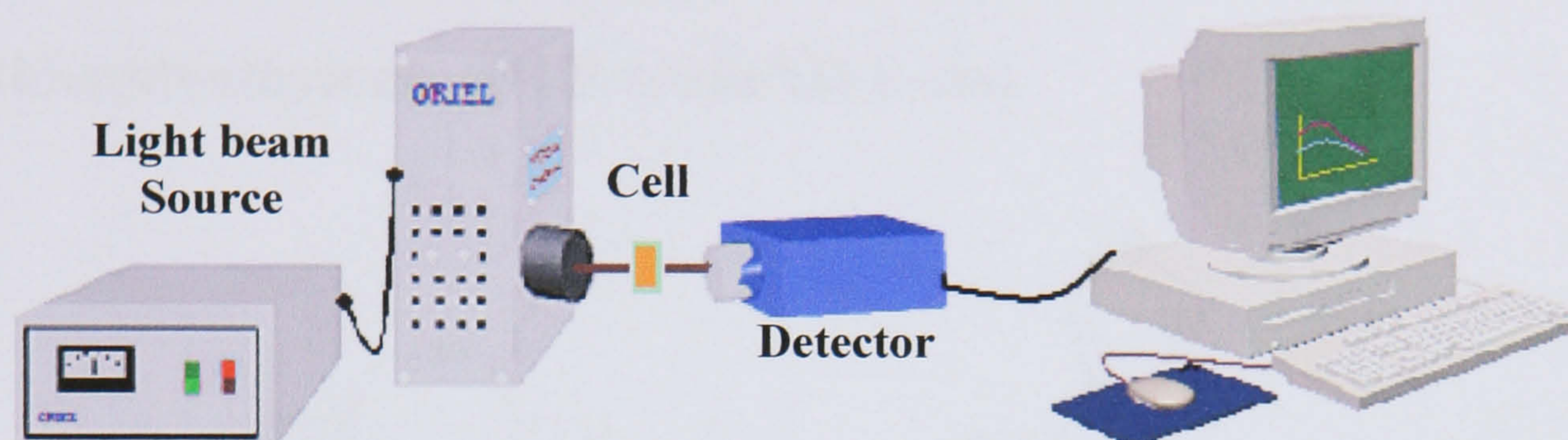


**Figure 2.07** - Schematic diagram of the UV-Visible set-up.

Measurements were conducted in the accumulation mode (1000 spectra were taken at each selected potential) and the results analysed using IntaSpec for Windows version 1.02 software. Mercury and Neon lamps were used to calibrate the detector that was optimised for operation over the wavelength range 280-1250 nm.



## 2.2 Chemical Synthesis

### 2.2.1 Synthesis of *trans*-1,2-di(3-thienyl)ethylene and *cis*-1,2-di(3-thienyl)ethylene (DTE-*trans*/DTE-*cis*)

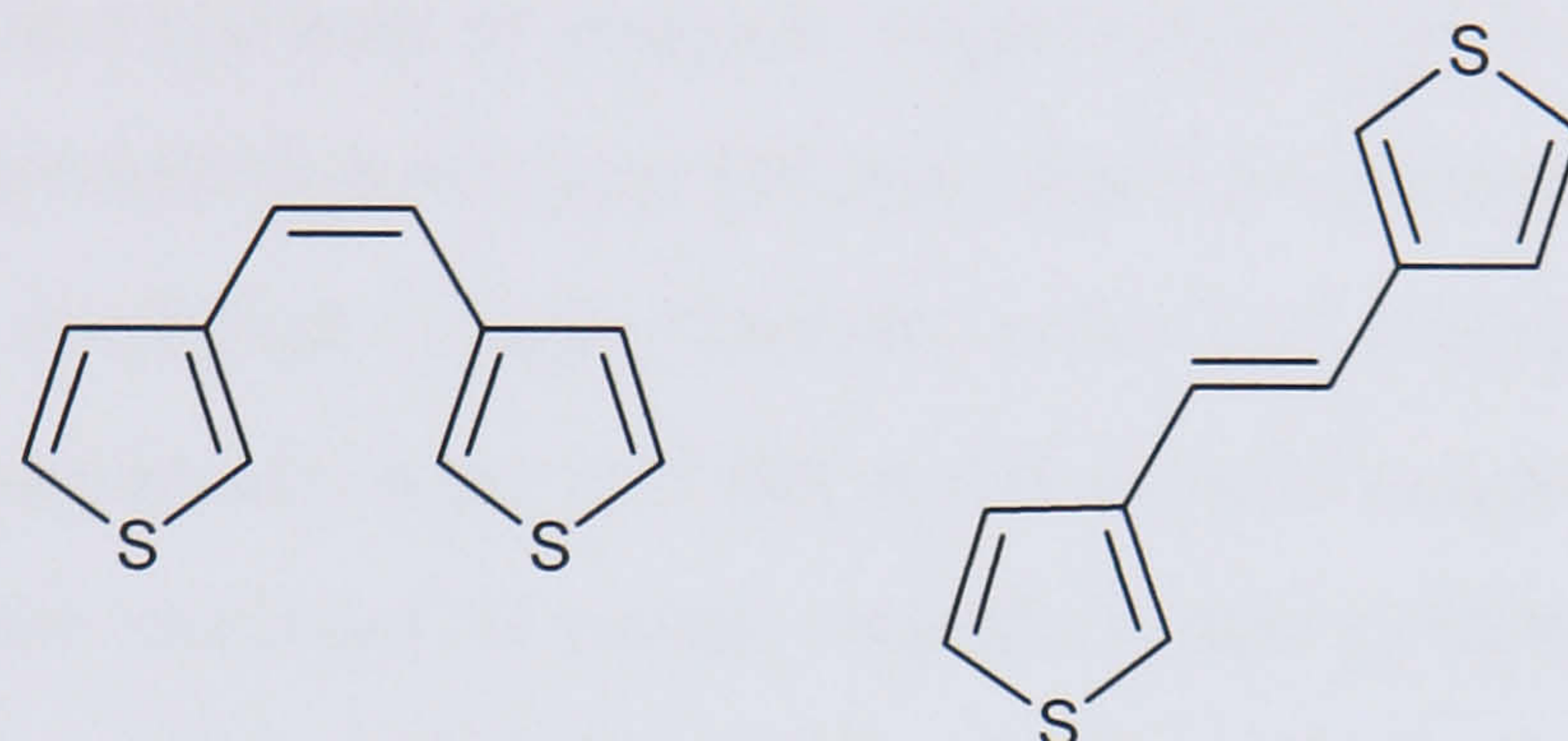
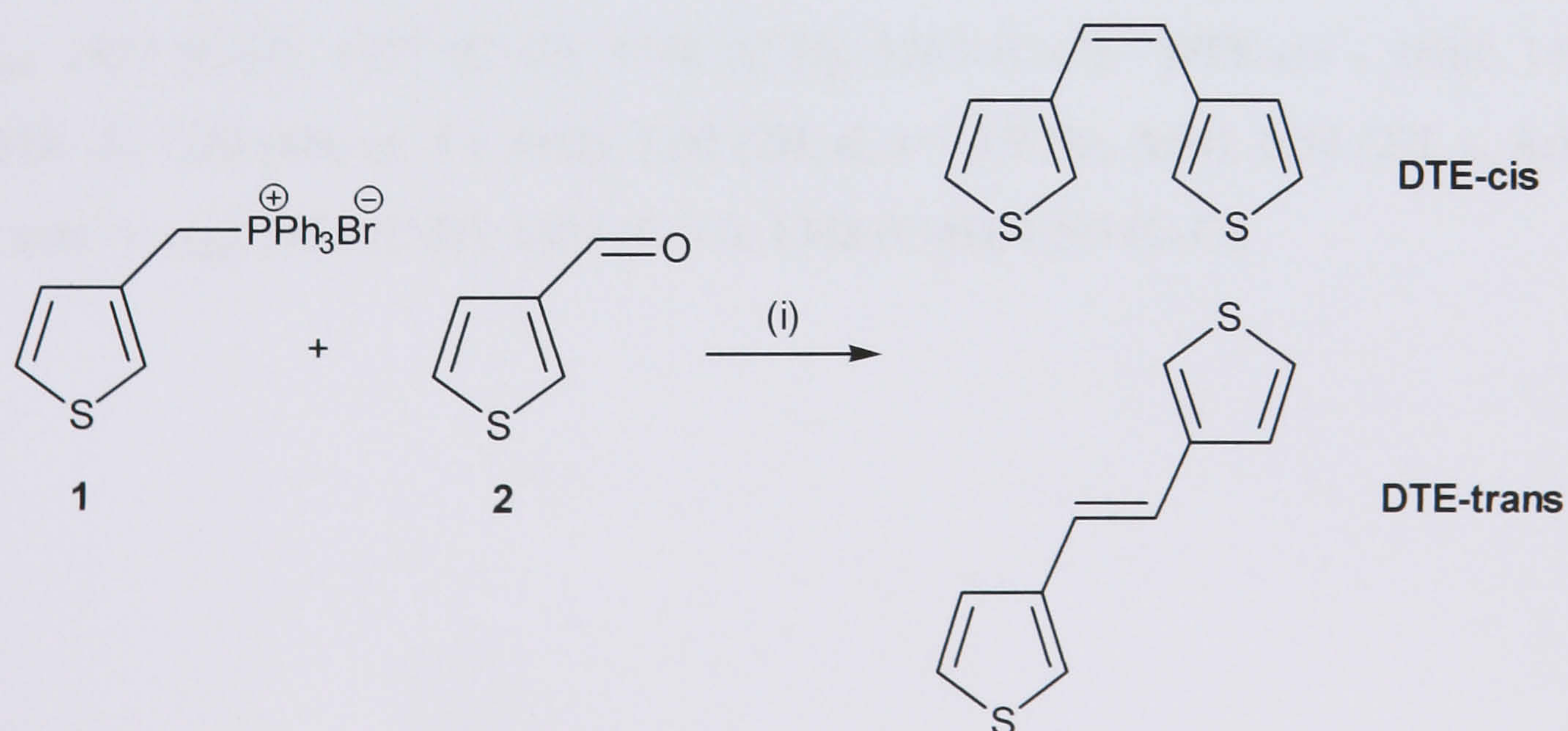


**Figure 2.08** - Structure of *cis*-1,2-di(3-thienyl)ethylene **DTE-*cis*** (left) and *trans*-1,2-di(3-thienyl)ethylene **DTE-*trans*** (right).

Dithienylethylenes can be synthesised in three steps starting with the bromination of 3-methyl-thiophene.<sup>17,27</sup> The resultant product is then reacted with triphenylphosphine in toluene to form a phosphonium salt. The final step of the synthesis, the formation of **DTE-*cis*** and **DTE-*trans***, is accomplished by a Wittig reaction as seen in Scheme 2.01.



**Scheme 2.01** - Reagents and conditions: (i) *n*-BuLi, 2 h, -78 °C.



The phosphonium salt **1** used as precursor for this synthesis was prepared within the Chemistry Department.<sup>17</sup>

To a cooled (0 °C) stirred solution of the salt **1** (3.02 g, 6.82 mmol) in tetrahydrofuran (30 ml), *n*-butyl lithium (3.51 ml, 7.54 mmol) was added and the reaction stirred for 30 minutes. The reaction was then cooled to -78 °C and compound **2** (0.97 g, 8.65 mmol) was added dropwise. This solution was stirred for 2 hours at -78 °C and allowed to warm to room temperature slowly. The reaction was quenched by the addition of water (50 ml), and was extracted with diethyl ether (3 × 50 ml). The combined organic fractions were then washed with hydrochloric acid (150 ml), sodium bicarbonate (150 ml) and dried with magnesium sulphate.

Solvents were removed *in vacuo*, and the crude products were purified by column chromatography using 3:97, 5:95, 10:90 diethyl ether:petrol as eluent. Sample vials containing  $R_f = 0.85$  (diethyl ether/petrol 5:95) were combined producing a clear oil of **DTE-cis** (0.18 g, 0.93 mmol) and sample vials combining  $R_f = 0.90$  were combined producing the white crystalline solid **DTE-trans** (0.55 g, 2.86 mmol).

The *cis:trans* ratio of this synthesis was 1:3, with an overall yield of 56%. The *trans* product was found to be the more thermodynamically stable isomer. **DTE-trans** - yield: 42%; mp 163-165 °C (lit.<sup>28</sup>, 166-167 °C); NMR:  $\delta_H$  7.32 (4H, d,  $J = 1.8$  Hz, ArH), 7.24 (2H, t,  $J = 2.2$  Hz, 2 × ArH), 6.99 (2H, s, ArH); IR ( $\text{cm}^{-1}$ ):  $\nu_{\text{max}}$  2922 (C-H), 1427 (C=C), 1348 (C-H), 1263 (C-C). **DTE-cis** - yield: 14%; NMR:  $\delta_H$  7.20 (4H, m, 4 × ArH), 7.02 (2H, d,  $J = 4.9$  Hz, ArH), 6.54 (2H, s, ArH); IR ( $\text{cm}^{-1}$ ):  $\nu_{\text{max}}$  2922 (C-H), 1427 (C=C), 1348 (C-H), 1263 (C-C).



### 2.2.2 Synthesis of 4,5-di-thiophen-3-yl-[1,3]dithiol-2-one (Th-3,3)

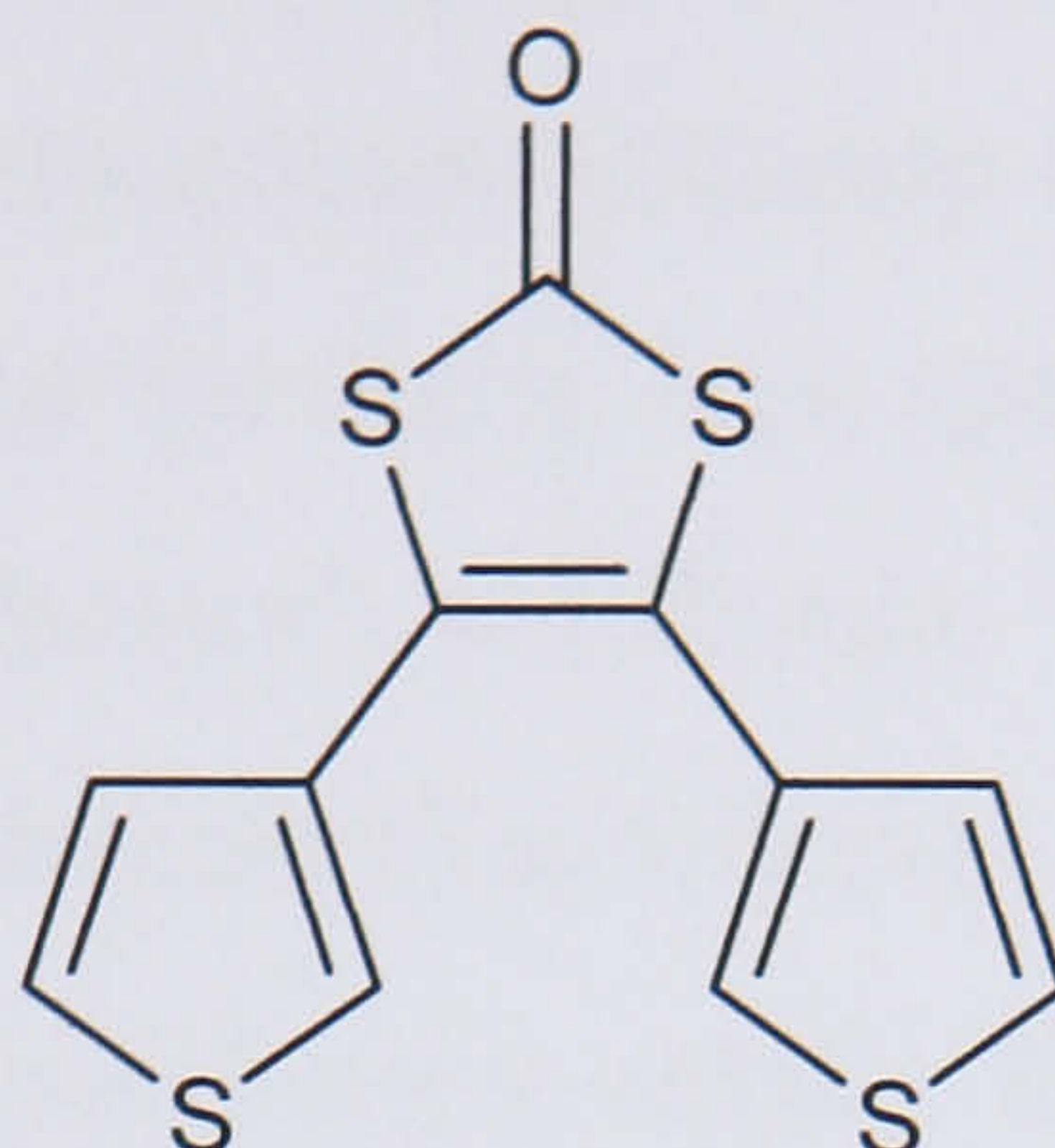
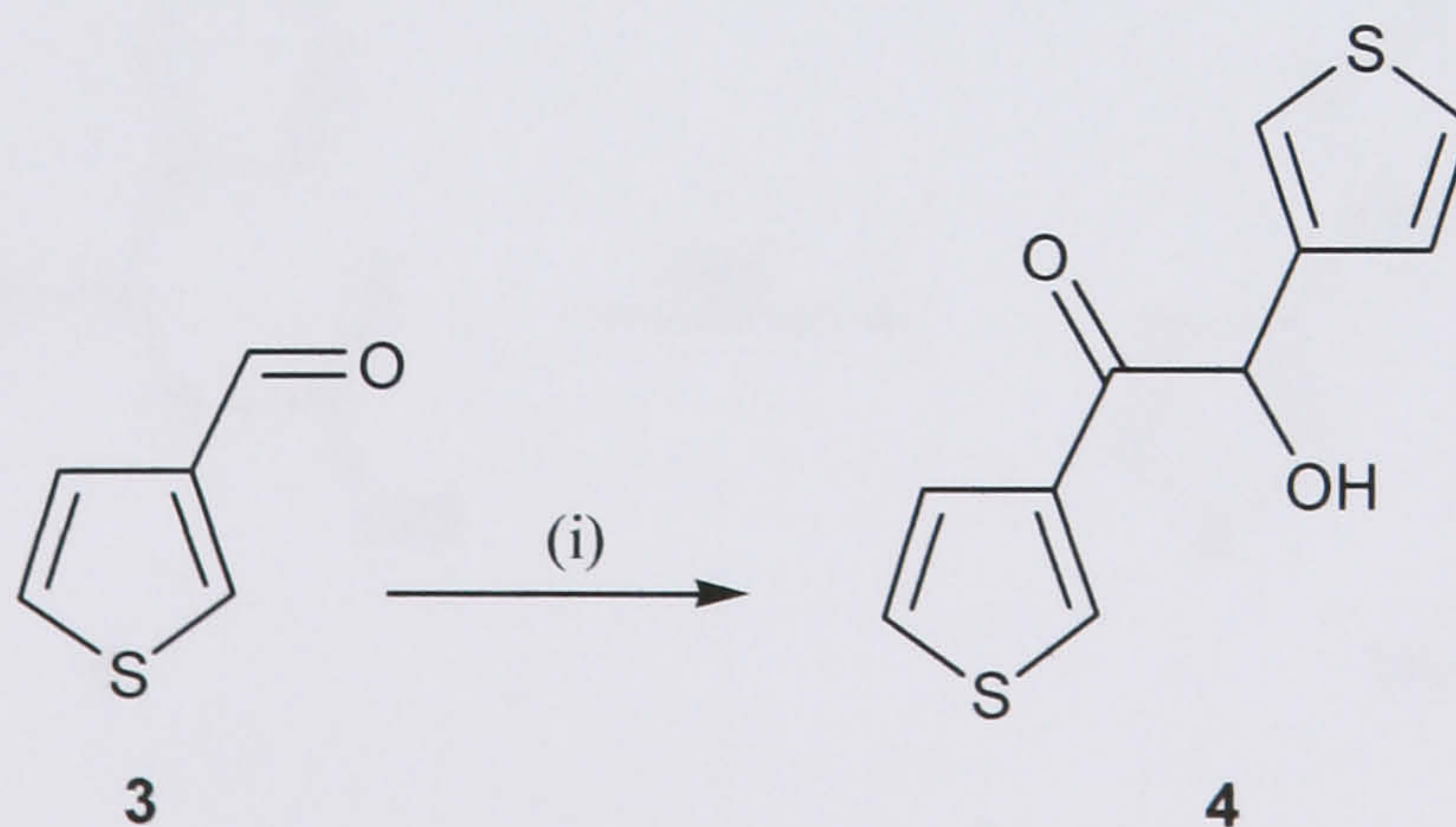


Figure 2.09 - Structure of 4,5-di-thiophen-3-yl-[1,3]dithiol-2-one Th-3,3.

The 4,5-di-thiophen-3-yl-[1,3]dithiol-2-one was first prepared by Charlton *et al.*<sup>29</sup> in 1998 as part of an on-going programme to incorporate tetrathiafulvalene (TTF) and thiophene into a single framework. The first step in the synthesis of **Th-3,3** involves the benzoin condensation of the thiophene-3-carboxaldehyde **3** (Scheme 2.02), followed by its reaction with triphenylphosphine and carbon tetrachloride to form chloride **5** (Scheme 2.03). Due to its unstable nature, this product is immediately treated with potassium ethyl xanthate to give compound **6**. The xanthate formed is then cyclised (HBr in acetic acid) resulting in the formation of **Th-3,3**.

#### Preparation of 2-hydroxy-1,2-di-thiophen-3-yl-ethanone (3,3'-theonin) 4

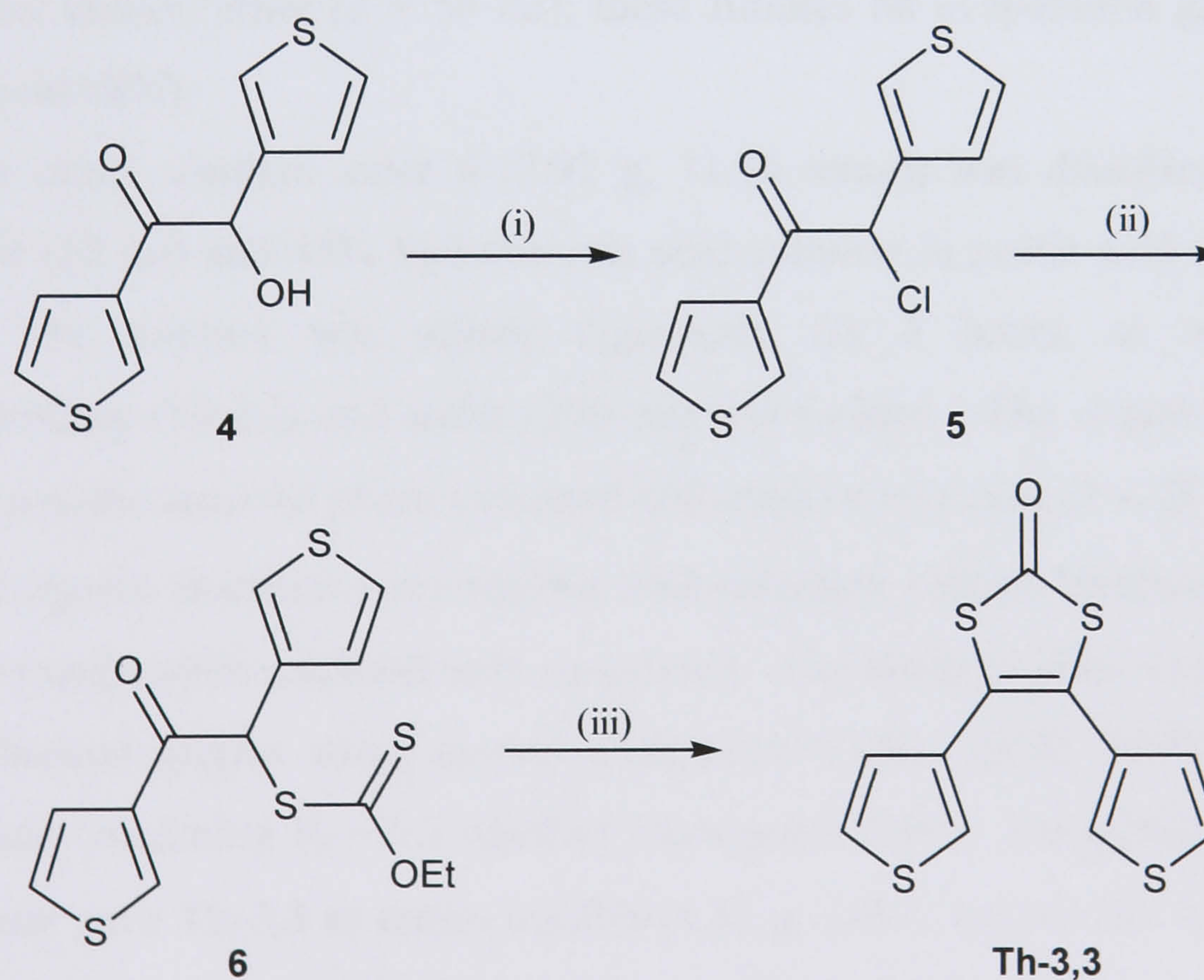


Scheme 2.02 - Reagents and conditions: (i) 3-benzyl-5-(2-hydroxymethyl)-4-methyl-1,3-thiazolium chloride,  $\text{NEt}_3$ , EtOH.



3-Thiophene carboxaldehyde **3** (25.03 g, 223.26 mmol) was dissolved in absolute ethanol (67.5 ml) and triethylamine (9.3 ml, 70.34 mmol), and 3-benzyl-5-(2-hydroxyethyl)-4-methyl-1,3-thiazolium chloride (1.21g, 4.53 mmol) were added. The reaction was heated to reflux for 2.5 h, then cooled, diluted with water (750 ml) and extracted with dichloromethane ( $3 \times 100$  ml). The combined organic fractions were washed with sodium bicarbonate ( $3 \times 100$  ml), dried (magnesium sulphate) and evaporated *in vacuo* to give a pale brown solid. The solid was recrystallised from chloroform, producing white crystals of **4** (11.81 g, 52.48 mmol, 47%): mp 108 -109 °C (lit.,<sup>17</sup> 108 °C); NMR:  $\delta_{\text{H}}$  4.38 (1H, d,  $J = 5.8$  Hz, OH), 5.86 (1H, d,  $J = 5.8$  Hz, CH), 7.01 (1H, dd,  $J = 1.2, 2.8$  Hz, CH), 7.33 (3H, m,  $3 \times$  CH), 7.53 (1H, dd,  $J = 0.9, 4.9$  Hz, CH), 8.06 (1H, dd,  $J = 1.2, 2.8$  Hz, CH); IR ( $\text{cm}^{-1}$ ):  $\nu_{\text{max}}$  3428 (O-H), 3097 (C-H), 3018 (C-H), 1667 (C=O).

### Preparation of 4,5-dithiophen-3-yl-[1,3]dithiol-2-one Th-3,3



**Scheme 2.03** - Reagents and conditions: (i)  $\text{PPh}_3$ ,  $\text{CCl}_4/\text{CH}_2\text{CH}_2$  (2:1), 24 h; (ii)  $\text{KSC(S)OEt}$ ,  $\text{Me}_2\text{CO}$ , 1 h; (iii)  $\text{HBr}$ ,  $\text{AcOH}$ , 2 h.



3,3'-theonin **4** (5.42 g, 24.19 mmol) was dissolved in dichloromethane (25 ml) and added to a solution of triphenylphosphine (12.71 g, 48.44 mmol) in carbon tetrachloride (50 ml). The reaction mixture was stirred in the dark for 24 hours at room temperature and then diluted with ether (100 ml) which caused the precipitation of a yellow solid. The solution was filtered through a silica pad and the yellow precipitate re-dissolved in dichloromethane (20 ml) and precipitated again by the sequential addition of diethyl ether (100 ml) and petroleum ether (50 ml). The supernatant layer was decanted and filtered as before and this precipitation process was repeated twice more. After evaporation of the combined filtrates, the product was purified by column chromatography using diethyl ether/petrol (30:70 collecting sample vials containing  $R_f = 0.2$ ) as eluent to give **5** as a white solid (4.23 g, yield: 71%) of sufficient purity to be used immediately in the next step.

Crude chloride **5** (4.23 g, 17.42 mmol) was dissolved in acetone (10 ml) and added to a solution of potassium ethyl xanthate (3.47 g, 21.33 mmol) in acetone (100 ml). The reaction mixture was stirred for 1 hour and then diluted with diethyl ether (200 ml). The resultant solution was filtered through a silica pad, which was washed with further diethyl ether ( $2 \times 50$  ml); these filtrates on evaporation gave crude **6** (3.92 g, yield 68%).

The crude xanthate ester **6** (3.92 g, 11.86 mmol) was dissolved in glacial acetic acid (15 ml) and 45% hydrobromic acid solution in acetic acid (15 ml) was added. The mixture was stirred vigorously for 2 hours, at which point dichloromethane (50 ml) and water (200 ml) were added. The organic phase was separated and the aqueous phase extracted with dichloromethane ( $3 \times 25$  ml) and the combined organic fractions were washed with saturated sodium bicarbonate ( $3 \times 25$  ml), dried (magnesium sulphate) and evaporated. The crude product was purified by column chromatography using diethyl ether/petrol (3:97, 10:90, 30:70) collecting sample vials containing  $R_f = 0.3$  (diethyl ether/petrol 3:97). Recrystallisation from ether/hexane gave **Th-3,3** as cream needles (1.51 g, 46%): mp 99-101 °C (lit.,<sup>17</sup> 102 °C); NMR:  $\delta_H$  6.86 (2H, dd,  $J = 4.9, 1.2$  Hz,  $2 \times$  CH), 7.24 (2H, dd,  $J = 3, 1.2$  Hz,  $2 \times$  CH), 7.29 (2H, dd,  $J = 4.9, 3.1$  Hz,  $2 \times$  H); IR ( $\text{cm}^{-1}$ ):  $\nu_{\text{max}}$  3111 (C-H), 1655 (C=O), 1632 (C=C).



### 2.2.3 Synthesis of 4,5-di-thiophen-2-yl-[1,3]dithiol-2-one (Th-2,2)

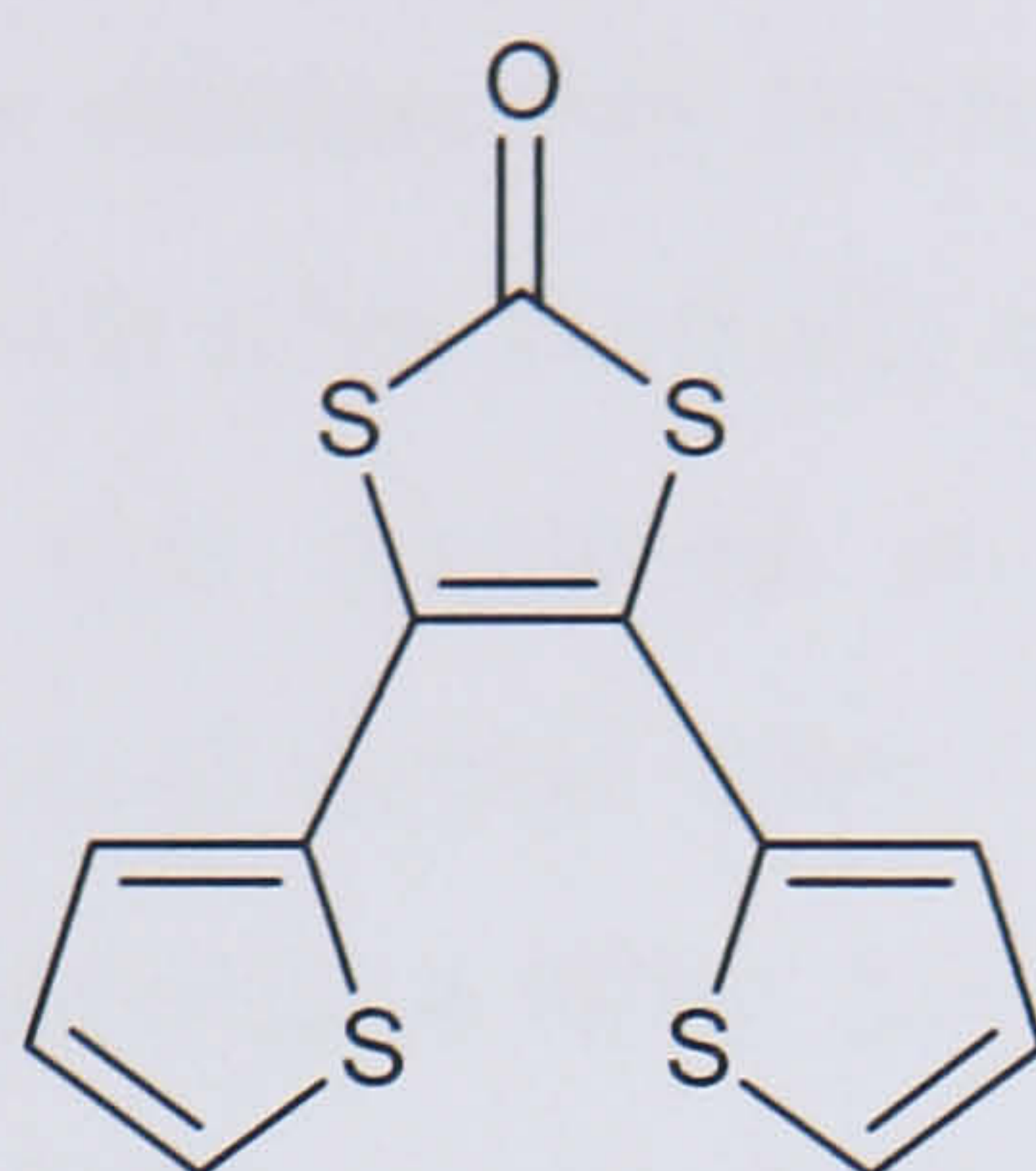
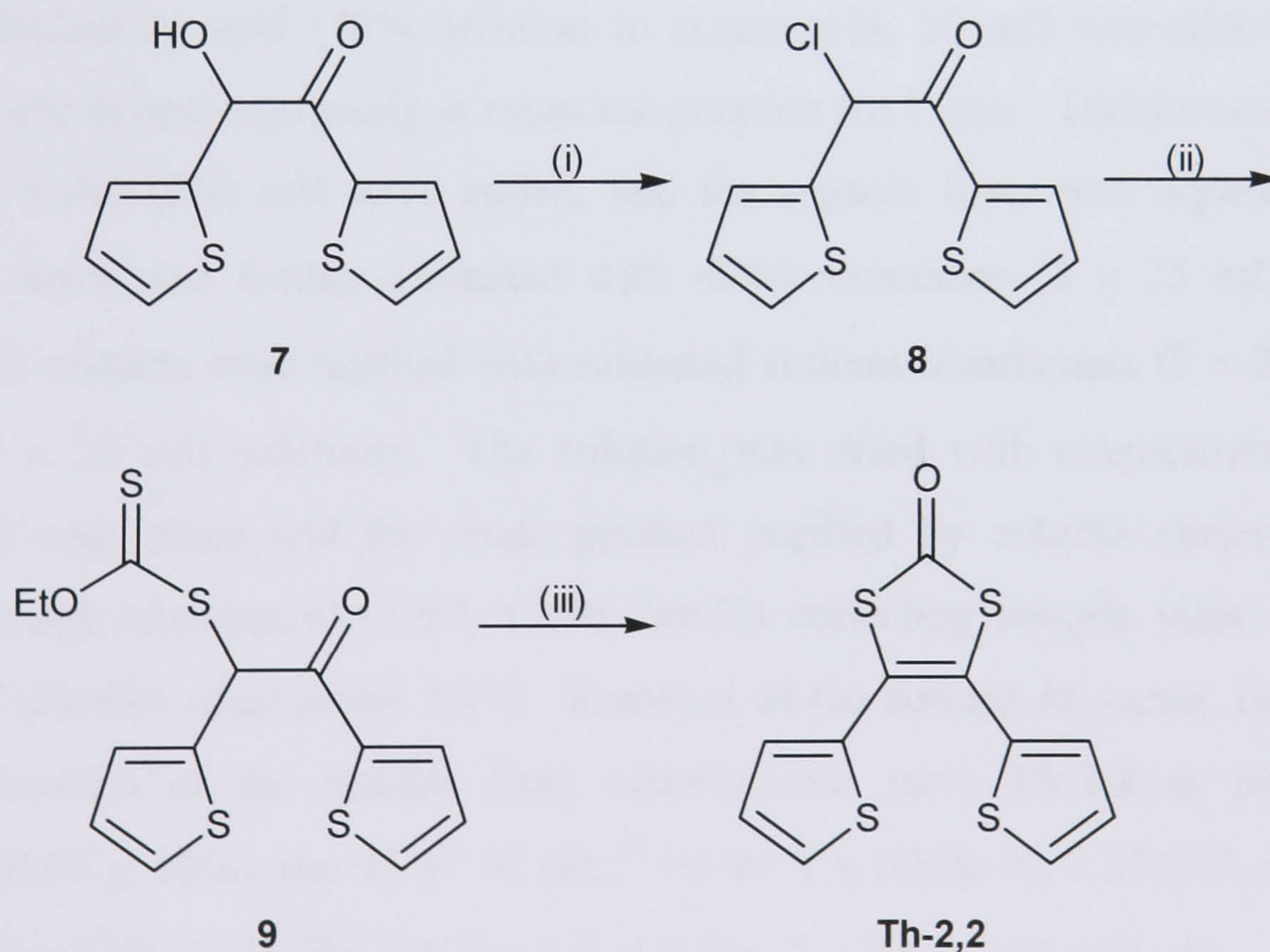


Figure 2.10 - 4,5-di-thiophen-2-yl-[1,3]dithiol-2-one **Th-2,2**.

The 4,5-di-thiophen-2-yl-[1,3]dithiol-2-one was initially synthesized in 1996 by Charlton *et al*<sup>30</sup> by reaction of the commercially available 2,2'-thionin **7** with triphenylphosphine in tetrachloromethane (Scheme 2.04). The obtained chloride **8** is then allowed to react with potassium ethyl xanthate to yield the product **9**, which on treatment with a solution of HBr in acetic acid gives **Th-2,2**.



Scheme 2.04 - Reagents and conditions: (i) PPh<sub>3</sub>, CCl<sub>4</sub>/CH<sub>2</sub>CH<sub>2</sub> (2:1), 24 h; (ii) KSC(S)OEt, Me<sub>2</sub>CO, 15 min; (iii) HBr, AcOH, 1 h.



2,2'-Theonin **7** (5.42 g, 24.19 mmol) was dissolved in a mixture of carbon tetrachloride (50 ml) and dichloromethane (25 ml). Triphenylphosphine (12.74 g, 48.55 mmol) was added, and the mixture was stirred overnight at room temperature. The solution was then diluted with ether (100 ml) and filtered through a silica plug. The remaining solid residue was dissolved in dichloromethane (20 ml) and precipitated again by the addition of diethyl ether (100 ml) and petroleum ether (50 ml). The solution was passed through a silica pad, and after adsorption onto silica the combined filtrates were further purified by column chromatography using ether/petrol (30:70 collecting sample vials containing  $R_f = 0.2$ ) as eluent to give **8** as a yellow oil (4.31 g, yield: 73%) which was used immediately in the next step.

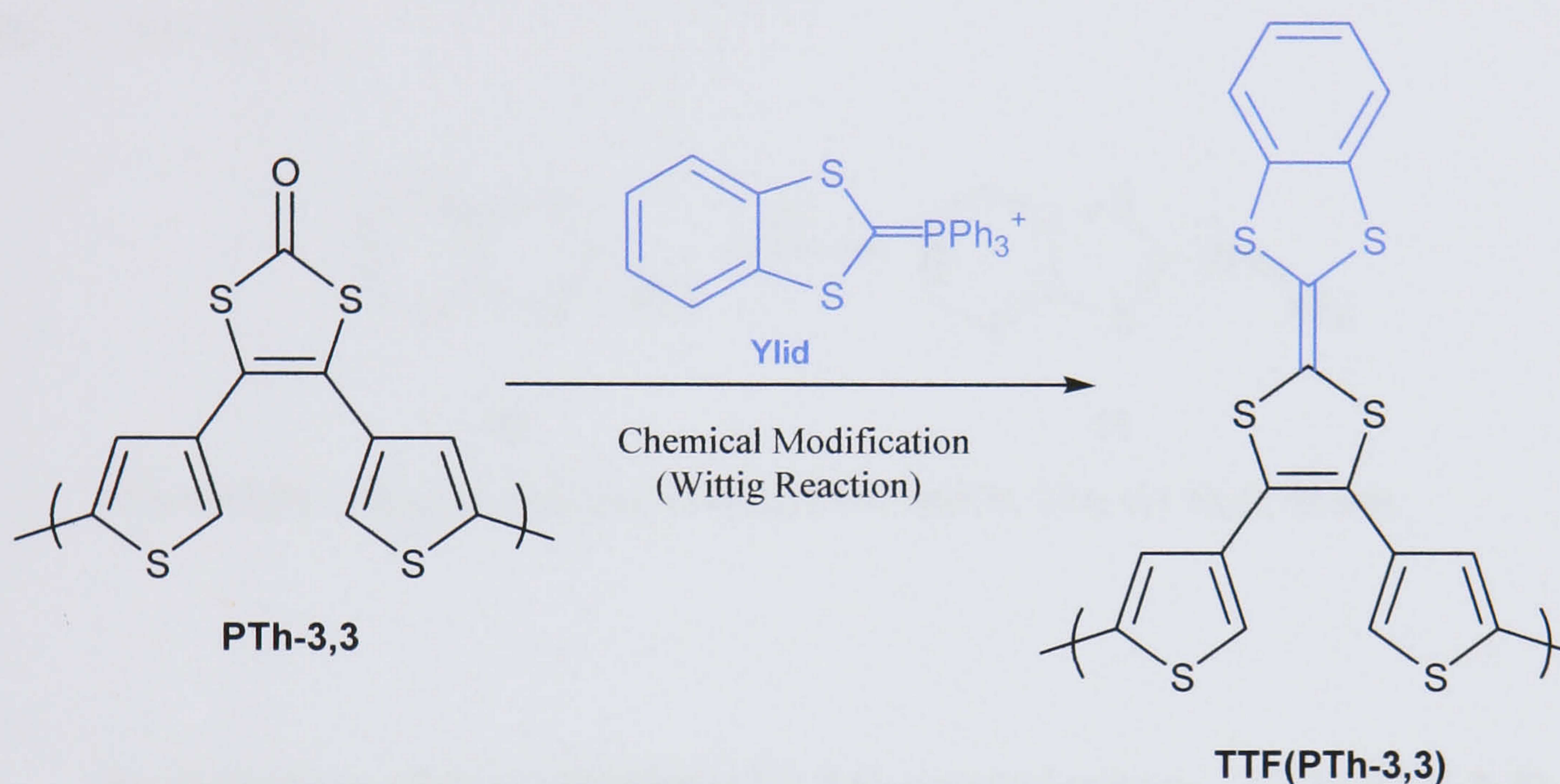
Chloride **8** (4.31 g, 17.73 mmol) was dissolved in acetone (20 ml), and potassium *o*-ethyl xanthate (3.12 g, 19.63 mmol) was added. After the mixture was stirred at room temperature for 15 min, ether (150 ml) was added and the solution was filtered through a silica pad, which was washed with further diethyl ether ( $2 \times 50$  ml). These filtrates on evaporation gave the yellow oil **9** (3.26 g, yield 56%).

Xanthate ester **9** (3.26 g 9.88 mmol) was dissolved in glacial acetic acid (10 ml), hydrobromic acid (45% solution in acetic acid, 20 ml) was added, and the mixture was stirred vigorously at room temperature for 1 hour. Dichloromethane (50 ml) and water (200 ml) were added, and the organic layer was separated. The aqueous layer was further extracted with dichloromethane ( $3 \times 25$  ml), and the combined extracts were washed with saturated sodium bicarbonate ( $3 \times 25$  ml) and brine ( $2 \times 20$  ml) solutions. The solution was dried with magnesium sulphate, adsorbed onto silica and the crude product purified by column chromatography using diethyl ether/petrol (3:97, 10:90, 30:70) collecting sample vials containing  $R_f = 0.3$  (diethyl ether/petrol 3:97). Removal of the solvent *in vacuo*, followed by recrystallisation of the residue from ether/hexane, gave **Th-2,2** as pale yellow needles (0.97 g, 32%): mp 95-97 °C (lit.,<sup>31</sup> 93-95 °C); NMR:  $\delta_H$  7.37 (2H, dd,  $J = 5.2, 1.2$  Hz,  $2 \times$  CH), 7.10 (2H, dd,  $J = 3.7, 1.2$  Hz,  $2 \times$  CH), 7.02 (2H, dd,  $J = 5.2, 3.7$  Hz,  $2 \times$  H); IR ( $\text{cm}^{-1}$ ):  $\nu_{\text{max}}$  3112 (C-H), 1660 (C=O), 1632 (C=C).



### 2.2.4 Solid-state modification of electrochemically synthesised poly-4,5-di-thiophen-3-yl-[1,3]dithiol-2-one (PTh-3,3)

After the electrochemical growth of PTh-2,3, PTh-3,3 and PTh-2,2 films, their modification by *in situ* reaction was attempted as shown in the following reaction scheme (exemplified for PTh-3,3):



**Scheme 2.05** - Reactional scheme for *in situ* modification of the polythiophene dithiolenes, deposited at an electrode surface.

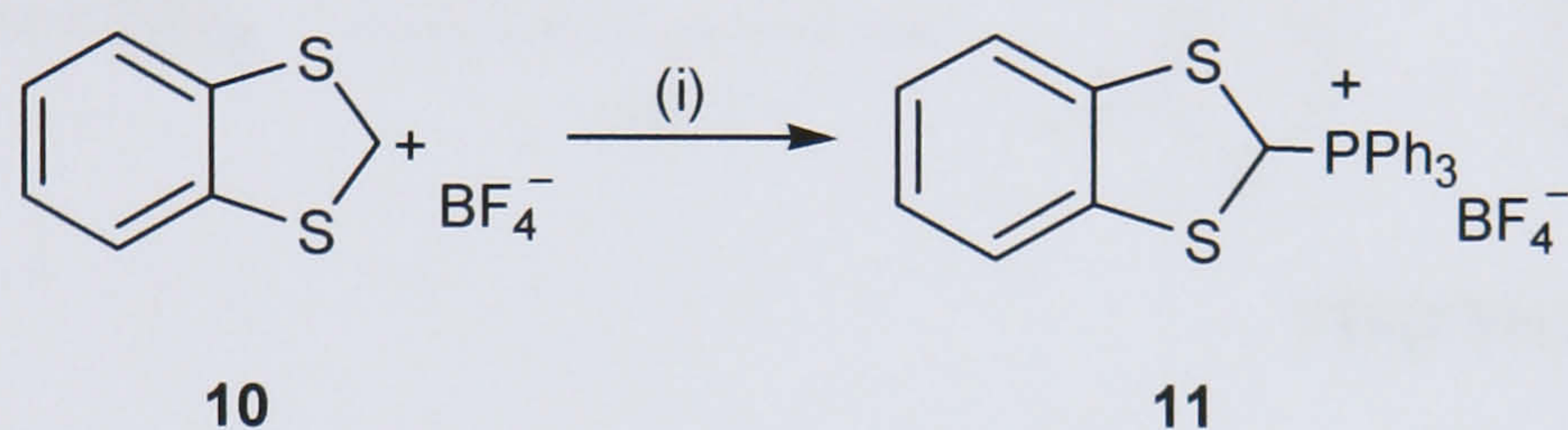
The reaction was performed using Wittig conditions: an ylid intermediate, generated from the action of *n*-BuLi on phosphorane (benzo[1,3] dithiol-2-yl-triphenyl-phosphonium tetrafluoroborate), reacts with the polymeric film deposited on the electrode.<sup>17</sup> A detailed description of the synthetic procedure is given in the following pages.

#### Preparation of benzo [1,3] dithiol-2-yl-triphenyl-phosphonium tetrafluoroborate 11

Following the procedure reported by Ishikawa *et al.*<sup>32</sup> for the synthesis of phosphonium salts, triphenylphosphine (0.95 g, 3.62 mmol, in excess) was added to a



solution of 1,3-benzodithiol-2-ylum tetrafluoroborate **10** (0.75g, 3.09 mmol) in acetonitrile (30 ml) and stirred for 30 hours under nitrogen. Dry ether (70 ml) was then added to the solution and the reaction mixture stirred for 30 min which precipitated the product **11** (1.34 g, 2.67 mmol, 87%). This compound was filtered from the reaction, washed with diethyl ether and dried under high vacuum for 24 hours. Mp 209-211 °C (lit.,<sup>32</sup> 211.5-212.5 °C); NMR:  $\delta_{\text{H}}$  6.26 (15H, m, PPh<sub>3</sub>), 5.41 (4H, m, ArH), 3.38 (1H, s, CH); IR (cm<sup>-1</sup>):  $\nu_{\text{max}}$  3069 (C-H), 1439 (C=C), 1064 (BF<sub>4</sub><sup>-</sup>), 945 (C-S).

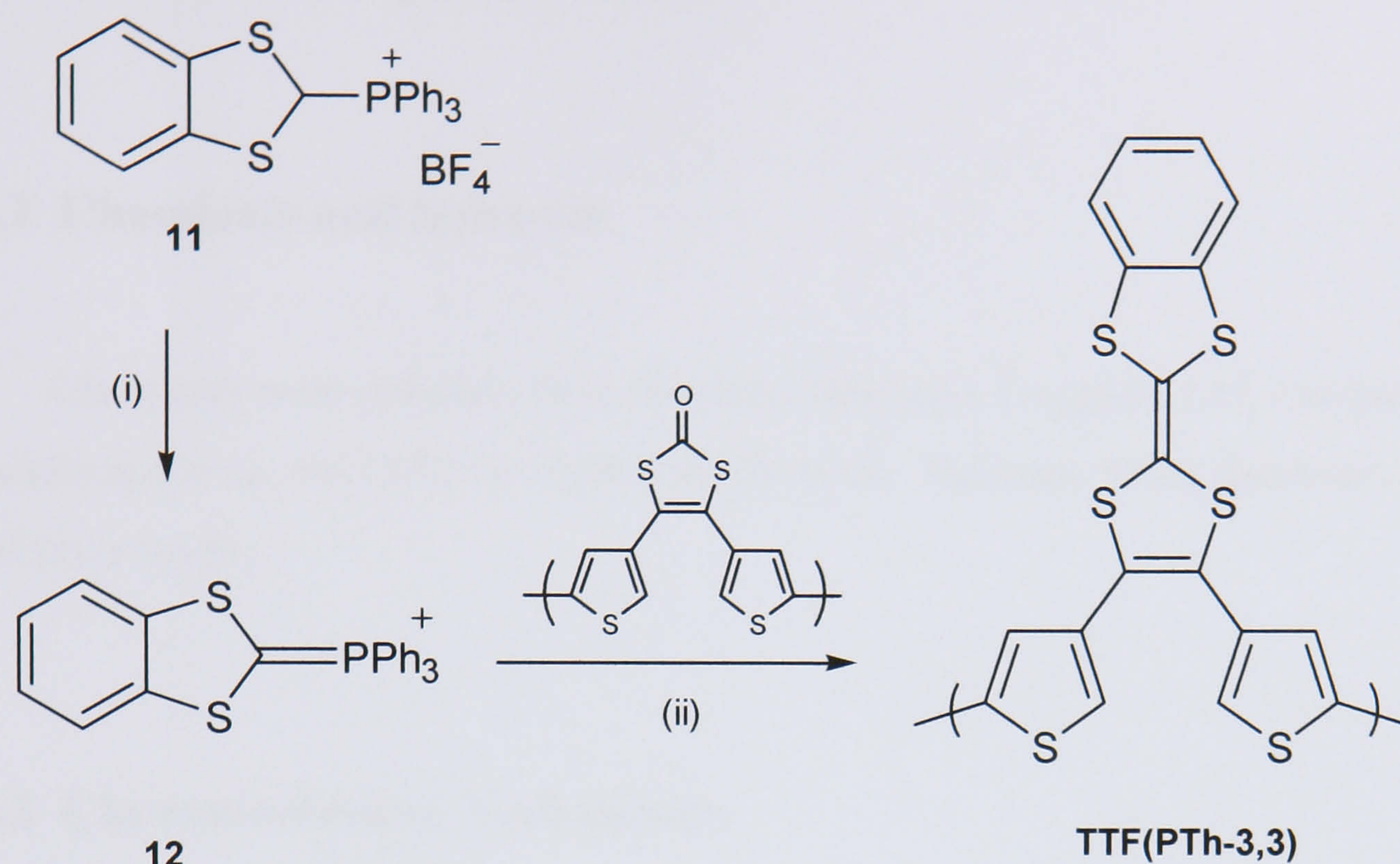


**Scheme 2.06** - Reagents and conditions: (i) PPh<sub>3</sub>, MeCN, 30 h, dry Et<sub>2</sub>O, 30 min.

### Preparation of the substituted TTF-polythiophene TTF(PTh-3,3)

The previously synthesised benzo [1,3] dithiol-2-yl-triphenyl-phosphonium tetra-fluoroborate (0.32g, 0.64 mmol) **11** was dissolved in dry ether (20 mL) at 0° C and stirred for 10 minutes. To produce the ylid **12**, *n*-BuLi (0.51 mL, 0.8 mmol) was added dropwise to this solution at 0 °C under stirring for 10 minutes (Scheme 2.6, step i). The electrode, with the polymer **PTh-3,3** deposited at its surface, was then introduced (under inert conditions) into the ylid solution and left overnight, allowing the Wittig reaction to proceed as the temperature slowly rose to room temperature (Scheme 2.07, step ii).





**Scheme 2.07** - Reagents and conditions: (i) dry  $\text{Et}_2\text{O}$ ,  $n\text{-BuLi}$ ,  $0\text{ }^\circ\text{C}$ ; (ii) **PTh-3,3**, 24 h.

The now modified polymer was carefully washed with acetonitrile to remove any traces of unreacted ylide and was afterwards characterised electrochemically.

This experimental procedure was also followed to attempt the *in situ* solid-state modification of **PTh-2,3** and **PTh-2,2**.



## 2.3 General Experimental

### 2.3.1 Chemicals and Solvents

Chemicals were obtained from Aldrich Chemicals Company Ltd, Lancaster or Avocado and were used without further purification. Solvents, when necessary, were dried prior to use.

### 2.3.2 Characterisation Techniques

#### Nuclear Magnetic Resonance (NMR)

NMR spectra for routine samples were recorded in CDCl<sub>3</sub> using a Bruker AC250 Spectrometer (<sup>1</sup>H-250 MHz) (s = singlet, bs = broad singlet, d = doublet, t = triplet, q = quartet, dd = doublet of doublets, dt = doublet of triplets, m = multiplet).

#### Infrared Spectroscopy (IR)

IR spectra were recorded on a Bruker Tensor 27 Spectrometer. Solid samples were recorded as a KBr disc or dissolved in chloroform.

#### Melting Point Measurements

Melting points were recorded on a Gallenkamp melting point apparatus.



## 2.4 References

1. P. T. Kissinger and W. R. Heineman, *J. Chem. Ed.*, 60 (1983) 702.
2. A.J. Bard and L.R. Faulkner, in "Electrochemical Methods - Fundamentals and Applications", John Wiley & Sons, 2nd ed., New York, (2000).
3. J. Wang, in "Analytical Electrochemistry", Wiley-Vch, 2nd ed., New York, (2000).
4. M. Gerard, A. Chaubey and B.D. Malhotra, *Biosens. Bioelec.*, 17 (2002) 345.
5. P. Marque, J. Roncali and F. Garnier, *J. Electroanal. Chem.*, 218 (1987) 107.
6. H.S. Nalwa, ed., "Handbook of organic conductive molecules and polymers Conductive polymers: Synthesis and electrical properties", Vol. 2, J. Wiley & Sons Ltd., UK, (1997).
7. D. Pletcher, R. Greff, R. Peat, L. M. Peter and J. Robinson, in "Instrumental Methods in Electrochemistry", Halsted Press, Southampton, (1985).
8. A. Charlton, Ph.D. Thesis, University of Wales, Bangor (1994).
9. G. Tourillon and F. Garnier, *J. Electrochem. Soc.*, 130 (1983) 2042.
10. H.S. Nalwa, ed., "Handbook of organic conductive molecules and polymers – Conductive polymers: Spectroscopy and Physical Properties", Vol. 3, J. Wiley & Sons Ltd., UK, (1997).
11. E. Lankinen, G. Sundholm, P. Talonen, T. Laitinen and T. Saario, *J. Electroanal. Chem.*, 447 (1998) 135.
12. B. Rasch and W. Vielstich, *J. Electroanal. Chem.*, 370 (1994) 109.
13. M. Pohjakallio, G. Sundholm and P. Talonen, *J. Electroanal. Chem.*, 406 (1996) 165.
14. H. Neugebauer, *J. Electroanal. Chem.*, 563 (2004) 153.
15. M. J. Nowak, S. D. D. V. Rughooputh, S. Hotta and A. J. Heeger, *Macromolecules*, 20 (1987) 965.
16. C. Ehrendorfer, H. Neugebauer, A. Neckel and P. Bauerle, *Synth. Met.*, 55 (1993) 493.
17. S. J. Roberts-Bleming, Ph.D. thesis. University of Wales, Bangor (2001).
18. R. J. Gale, in "Spectroelectrochemistry, Theory and Practice", Plenum Press (1988).



19. C. Kvarnstrom, H. Neugebauer, S. Blomquist, H.J. Ahonen, J. Kankare and A. Ivaska, *Electrochim. Acta*, 44 (1999) 2739.
20. D.N. Tito, Ph.D. Thesis, University of Wales, Bangor (2005).
21. G. Tourillon and F. Garnier, *J. Electroanal. Chem.*, 161 (1984) 51.
22. S. Hotta, S. Rughooputh, A.J. Heeger and F. Wudl, *Macromolecules*, 20 (1987) 212.
23. T.A. Skotheim, ed., "Handbook of Conducting Polymers", Vol. 1, Marcel Dekker Inc., New York, (1986).
24. M.R. Fernandes, J.R. Garcia, M.S. Schultz and F.C. Nart, *Thin Solid Films*, 474 (2005) 279.
25. H.S. Nalwa, ed., "Handbook of organic conductive molecules and polymers – Conductive polymers: Synthesis and electrical properties", Vol. 2, J. Wiley & Sons Ltd., UK, (1997).
26. M. Onoda, T. Iwasa, T. Kawai and K. Yoshino, *J. Phys. D: Appl. Phys.*, 24 (1991) 2076.
27. J. Lamy, D. Lavit and N.P. Buu-Hoi, *J. Chem. Soc.*, (1958) 4204.
28. R.M. Kellogg, M.B. Groen and H. Wynberg, *J. Org. Chem.*, 32 (1967) 3093.
29. A. Charlton, M. Kalaji, P.J. Murphy, S. Salmaso, A.E. Underhill, G. Williams, M.B. Hursthouse and K.M. Abdul Malik, *Synth. Met.*, 95 (1998) 75.
30. A. Charlton, A. Underhill, G. Williams, M. Kalaji, P.J. Murphy, D.E. Hibbs, M.B. Hursthouse and K.M.A. Malik, *Chem. Commu.*, (1996) 2423.
31. A. Charlton, A. Underhill, G. Williams, M. Kalaji, P.J. Murphy, K.M.A. Malik and M.B. Hursthouse, *J. Org. Chem.*, 62 (1997) 3098.
32. K. Ishikawa, K. Akiba and N. Inamoto, *Tetrahedron Lett.*, 17 (1976) 3695.



**Chapter 3**

**Studies on  
Dithienylethylenes**



### 3.1 Introduction

In this Chapter, electrochemical and spectroelectrochemical studies carried out on the two thienylethylenes isomers shown in Figure 3.01 are described.

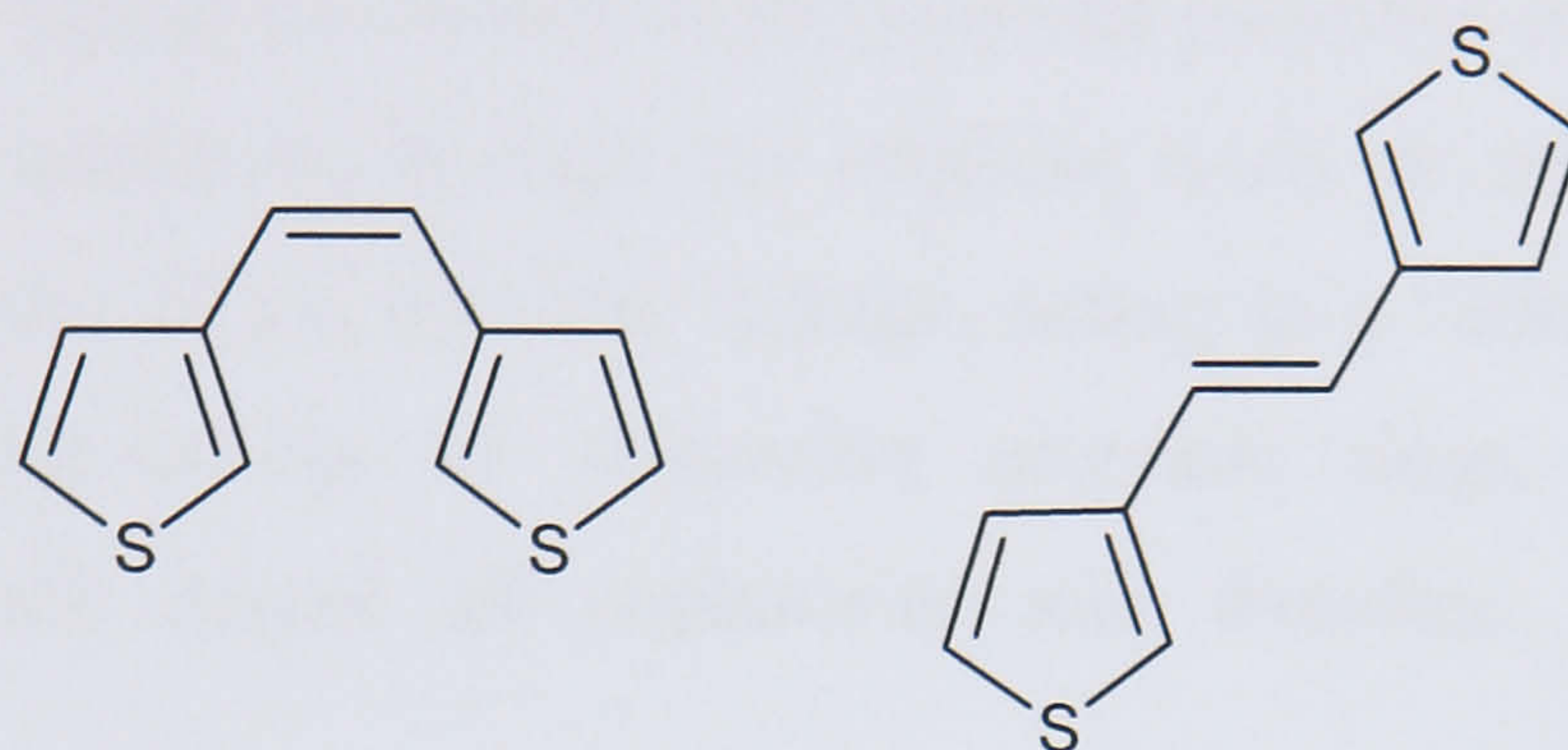


**Figure 3.01** - Structures of *cis*-1,2-di(3-thienyl)ethylene **DTE-cis** (left) and *trans*-1,2-di(3-thienyl)ethylene **DTE-trans** (right).

This class of compounds can be viewed as a combination of the structures of thiophene and polyacetylene.<sup>1,2</sup> In such systems, the presence of double bonds produces both a decrease in the overall aromatic character of the molecule allowing a better delocalisation of  $\pi$ -electrons over the polymeric chain, and a limitation of the rotational disorder.<sup>3,4</sup> The combination of these two effects has been confirmed in polymers like poly-thienylenevinylene (PVT)<sup>2,5</sup> and poly-dithienylethylene (PDTE)<sup>1,6</sup>, exhibiting lower bandgaps by about 0.3 eV than that of polythiophene.

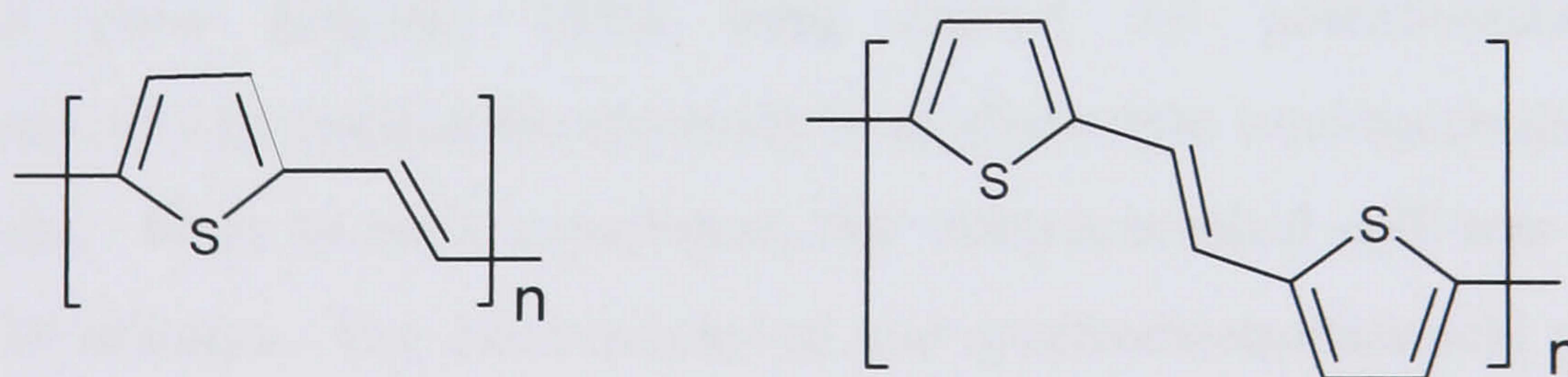


**Figure 3.02** - Structures of poly(thienylenevinylene) (left) and poly-dithienylethylene (right).

A major drawback in the study of ethylene linked thiophene derivatives lies in the enhanced stability of the corresponding radicals which exerts detrimental consequences for the efficiency of the electropolymerisation process.<sup>1</sup> The existence of a poorly soluble precursor will lead to a limited number of couplings, thus



preventing the formation of extensively conjugated polymer chains.<sup>6</sup> Also, the oxidation of the alkene spacer linkage can lead to the formation of a crosslinked polymer film with low conductivities.<sup>7</sup>

The interest in investigating the polymerisation of dithienylethylenes, with the ethylenic double bond bridging two thiophene rings in the  $\beta$ -position, arises from the possibility that the charge movement in the resultant polymers could occur either *via* the polythiophene backbone, through the ethylene bond, or using both routes. In addition, the presence of the ethylene linkage, acting as a “conjugated spacer” and reducing steric interactions on successive aromatic rings, could lead to an enhancement of the degree of coplanarity and therefore, increased polymer conjugation.<sup>5</sup>

## 3.2 Experimental

Cyclic voltammetric studies on the thienylethylenes isomers **DTE-trans** and **DTE-cis** were performed using a three-electrode cell with a platinum disc as the working electrode. A silver wire immersed in a solution of supporting electrolyte (0.1 M TBAPF<sub>6</sub> / MeCN) containing 0.01 mol dm<sup>-3</sup> AgNO<sub>3</sub> was used as reference electrode. This reference lies +0.32 V relative to the saturated calomel electrode (SCE). All potential values presented in this Chapter are quoted against the SCE. Attempts to grow polymer films were carried out potentiostatically or potentiodynamically by cycling the electrode in an electrolyte solution containing the monomer units. Prior to each experiment, the electrochemical cell was de-gassed with N<sub>2</sub> for 30 minutes. The electrochemical and spectroelectrochemical procedure followed in the study of synthesised polymers, **PDTE-trans** and **PDTE-cis**, was the same as previously described in Chapter Two.

Chemical doping was performed by exposing the electropolymerised films to iodine vapour for a period of 24 hours at 40 °C. Subsequently, the doped polymers were carefully washed with acetonitrile to remove any excess of I<sub>2</sub> and analysed by CV and SNIFTIRS.



### 3.3 Results and Discussion

#### 3.3.1 Studies on *trans*-dithienylethylene DTE-trans

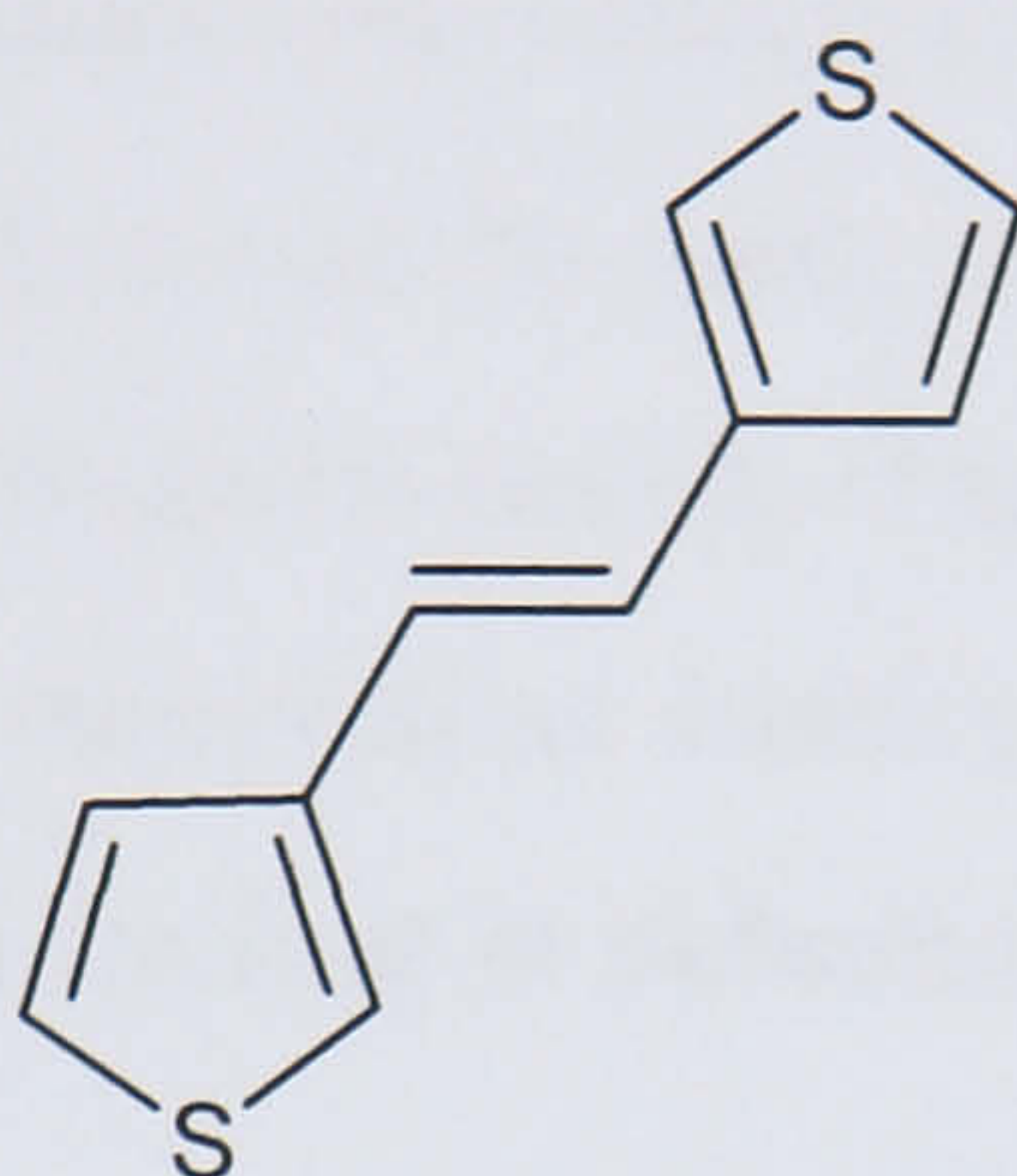


Figure 3.03 - Structure of *trans*-1,2-di(3-thienyl) ethylene **DTE-trans**.

#### Electrochemical and Spectroelectrochemical Studies

The voltammetric response of **DTE-trans** is shown in Figure 3.04. Two oxidation and two reduction peaks can be seen at  $E_{\text{ox}}^1 = 0.74$  V,  $E_{\text{ox}}^2 = 1.01$  V,  $E_{\text{red}}^1 = 0.63$  V, and  $E_{\text{red}}^2 = 0.86$  V.

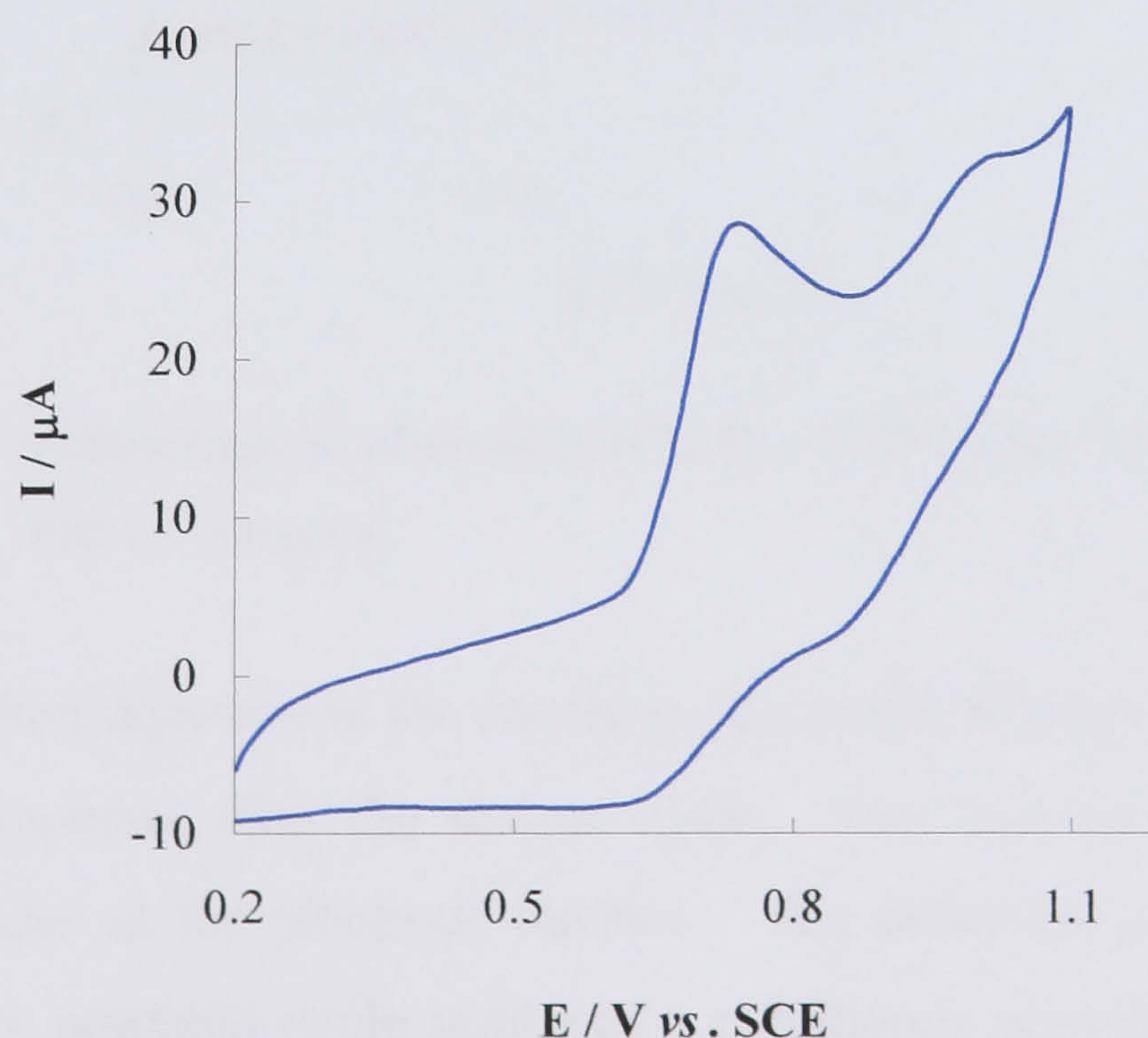
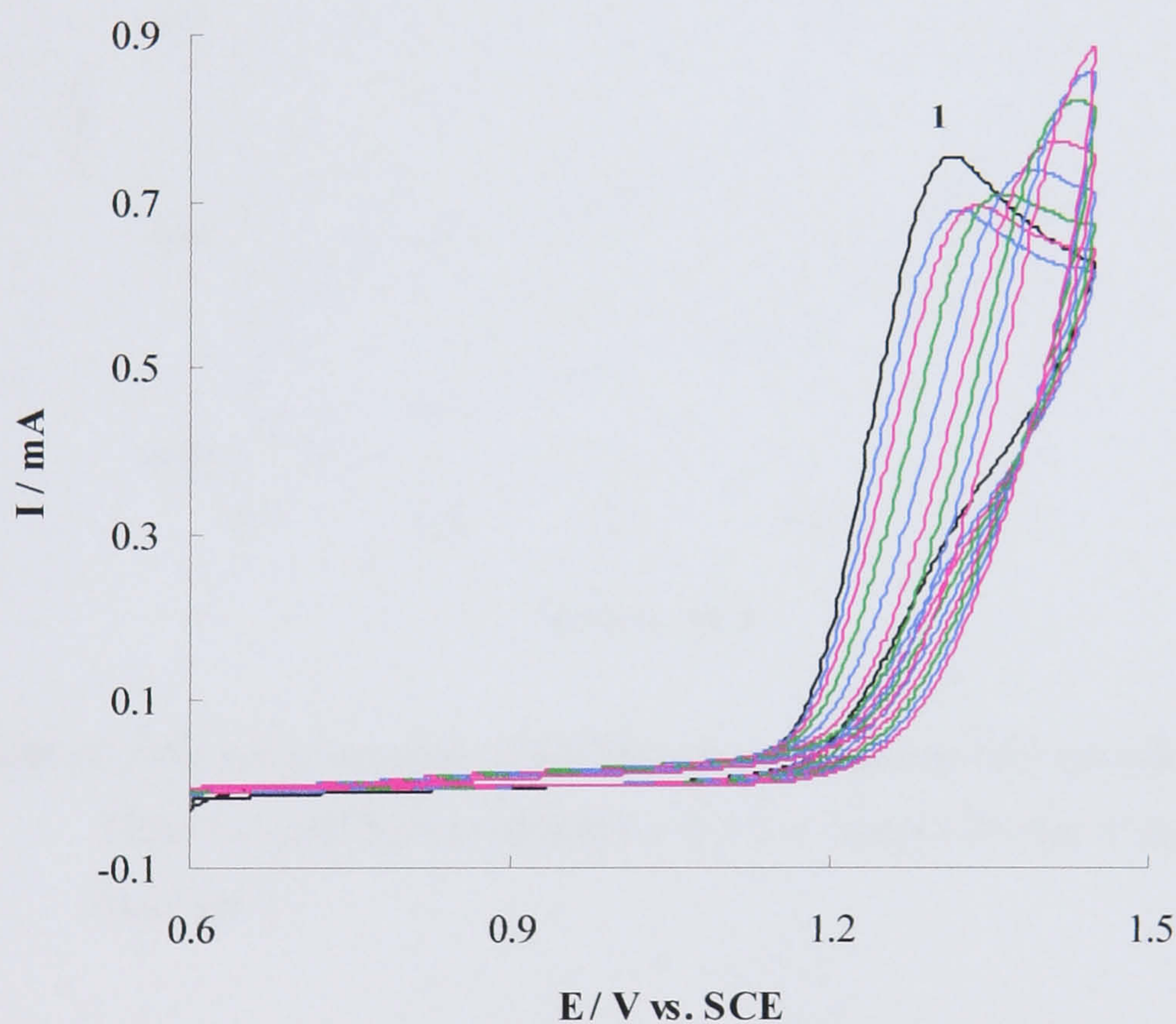


Figure 3.04 - Voltammogram of a **DTE-trans** solution ( $0.003 \text{ mol dm}^{-3}$ ) in electrolyte recorded at  $v = 0.1 \text{ V s}^{-1}$ .



These redox couples correspond to the formation of a radical cation ( $E_{\text{ox}}^1 / E_{\text{red}}^1$ ) and a dication ( $E_{\text{ox}}^2 / E_{\text{red}}^2$ ). The reversible one electron oxidation of oligothiophenes to radical cations and dications has been very well documented.<sup>8-12</sup> However, electrochemical reversibility is very unusual in monomers with three or fewer thiophene rings.<sup>13</sup> This fact can explain the large peak separation and therefore low reversibility observed in the voltammetric behaviour of **DTE-trans**.

A third irreversible oxidation can be seen at  $E_{\text{ox}}^3 = 1.34$  V, corresponding to the potential at which the polymerisation occurs (Figure 3.05). Prior to this potential, no polymer formation could be observed as confirmed by the lack of an increase in current upon successive potential cycling at potentials lower than 1.34 V.



**Figure 3.05** - Voltammograms of the polymerisation of **DTE-trans** recorded at  $\nu = 0.1 \text{ V s}^{-1}$  with 1 - first cycle.

After an initial decrease in the anodic peak current density at  $E_{\text{ox}}^3 = 1.34$  V, the current starts to increase after the second cycle. This may be due to the need to initially form nuclei at the electrode surface. The observed increase in the peak current with every potential cycle indicates a continuous growth of material on the electrode leading to an increase in the effective surface area of the electrode.<sup>14,15</sup>



As the polymerisation proceeds, the peak potential shifts gradually towards higher values. This potential shift, also seen during the growth of many polythiophene derivatives has been attributed to heterogeneous electron-transfer kinetics, the  $iR$  drop across the film and a decrease in the film conductivity.<sup>16-18</sup>

The redox behaviour of the electrochemically polymerised light-yellow **PDTE-trans** film was investigated using cyclic voltammetry in a monomer-free electrolyte solution. The obtained voltammogram is shown in the Figure 3.06.

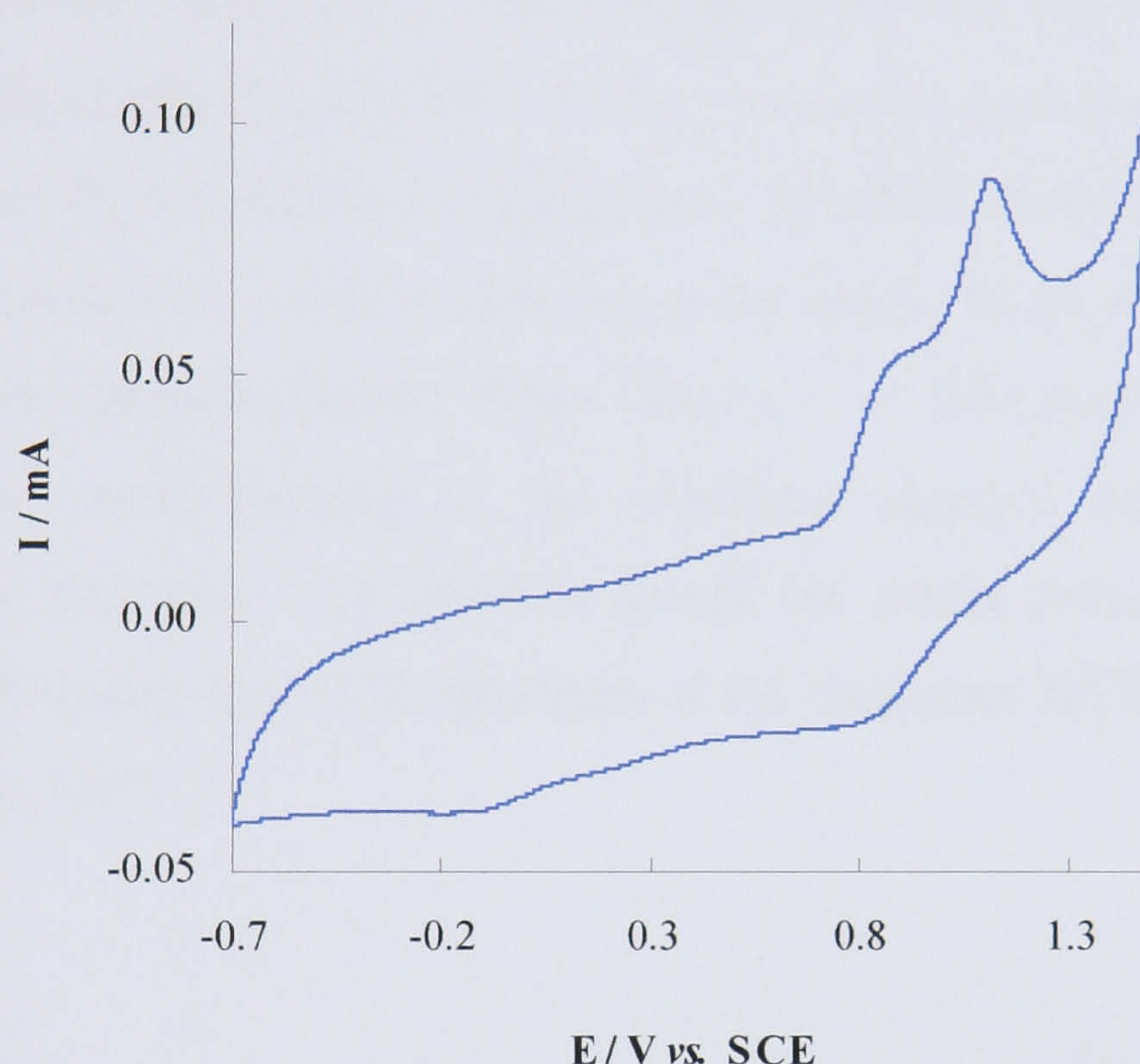


**Figure 3.06** - Cyclic voltammogram of **PDTE-trans** in monomer free solution (0.1 M TBAPF<sub>6</sub>/MECN) recorded at  $\nu = 0.1 \text{ V s}^{-1}$  using a Pt disc working electrode (0.44 cm<sup>2</sup>).

The cyclic voltammogram of **PDTE-trans** shows a one electron redox process at  $E^1_{\text{ox}} = 0.89 \text{ V} / E^1_{\text{red}} = 0.83 \text{ V}$  and a second oxidation at  $E^2_{\text{ox}} = 1.12 \text{ V}$ . These peaks can be assigned to the sequential oxidation of the conjugated polymer chain to form polarons and bipolarons.<sup>18-21</sup> Even though previous studies on the electroactivity of polythiophene films indicate that the formation of polarons and bipolarons usually occurs at essentially the same potential, variations in the electrolyte medium or temperature may facilitate its detection by cyclic voltammetry.<sup>19</sup> For example, using a Pt ultramicroelectrode at low temperature, Chen *et al.*<sup>20</sup> were able to distinguish the reversible formation of the polaron, bipolaron and even a metallic state in (3,4-ethylenedioxythiophene) (PEDOT) and poly(3-methylthiophene).



Taking the potential towards more negative values reveals further reduction of the polymeric chain at  $E_{\text{red}}^2 = -0.11$  V. This peak might be attributed to the removal of trapped positive charges remaining in the polymer after being cycled through the p-doped state.<sup>22,23,24</sup> The film was found to be stable from -1.0 to 2.0 V. Potential cycling outside this potential interval leads to polymer degradation.

The oxidation of **PDTE-trans** (Figure 3.06) takes place at a lower potential than that of polythiophene (1.1 V vs. SCE)<sup>25</sup>. It can then be concluded that, as already seen for PVT<sup>26</sup> and PDTE<sup>27</sup>, the introduction of the ethylene linkage between the thiophene rings induces a negative shift of the anodic peak potential.

The spectroelectrochemical investigation of **PDTE-trans** was performed in a monomer-free electrolyte solution and using the same range of potentials as those applied during the characterisation of the film by CV. The aim of this study was to achieve a better understanding of the structural changes occurring during the oxidation of the polymer. In order to assign the peaks present in the SNIFTIR spectra of **PDTE-trans**, the FTIR spectrum of the monomer **DTE-trans** was initially recorded (Figure 3.07).

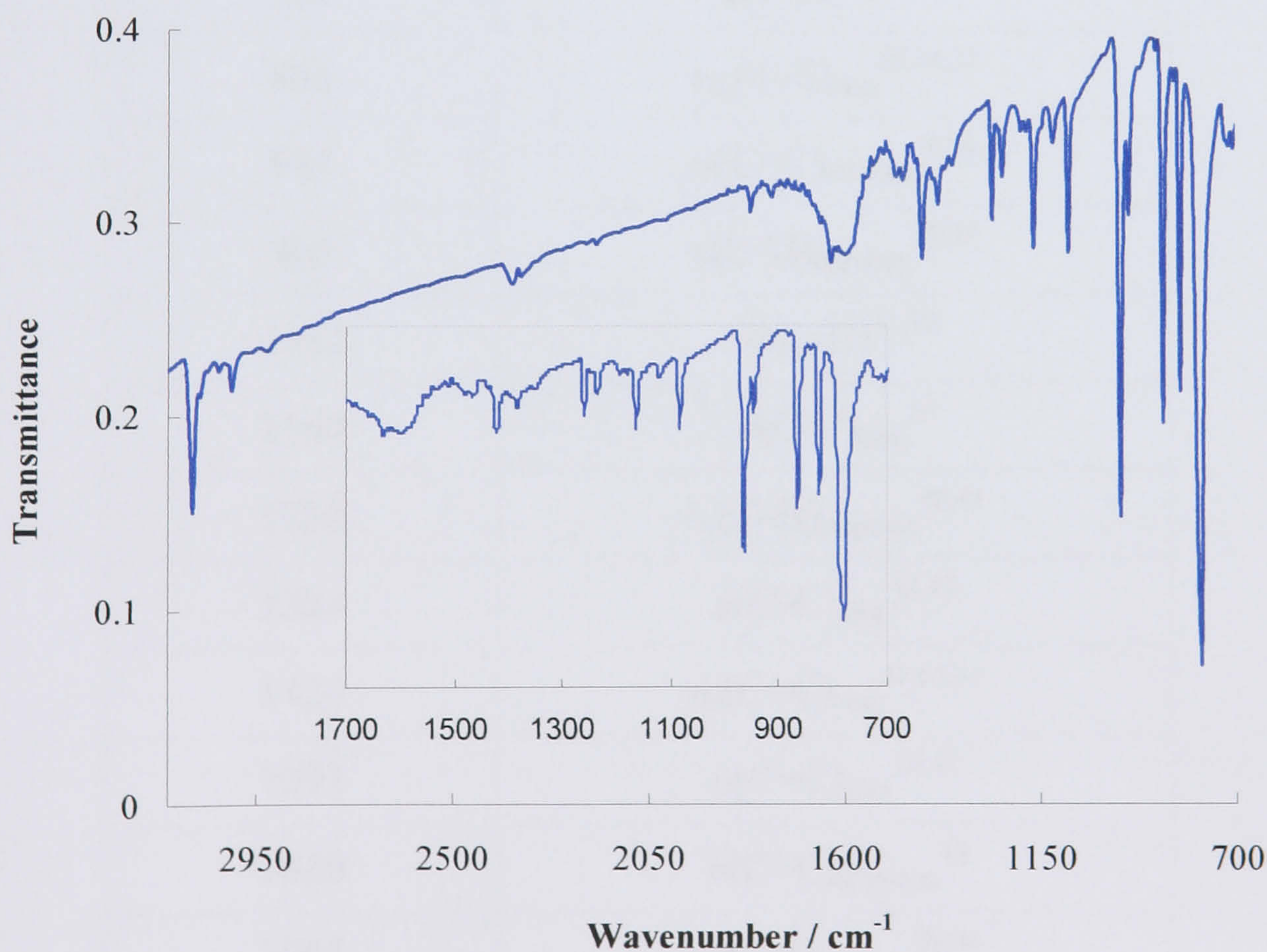


**Figure 3.07** - Infrared spectrum of **DTE-trans** in KBr disc pellet and expansion of the IR spectrum between 1700 and 700 cm<sup>-1</sup>.



The FTIR spectrum of **DTE-trans** displays its strongest bands at 780 and 965  $\text{cm}^{-1}$ . These signals are due to the out-of-plane  $\text{C}_\beta\text{-H}$  deformation in the thiophene ring and C-H out-of-plane bending of the *trans*-vinylene linkage, respectively.<sup>11,26,28,29</sup> The vibrations between 1000-1400  $\text{cm}^{-1}$  are in the range of the stretching frequencies of C-C, C=C and C-S bonds and of the bending frequencies of C-H bonds in thiophene.<sup>30</sup> The C-H stretching vibration and out-of-plane deformation due to  $\alpha$ -hydrogen in the thiophene rings are found at 3095 and 703  $\text{cm}^{-1}$ , respectively.<sup>31,32</sup> The main IR bands for **DTE-trans** and their assignment are listed in Table 3.01 ( $\nu$  – stretching,  $\delta$  - in-plane deformation,  $\gamma$  - out-of-plane deformation,  $s$  – symmetric and  $as$  – asymmetric).

**Table 3.01** - FTIR bands frequency assignments for **DTE-trans**.

FTIR Band ( $\text{cm}^{-1}$ )	Band assignment
703	$\gamma(\text{C}_\alpha\text{-H})^{28,33}$
780	$\gamma(\text{C}_\beta\text{-H})^{11,15,34}$
825	$\gamma(\text{C-H})^{28,35,36}$
868	$\nu_{as}(\text{C-S})_{\text{ring}}^{14,34,37}$
945	$\nu(\text{C=C})_{\text{ethylene}}^{2,26}$
965	$\gamma(\text{C-H})_{\text{ethylene}}^{29,38}$
1082	$\delta(\text{C}_\alpha\text{-H})^{31,39}$
1164	$\nu(\text{C-C})_{\text{ring}}^{14}$
1238	$\delta_s(\text{C-H})_{\text{ethylene}}^{40,41}$
1384	$\nu(\text{C-C})_{\text{ring}}^{42,43}$
1424	$\nu_s(\text{C=C})_{\text{ring}}^{31,44,45}$
1597	$\nu(\text{C=C})_{\text{ring}}^{46,47}$
1630	$\nu(\text{C=C})_{\text{ethylene}}^{48}$
3005	$\nu(\text{C-H})_{\text{ethylene}}^{26,40}$
3037	$\nu(\text{C}_\beta\text{-H})^{35,39}$
3095	$\nu(\text{C}_\alpha\text{-H})^{31,32}$



Figure 3.08 shows the SNIFTIR spectra of **PDTE-trans** collected at successively increasing positive potentials and normalised to the reference spectrum taken at 0 V. These spectra were obtained by application of Equation 2.01 (Chapter Two - page 43) and in such spectra, positive bands represent a decrease in absorbance at the applied potential relative to the reference potential, and negative bands are associated with an increase in absorbance under the same conditions.

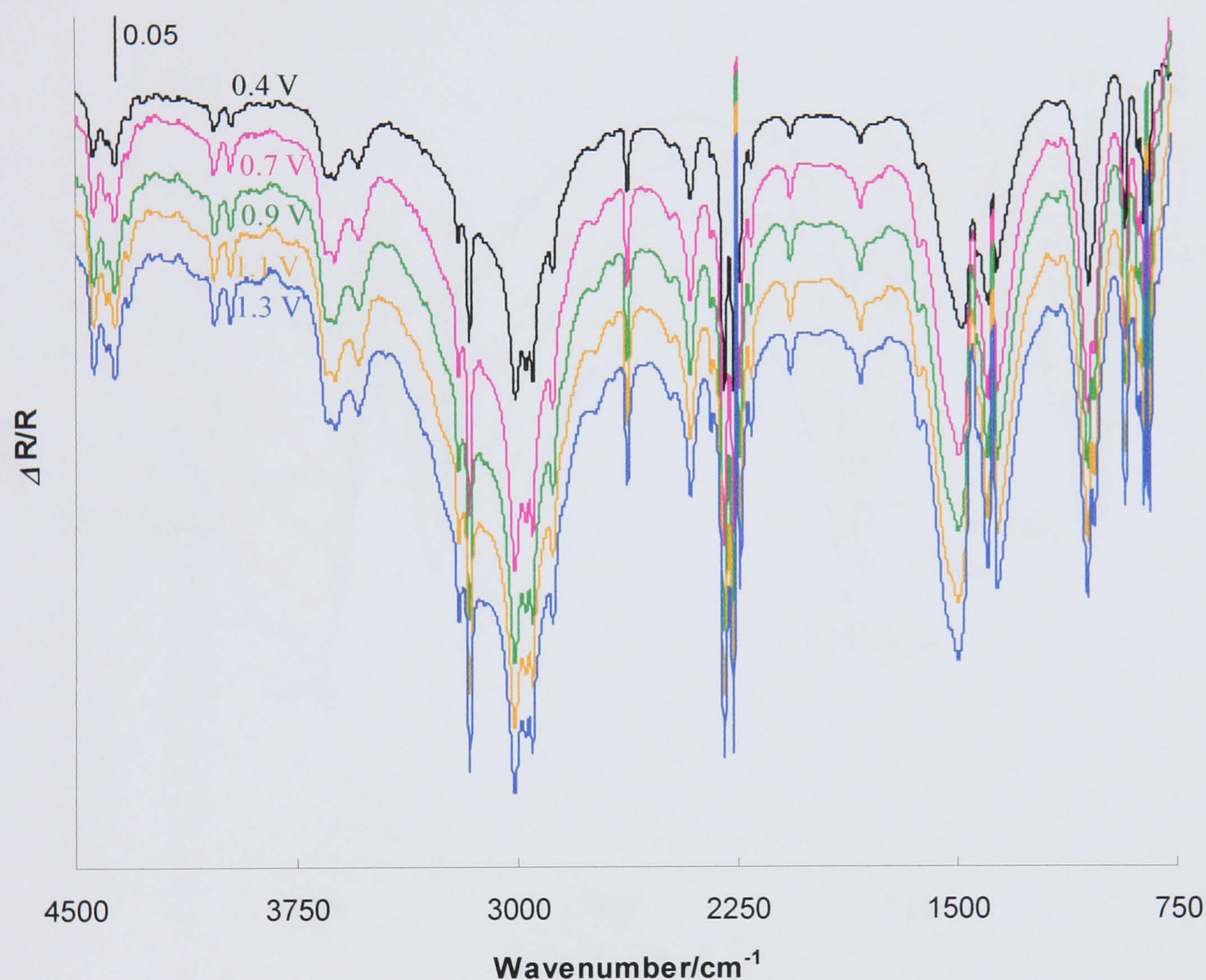


**Figure 3.08** - SNIFTIRS spectra of **PDTE-trans** taken from 0.4 to 1.3 V. Reference spectra collected at 0 V. Spectra were shifted for clarity.

The spectra obtained between 4500 and 750  $\text{cm}^{-1}$  show an increase in the intensity of the IR absorbance peaks as the polymer is oxidised from 0.4 to 1.3 V. Solvent bands are seen at 2250  $\text{cm}^{-1}$  (acetonitrile  $\text{C}\equiv\text{N}$  stretch) and centred at 3000  $\text{cm}^{-1}$  (symmetric and asymmetric stretching modes of  $\text{CH}_2$  and  $\text{CH}_3$  due to the electrolyte salt - tetrabutyl ammonium salt).<sup>14,49</sup>



The absence of the peaks at 3095 and 1082  $\text{cm}^{-1}$  related with the  $\text{C}_\alpha\text{-H}$  stretching vibration and in-plane deformation, respectively, indicates that the coupling of thiophene units occurs mainly through the  $\alpha,\alpha$ -positions. However, a decrease in the intensity of the  $\text{C}_\beta\text{-H}$  vibration at 780  $\text{cm}^{-1}$  is also seen in the spectra of **PDTE-trans** when compared with the IR of the monomer. This might be attributed to the presence of cross-linked thiophene units or the occurrence of mislinkages through the  $\beta$ -positions.<sup>32,50</sup>

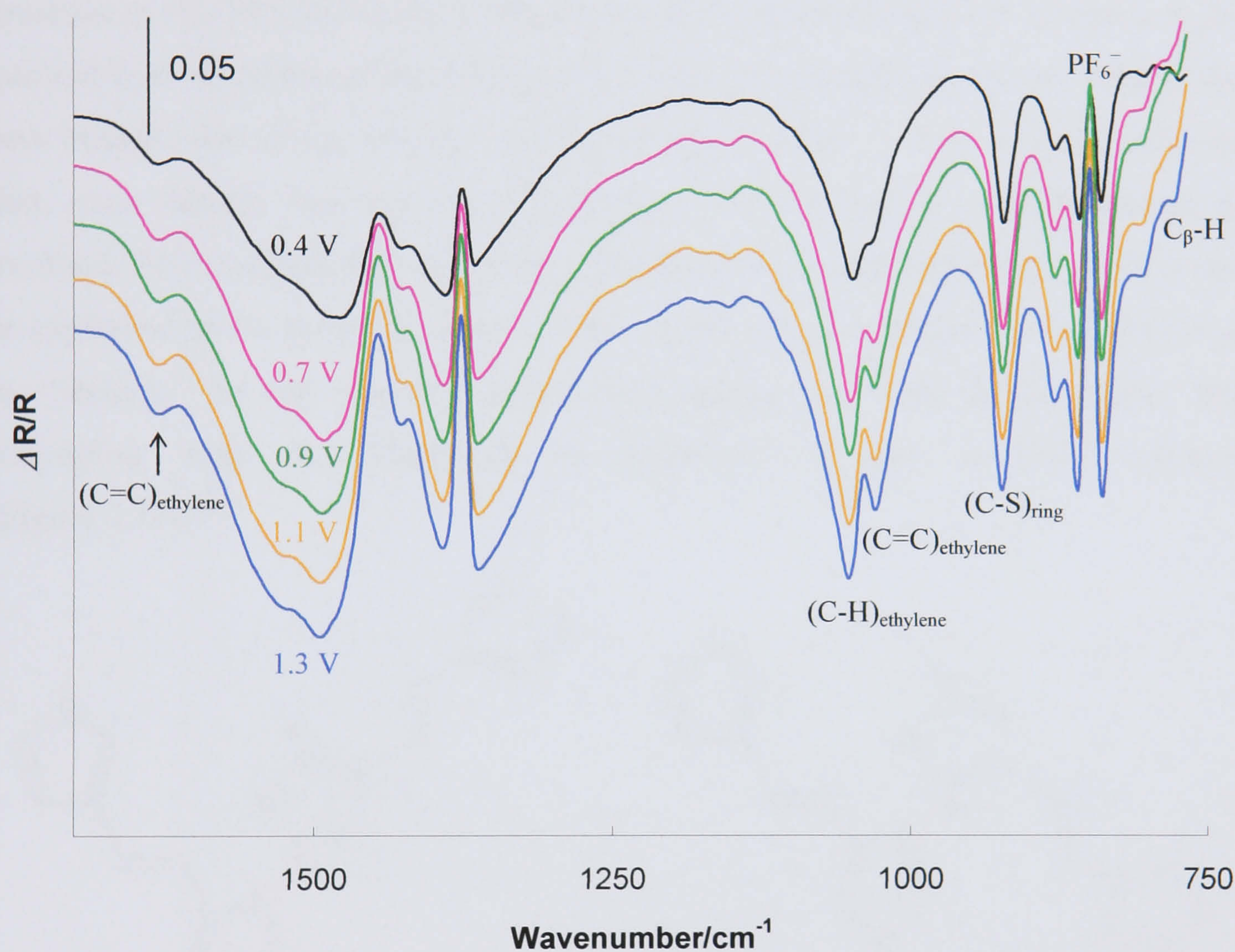


**Figure 3.09** - SNIFTIRS spectra of **PDTE-trans** between 1750 and 750  $\text{cm}^{-1}$ . Reference spectra collected at 0 V. Spectra were shifted for clarity.

SNIFTIRS peaks at 1631, 923/ 858 and 839  $\text{cm}^{-1}$  are in good agreement with the  $\nu(\text{C}=\text{C})_{\text{ethylene}}$ ,  $\nu(\text{C}-\text{S})_{\text{ring}}$  and  $\gamma(\text{C}-\text{H})$  vibrations found in the FTIR spectrum of **DTE-trans**. Peaks at 1049 and 1032  $\text{cm}^{-1}$  can be related with the out-of plane deformation  $(\text{C}-\text{H})_{\text{ethylene}}$  and stretching vibration  $(\text{C}=\text{C})_{\text{ethylene}}$  seen in the IR spectrum of the monomer at 965 and 945  $\text{cm}^{-1}$ .



New absorption peaks are observed at 1365, 1390 and 1476  $\text{cm}^{-1}$  (shifts to 1493  $\text{cm}^{-1}$  as the polymer oxidised). The emergence of these bands upon p-doping is due to the displacement of the position of the double bonds forming quinoid structures.<sup>51,52</sup> The incorporation of electrolyte anions ( $\text{PF}_6^-$ ) into the film during oxidation of **PDTE-trans** is seen 848  $\text{cm}^{-1}$  as an increasing positive band.<sup>14,53</sup>

The SNIFTIR spectra of **PDTE-trans** seems to lack some of the characteristic features usually found in IR spectra of polythiophenes as they are p-doped, i.e. the presence of the Infra Red Active Vibrations - IRAV (created from the coupling of the quinoid-type vibrations of the polymer backbone), or a broad absorbance band in the near infrared due to the existence of free charge carriers.<sup>54</sup> Their absence indicates that, even though polarons and bipolarons could be formed as **PDTE-trans** is oxidised, their mobility throughout the chain must be considerably limited. This can be explained by the presence of mislinkages through the  $\beta$ -positions that would result in “defects” in the polymer backbone, reducing the conjugation length and interfering with the formation of bipolarons in the oxidised polymer (Figure 3.10).<sup>50,55</sup>

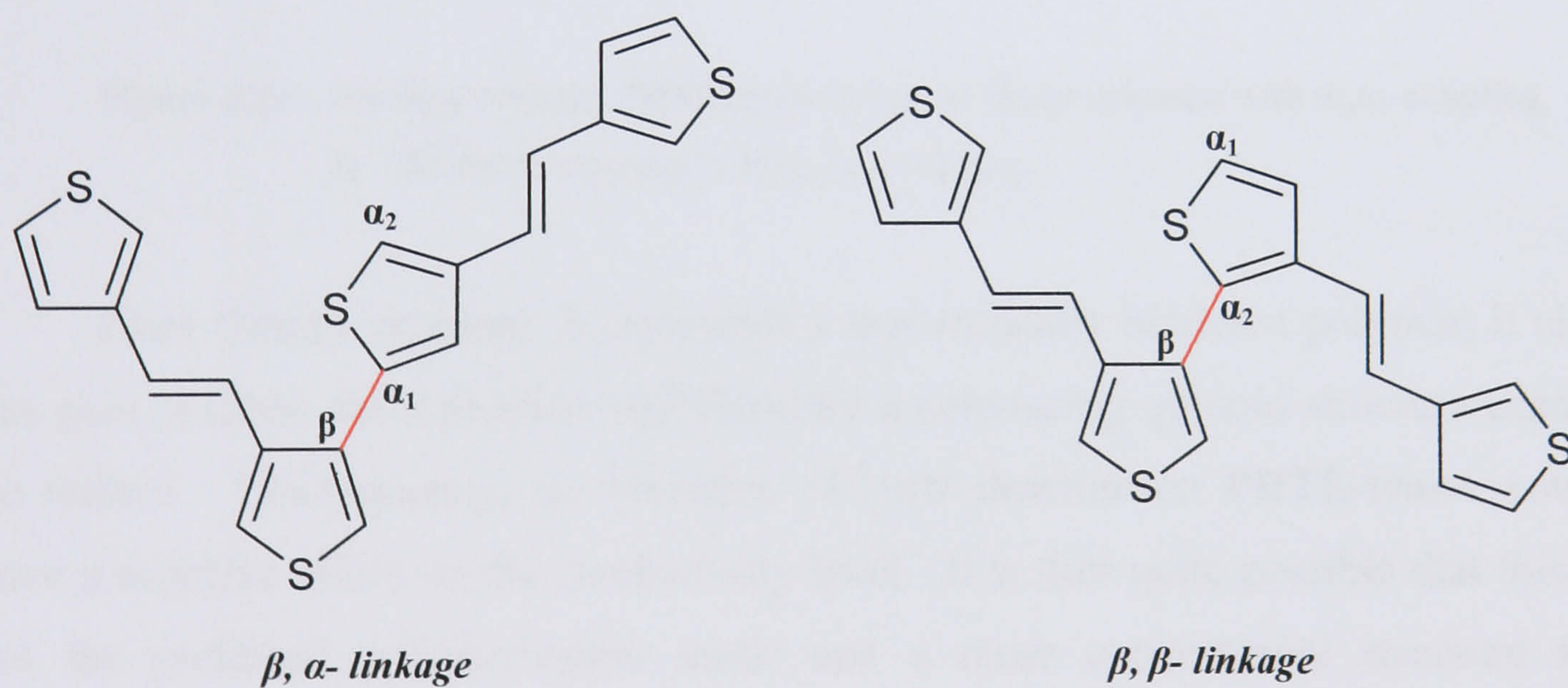
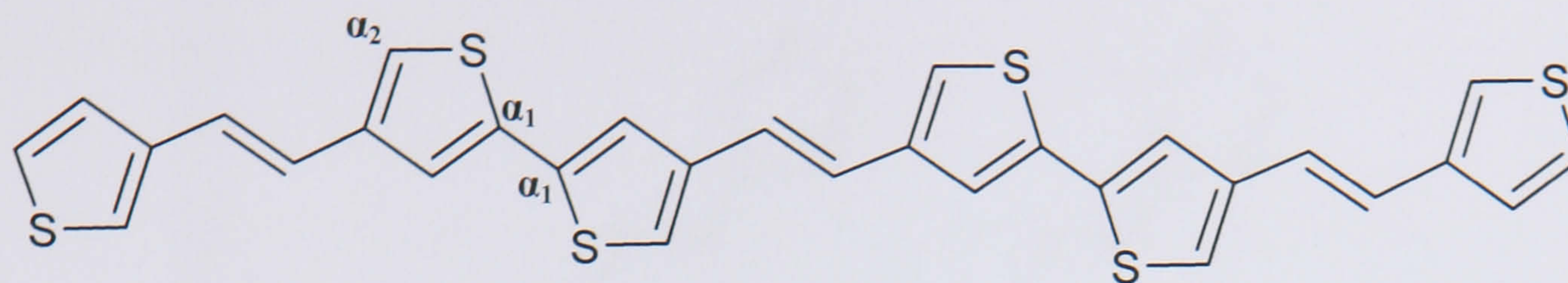


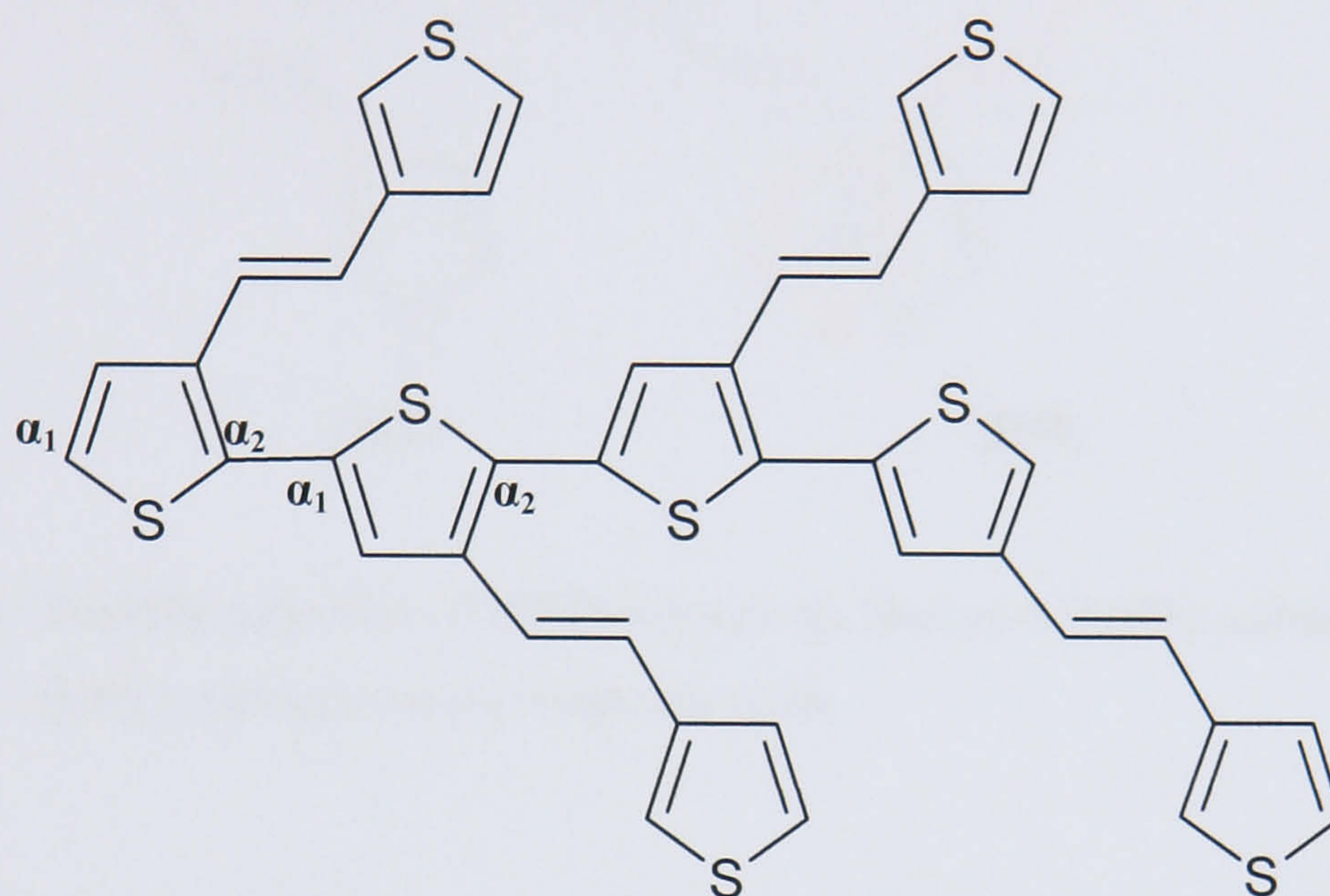
**Figure 3.10** - Bonding between **PDTE-trans** units;  $\beta, \alpha_1$ - and  $\beta, \alpha_2$ - linkage.

Moreover, considering that polymerisation is likely to occur through the  $\alpha$ -positions of the thiophene rings, two different **PDTE-trans** structures can be obtained as shown in Figure 3.11:





A – Linear Structure



B – Branched Structure (with head-to-tail couplings, HT)

**Figure 3.11** - Bonding between **PDTE-trans** units; A- linear structure with  $\alpha_1, \alpha_1$ -coupling, B – Branched structure with  $\alpha_1, \alpha_2$ -coupling.

Even though structure A represents a less sterically hindered polymer, it also has poor electron delocalisation and therefore a convincing quinoid structure cannot be formed. Consequently, the presence of such structure on **PDTE-trans** would have a negative effect on the conductivity level. It is thus quite possible that this is not the preferred polymerisation mode and a more conventional structure for **PDTE-trans** would be the one shown in Figure 3.11 B. In the branched **PDTE-trans** polymer the occurrence of head-to-head couplings (Figure 3.12) during the electropolymerisation, can induce a considerable deviation from coplanarity between adjacent rings leading to poor  $\pi$ -orbital overlap and consequently, a reduction in the electrical conductivity.<sup>15,50</sup>



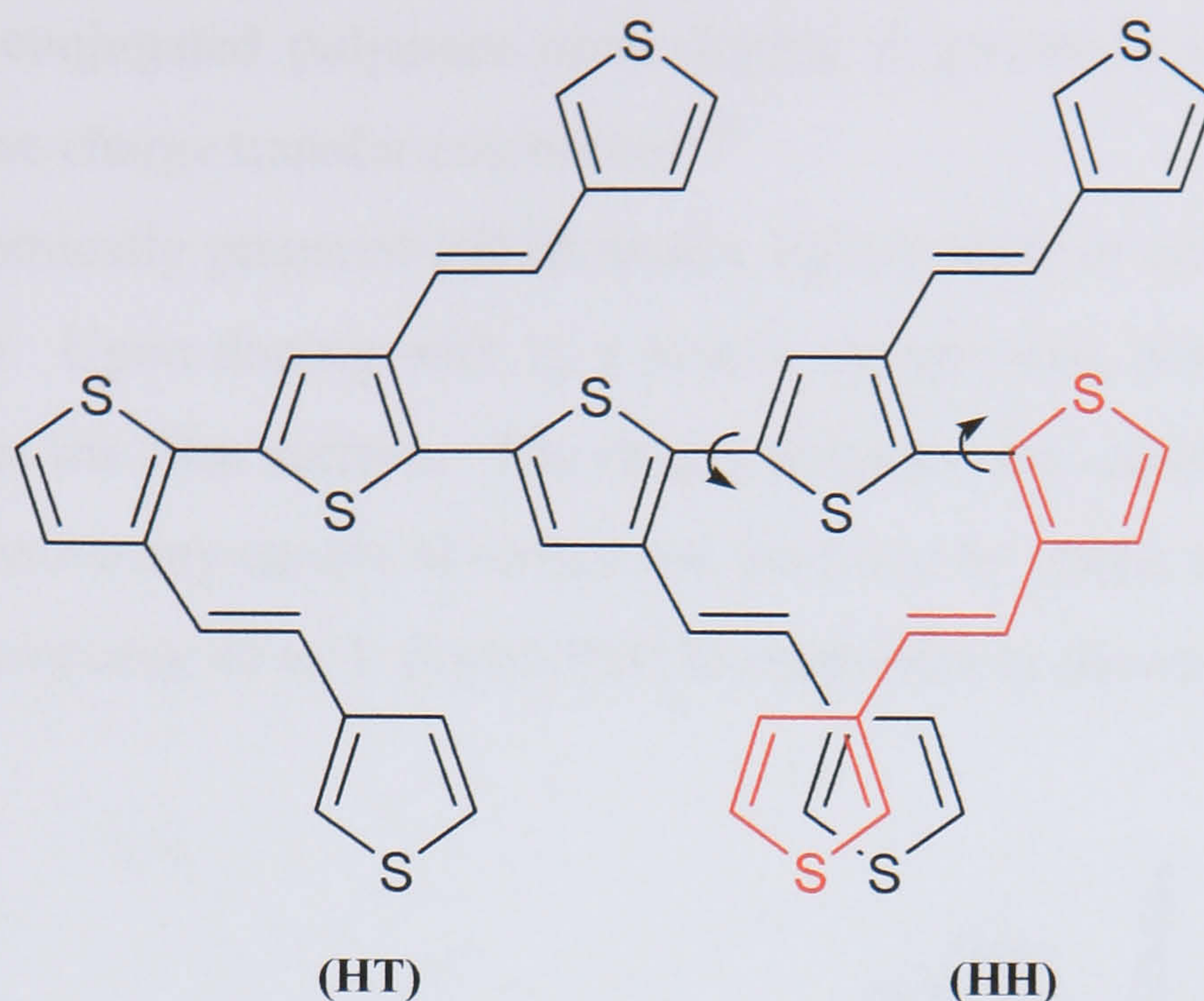
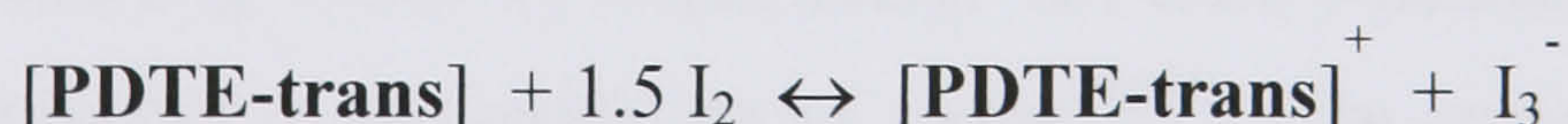


**Figure 3.12** - Possible structures of **PDTE-trans** with head-to-tail (HT) and head-to-head (HH) coupling between thiophene units.

### Electrochemical and Spectroelectrochemical Studies on Iodine-doped PDTE-trans

In order to improve the electrical properties of the neutral and doped state of **PDTE-trans**, iodine (an electron acceptor) was used as a chemical p-doping agent. Iodine has been frequently employed as an oxidant for the doping of conducting polymers due to the ease of the doping procedure.<sup>28,56,57</sup> Upon exposure to iodine vapour, an ionic complex consisting of positively charged polymer chains and counter anions ( $I_3^-$ ) is formed.<sup>58,59</sup> The reaction between **PDTE-trans** and iodine can be summarised as follows<sup>60,61</sup>:



The presence of charge transfer (CT) complexes in the form of  $I_3^-$ , or even  $I_5^-$ , next to the absorbed  $I_2$  has been confirmed by several techniques such as Raman spectroscopy, and UV-Vis spectroscopy.<sup>34,62,63</sup> It is now widely accepted that the



conductivity of conjugated polymers upon doping is governed by charge carriers generated by these charge transfer complexes.<sup>28</sup>

Electrochemically prepared **PDTE-trans**, light-yellow in colour, was exposed to iodine vapour. Upon doping with  $I_2$ , a colour change took place to dark-orange due to extra  $I_2$  on the film surface. The doped polymer was carefully washed with acetonitrile to remove any excess of iodine and analysed by cyclic voltammetry. The electrochemical response of an  $I_2$  doped **PDTE-trans** film is shown in Figure 3.13.

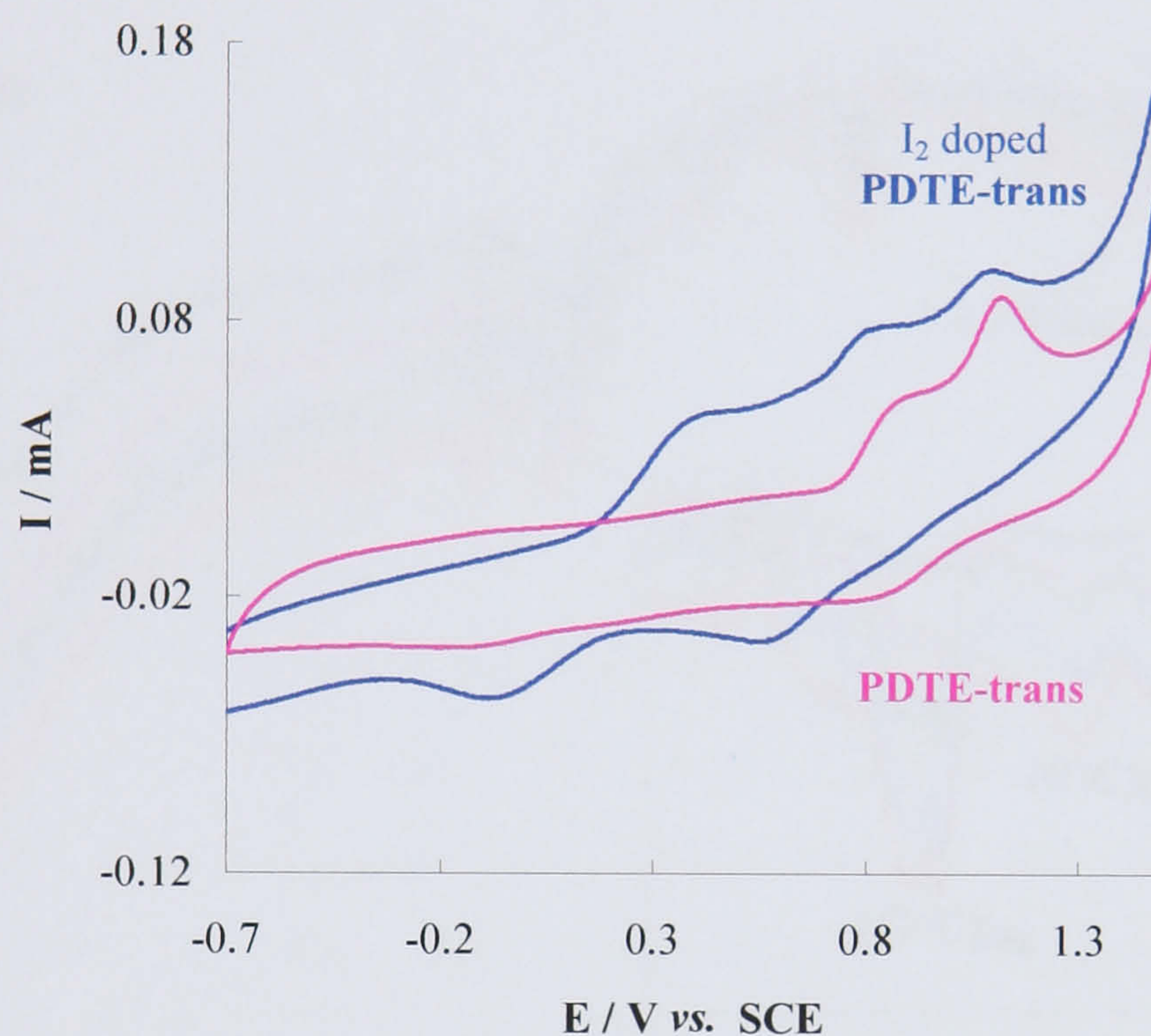


**Figure 3.13** - Cyclic voltammogram of **PDTE-trans** in monomer free solution (0.1 M TBAPF<sub>6</sub>/MECN) before and after  $I_2$  doping recorded at  $v = 0.1 \text{ V s}^{-1}$  using a Pt disc working electrode ( $0.44 \text{ cm}^2$ ).

The voltammogram of iodine doped **PDTE-trans** is very similar to that of the undoped polymer with the sequential oxidation to polarons and bipolarons taking place at  $E^1_{\text{ox}} = 0.80$  and  $E^2_{\text{ox}} = 1.09 \text{ V}$ , respectively. An extra oxidation peak is seen at  $E^3_{\text{ox}} = 0.36 \text{ V}$  attributed to the oxidation of iodine.<sup>61,62</sup> The comparison of the voltammetric response of **PDTE-trans** (Figure 3.13) before and after exposure to iodine vapour reveals a decrease in the oxidation potential values. This might be related with the presence of  $I_3^-$  ions incorporated into the film, which can induce the existence of partially oxidised areas in **PDTE-trans** facilitating the formation of polarons and bipolarons. The reduction of  $I_2$  doped **PDTE-trans** occurs at  $E^1_{\text{red}} = 0.57 \text{ V}$ , a considerable lower potential value than the one observed for



**PDTE-Trans** before chemical doping ( $E_{\text{red}}^1 = 0.83 \text{ V}$ ). This shift in the reduction peak potential can indicate an increased stability of the p-doped state upon exposure to iodine vapour.<sup>64</sup> A second reduction peak, attributed to the removal of trapped positive charges remaining on the polymer can be seen at  $E_{\text{red}}^2 = -0.11 \text{ V}$ .<sup>22,24</sup>

The redox response of  $\text{I}_2$  doped **PDTE-trans** was investigated by SNIFTIRS. Using as reference the spectrum taken at 0 V, the stepwise oxidation is shown in Figure 3.14.

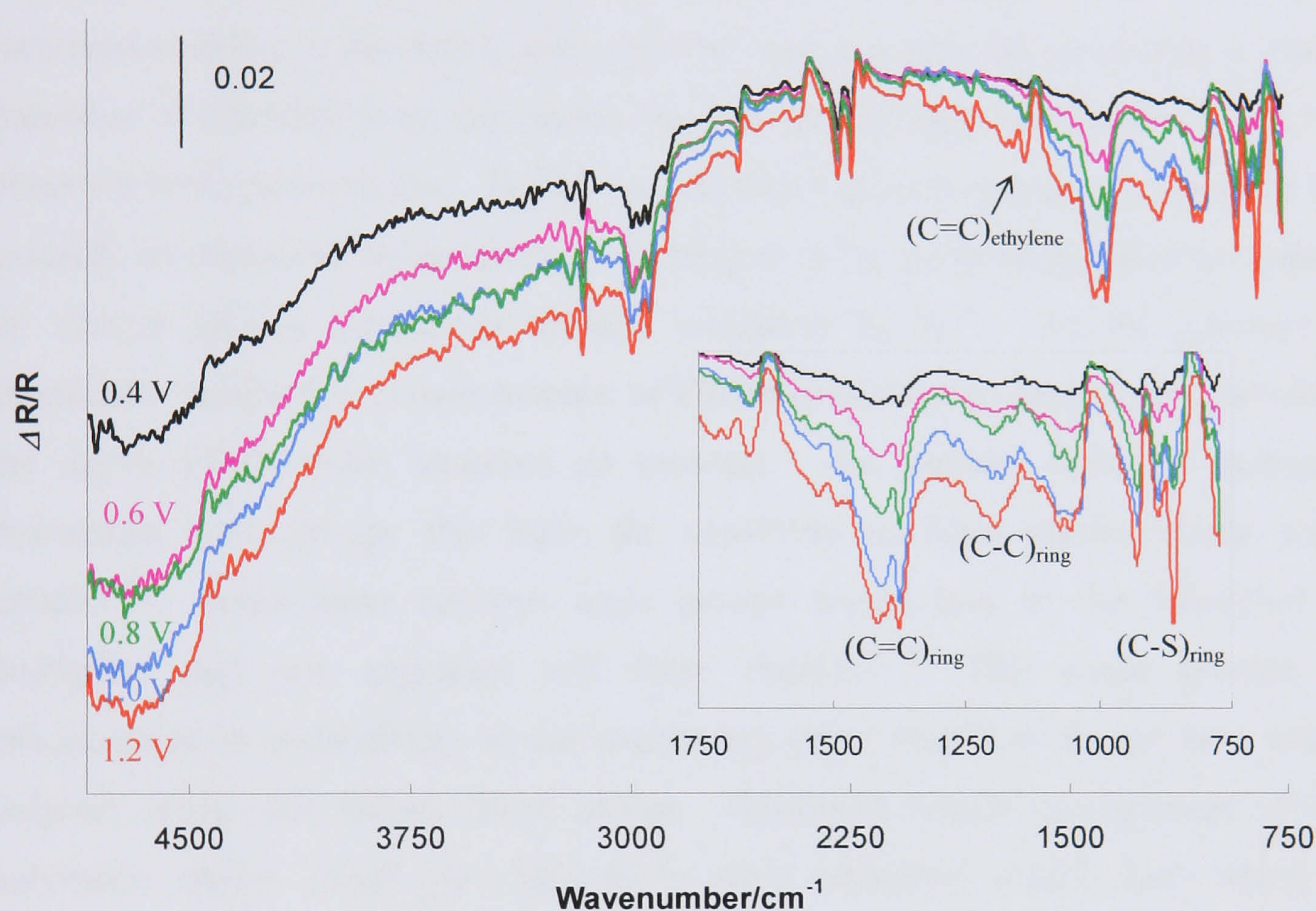


**Figure 3.14** - SNIFTIRS spectra of iodine doped **PDTE-trans** taken from 0.4 to 1.2 V and expansion of the SNIFTIRS spectra between 1750 and 750  $\text{cm}^{-1}$ . Reference spectra collected at 0 V. Spectra were shifted for clarity.

**PDTE-trans** exhibits a significantly different spectroelectrochemical behaviour after chemical doping displaying similar IR characteristics to those of polythiophenes. As the polymer is oxidised, a very large broad band, extending into the near IR region is seen. This band is caused by the transition of electrons from the valence band to new electronic states in the bandgap.<sup>21,32</sup> In addition, new infrared vibrations bands (IRAV) at 1072, 1116, 1193 and 1373  $\text{cm}^{-1}$ , not seen in the spectra



of **PDTE-trans**, are observed. Previous studies have shown that these peaks are due to the selective enhancement of four thiophene ring modes associated with the formation of polaronic or bipolaronic structures in the polymer chain.<sup>39,65</sup> Peaks at 1521/1413  $\text{cm}^{-1}$  and 1373/1193  $\text{cm}^{-1}$  are assigned to C=C and C-C ring stretching vibrations.<sup>14,21</sup> Strong C-S ring vibrations appear at 923, 888, and 860  $\text{cm}^{-1}$ .<sup>37</sup> The C=C ethylenic stretching vibration can be seen at 1650  $\text{cm}^{-1}$ .<sup>48</sup>

From the cyclic voltammetry and SNIFTIRS data it is clear that, on exposure to  $\text{I}_2$  vapour, changes occur in the electrical properties of **PDTE-trans**. Not only an increased stability in the doped state was achieved, but also, the previously not seen transition of electrons from the valence band to intermediate energy levels could be observed in the near infrared. Studies on polythiophenes have suggested that this can possibly be explained by occurrence of changes in the polymer morphology caused by charge species introduced through oxidation by  $\text{I}_2$ .<sup>66</sup> As the polymer is chemically oxidised, a certain amount of **PDTE-trans** salt is formed and therefore, the doped **PDTE-trans** becomes an ionomer. An ionomer refers to polymers containing ionic groups that have the capability to form intermolecular ionic bonds.<sup>66,67</sup> Association between ionic groups would lead to the formation of multiplets that can aggregate and form clusters.<sup>67,68</sup> This could prompt an enhancement in conductivity as the conducting entity would no longer be a single polymer chain, but rather, many chains. Increased spatial arrangement of the polymeric chains could also lead to a more stabilised doped state which is responsible for higher conductivity levels.<sup>66</sup>



### 3.3.2 Studies on *cis*-dithienylethylene DTE-cis

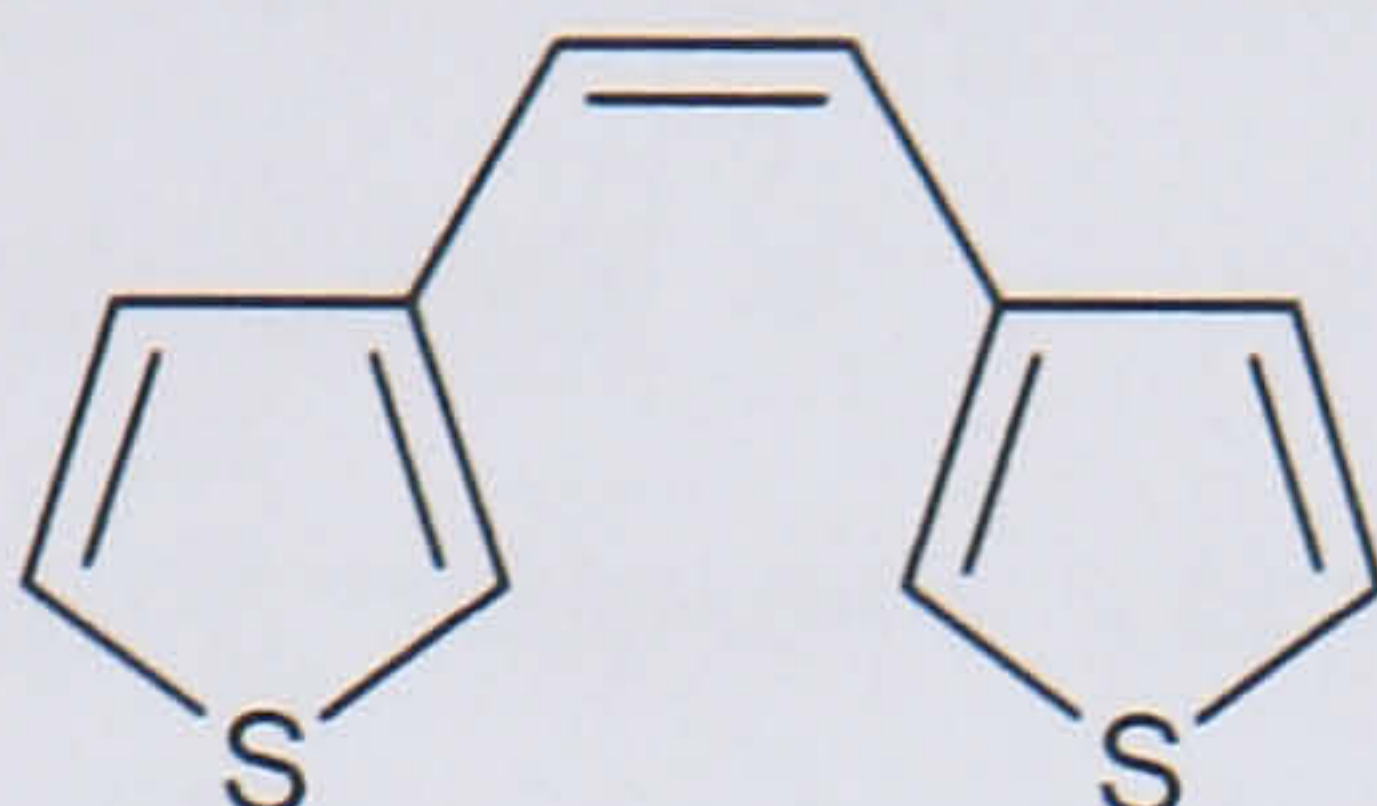


Figure 3.15 - Structure of *cis*-1,2-di(3-thienyl) ethylene **DTE-cis**.

#### Electrochemical and Spectroelectrochemical Studies

The electrochemical behaviour of **DTE-cis** was investigated by CV. A typical voltammogram of **DTE-cis** in electrolyte solution is shown in Figure 3.16.

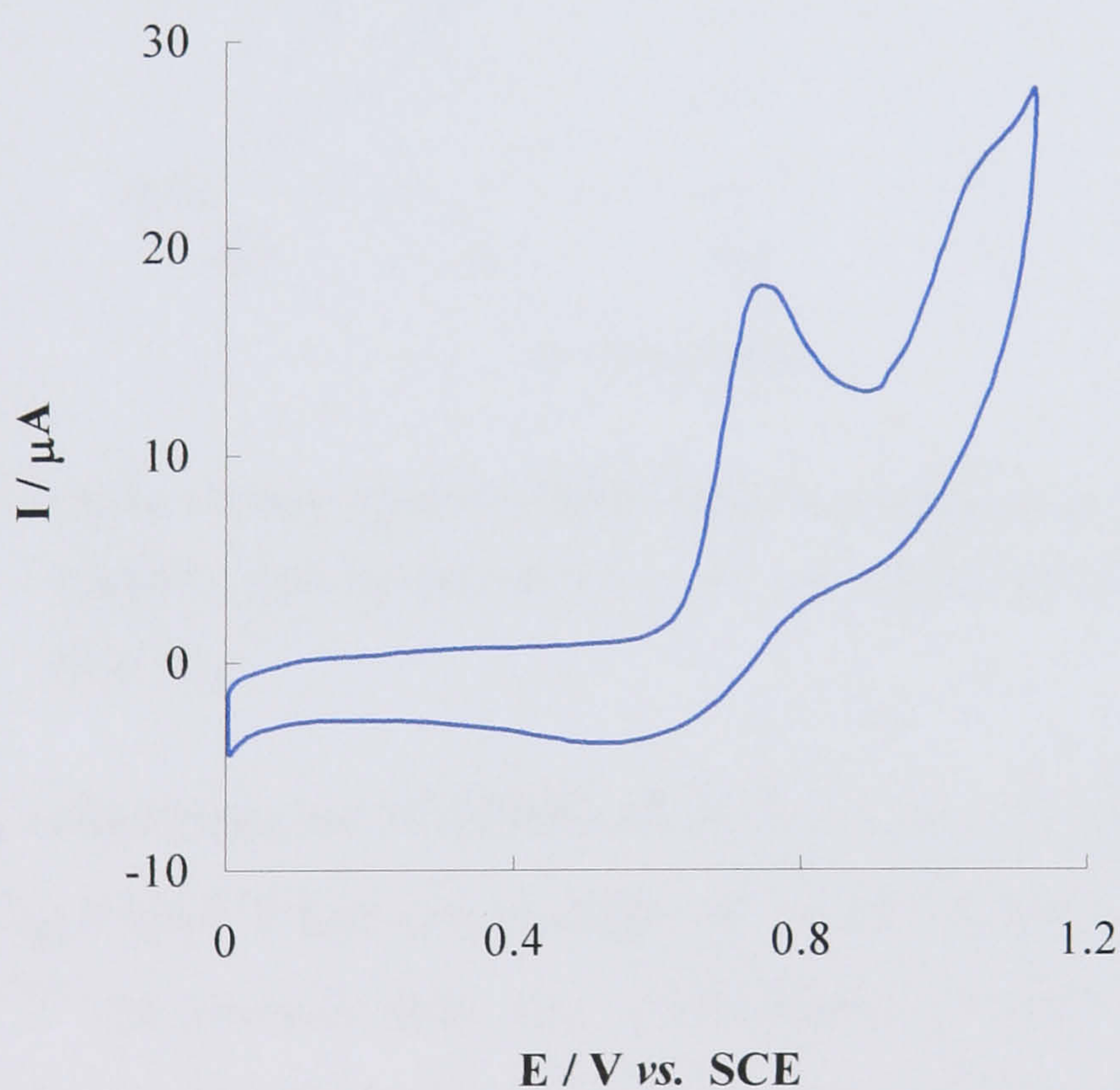


Figure 3.16 - Voltammogram of a **DTE-cis** solution ( $0.003 \text{ mol dm}^{-3}$ ) recorded in electrolyte at  $\nu = 0.1 \text{ V s}^{-1}$ .

As already reported for the electrochemical study of **DTE-trans**, two redox couples corresponding to the formation of a radical cation ( $E_{\text{ox}}^1 = 0.75 \text{ V} / E_{\text{red}}^1 = 0.61 \text{ V}$ ) and a dication ( $E_{\text{ox}}^2 = 1.04 \text{ V} / E_{\text{red}}^2 = 0.88 \text{ V}$ ) can be distinguished in the cyclic voltammogram of **DTE-cis**. These peaks occur at approximately the same



potentials as the ones seen in **DTE-trans**, which lead to the conclusion that the different structure of the two isomers does not influence their electroactivity.

A **PDTE-cis** film was grown potentiostatically at 1.6 V. The resultant light-yellow polymer was characterised in a monomer-free electrolyte solution. Figure 3.17 shows the voltammetric response obtained between different potential limits.

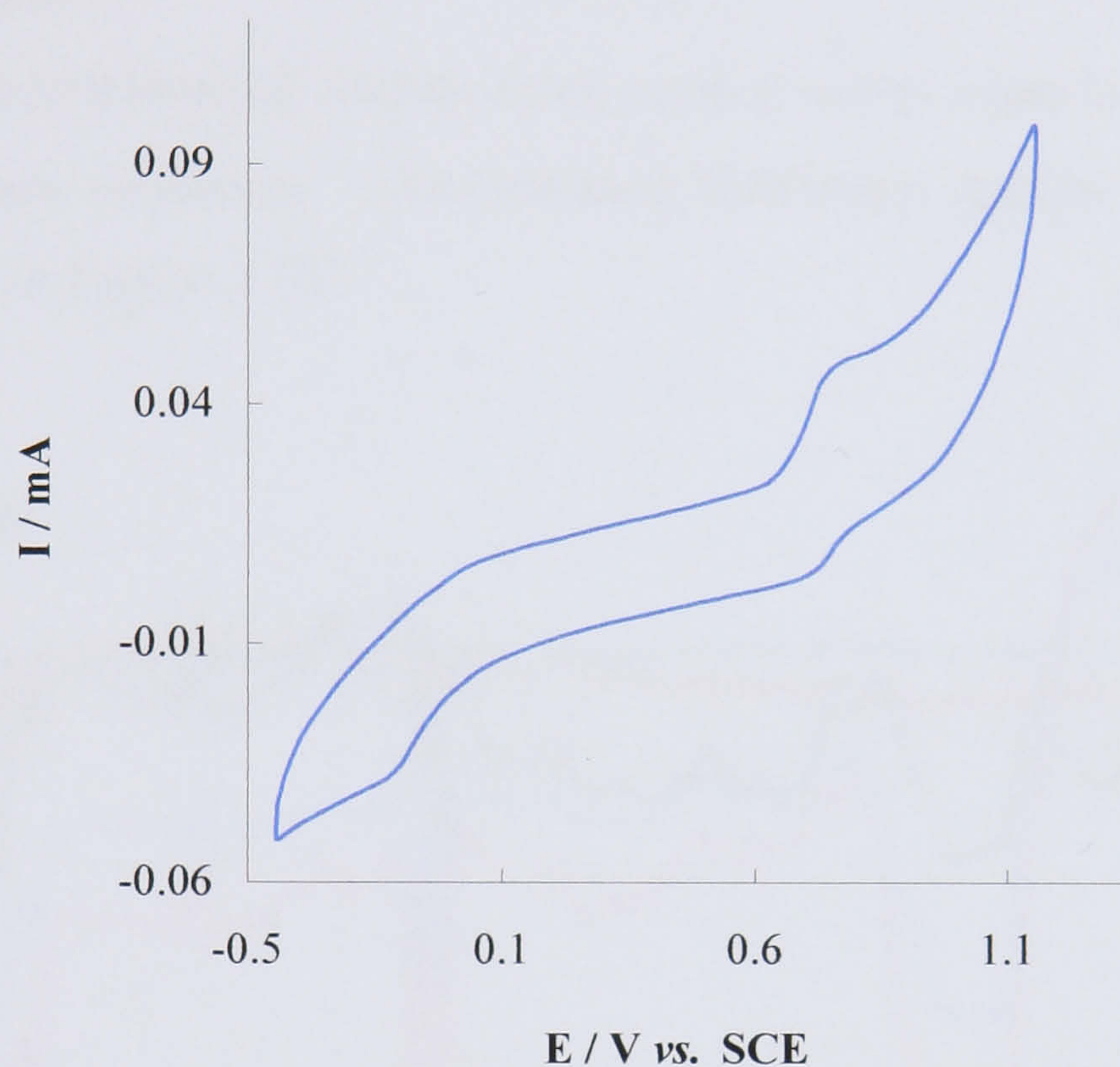


**Figure 3.17** - Cyclic voltammogram of **PDTE-cis** in monomer free solution (0.1 M TBAPF<sub>6</sub>/MECN) recorded at  $\nu = 0.1 \text{ V s}^{-1}$  using a Pt disc working electrode (0.44 cm<sup>2</sup>).

The cyclic voltammogram of **PDTE-cis** shows a one electron redox process at  $E^1_{\text{ox}} = 0.71 \text{ V} / E^1_{\text{red}} = 0.65 \text{ V}$  that can be assigned to the formation of polarons in the polymer chain.<sup>18,19</sup> In contrast with the electrochemical behaviour observed for **PDTE-trans**, the formation of a bipolaronic state at higher potential values cannot be identified by CV. The reduction of **PDTE-cis** occurs at  $E^2_{\text{red}} = -0.17 \text{ V}$  (Figure 3.17). Reproducible voltammograms could only be obtained when cycling in the potential range between -0.6 and 1.3 V. Moreover, **PDTE-cis** would start losing its electroactivity when cycled beyond this potential range. This is a significantly shorter stability interval than the one previously seen in **PDTE-trans** (from -1.0 to 2.0 V). In addition, the oxidation of **PDTE-cis** ( $E^1_{\text{ox}} = 0.71 \text{ V}$ ) is considerably easier than that of the **PDTE-trans** isomer ( $E^1_{\text{ox}} = 0.89 \text{ V}$ ), occurring at a lower potential.



These observations suggest that the electropolymerised **PDTE-cis** is less stable than the **PDTE-trans** isomer. The diminished stability of the *cis* isomer is consistent with reported data for both polyacetylene and poly-dithienylethylene.<sup>69,70</sup> For polyacetylene, the *cis* form was found to be thermodynamically less stable than the *trans* one, undergoing isomerisation upon doping.<sup>71,72</sup> In the case of dithienylethylene, the polymerisation of the *trans* and *cis* isomers has produced the same *trans* polymer.<sup>70</sup>

Spectroelectrochemical studies were carried out to examine the IR properties of **PDTE-cis** upon oxidation. The obtained difference spectra taken from 0.5 to 1.1 V are shown in Figure 3.18.

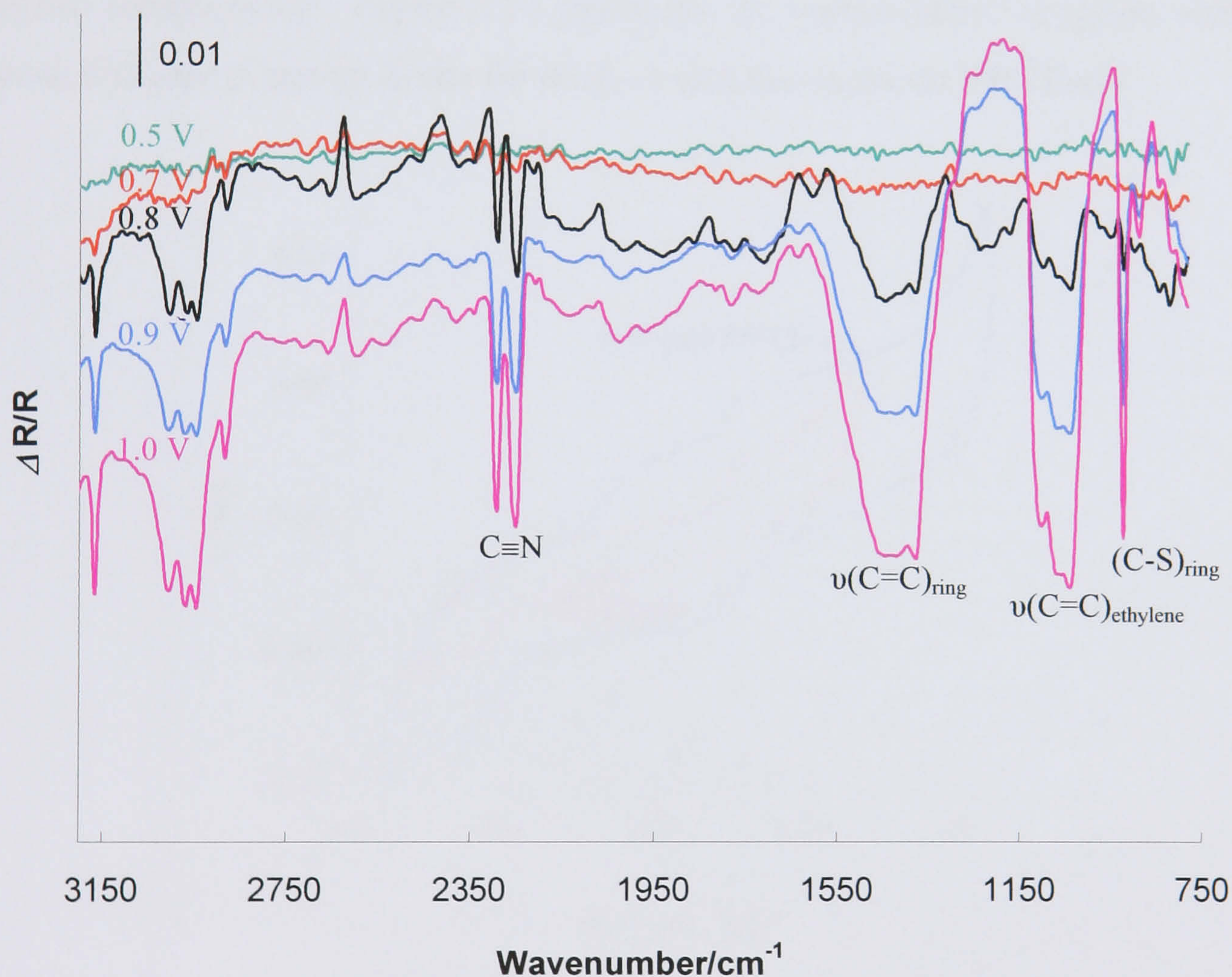


**Figure 3.18** - SNIFTIRS spectra of **PDTE-cis** taken from 0.5 to 1.0 V. Reference spectra collected at 0 V. Spectra were shifted for clarity.

A significant increase of infrared vibrations is observed from 0.8 V, coinciding with the polymer oxidation at  $E_{ox} = 0.71$  V seen in the cyclic voltammogram of **PDTE-cis** (Figure 3.17). Electrolyte absorption peaks appear around 2250 and



$3000\text{ cm}^{-1}$ .<sup>14</sup> Large peaks centred at  $1420$  and  $1056\text{ cm}^{-1}$  are assigned to  $\nu(\text{C}=\text{C})_{\text{ring}}$  and  $\nu(\text{C}=\text{C})_{\text{ethylene}}$ , respectively.<sup>2,43</sup> The broadness of these peaks is probably obscuring  $(\text{C}-\text{C})_{\text{ring}}$  and  $(\text{C}-\text{H})_{\text{ethylene}}$  vibrations expected in this frequency region. Vibration of the C-S bonds in the thiophene rings can be seen at  $923\text{ cm}^{-1}$ .

## Electrochemical and Spectroelectrochemical Studies on

### Iodine-doped PDTE-cis

Chemical doping of **PDTE-cis** was achieved by oxidation with iodine vapour. The doped polymer was washed with acetonitrile to remove any  $\text{I}_2$  excess and studied by cyclic voltammetry. Figure 3.19 illustrates the voltammetric response obtained between different potential limits for the  $\text{I}_2$ -doped and undoped **PDTE-cis**.

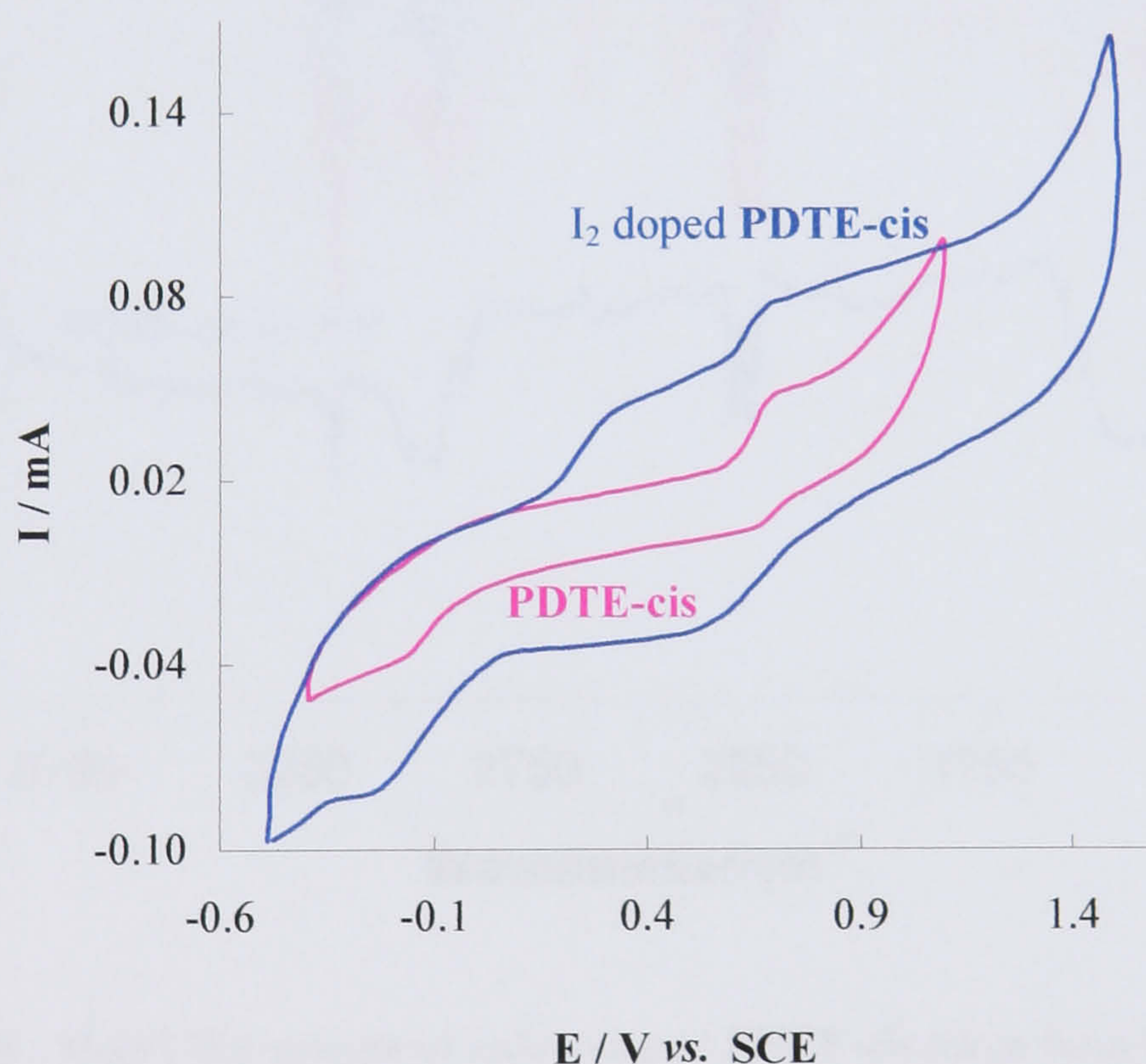


**Figure 3.19** - Cyclic voltammogram of **PDTE-cis** in monomer free solution ( $0.1\text{ M}$   $\text{TBAPF}_6/\text{MECN}$ ) before and after  $\text{I}_2$  doping recorded at  $\nu = 0.1\text{ V s}^{-1}$  using a Pt disc working electrode ( $0.44\text{ cm}^2$ ).

The presence of iodine incorporated into the polymeric film is shown by an oxidation peak at  $E_{\text{ox}} = 0.33\text{ V}$ . The oxidation of **PDTE-cis** does not appear to be affected by the exposure to  $\text{I}_2$  vapour, taking place at  $E_{\text{ox}}^1 = 0.70\text{ V}$ . Two clear



reduction peaks ( $E_{\text{red}}^1 = 0.55 \text{ V}$ ,  $E_{\text{red}}^2 = -0.25 \text{ V}$ ) can be observed at lower potential values in comparison with the ones seen prior to chemical doping. This can imply an increased stability of the p-doped state upon exposure to iodine vapour as already described for  $\text{I}_2$  doped **PDTE-trans**.

The redox behaviour of  $\text{I}_2$  doped **PDTE-cis** film was investigated by SNIFTIRS. The obtained IR spectra taken during the stepwise oxidation are shown in Figure 3.20 alongside with the SNIFTIR spectrum of **PDTE-cis** at 0.9 V.

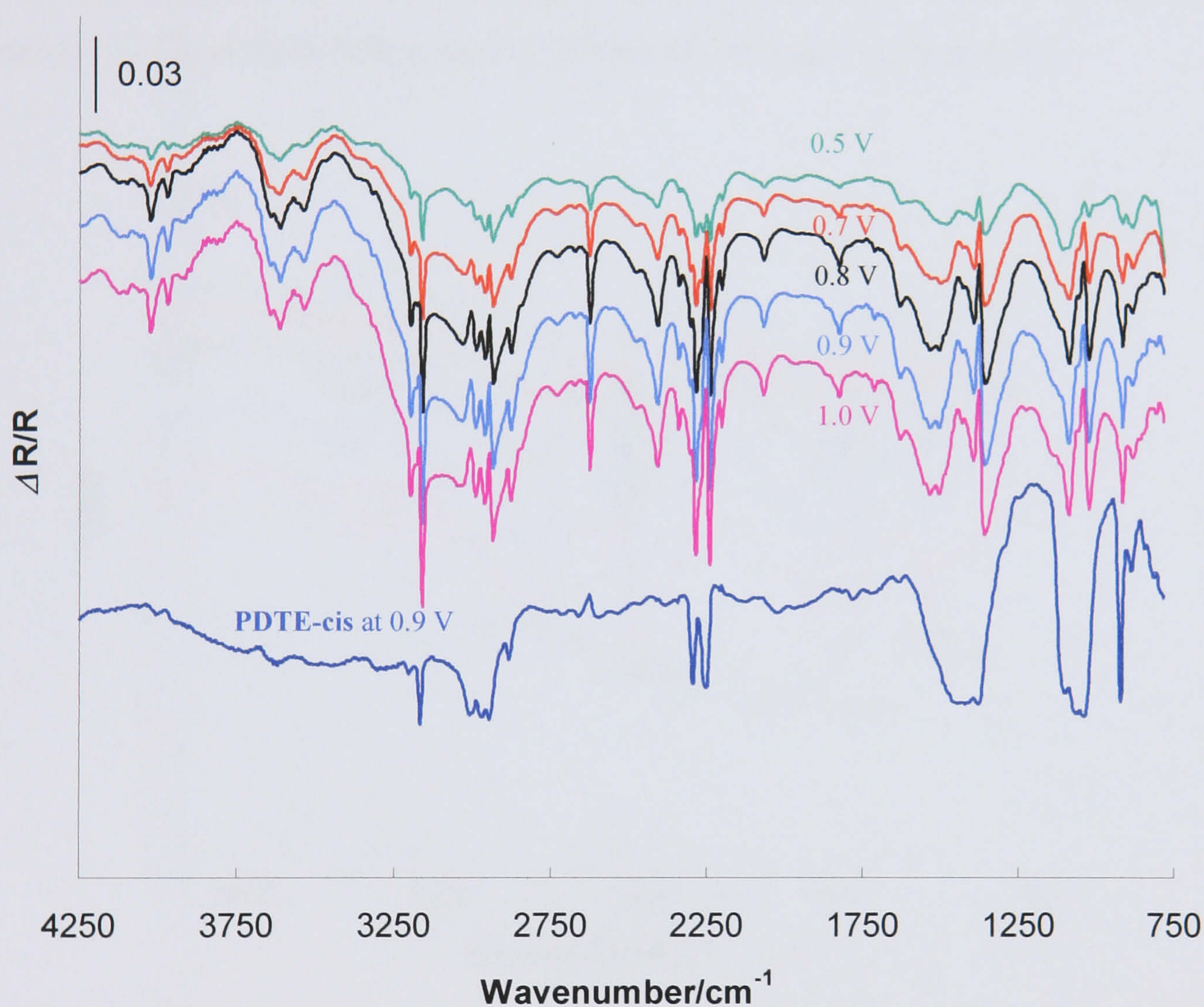


**Figure 3.20** - SNIFTIRS spectra of iodine doped **PDTE-cis** taken from 0.5 to 1.0 V. Reference spectra collected at 0 V. Spectra were shifted for clarity.

From Figure 3.20 it can be seen that the  $\text{I}_2$  doped and the undoped **PDTE-cis** polymers exhibit a relatively similar IR response upon oxidation. In comparison with **PDTE-cis**, the iodine doped film presents much better defined spectra, with sharper infrared absorption peaks. It appears that, the chemical doping with iodine leads to the enhancement of the IR characteristics of the polymer. This might be prompted by the occurrence of morphology changes in the polymeric film, caused by



the charged species introduced through  $I_2$  doping, as previously suggested for  $I_2$  doped **PDTE-trans**. However, in contrast with the spectroelectrochemical response of  $I_2$  doped **PDTE-trans**, the chemical doping of **PDTE-cis** does not lead to the appearance of a baseline drop in the near infrared which is a typical feature of conjugated polymers as they become conductive.

Peaks due to the C=C, C-C and C-S ring vibrations can be seen at 1506, 1355 and 916  $cm^{-1}$ , respectively. A closer look into the SNIFTIR spectra (Figure 3.21) reveals the presence of the C-H out-of-plane deformation and C=C stretching vibration (C=C) of the ethylene unit at 1089 and 1022  $cm^{-1}$ , respectively.

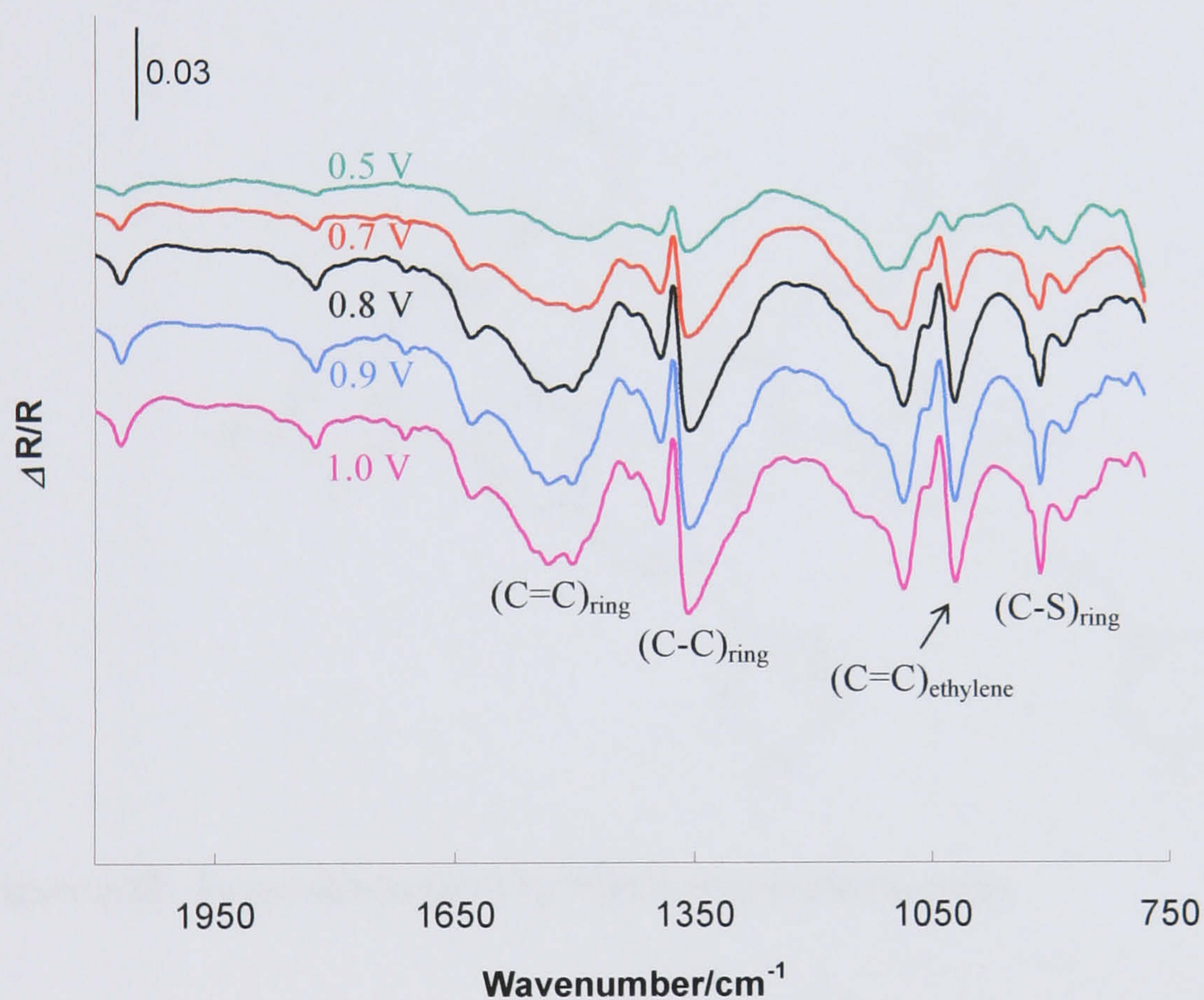


**Figure 3.21** - SNIFTIRS spectra of iodine doped **PDTE-cis** from 2100 to 750  $cm^{-1}$ .

Reference spectra collected at 0 V. Spectra were shifted for clarity.

As the polymer is oxidised, the intensity of the  $\nu(C=C)_{ethylene}$  vibration is considerably increased. This IR behaviour was not observed for **PDTE-trans** either before or after iodine doping indicating that in the *trans* isomer the ethylene bond is not particularly affected by doping. Also, as previously described in this Chapter, upon doping, **PDTE-trans** assumes an IR response characteristic of polythiophenes. This suggests that the ethylene linkage might be involved in the charge transport



mechanism across the polymer chains in **PDTE-cis** but not in **PDTE-trans**. Taking this into account, and bearing in mind that the coupling between the thiophene units occurs mostly through the  $\alpha,\alpha'$ - positions, a possible representation of the **PDTE-cis** and **PDTE-trans** polymer structures is shown in Figure 3.22.

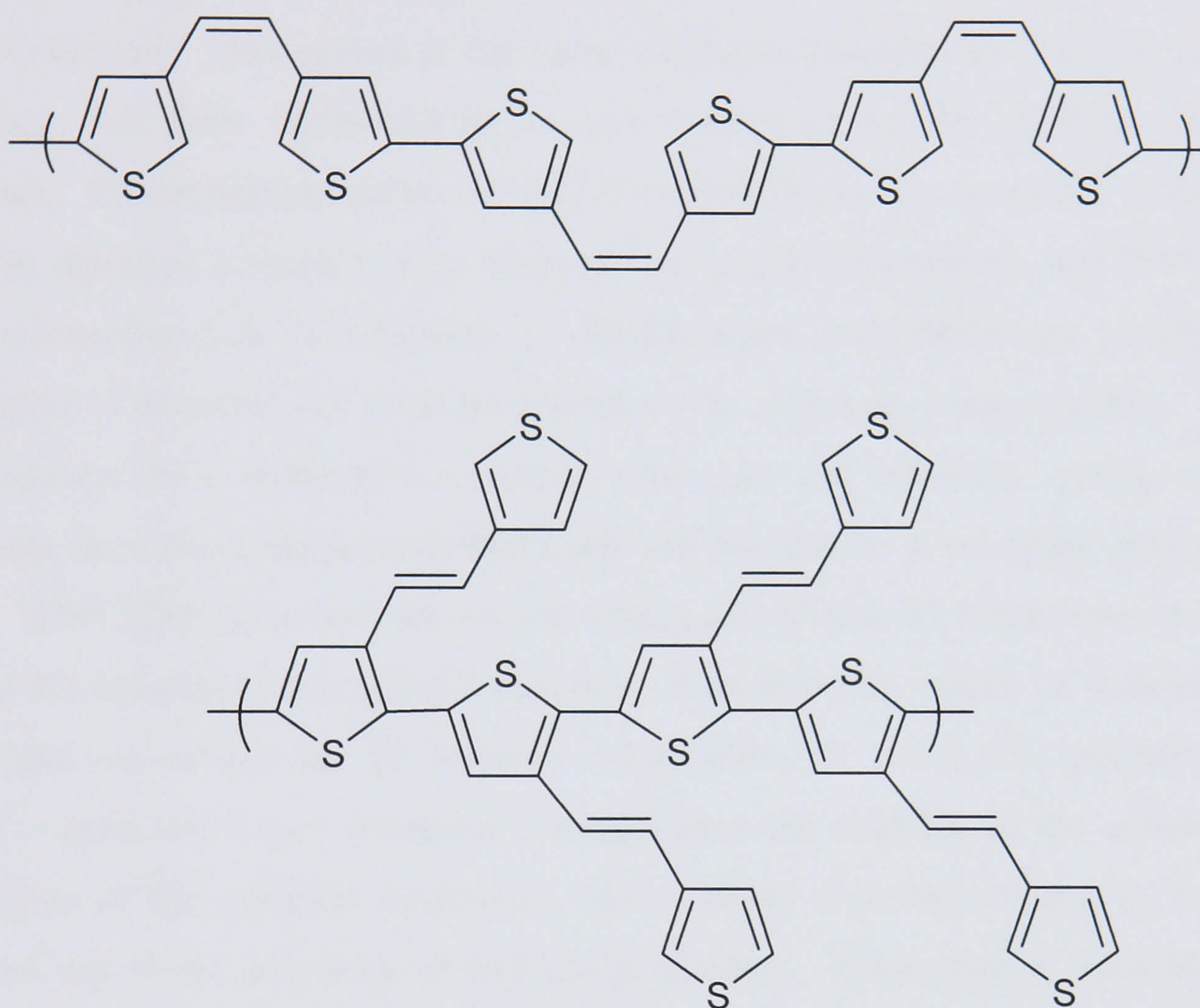


**Figure 3.22** - Proposed structures for **PDTE-cis** and **PDTE-trans**.

Considering the polymer structures suggested in Figure 3.22, charge movement in **PDTE-trans** occurs all the way through the polythiophene backbone, whereas **PDTE-cis** presents a charge transfer mechanism similar, at some extent, to that of polyacetylene in which the ethylene linkage is involved in the movement of electrons.



### 3.4 Conclusions

Electrochemical and spectroelectrochemical investigations have been carried out on two thienylethylene isomers, **DTE-trans** and **DTE-cis**. Their voltammetric study has clearly shown the sequential formation of radical cations and dications upon oxidation. This occurs at the same oxidation potential for the two isomers, implying that their electroactivity is not influenced by the different isomeric structure. Electropolymerisation of both thienylethylenes was successfully achieved and the resultant polymers were analysed by cyclic voltammetry and SNIFTIRS. The electrochemical investigation of **PDTE-trans** and **PDTE-cis** revealed the formation of polarons and even bipolarons as the polymers were oxidised. Taking into account their distinctive oxidation potentials and potential cycling stability intervals, the electropolymerised **PDTE-cis** was found to be a less stable polymer.

SNIFTIRS data have shown the emergence of new IR bands upon p-doping due to the formation of a quinoid structure. However, the spectra of both isomeric films did not exhibit the IR features characteristic of conductive polymers e.g., IRAV – infra red active vibrations (created from the coupling of the quinoid-type vibrations of the polymer backbone), and a broad absorbance band in the near infrared due to the existence of free charge carriers. These lead to the conclusion that only a low conductivity level could be achieved upon electrochemical doping of both **PDTE-trans** and **PDTE-cis**.

In order to improve the electrical properties of the neutral and doped state of **PDTE-trans** and **PDTE-cis**, iodine (an electron acceptor) was used as a chemical p-doping agent.

The comparison between the electrochemical responses of **PDTE-trans** before and after exposure to iodine vapour showed a decrease in the oxidation and reduction potential values upon  $I_2$  doping. These shifts are associated with the presence of  $I_3^-$  ions incorporated into the polymer film, which can induce the existence of partially oxidised areas in **PDTE-trans** promoting the oxidation to polarons and bipolarons. The observed shift in the reduction peak potential towards a more negative value could also imply an increased stability of the p-doped state upon exposure to iodine vapour. Iodine doped **PDTE-trans** has shown a significantly different



spectroelectrochemical behaviour from **PDTE-trans** displaying similar IR characteristics to those of polythiophenes. This might be explained by the occurrence of changes in the polymer morphology caused by charged species introduced through oxidation by  $I_2$ . With  $I_2$  doping, a certain amount of **PDTE-trans** salt was formed and therefore the doped **PDTE-trans** would become an ionomer - a polymer containing ionic groups that have the capability to form intermolecular ionic bonds. Association between these ionic groups would lead to the formation of multiplets with the capability to aggregate and form clusters. This could originate an increase in the conductivity levels since the conducting entity would no longer be a single polymer chain, but rather, many chains. Increased spatial arrangement of the polymeric chains could also lead to a more stabilised doped state which would be responsible for higher conductivity levels.

The iodine doping of **PDTE-cis** brought about a negative shift of the reduction peak potential which could indicate an increased stability of the p-doped state, as previously described for  $I_2$  doped **PDTE-trans**. The SNIFTIRS data have shown an enhancement of the IR characteristics of the polymer upon iodine doping but, in contrast with the spectroelectrochemical behaviour of  $I_2$  doped **PDTE-trans**, the chemical doping of **PDTE-cis** did not seem to trigger the appearance of a baseline drop in the near infrared. The oxidation of  $I_2$  doped **PDTE-cis** caused an increase in the intensity of the  $(C=C)_{\text{ethylene}}$  vibration that could be monitored by SNIFTIRS. This IR behaviour has not been observed in **PDTE-trans** either before or after iodine doping indicating that in the *trans* isomer the ethylene bond is not particularly affected by doping. This has led to the suggestion that the ethylene linkage should be involved in the charge transport mechanism across the polymer chains in the **PDTE-cis** film but not in **PDTE-trans**. Therefore, it was proposed that the charge movement in **PDTE-trans** should occur all the way through the polythiophene backbone whereas **PDTE-cis** exhibits a charge-transfer mechanism resembling that of polyacetylene.



### 3.5 References

1. J. Roncali, *Chem. Rev.*, 97 (1997) 173.
2. S. Yamada, S. Tokito, T. Tsutsui and S. Saito, *J. Chem. Soc., Chem. Commun.*, 19 (1987) 1448.
3. J. Roncali, *Acc. Chem. Res.*, 33 (2000) 147.
4. J. Roncali, C. Thobie-Gautier, E.H. Elandaloussi and P. Frere, *J. Chem. Soc., Chem. Commun.*, (1994) 2249.
5. Y. Fu, H. Cheng and R.L. Elsenbaumer, *Chem. Mater.*, 9 (1997) 1720.
6. P. Blanchard, H. Brisset, B. Illien, A. Riou and J. Roncali, *J. Org. Chem.*, 62 (1997) 2401.
7. J.R. Smith, N.M. Ratcliffe and S.A. Campbell, *Synth. Met.*, 73 (1995) 171.
8. J. Guay, P. Kasai, A. Diaz, R. Wu, J.M. Tour and L.H. Dao, *Chem. Mater.*, 4 (1992) 1097.
9. I. Jestin, P. Frere, N. Mercier, E. Levillain, D. Stievenard and J. Roncali, *J. Am. Chem. Soc.*, 120 (1998) 8150.
10. G. Zotti, G. Schiavon, A. Berlin and G. Pagani, *Chem. Mater.*, 5 (1993) 430.
11. A. Berlin and G. Zotti, *Synth. Met.*, 106 (1999) 197.
12. P. Audebert, J. Catel, G. Coustumer, V. Duchenet and P. Hapiot, *J. Phys. Chem.*, 99 (1995) 11923.
13. R.G. Hicks and M.B. Nodwell, *J. Am. Chem. Soc.*, 122 (2000) 6746.
14. C. Kvarnstrom, H. Neugebauer, S. Blomquist, H.J. Ahonen, J. Kankare and A. Ivaska, *Electrochim. Acta*, 44 (1999) 2739.
15. J.R. Reynolds, J.P. Ruiz, A.D. Child, K. Nayak and D.S. Marynick, *Macromolecules*, 24 (1991) 678.
16. Y. Wei, C. Chan, J. Tian, G. Jang and K. Hsueh, *Chem. Mater.*, 3 (1991) 888.
17. A. Yassar, J. Roncali and F. Garnier, *Macromolecules*, 22 (1989) 804.
18. J.M. Pringle, M. Forsyth, D.R. MacFarlane, K. Wagner, S.B. Hall and D.L. Officer, *Polymer*, 46 (2005) 2047.
19. C. Jerome, C. Maertens, M. Mertens, R. Jerome, C. Quattrocchi, R. Lazzaroni and J.L. Bredas, *Synth. Met.*, 83 (1996) 103.
20. X. Chen and O. Inganas, *J. Phys. Chem.*, 100 (1996) 15202.



21. H.S. Nalwa, ed., "Handbook of organic conductive molecules and polymers - Conductive polymers: Spectroscopy and Physical Properties". Vol. 3, J. Wiley & Sons Ltd., UK, (1997).
22. G. Zotti, G. Schiavon and S. Zecchin, *Synth. Met.*, 72 (1995) 275.
23. V. Seshadri, L. Wu and G.A. Sotzing, *Langmuir*, 19 (2003) 9479.
24. O.A. Semenikhin, E.V. Ovsyannikova, M.R. Ehrenburg, N.M. Alpatova and V.E. Kazarinov, *J. Electroanal. Chem.*, 494 (2000) 1.
25. T.A. Skotheim, ed., "Handbook of Conducting Polymers", Vol. 1, Marcel Dekker Inc., New York, (1986).
26. M. Onoda, S. Iwasa, H. Nakayama, K. Yoshino and M. Laguna, *J. Chem. Phys.*, 95 (1991) 8584.
27. U. Schlick, F. Teichert and M. Hanack, *Synth. Met.*, 92 (1998) 75.
28. L.M.H. Groenewoud, G.H.M. Engbers, R. White and J. Feijen, *Synth. Met.*, 125 (2001) 429.
29. P. Frere, J. Raimundo, P. Blanchard, J. Delaunay, P. Richomme, J. Sauvajol, J. Orduna, J. Garin and J. Roncali, *J. Org. Chem.*, 68 (2003) 7254.
30. W. Hayes, F.L. Pratt, K.S. Wong, K. Kaneto and K. Yoshino, *J. Phys. C: Solid State Phys.*, 18 (1985) 555.
31. M. Pohjakallio, G. Sundholm and P. Talonen, *J. Electroanal. Chem.*, 401 (1996) 191.
32. B. Rasch and W. Vielstich, *J. Electroanal. Chem.*, 370 (1994) 109.
33. J.T. Lopez Navarrete, V. Hernandez, J. Casado, L. Favaretto and G. Distefano, *Synth. Met.*, 101 (1999) 590.
34. J. Casado, H.E. Katz, V. Hernandez and J.T. Lopez Navarrete, *Vibrational Spectroscopy*, 30 (2002) 175.
35. S. Hotta, S. Rughooputh, A.J. Heeger and F. Wudl, *Macromolecules*, 20 (1987) 212.
36. K.B. Becker, *Tetrahedron*, 36 (1980) 1717.
37. M. Pomerantz, Y. Cheng, R.K. Kasim and R.L. Elsenbaumer, *Synth. Met.*, 85 (1997) 1235.
38. M. Kofranek, T. Kovar, H. Lischka and A. Karpfen, *J. Molec. Struct.: THEOC.*, 259 (1992) 181.



39. C. Ehrendorfer, H. Neugebauer, A. Neckel and P. Bauerle, *Synth. Met.*, 55 (1993) 493.
40. O.S. Roshchupkina, O.N. Efimov and L.I. Tkachenko, *Synth. Met.*, 90 (1997) 89.
41. J. Casado, J.J.M. Puig, V. Hernandez, G. Zotti and J.T.L. Navarrete, *J. Phys. Chem.*, 104 (2000) 10656.
42. P. Camurlu, A. Cirpan and L. Toppare, *Mat. Chem. Phys.*, 92 (2005) 413.
43. G. Louarn, J.-Y. Mevellec, J.P. Buisson and S. Lefrant, *Synth. Met.*, 55 (1993) 587.
44. G.O. Williams, Ph.D. Thesis, University of Wales, Bangor (1999).
45. J.T. Lopez Navarrete, J. Casado, H. Muguruma, S. Hotta and V. Hernandez, *J. Mol. Struct.*, 521 (2000) 239.
46. D. Kumar, *Synth. Met.*, 114 (2000) 369.
47. C. Ehrendorfer, A. Karpfen, P. Bauerle, H. Neugebauer and A. Neckel, *J. Mol. Struct.*, 298 (1993) 65.
48. F. Cataldo, *Polymer Degradation and Stability*, 60 (1998) 223.
49. D.N. Tito, Ph.D. Thesis, University of Wales, Bangor (2005).
50. H.S.O. Chan and S.C. Ng, *Prog. Polym. Sci.*, 23 (1998) 1167.
51. H. Neugebauer, *J. Electroanal. Chem.*, 563 (2004) 153.
52. M.R. Fernandes, J.R. Garcia, M.S. Schultz and F.C. Nart, *Thin Solid Films*, 474 (2005) 279.
53. E. Lankinen, G. Sundholm, P. Talonen, T. Laitinen and T. Saario, *J. Electroanal. Chem.*, 447 (1998) 135.
54. G. Tourillon and F. Garnier, *J. Electrochem. Soc.*, 130 (1983) 2042.
55. H.A.M. van Mullekom, J.A.J.M. Vekemans, E.E. Havinga and E.W. Meijer, *Mat. Sci. Eng. R* 32 (2001) 1.
56. C.K. Chiang, C.R. Fincher, Y.W. Park, A.J. Heeger, H. Shirakawa, E.J. Louis, S.C. Gau and A.G. MacDiarmid, *Phys. Rev. Lett.*, 39 (1977) 1098.
57. T. Yamabe, K. Tanaka, H. Terama-e, K. Fukui, A. Imamura, H. Shirakawa and S. Ikeda, *J. Phys. C Solid State* 12 (1979) 257.
58. Y. Furukawa, *J. Phys. Chem.*, 100 (1996) 15644.
59. J.W. Hall and G.A. Arbuckle, *Macromolecules*, 29 (1996).



60. W.W. Chiu, J. Travas-Sejdic, R.P. Cooney and G.A. Bowmaker, *Synth. Met.*, 155 (2005) 80.
61. M.D. Levi, M.A. Vorotyntsev, A.M. Skundin and V.E. Kazarinov, *J. Electroanal. Chem.*, 319 (1991) 243.
62. T. Yamamoto, M. Omote, Y. Miyazaki, A. Kashiwazaki, B. Lee, T. Kanbara, K. Osakada, T. Inoue and K. Kubota, *Macromolecules*, 30 (1997) 7158.
63. K. Tashiro, M. Kobayashi, T. Kawai and K. Yoshino, *Polymer*, 38 (1997) 2867.
64. E.E. Havinga and C.M.J. Mutsaers, *Chem. Mater.*, 8 (1996) 769.
65. P.A. Christensen, A. Hamnett, A.R. Hillman, M.J. Swann and S.J. Higgins, *J. Chem. Soc. Faraday Trans.*, 88 (1992) 595.
66. D.Y. Zhang and T.L. Porter, *Synth. Met.*, 74 (1995) 55.
67. N. Sato, Y. Mazaki, K. Kobayashi and T. Kobayashi, *J. Chem. Soc. Perkin Trans*, 2 (1992) 765.
68. G. Tourillon and F. Gamier, *J. Polym. Sci.*, 22 (1984) 33.
69. K. Song, M. Peng, M. Xu, L. Wu, L. Zhang and C. Tung, *Tetrahedron Lett.*, 43 (2002) 6633.
70. M. Onoda, T. Iwasa, T. Kawai, K. Yochino, *J. Phys. Soc. Jpn.*, 60 (1991) 3768.
71. A. Patil, A.J. Heeger and F. Wudl, *Chem. Rev.*, 88 (1988) 183.
72. H. Shirakawa, *Synth. Met.*, 125 (2001) 3.



## **Chapter 4**

# **Studies on Thiophene**

## **Dithiolenes**



## 4.1 Introduction

Electrochemical and spectroelectrochemical studies have been carried out on the thiophene dithiolenes shown in Figures 4.01 - 4.02. With the exception of **Th-3,3Me**, which has two methyl groups, these thiophene derivatives only differ by the substitution pattern on the thiophene rings.

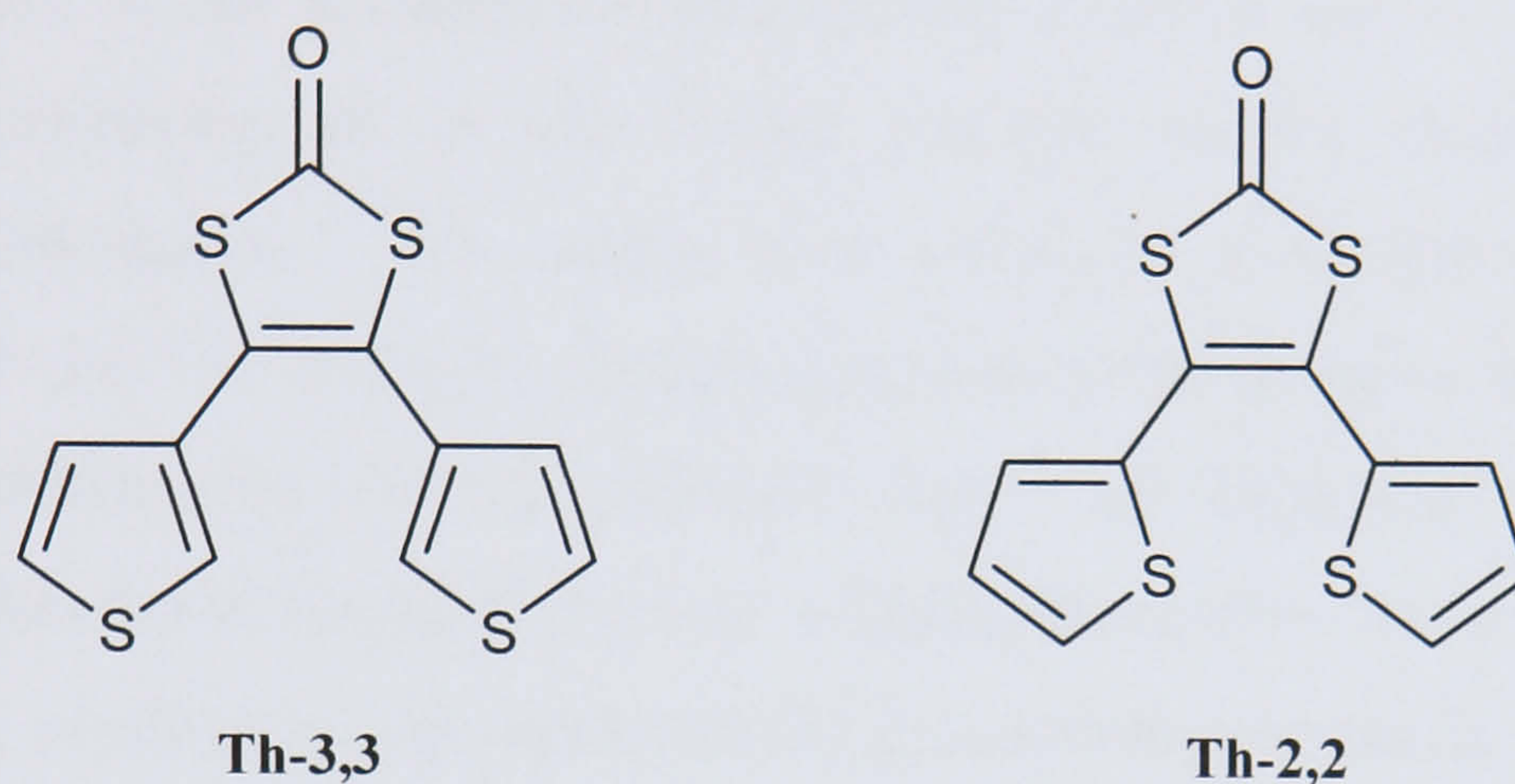


**Figure 4.01** - Structures of 4,5-di-thiophen-3-yl-[1,3]dithiol-2-one **Th-3,3** and 4,5-di-thiophen-2-yl-[1,3]dithiol-2-one **Th-2,2**.

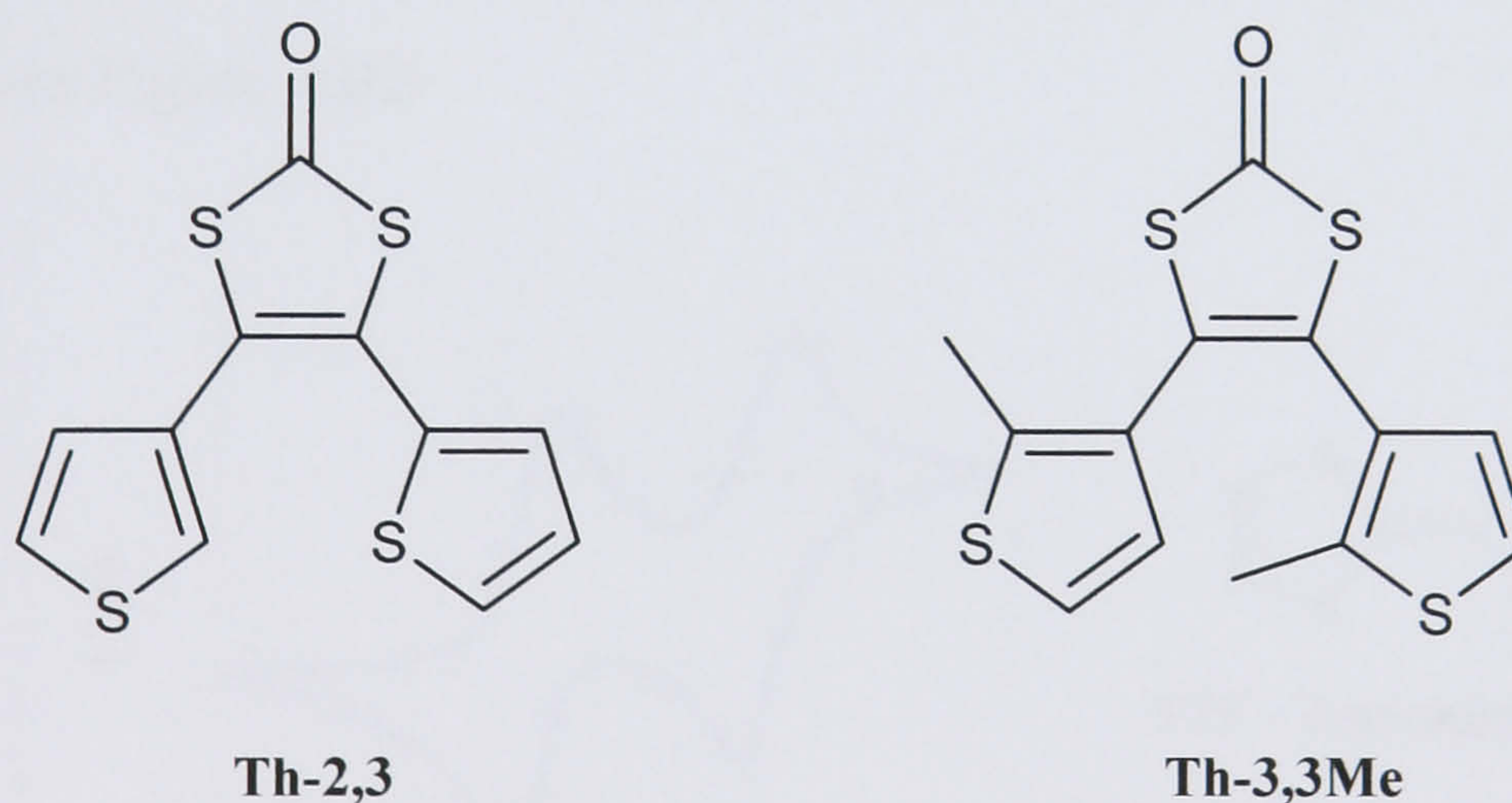


**Figure 4.02** - Structure of 4-thiophen-3-yl-5-thiophen-2-yl-[1,3]dithiol-2-one **Th-2,3** and 4,5-di-(5-methyl-thiophen-3-yl)-[1,3]dithiol-2-one **Th-3,3Me**.

Comparing with the structure of the thienylethylene **DTE-cis**, discussed in Chapter Three, these are a more complex type of thiophene derivatives due to the 1,3-dithiol-2-one unit. It was envisaged that its presence would allow the formation of a planar polymeric system where the two thiophenes adopt a restricted



*cis*-conformation. Such polymeric structure could extend  $\pi$ -conjugation along the polymer backbone, allowing an efficient electron delocalisation and therefore, enhance conductivity levels.

The polymerisation of the thiophene dithiolenes shown in Figure 4.01 and Figure 4.02 has been carried out potentiodynamically and the properties of the resultant films (**PTh-3,3**, **PTh-2,2**, **PTh-2,3** and **PTh-3,3Me**) analysed by CV, SNIFTIRS and UV-Visible spectroscopy.

Another aim of the research comprising this Chapter was to investigate the possibility of performing an *in situ* Wittig reaction on the electropolymerised polythiophene dithiolenes. This would give access to a thiophene based TTF polymer in which the TTF moiety is directly attached to the polymer backbone. The concept of combining the ordered polymers based on thiophene with the high conductivities observed in doped TTFs into a single framework opens the possibility to develop highly conducting and mechanically processable polymeric systems.<sup>1-3</sup>

The ability for TTF and its derivatives to behave as reversible electron donors, forming stable radical cations and dications upon oxidation, makes them ideal components in charge transfer complexes. The voltammetric response of compounds containing TTF units exhibits the characteristic TTF redox couples as shown by the voltammogram in Figure 4.03.

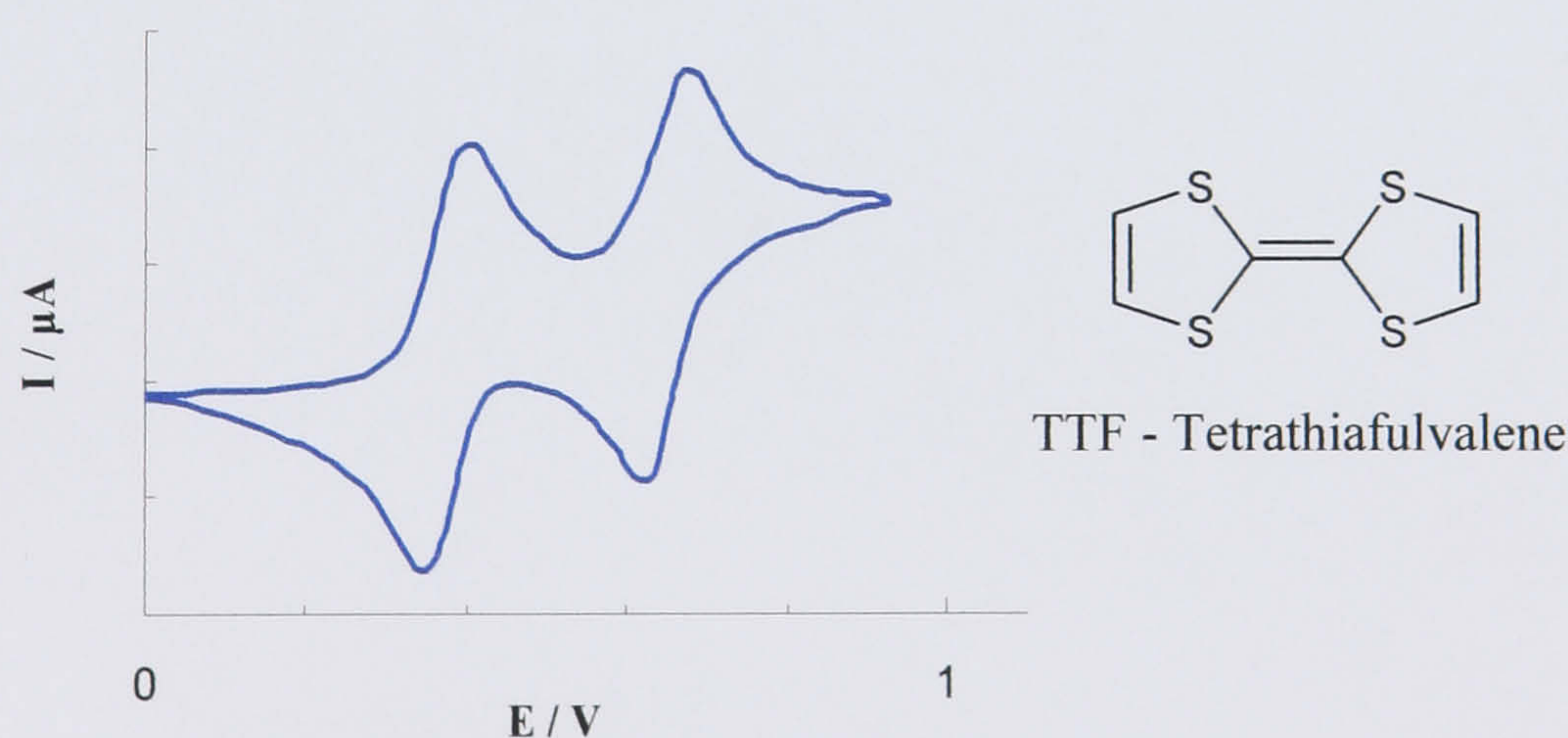


**Figure 4.03** - Typical voltammogram of a compound containing the TTF unit.<sup>4</sup>

For the TTF unit, the standard literature potentials for the oxidation to radical cation and dication are  $E_{1/2}^1 = 0.34$  V and  $E_{1/2}^2 = 0.71$  V ( $E_{1/2}$  refers to the half wave potentials – potentials mid-way between the oxidation and reduction peaks).<sup>5,6</sup>



## 4.2 Experimental

Cyclic voltammetry has been used to study the thiophene dithiolenes presented in Figure 4.01 and Figure 4.02, in order to attempt their electropolymerisation and characterise the resultant polymers. The electrochemical growth of polymeric films has been carried out potentiodynamically by cycling the electrode potential in an electrolyte solution (0.1 M TBAPF<sub>6</sub> / MeCN) containing monomer units (0.01 M). A silver wire immersed in a solution of AgNO<sub>3</sub> (0.01 M) in the same electrolyte solution was used as the reference electrode (+ 0.32 V vs. SCE).

The spectroelectrochemical investigation of polythiophene dithiolenes has been performed using SNIFTIRS and UV-Visible spectroscopy. The experimental procedure followed was described in Chapter Two.

Chemical modification of the polythiophene dithiolenes has been carried out at 0 °C using the Wittig reaction under inert conditions. All solvents used in the modification procedure have been previously dried by standard methods.<sup>7</sup> The modification of polythiophene dithiolenes took place over a period of 24 h, after which the resulting polymers were carefully washed with acetonitrile and analysed by CV and SNIFTIRS.



## 4.3 Results and Discussion

### 4.3.1 Studies on Thiophene Dithiolene Th-3,3

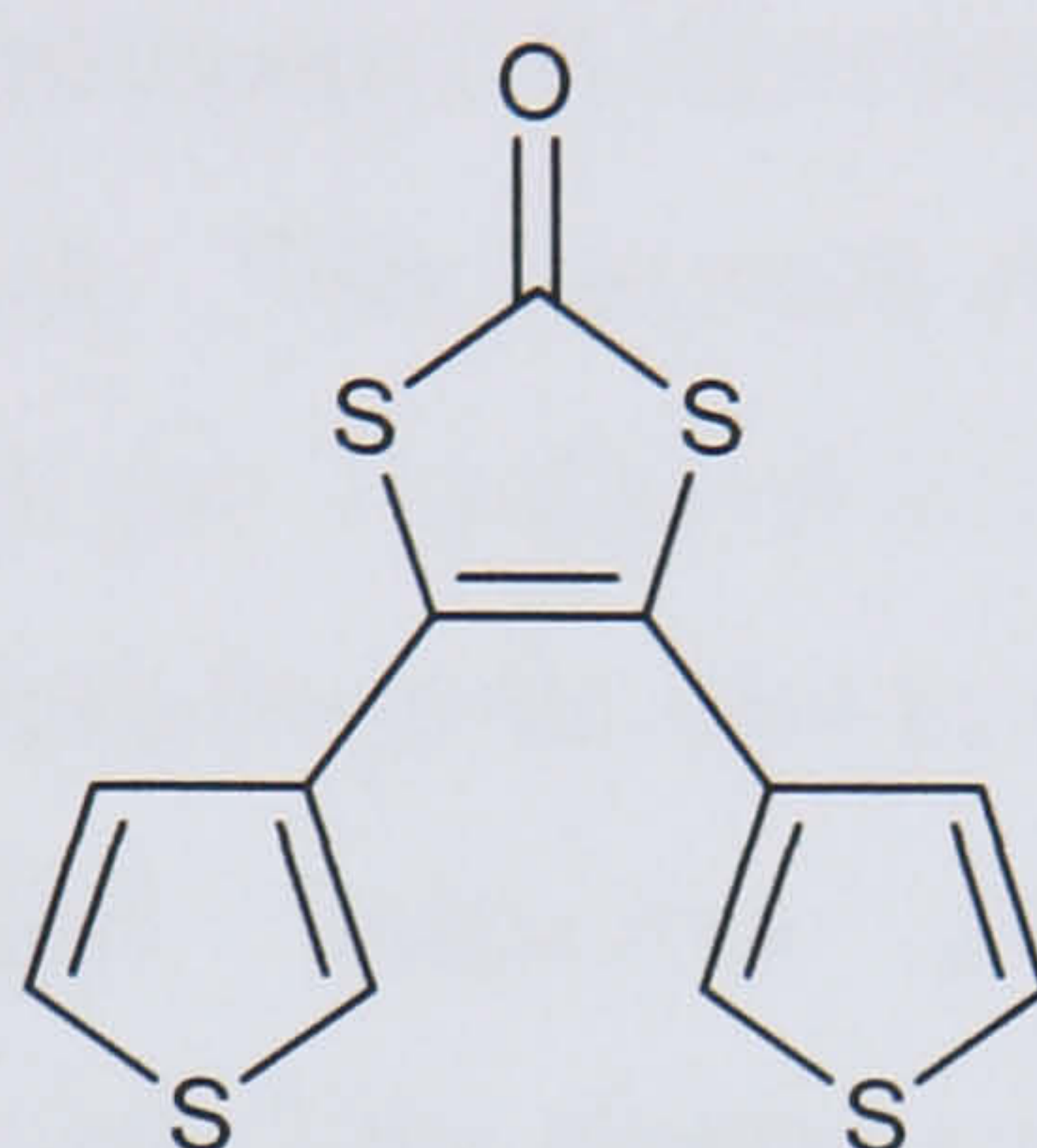


Figure 4.04 - Structure of 4,5-di-thiophen-3-yl-[1,3]dithiol-2-one **Th-3,3**.

#### Electrochemical Studies

A solution of thiophene dithiolene **Th-3,3** was analysed by cyclic voltammetry. Polymerisation was successfully achieved by cycling the electrode potential between 0.8 and 1.7 V as shown in the Figure 4.05:

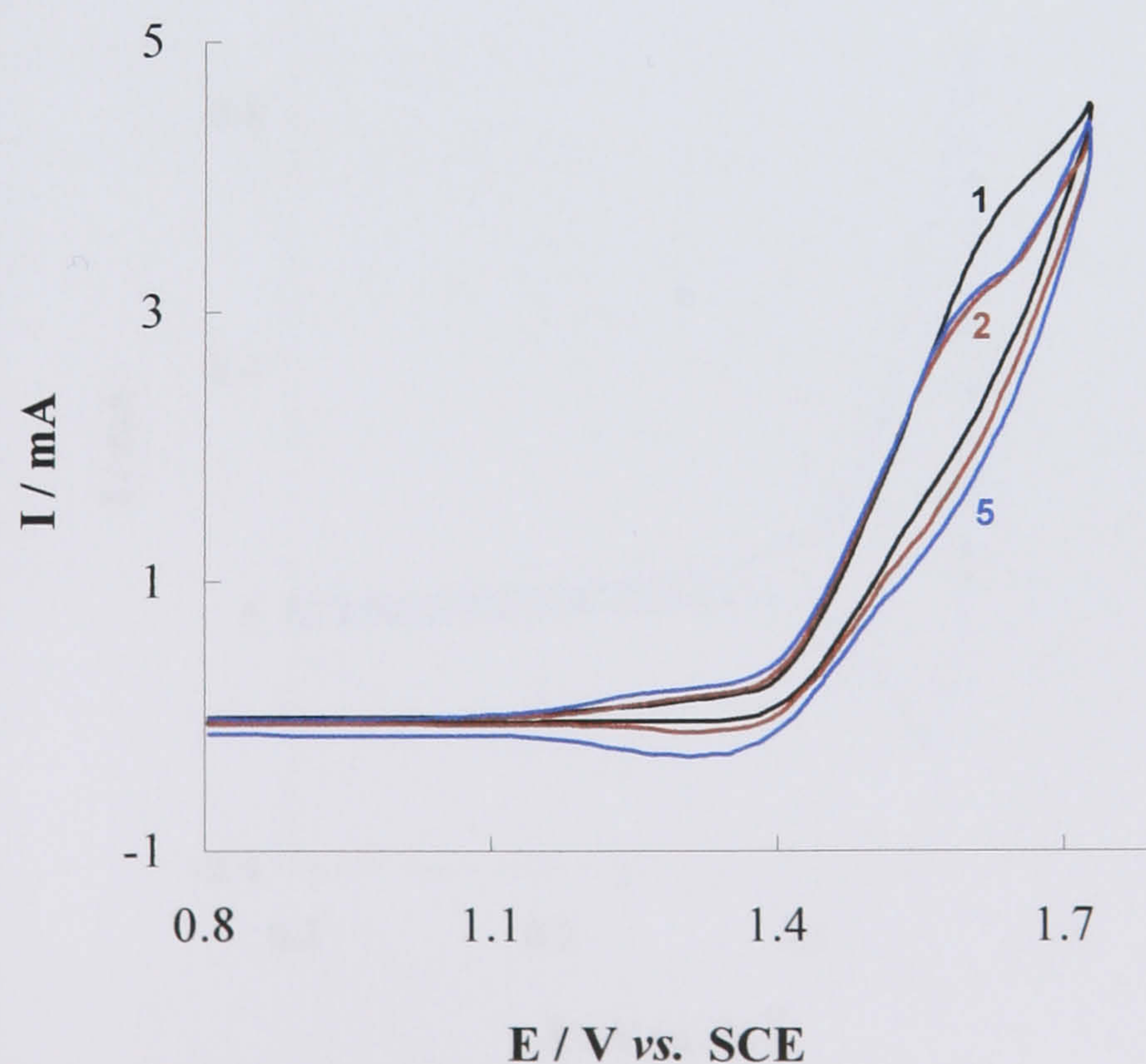
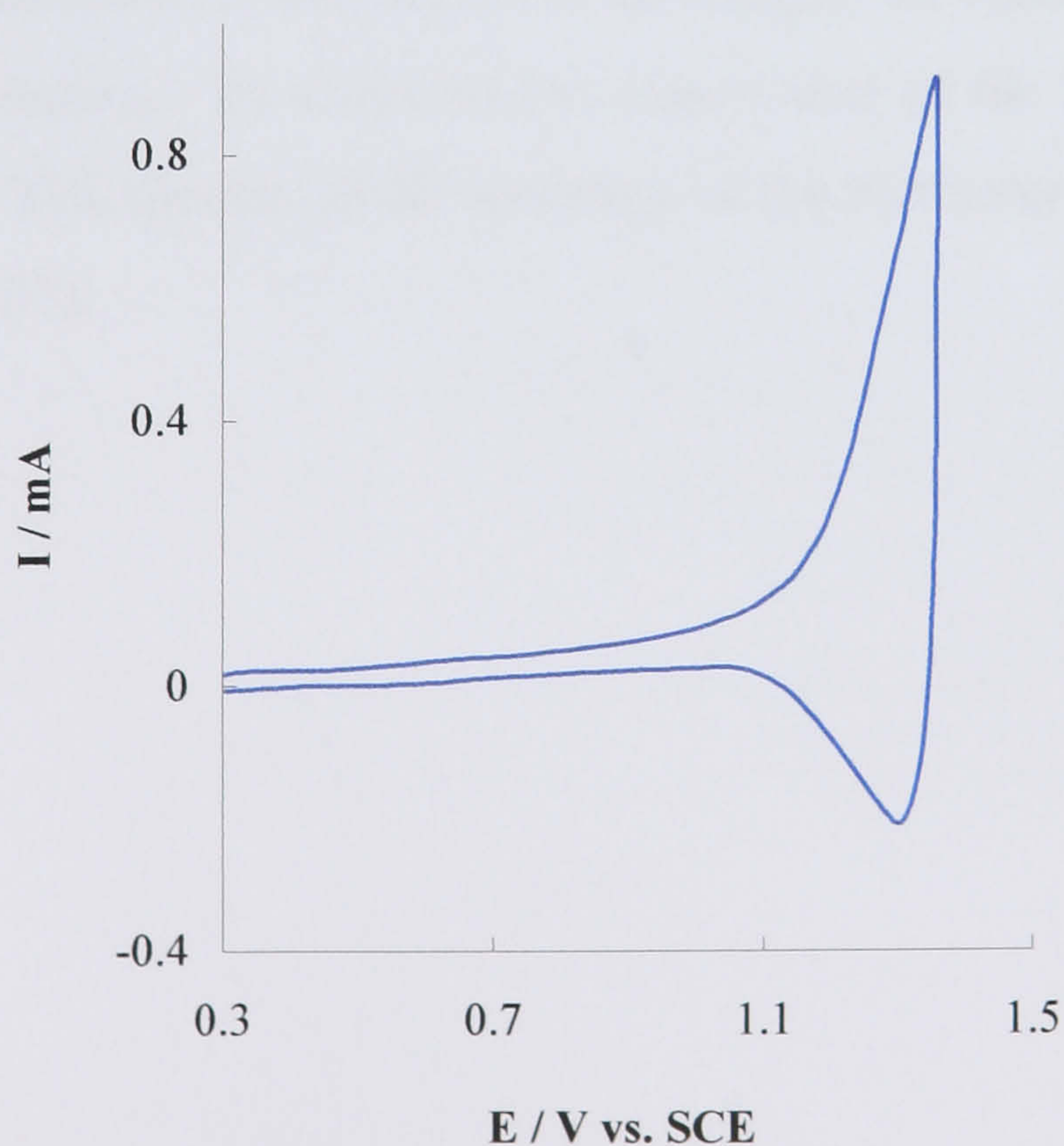


Figure 4.05 - Voltammograms of the polymerisation of **Th-3,3**, recorded at  $0.1 \text{ V.s}^{-1}$  (1<sup>st</sup>, 2<sup>nd</sup> and 5<sup>th</sup> cycles).



The first cycle shows that the oxidation of **Th-3,3** commences at about 1.4 V during the positive sweep with a peak appearing at 1.64 V owing to the formation of the monomer radical cation. This process is irreversible indicating that, as reported for many thiophenes, the radical cation formed upon oxidation is unstable and extremely reactive.<sup>8-10</sup> In comparison with the electrochemical response of thiophene derivative **DTE-cis**, presented in Chapter Three, the oxidation of **Th-3,3** occurs at higher potential values. This potential shift is likely to be caused by the electron withdrawing nature of the 1,3-dithiol-2-one unit. Figure 4.05 shows a decrease in the anodic peak current from the first to the second cycle, increasing then onwards. This electrochemical behaviour has been observed for the dithienylethylenes studied in the previous chapter and can be attributed to the need to initially form nuclei at the electrode surface.

Upon consecutive cycles, a gradual increase in the current intensity is seen, implying a continuous growth of material on the electrode.<sup>11,12</sup> The resultant polymer film was carefully washed in acetonitrile in order to remove the excess monomer and its electroactivity was investigated in a monomer-free electrolyte solution. Figure 4.06 shows the voltammetric response obtained between 0.3 and 1.35 V.



**Figure 4.06** - Cyclic voltammogram of **PTh-3,3** in monomer free solution recorded at  $\nu = 0.1 \text{ V}\cdot\text{s}^{-1}$  using a Pt disc working electrode ( $0.44 \text{ cm}^2$ ).



Polymer oxidation occurs when the potential is taken from 1.08 to 1.35 V. A clear reduction peak can then be seen in the reverse scan at 1.22 V. The film was cycled repeatedly between the -1.5 and 2.1 V without any significant loss of electroactivity.

The switching of **PTh-3,3** between the neutral and oxidised state was accompanied by a reversible colour change from yellow (neutral polymer) to black (oxidised polymer). The reversible change in colour of polythiophenes upon electrochemical doping has been well documented.<sup>13-16</sup> This phenomenon, generally referred to as electrochromism, results from the generation of different visible electronic absorption bands upon switching between redox states.<sup>17</sup> Whereas in the neutral state, the colour is determined by the band gap of the polymer, as electrons are added or removed (doping), new electronic states are formed in the band gap, giving rise to optical absorption at energies lower than the original band gap.<sup>12,18</sup>

### SNIFTIRS Studies

SNIFTIRS studies were carried out to investigate the changes in the IR spectra of **PTh-3,3** upon doping. To facilitate the assignment of the IR absorption peaks present in the SNIFTIR spectra, an IR spectrum of the monomer **Th-3,3** was initially recorded (Figure 4.07).



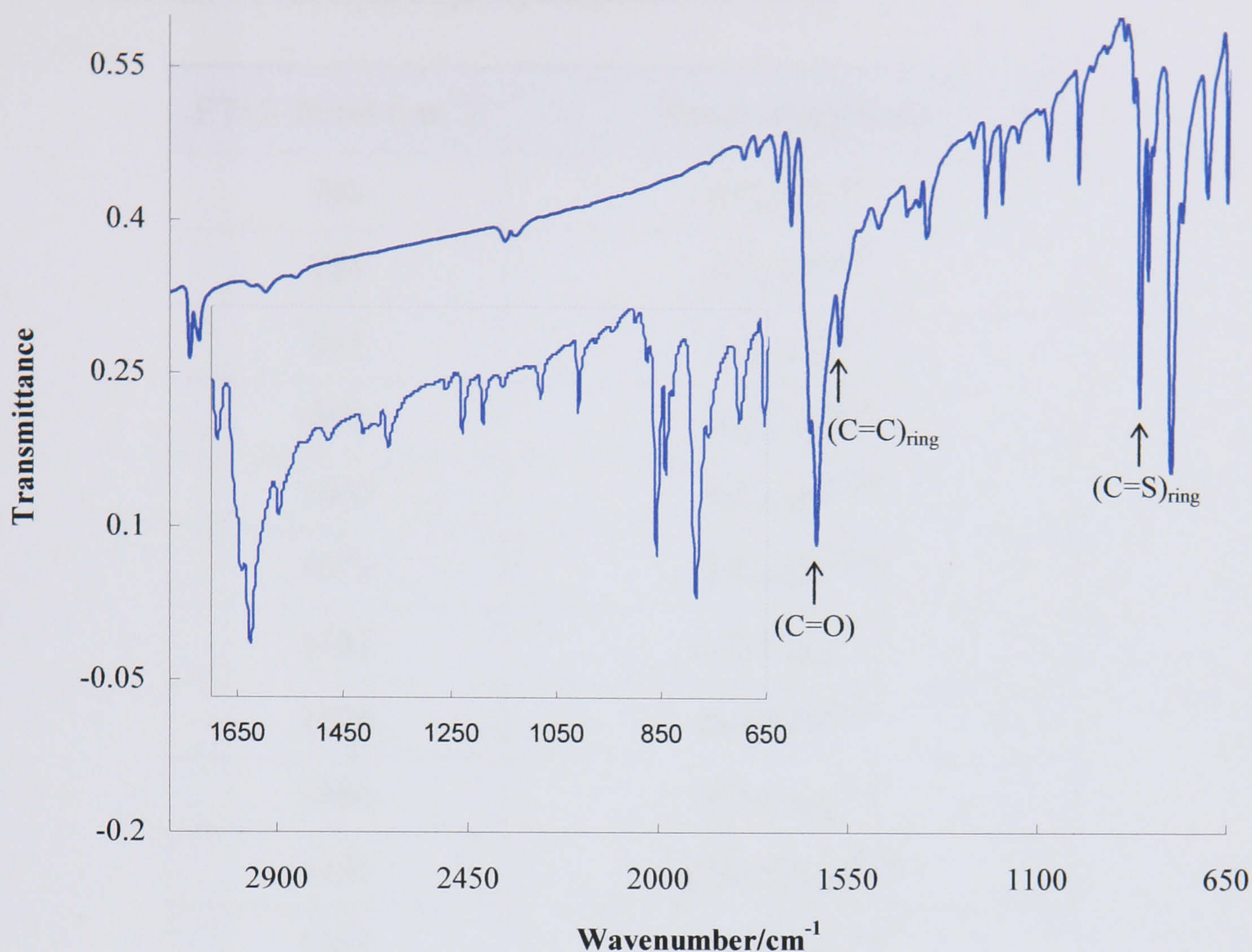


**Figure 4.07** - Infrared spectrum of **Th-3,3** in KBr disc pellet and expansion of the IR spectrum between 1650 and 650  $\text{cm}^{-1}$ .

As expected, the spectrum of **Th-3,3** displays some similarities with the IR absorption spectrum of **DTE-cis**, showing peaks at 3103 and 3081  $\text{cm}^{-1}$  assigned to  $\text{C}_\alpha\text{-H}$  and  $\text{C}_\beta\text{-H}$  stretching vibrations, respectively.<sup>19,20</sup> The C-S stretching vibrations can be found at 859 and 841  $\text{cm}^{-1}$ . A strong peak arising from the C=O stretching is seen at 1630  $\text{cm}^{-1}$ . Smaller bands at 1571 and 1481  $\text{cm}^{-1}$  are assigned to the C=C ring vibration.<sup>4,21</sup>

The main IR bands for **Th-3,3** and their assignment are outlined in the following table ( $\nu$  – stretching,  $\delta$  – in-plane deformation,  $\gamma$  – out-of-plane deformation,  $s$  – symmetric and  $as$  – asymmetric).



Table 4.01 – FTIR bands frequency assignments for Th-3,3.

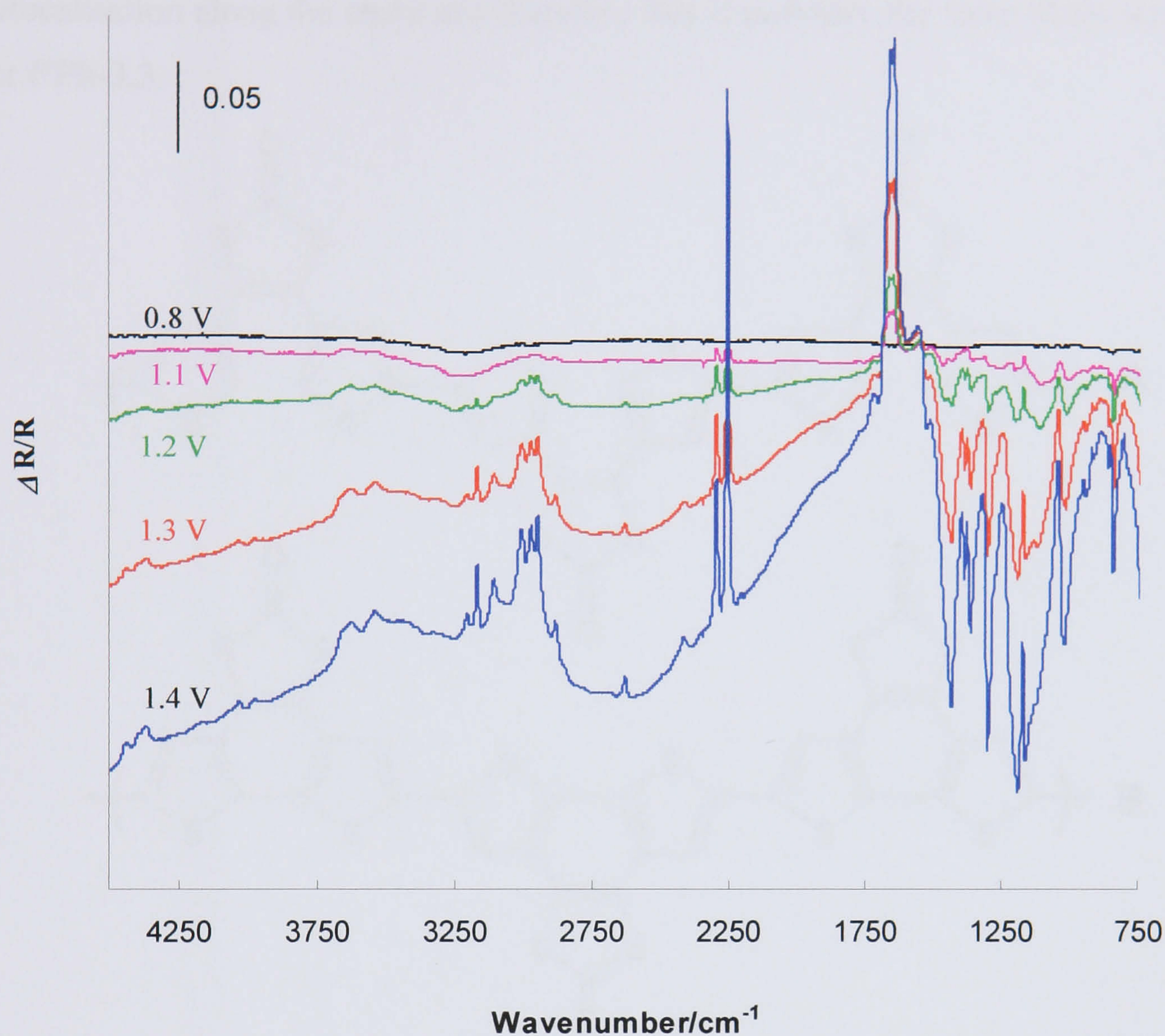
FTIR Band (cm <sup>-1</sup> )	Band assignment
703	$\gamma(\text{C}_\alpha\text{-H})^{22,23}$
784	$\gamma(\text{C}_\beta\text{-H})^{24,25}$
841	$\nu_s(\text{C-S})^{26,27}$
859	$\nu_a(\text{C-S})^{28,29}$
1007	$\delta(\text{C}_\alpha\text{-H})^{12,26}$
1078	$\delta(\text{C}_\alpha\text{-H})^{29,30}$
1187	$\nu(\text{C-C})_{\text{ring}}^{22,27}$
1226	$\delta_{\text{as}}(\text{C-H})^{30,31}$
1366	$\nu(\text{C-C})_{\text{ring}}^{12,32}$
1481	$\nu_a(\text{C=C})_{\text{ring}}^{33,34}$
1571	$\nu_s(\text{C=C})_{\text{ring}}^{21,35}$
1630	$\nu(\text{C=O})^{29,36}$
3081	$\nu(\text{C}_\beta\text{-H})^{20,30}$
3103	$\nu(\text{C}_\alpha\text{-H})^{19,37}$

Figure 4.08 shows the SNIFTIR spectra of **PTh-3,3** collected at successively higher potentials and normalised to the reference spectrum taken at 0.3 V. Upon oxidation, new IR vibrations can be seen at 1298, 1190, 1156 and 1013 cm<sup>-1</sup>. These bands (IRAV - Infra Red Active Vibrations) appear roughly at about the same position in the FTIR spectra of doped PT and are due to the selective enhancement of four thiophene ring modes caused by the coupling of the movement of charge carriers with the polymer lattice vibrations.<sup>38-41</sup> In addition, it can be noticed that the shape and position of the IRAV bands are not changed with p-doping indicating that the same type of charge carriers are responsible for the conduction in the potential range studied.<sup>36</sup>

The spectra of **PTh-3,3** also reveal a very broad absorbance extending from about 1950 cm<sup>-1</sup> (0.24 eV) into the near-IR. This band is believed to be due to the



electronic transition between the valence band and the lowest polaron or bipolaron state.<sup>42,43</sup>



**Figure 4.08** - SNIFTIRS spectra of **PTh-3,3** taken from 0.8 to 1.4 V. Reference spectra collected at 0.3 V.

The incorporation of anions, the main charge compensation process during the oxidation of polythiophenes, can be observed as an increasing negative band related to the insertion into the film of  $\text{PF}_6^-$  (anion present in the electrolyte used in the SNIFTIRS analysis) at  $839\text{ cm}^{-1}$ .<sup>44,45</sup> Other electrolyte bands are seen pointing upwards at  $2250\text{ cm}^{-1}$  (acetonitrile  $\text{C}\equiv\text{N}$  stretch) and centred at  $3000\text{ cm}^{-1}$  ( $\text{TBA}^+$ ).<sup>27</sup>

The absence of the  $\text{C}_\alpha\text{-H}$  stretching vibration peak at  $3103\text{ cm}^{-1}$  indicates that the coupling of thiophene units takes place mainly through the  $\alpha$ -positions. Taking into account the proposed structure for **PDTE-cis** in the previous Chapter, a possible structure of **PTh-3,3** is shown in Figure 4.09 - A. Also, the proximity of the  $\text{C}_\alpha\text{-H}$  bonds in the thiophene rings of each monomeric unit suggests the occurrence of



intramolecular cyclisation during the polymerisation or even after the polymer chain is formed. Such a polymer (Figure 4.09 - B) would have a better electron delocalisation along the chain and therefore this is probably the more likely structure for **PTh-3,3**.

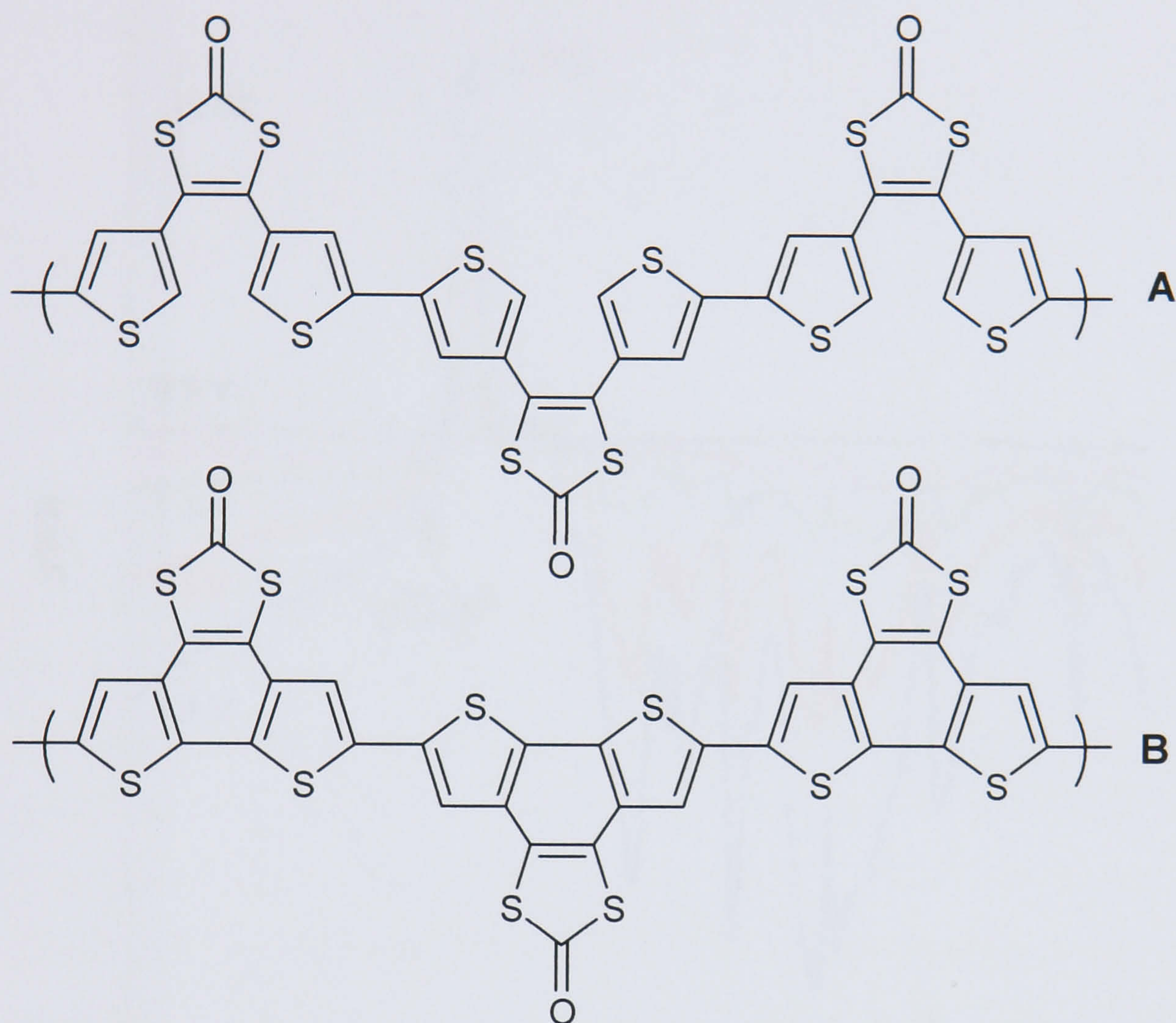
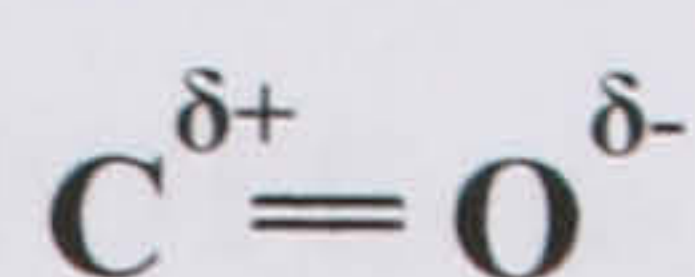


Figure 4.09 - Proposed structures for **PTh-3,3**.

In the SNIFTIRS spectra of **PTh-3,3** low intensity bands appearing at 1524, 1363 and 939/855  $\text{cm}^{-1}$  can be assigned to the stretching vibrations of C=C, C-C and C-S, correspondingly.<sup>26,27,44</sup> Another important region to highlight is that around 1700  $\text{cm}^{-1}$  better seen in Figure 4.10. This spectral region is especially informative about the effect of the doping process on the strength of the C=O bond. This bond is affected by the electronic changes within the polymer backbone as reported by Beyer *et al.*<sup>45</sup>. Upon p-doping the positive charge on the carbonyl carbon atom increases which creates a polarised bond resulting in increased bond strength. This will be manifested by a shift, in the carbonyl group frequency, to a higher wavenumber (blue shift):





Experimental evidence of this phenomenon is indeed observed upon p-doping with the peak corresponding to the neutral carbonyl group at  $1664\text{ cm}^{-1}$  being gradually lost (positive band) and the peak associated with the oxidised polymer at  $1710\text{ cm}^{-1}$  becoming increasingly dominant (negative band).

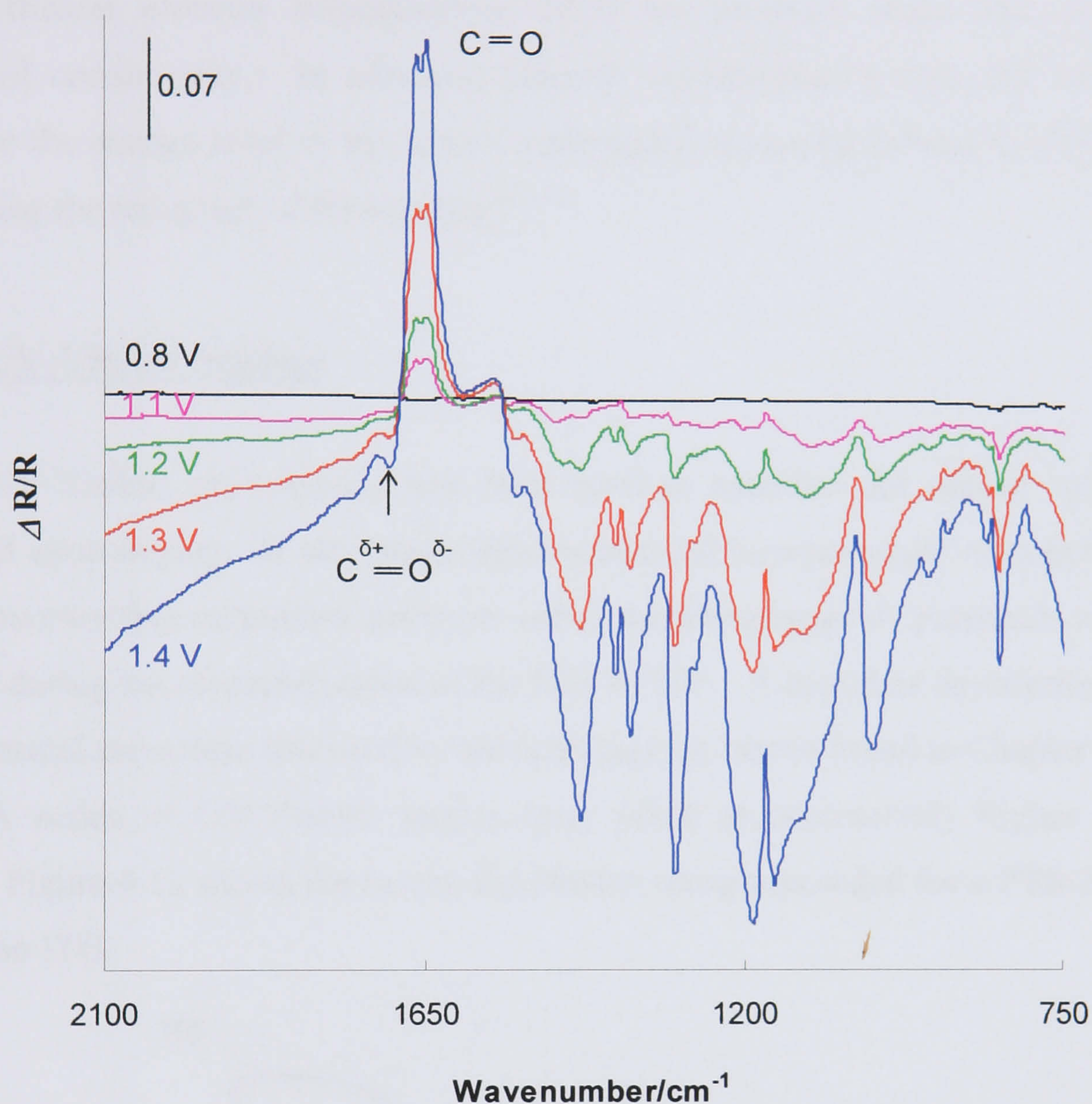


**Figure 4.10** - SNIFTIRS spectra of **PTh-3,3** between  $2100$  and  $750\text{ cm}^{-1}$ . Reference spectra collected at  $0.3\text{ V}$ .

In contrast with the spectroelectrochemical response of **PDTE-cis** (Chapter Three, Figure 3.18), the doping of **PTh-3,3** (Figure 4.08) induces the appearance of IRAV bands and a broad band extending from  $2000\text{ cm}^{-1}$  into the near-IR. As previously stated, these are a direct consequence of new transitions below the optical gap (subgap transitions) that are accompanied by specific vibrational modes in the mid IR-region.<sup>40</sup> It is widely accepted that these are features typical of organic conductive polymers as they are converted from the insulating to the conducting state.<sup>45</sup> This implies that whereas **PDTE-cis** is a poorly conducting polymer, the



conductivity level in **PTh-3,3** can be significantly enhanced upon doping. Considering that the main structural difference between the two polymers in question lies in electron withdrawing 1,3-dithiol-2-one unit, it can be concluded that its presence seems have the effect of extending the  $\pi$ -conjugated system allowing a more efficient electron delocalisation along the polymer chain and therefore, improved conductivity. In addition, electron withdrawing groups are known to decrease the energy level of the lowest unoccupied molecular orbital (LUMO) thus promoting the reduction of the bandgap.<sup>46,47</sup>

### UV-Visible Studies

UV-Visible spectroscopy has been used to examine the optical behaviour **PTh-3,3** upon doping. *In situ* spectroelectrochemical measurements were performed in a monomer-free electrolyte solution, using the same range of potentials as those applied during the characterisation of the film by CV. A complete description of the experimental procedure followed in this investigation can be found in Chapter Two.

A series of UV-Visible spectra were taken at successively higher doping levels. Figure 4.11 shows the *in situ* absorbance spectra recorded for a **PTh-3,3** film grown on ITO.

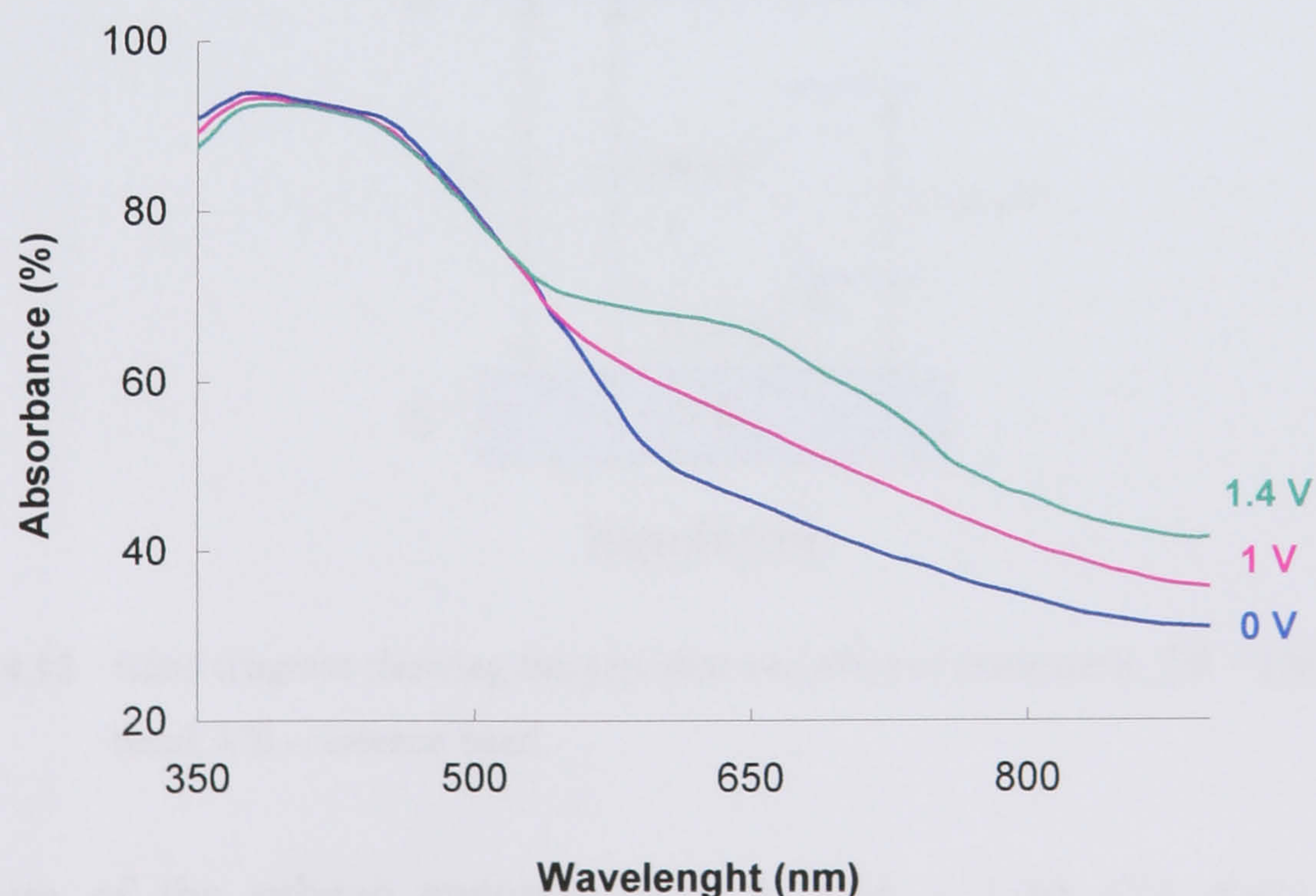


**Figure 4.11** - UV-Visible spectra of **PTh-3,3** taken at 0 V (neutral film), 1 V and 1.4 V (doped film).



Neutral **PTh-3,3** exhibits an absorption maximum centred at 410 nm that can be assigned to the  $\pi$ - $\pi^*$  transition.<sup>48</sup> The electronic bandgap of the polymer, defined as the onset for the  $\pi$ - $\pi^*$  absorbance, is approximately 2.04 eV. The oxidation of **PTh-3,3** is characterised by the emergence of a new band at  $\lambda_{\text{max}} = 655$  nm (onset at 1.64 eV) corresponding to the formation of (bi)polaronic states.<sup>49</sup> An isosbestic point is perceptible around 525 nm implying the coexistence of two regions in doped **PTh-3,3** - a neutral region where the  $\pi$ - $\pi^*$  transition is unchanged and localised regions surrounding the charge-storage configuration (fully doped polymeric chains).<sup>50-53</sup>

Using SNIFTIRS, a second subgap electronic transition has been previously identified at 0.24 eV (Figure 4.08). Therefore, two electronic transitions took place below the bandgap energy level upon electrochemical oxidation. As described in Chapter Two, it has been recognised that associated with the formation of the bipolaron and polaron state, two and three subgap electronic transition are expected, respectively.<sup>15,54,55</sup> Therefore, since **PTh-3,3** only displays two new optical transitions upon doping, it can be assumed that bipolarons are the most likely charge carriers, as shown in the energy level diagram of Figure 4.12.

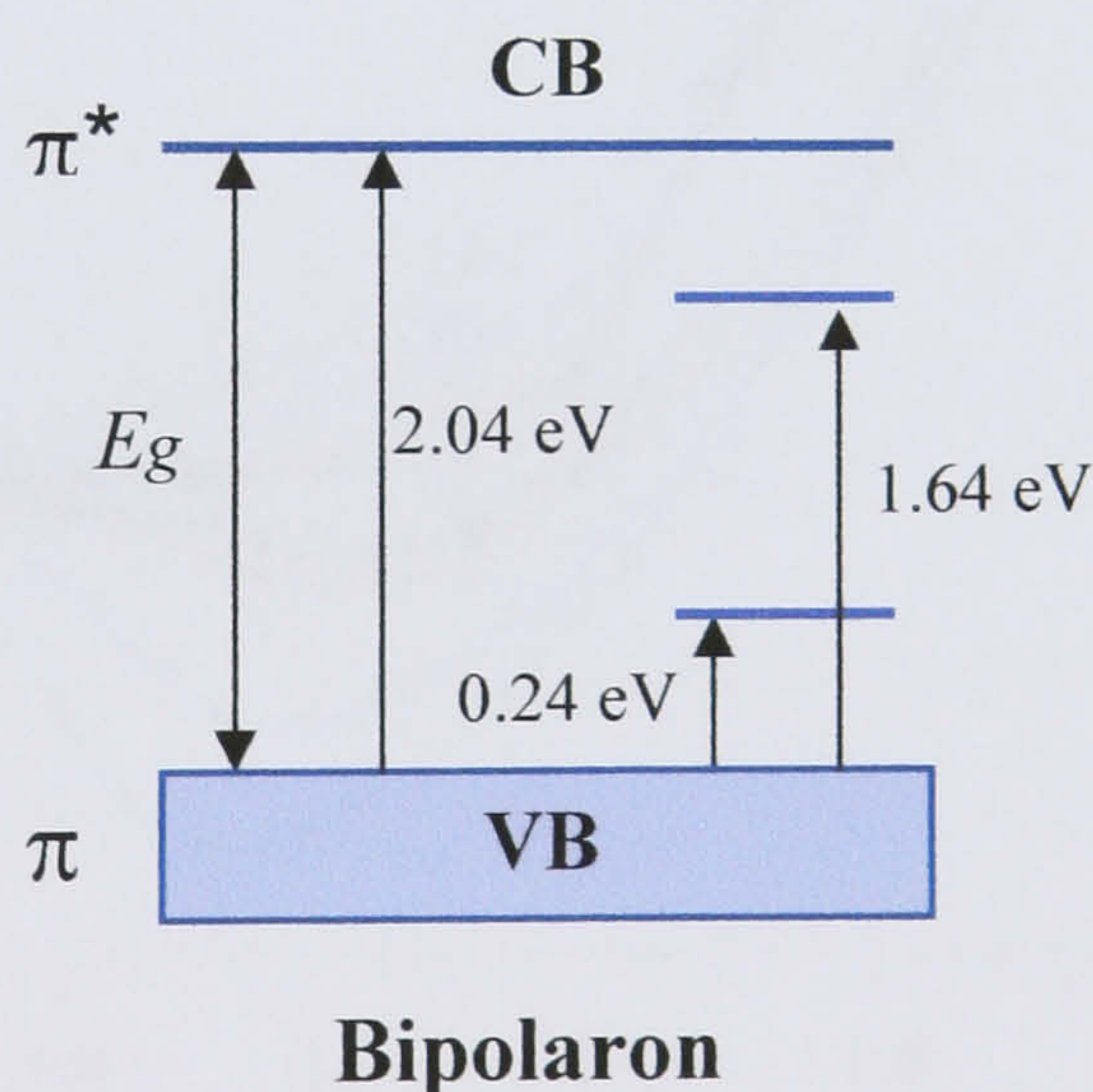


**Figure 4.12** - Band diagram showing the gap state and allowed transitions; CB – conduction band, VB – valence band.

The sum of the subgap energies ( $0.24 + 1.64 \approx 1.84$  eV) gives a good approximation to the value of the  $\pi$ - $\pi^*$  transition energy ( $E_g \approx 2.04$  eV).



### 4.3.2 Studies on Thiophene Dithiolene Th-2,2

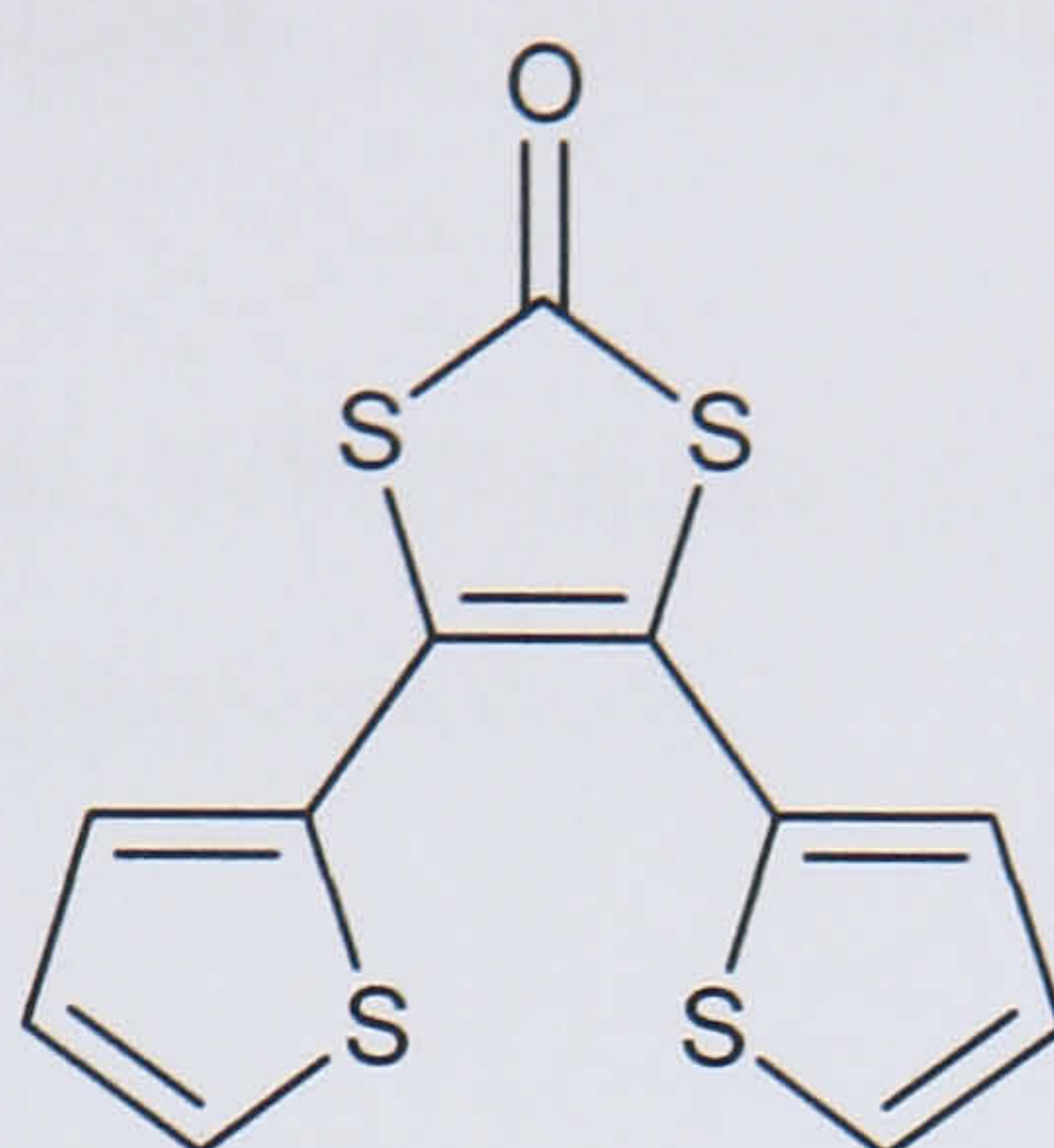


Figure 4.13 - Structure of 4,5-Di-thiophen-2-yl-[1,3]dithiol-2-one **Th-2,2**.

#### Electrochemical Studies

Figure 4.14 shows the potentiodynamic growth of **PTh-2,2** by cyclic voltammetry.

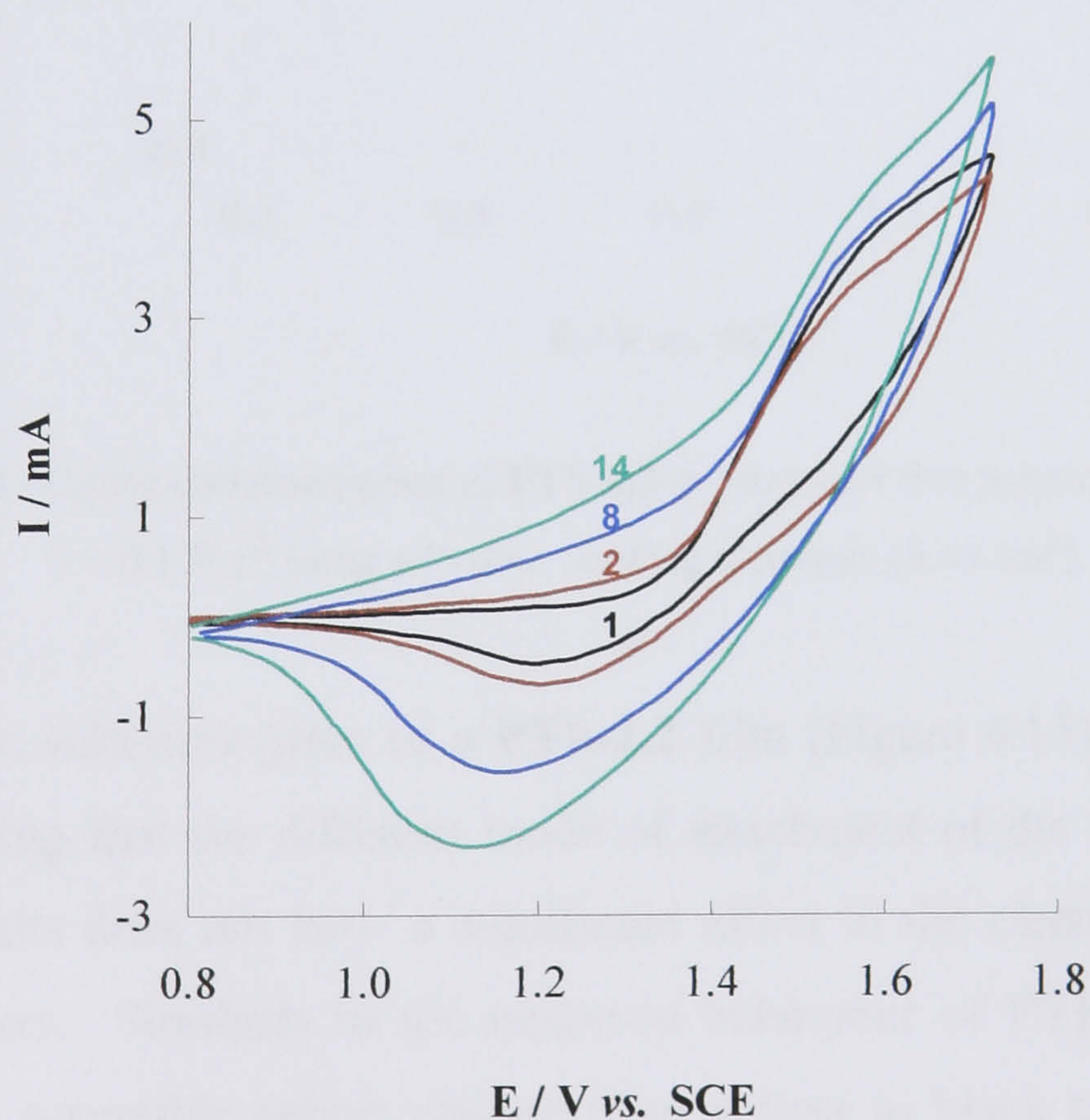


Figure 4.14 - Voltammograms of the polymerisation of **Th-2,2** recorded at  $\nu = 0.1 \text{ V.s}^{-1}$  (1<sup>st</sup>, 2<sup>nd</sup>, 8<sup>th</sup> and 14<sup>th</sup> cycles).

The irreversible oxidation of **Th-2,2** occurs at 1.56 V. The voltammograms presented in Figure 4.14 are similar to those previously observed during the growth



of **PTh-3,3** in the sense that a decrease in the anodic current is observed from the first to the second potential cycle. The steady increase in the cathodic current from the third cycle onwards indicates a continuous growth of material on the electrode.<sup>12,27</sup>

Figure 4.15 illustrates the voltammetric response of **PTh-2,2** from 0.3 to 1.35 V in a monomer-free electrolyte solution.

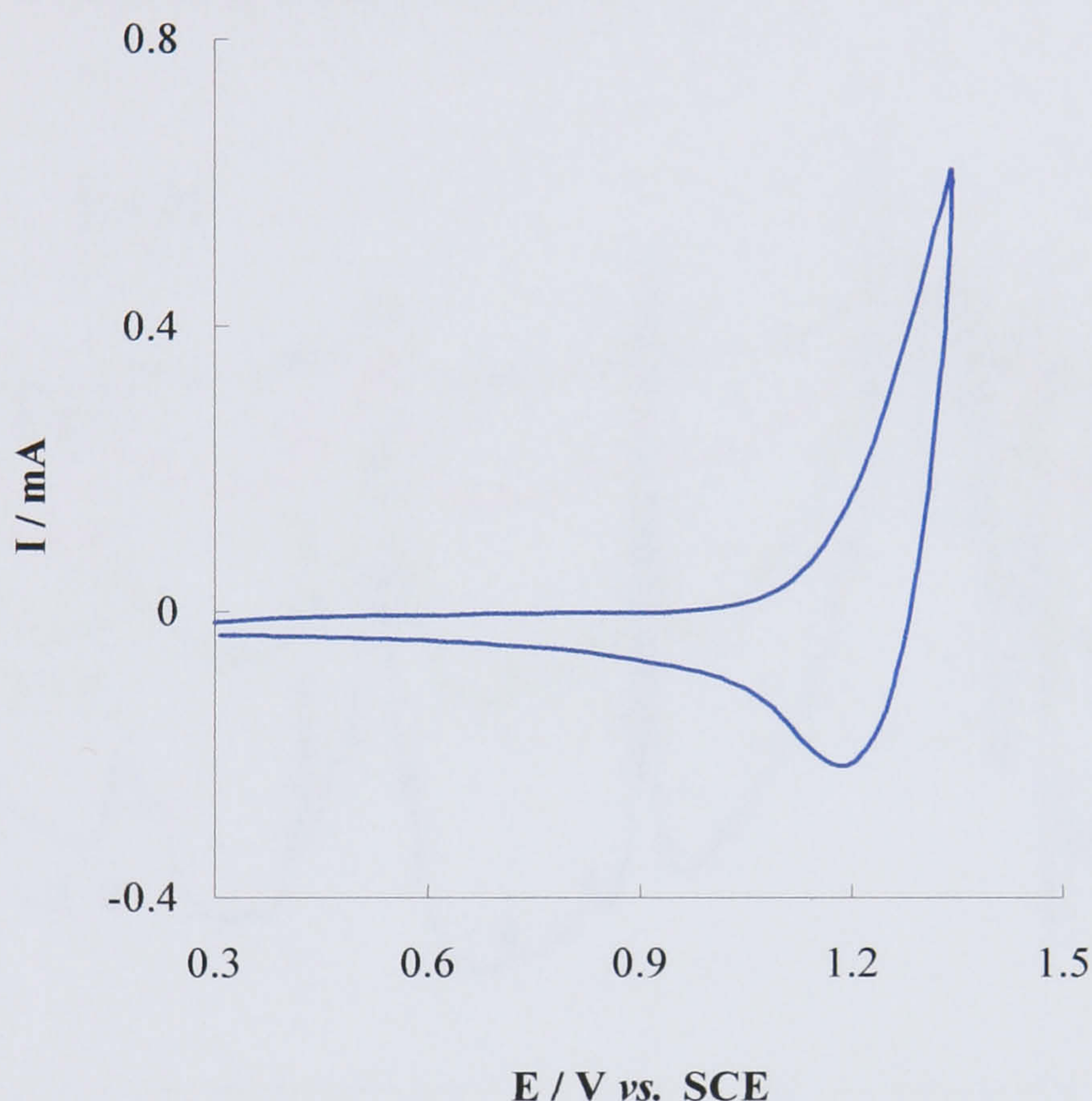


**Figure 4.15** - Cyclic voltammogram of **PTh-2,2** in monomer free solution recorded at  $\nu = 0.1 \text{ V}\cdot\text{s}^{-1}$  using a Pt disc working electrode ( $0.44 \text{ cm}^2$ ).

The cyclic voltammogram of a **PTh-2,2** film (Figure 4.15) resembles that of **PTh-3,3** indicating that the different mode of attachment of the thiophene rings in the monomer units does not have a significant effect in the electrochemistry of the resultant polymers. Similarly to the observed behaviour of **PTh-3,3**, the **PTh-2,2** film exhibited a reversible colour change from yellow to black upon oxidation and showed a reproducible electrochemical response when cycled from -1.1 to 2.1 V.



### SNIFTIRS Studies

The spectroelectrochemical investigation of **PTh-2,2** was performed employing a monomer-free electrolyte solution and using the same range of potentials as those applied during the characterisation of the film by CV. Figure 4.16 shows the acquired SNIFTIRS spectra collected at successively higher potentials and normalised to the reference spectrum taken at 0.3 V.

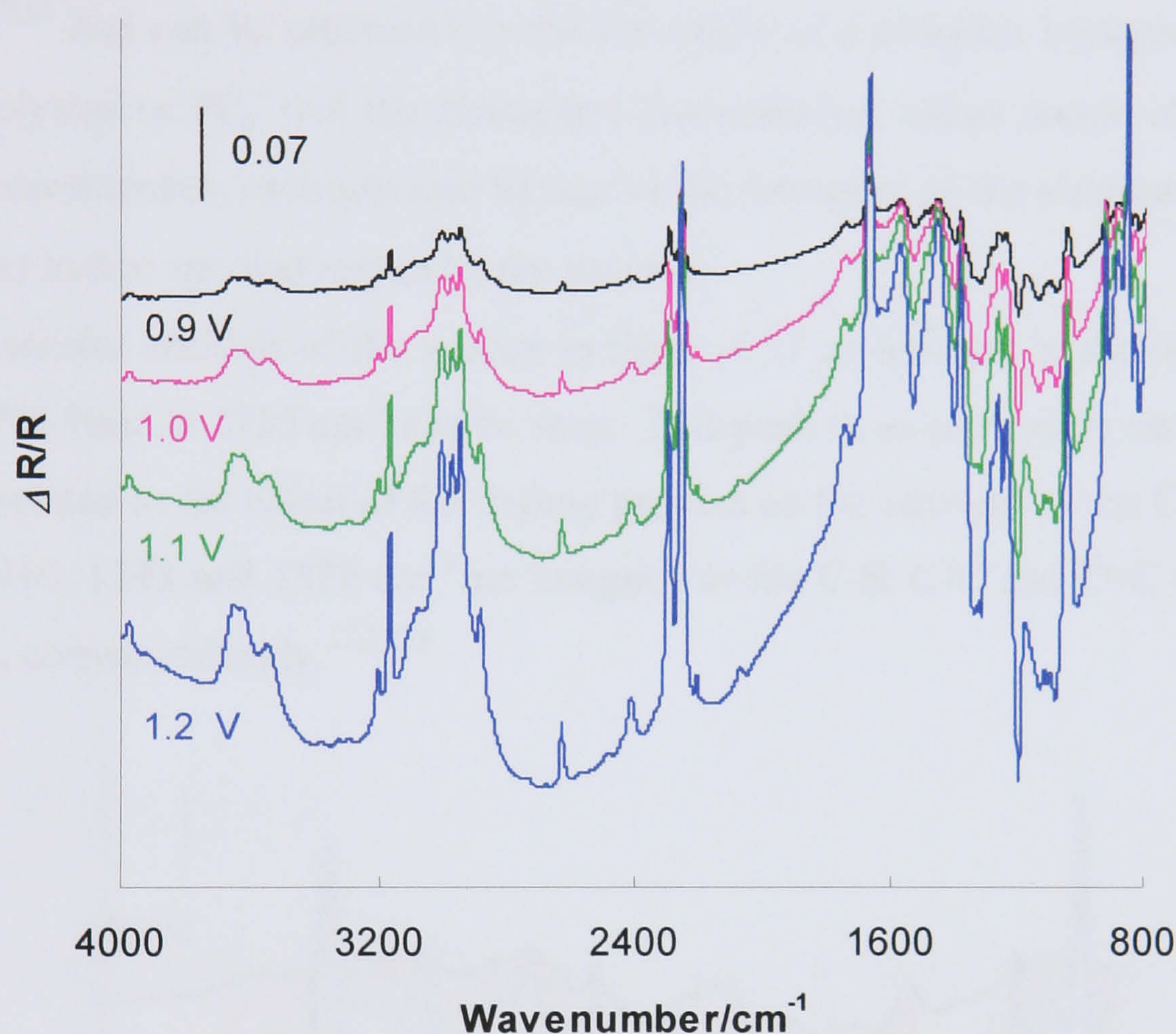


**Figure 4.16** - SNIFTIRS spectra of **PTh-2,2** taken from 0.9 to 1.2 V. Reference spectra collected at 0.3 V.

Analysis of the spectra between  $800\text{ cm}^{-1}$  and  $1600\text{ cm}^{-1}$  confirms the presence of the IRAV bands. These bands originate from the coupling of the quinoid-type vibrations of the polymer backbone and become increasingly dominant upon doping (as the film is oxidised) when the aromatic character is lost.<sup>4,56</sup> A very broad absorbance ( $\Delta\nu = 2000\text{ cm}^{-1}$ ), attributed to the electronic transition between the valence band and the lowest polaron or bipolaron state, is observed at  $2500\text{ cm}^{-1}$ .<sup>42,45</sup> Solvent bands can be seen pointing upwardly at  $2250\text{ cm}^{-1}$  (acetonitrile  $\text{C}\equiv\text{N}$  stretch) and centred around  $3000\text{ cm}^{-1}$  (symmetric and asymmetric stretching modes of  $\text{CH}_2$



and  $\text{CH}_3$  due to the electrolyte salt - tetrabutyl ammonium salt).<sup>27,57</sup> The incorporation of electrolyte anions ( $\text{PF}_6^-$ ) as a means of maintaining charge neutrality of **PTh-2,2** upon p-doping should give rise to an increasing negative band, as it occurred in the case of **PTh-3,3**. Nonetheless, analysis of the SNIFTIR spectra presented in Figure 4.17 shows that the band associated with  $\text{PF}_6^-$  at  $845\text{ cm}^{-1}$  is positive, implying a decrease of the anion absorbance when the polymer is being oxidised. Such behaviour has been reported for polyaniline<sup>58</sup> and many other polymers<sup>59,60</sup> and can be attributed to the formation of a complex between the  $\text{PF}_6^-$  and the polymer or  $\text{PF}_6^-$  and the electrolyte (acetonitrile), which would absorb at a different wavenumber, or might also be due to the screening of the absorbance of the  $\text{PF}_6^-$  anions in that spectral region by the polymer.

By careful analysis of the spectra in figure 4.17 an increase in the intensity of the SNIFTIR band at  $1725\text{ cm}^{-1}$  can be seen. This peak is, as previously observed for **PTh-3,3**, related to the effect of the doping process on the strength of the  $\text{C}=\text{O}$  bond. Bands at  $910$ ,  $1398$  and  $1529\text{ cm}^{-1}$  are assigned to the  $\text{C}-\text{S}$ ,  $\text{C}-\text{C}$  and  $\text{C}=\text{C}$  stretching vibrations, correspondingly.<sup>12,23,29</sup>

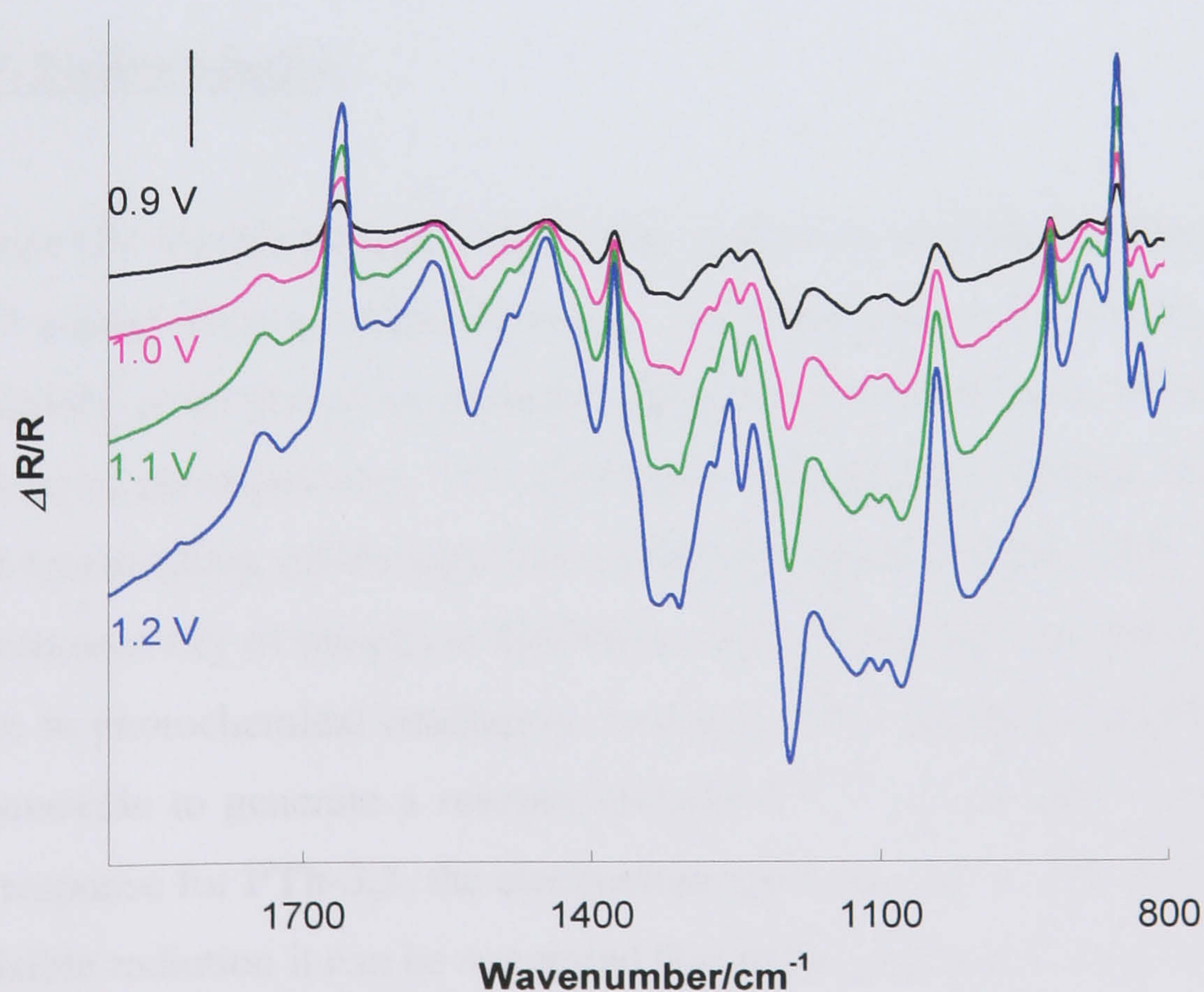


**Figure 4.17** - SNIFTIRS spectra of **PTh-2,2** between  $1900$  and  $800\text{ cm}^{-1}$ . Reference spectra collected at  $0.3\text{ V}$



The absence of the  $C_{\alpha}$ -H stretching vibration peak around  $3103\text{ cm}^{-1}$  indicates that **Th-2,2** polymerises *via* the available  $\alpha$ -positions in the thiophene rings. This is in agreement with the higher reactivity of the  $C_{\alpha}$ -H radical in relation to the one formed in the  $\beta$ -position.<sup>9,43</sup>

Considering this information, the most likely structure of the polymer formed upon electropolymerisation of the **Th-2,2** monomer is shown in Figure 4.18.

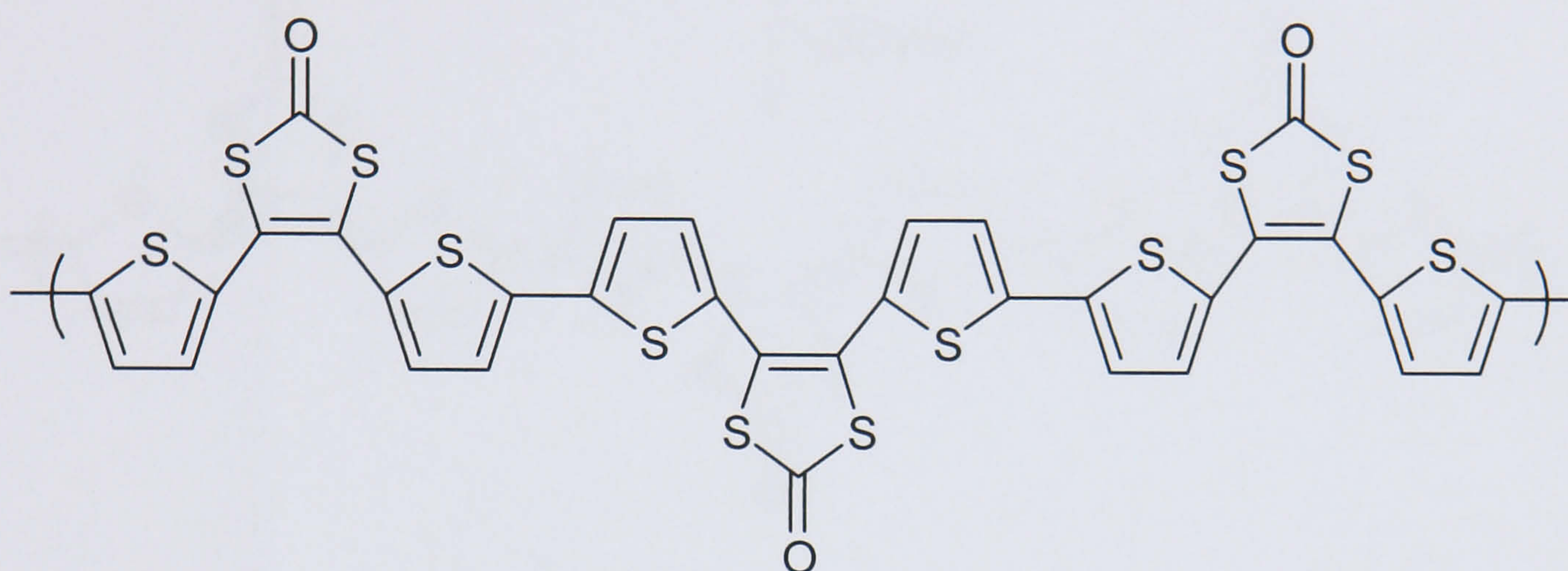
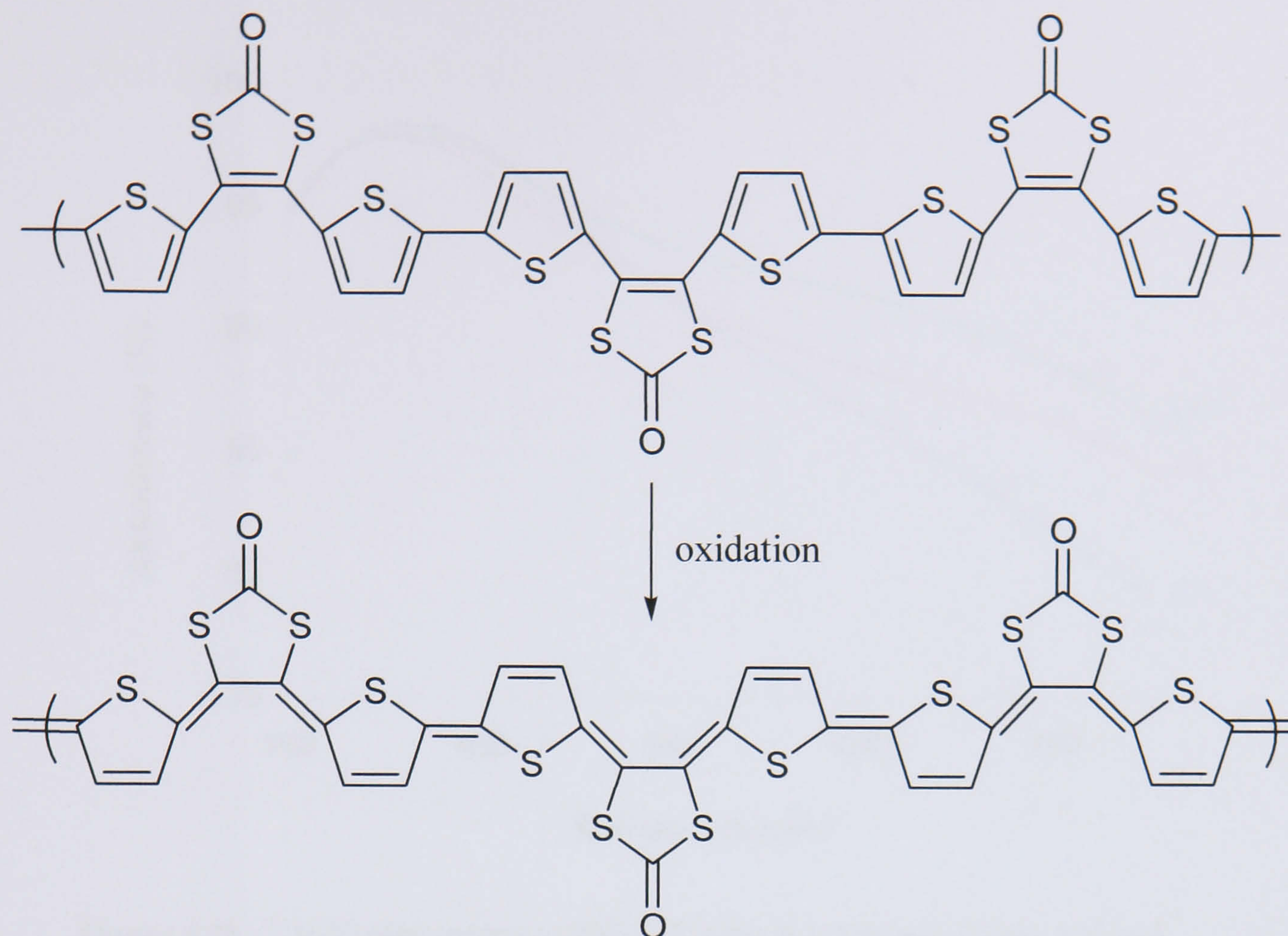


Figure 4.18 - Proposed structure for PTh-2,2.

### UV-Visible Studies

*In-situ* UV-Visible measurements were carried out on **PTh-2,2** films deposited on an ITO coated glass working electrode. The films revealed a certain degree of photosensitivity given that a few minutes of exposure to UV-Visible radiation would originate loss of electroactivity. For this reason, spectroscopic studies could only be performed by switching off the light source between measurements. Previous reports on the photoreactivity of thiophene dithiolenes have shown that the dithiolene unit is susceptible to photochemical irradiation, leading to ring cleavage and elimination of carbon monoxide to generate a reactive di-radical.<sup>61,62</sup> Given that, contrary to the observed response for **PTh-3,3**, the electrochemical behaviour of **PTh-2,2** is affected by UV-Visible radiation it can be suggested that in this polymer the dithiolene unit is directly involved in the movement of charge upon oxidation (Figure 4.19).





**Figure 4.19** - Proposed structure for neutral and oxidised **PTh-2,2**.

Consequently, the disruption of the dithiolenone group would reduce the electroactivity of **PTh-2,2**. Since **PTh-3,3** does not appear to show photosensitivity when subject to UV-Visible radiation, it can be concluded that the dithiolenone unit is only partially involved in the conduction mechanism that would essentially occur through the polythiophene backbone of the polymer.

Figure 4.20 shows the spectra recorded for a **PTh-2,2** as the potential was stepped from 0 V to 1.2 V.



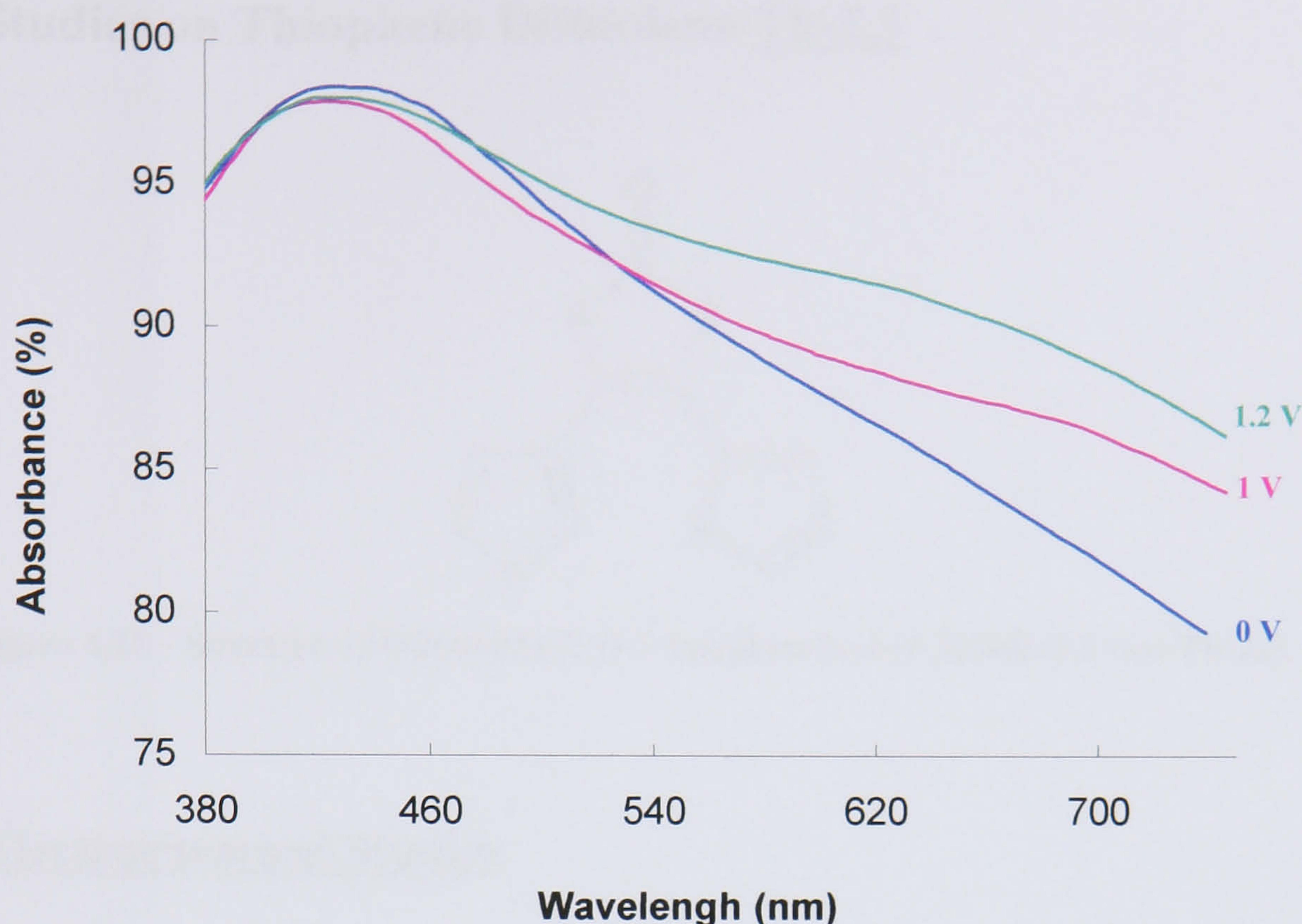


**Figure 4.20** - UV-Visible spectra of **PTh-2,2** taken at 0 V (neutral film), 1 V and 1.4 V (doped film).

The UV-Visible absorption spectra of **PTh-2,2** at 0 V is characterised by an intense broad absorbance band with a maximum at 440 nm related with the  $\pi$ - $\pi^*$  transition.<sup>63</sup> The onset of this band is observed at approximately 540 nm which means that the polymer has a bandgap of 2.3 eV. Upon oxidation, a gradual increase in the absorbance around 650 nm reveals the formation of the charge carriers typical p-type conducting polymer.<sup>12,64</sup>

Prompted by electrochemical doping, two new electronic subgap transitions have been identified: one by UV-Visible spectroscopy (Figure 4.20) and the other by SNIFTIRS (Figure 4.16). The existence of two mid-gap transitions is consistent with charge storage predominantly in bipolarons as observed in the study of **PTh-3,3**.



### 4.3.3 Studies on Thiophene Dithiolenes Th-2,3

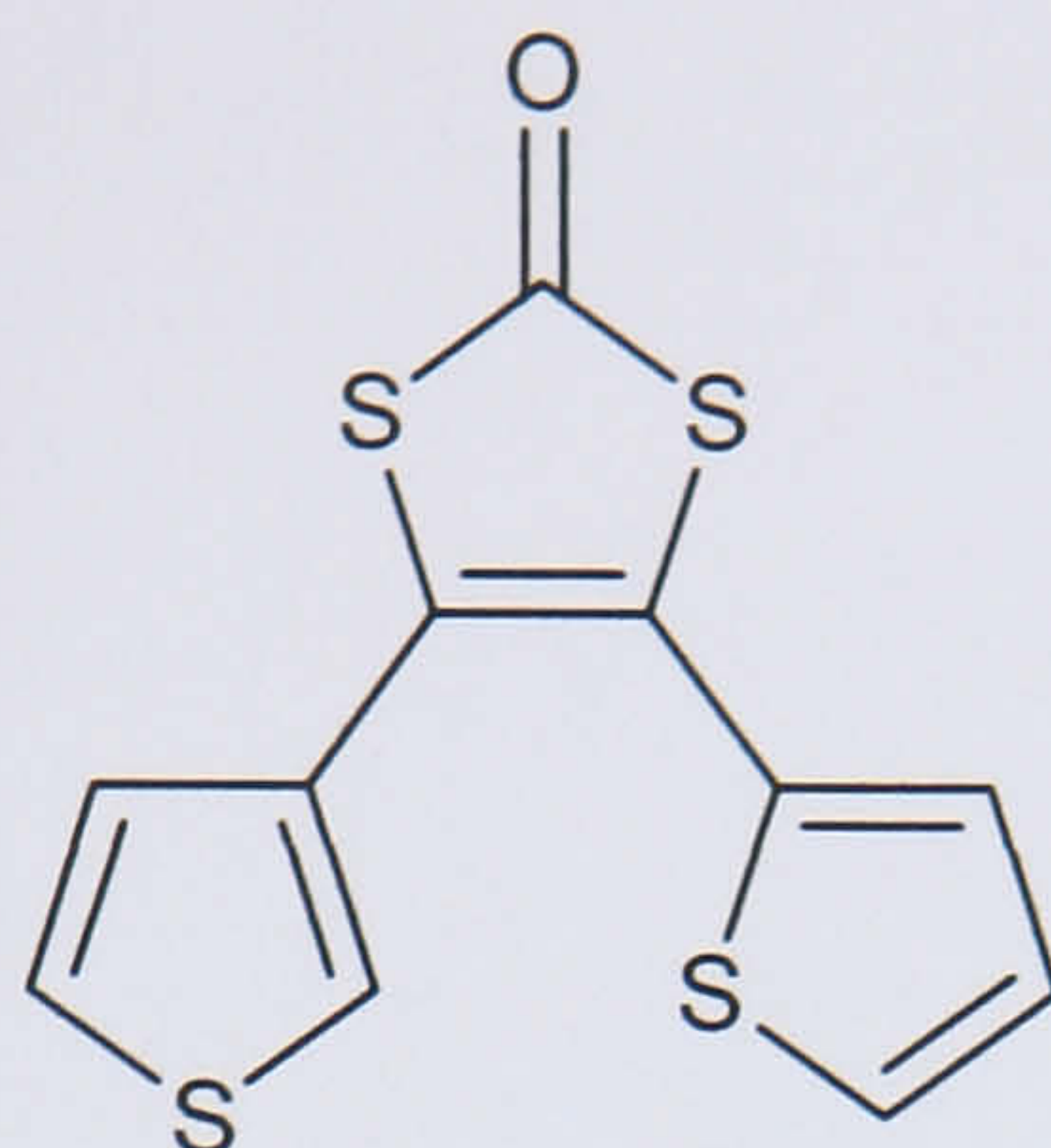


Figure 4.21 - Structure of 4-thiophen-3-yl-5-thiophen-2-yl-[1,3]dithiol-2-one **Th-2,3**.

#### Electrochemical Studies

Figure 4.22 shows the voltammograms recorded during potentiodynamic growth of **PTh-2,3** between 0.8 and 1.7 V.

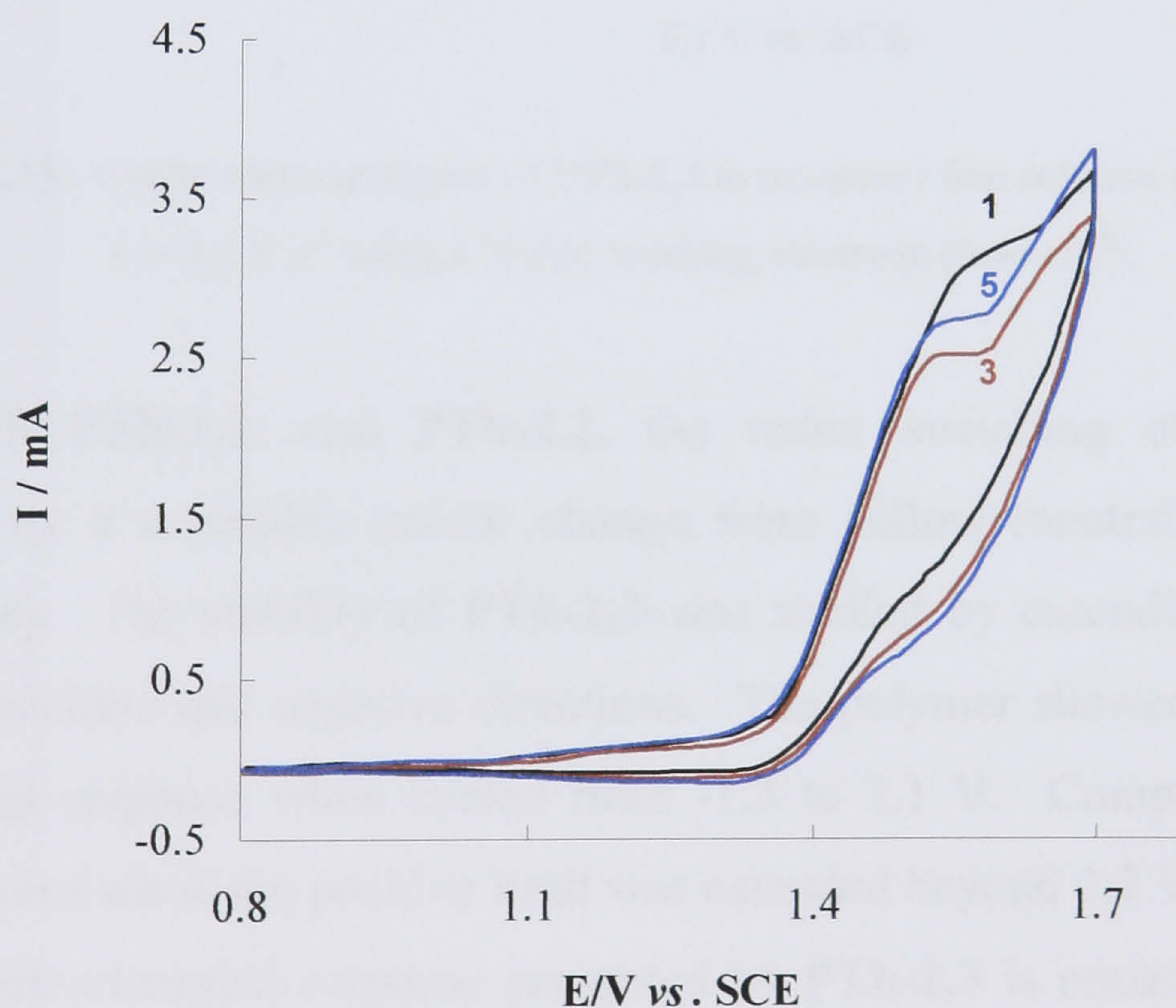
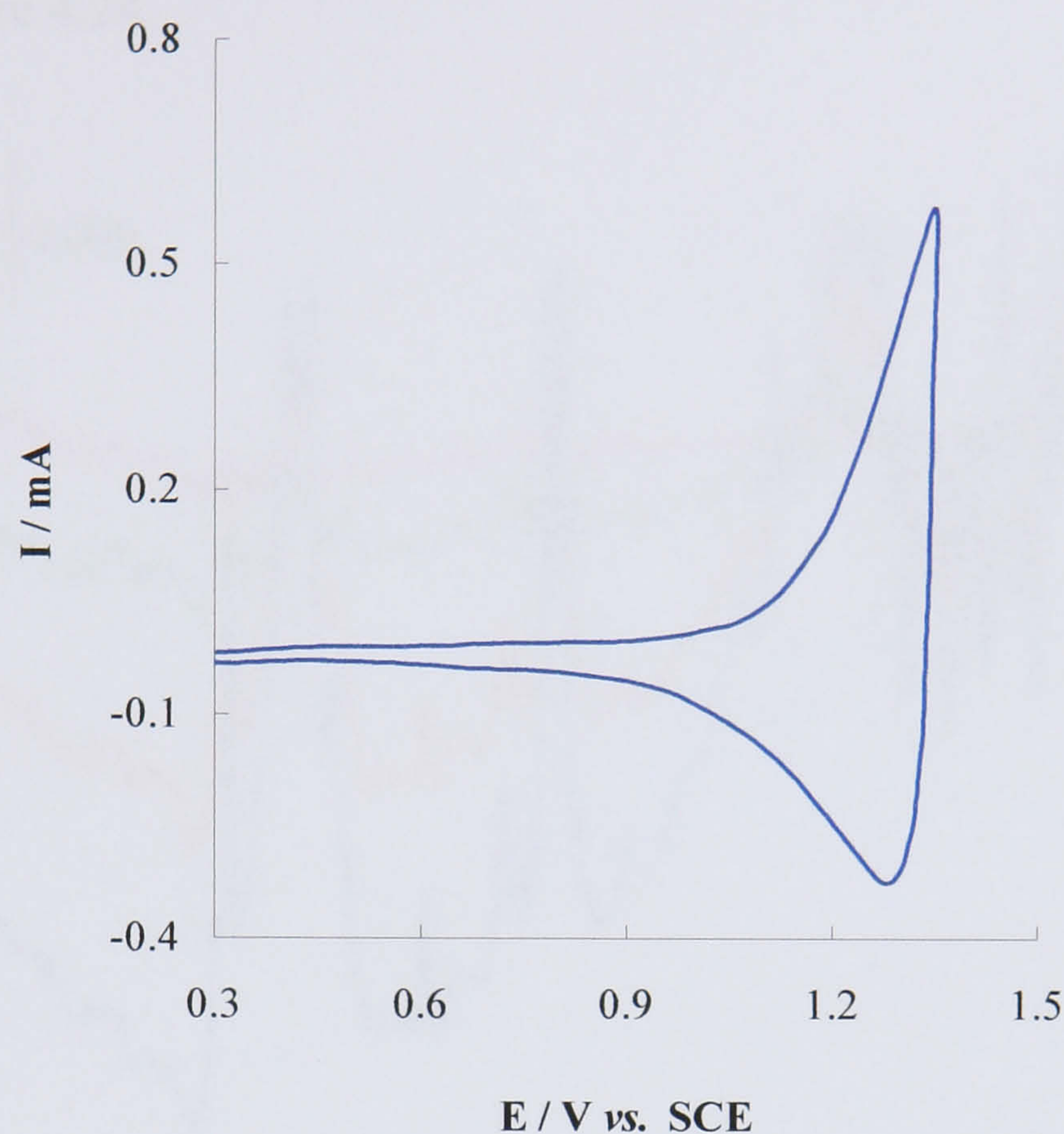


Figure 4.22 - Voltammograms of the polymerisation of **Th-2,3** recorded at  $\nu = 0.1 \text{ V.s}^{-1}$  (1<sup>st</sup>, 3<sup>rd</sup> and 5<sup>th</sup> cycles).

The irreversible oxidation of **Th-2,3** occurs at 1.6 V. After the initial cycles, a steady increase in the anodic and cathodic currents is observed indicating continuous polymer deposition at the surface of the electrode.



The electropolymerised film was studied by cyclic voltammetry in a monomer-free electrolyte solution. Figure 4.23 illustrates the voltammetric response of **PTh-2,3** from 0.3 to 1.35 V.



**Figure 4.23** - Cyclic voltammogram of **PTh-2,3** in monomer free solution recorded at  $\nu = 0.1 \text{ V}\cdot\text{s}^{-1}$  using a Pt disc working electrode ( $0.44 \text{ cm}^2$ ).

As with **PTh-3,3**, and **PTh-2,2**, the redox switching of **PTh-2,3** was accompanied by a reversible colour change from yellow (neutral state) to black (oxidised state). The stability of **PTh-2,3** was studied by extending the potential limits in the positive and negative directions. The polymer showed a reproducible electrochemical response when cycled from -1.3 to 2.1 V. Complete inactivation could be achieved when the positive limit was extended beyond 2.7 V.

The electrochemical response presented by **PTh-2,3** is remarkably similar to the one of **PTh-3,3** and **PTh-2,2**, resembling that of many polythiophenes. It is clear that all the three polythiophene dithiolenes investigated could be reversibly (and easily) p-doped and yet, none of the films underwent n-doping within the potential range studied.



### SNIFTIRS Studies

The SNIFTIRS spectra taken during the stepwise oxidation of **PTh-2,3** are presented in the Figure 4.24.

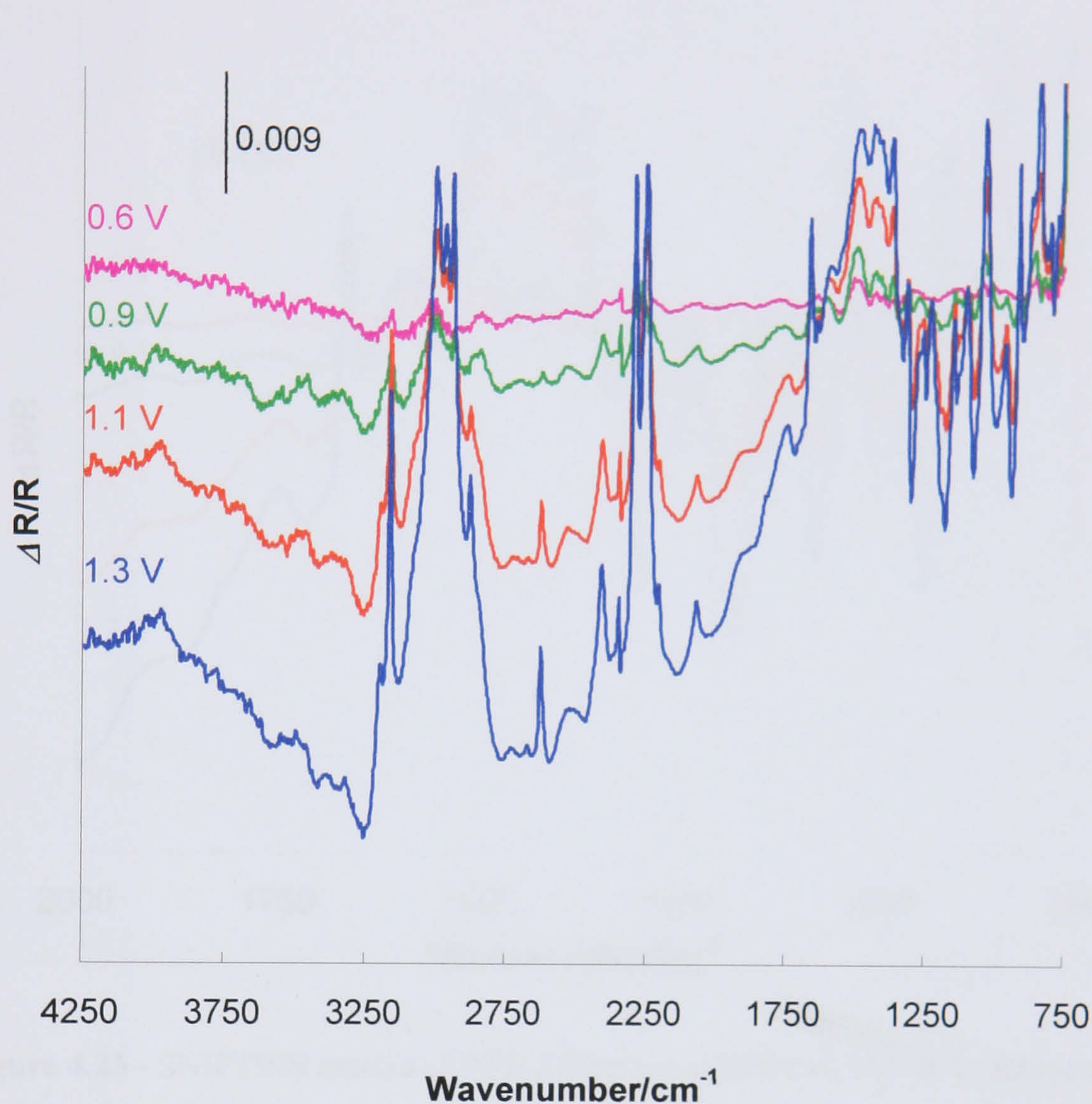


**Figure 4.24** - SNIFTIRS spectra of **PTh-2,3** taken from 0.6 to 1.3 V. Reference spectra collected at 0.3 V.

As the film is oxidised, the distinct bands that are characteristic of conducting polymers are observed: a broad band above  $2500\text{ cm}^{-1}$  (onset at  $0.23\text{ eV}$ ) and several bands in the  $1500\text{ to }800\text{ cm}^{-1}$  region. As previously stated, these bands are assigned to (bi)polaron type charge carriers; the former is due to transition from the valence band to the lowest subgap state, and the latter are caused by the coupling of this electronic excitation to the lattice vibrations of the polymer. The potential range at which these main spectral changes occur coincides well with the potential where the current peak of the **PTh-2,3** film is observed in the cyclic voltammogram.



Vibrations at 1564 and 1334  $\text{cm}^{-1}$  (best seen in figure 4.25) originate from the stretching of C=C and C-C in the thiophene ring.<sup>23</sup> As with **PTh-3,3** and **PTh-2,2**, solvent features are observed as positive bands around 3000 and 2500  $\text{cm}^{-1}$ .

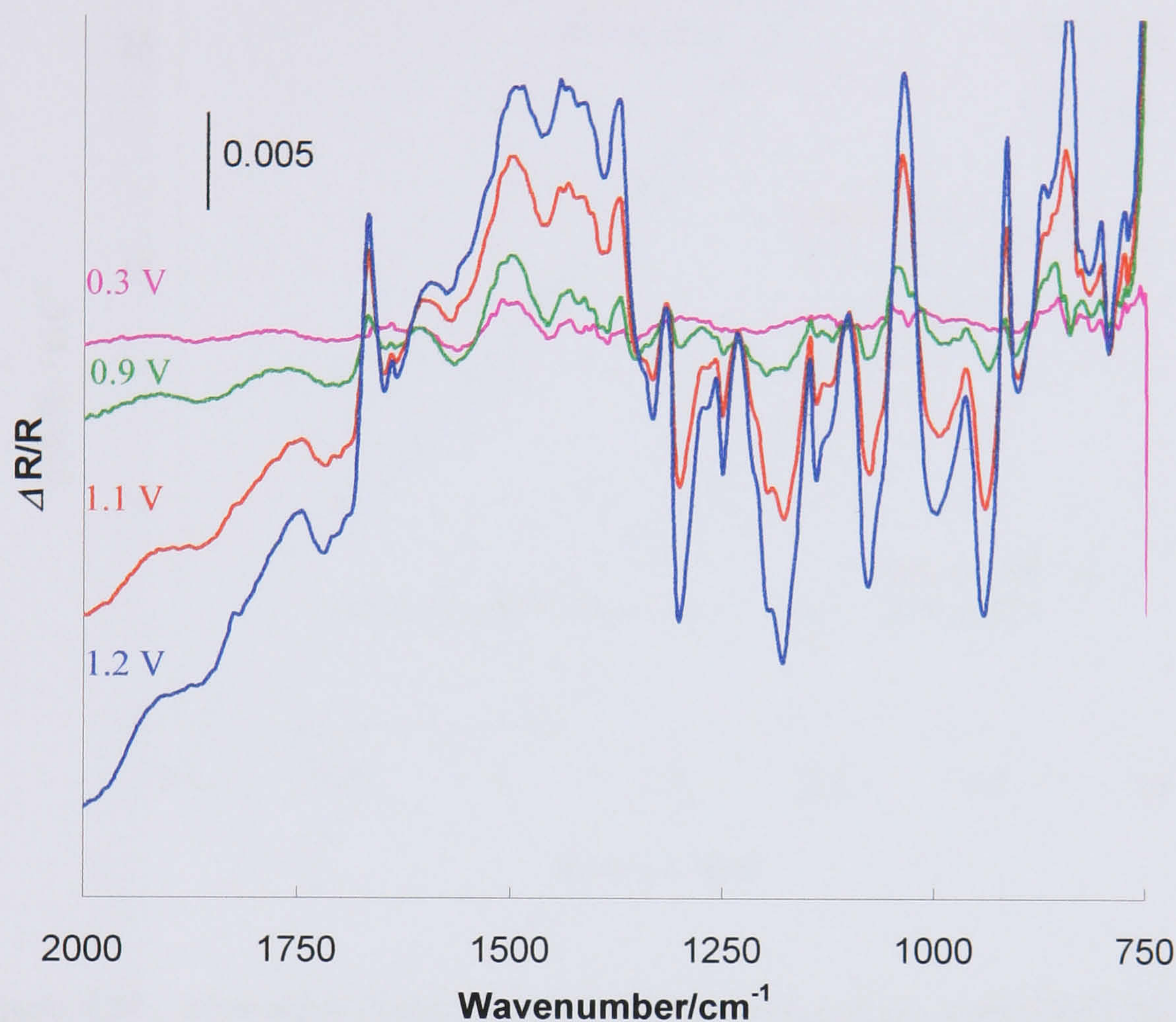


**Figure 4.25** - SNIFTIRS spectra of **PTh-2,3** between 2100 and 750  $\text{cm}^{-1}$ . Reference spectra collected at 0.3 V.

Once more, the increase in the C=O bond strength upon p-doping is manifested by the shift of the carbonyl group frequency to a higher wavenumber. The development of a sharp peak at 795  $\text{cm}^{-1}$  assigned to the  $\text{C}_\beta\text{-H}$  out-of-plane deformation<sup>24</sup> implies that the bonding between thiophene units occurs mainly through the  $\alpha$ - position.

Even though the three polythiophene dithiolenes investigated have shown very similar SNIFTIR spectra, the observed subtle differences between them can give an insight about their structures. One major distinction lies in the fact that the relative change of reflectance ( $\Delta R/R$ ) in the **PTh-3,3** and **PTh-2,2** spectra (Figures 4.08 and 4.16) was found to be about 5 times bigger than that for **PTh-2,3** (Figure 4.24). This different IR behaviour seen for the polythiophene dithiolenes is clearly illustrated by



plotting the normalised change in reflectance of the broad band centred around  $3000\text{ cm}^{-1}$  as a function of the applied potential.

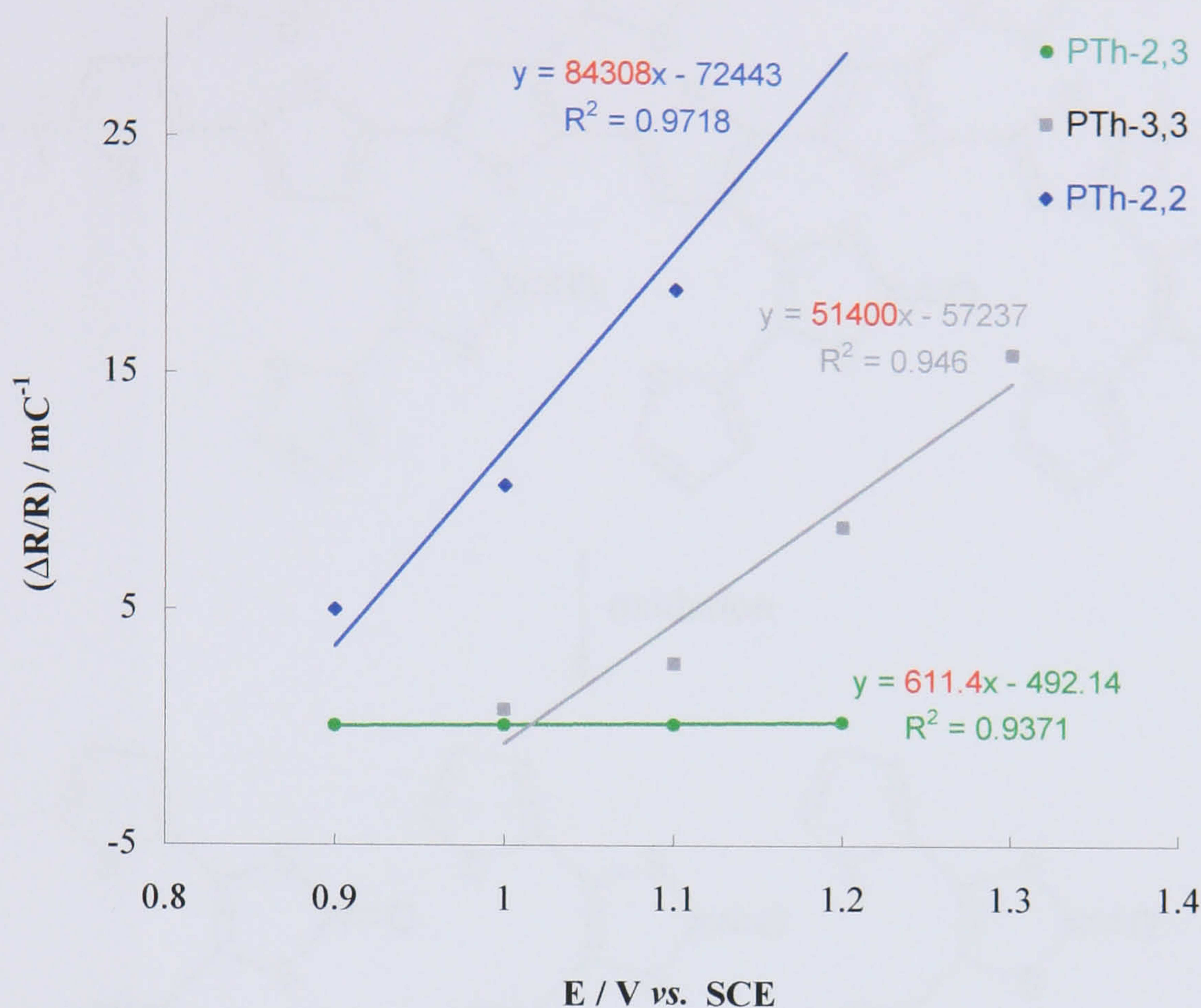


**Figure 4.26** – Normalised change in reflectivity as a function of potential for **PTh-2,3**, **PTh-3,3** and **PTh-2,2**.

From Figure 4.26 it can be seen that, contrary to the response observed for **PTh-2,3**, the oxidation of **PTh-3,3** and **PTh-2,2** induces a strong increase in the intensity of the IR electronic absorption prompting a higher slope in the regression curves. One possible explanation is that in these two polymers, and according to their previous suggested structure, all thiophene rings are involved in the movement of electrons. Also, and especially in **PTh-2,2**, there is an important contribution from the dithiolene group in the conduction mechanism, leading to increased levels of conductivity. In the case of the monomer **Th-2,3**, polymerisation probably occurs *via* the only thiophene ring with two  $\alpha$ - positions available for bonding. Therefore, in the resultant **PTh-2,3** polymer, just a small part of the molecule participates in the transport of charge across the polythiophene backbone. Taking this into account, Figure 4.27 shows the proposed structure for **PTh-2,3** and the expected quinoid form of this polymer, generated upon oxidation.



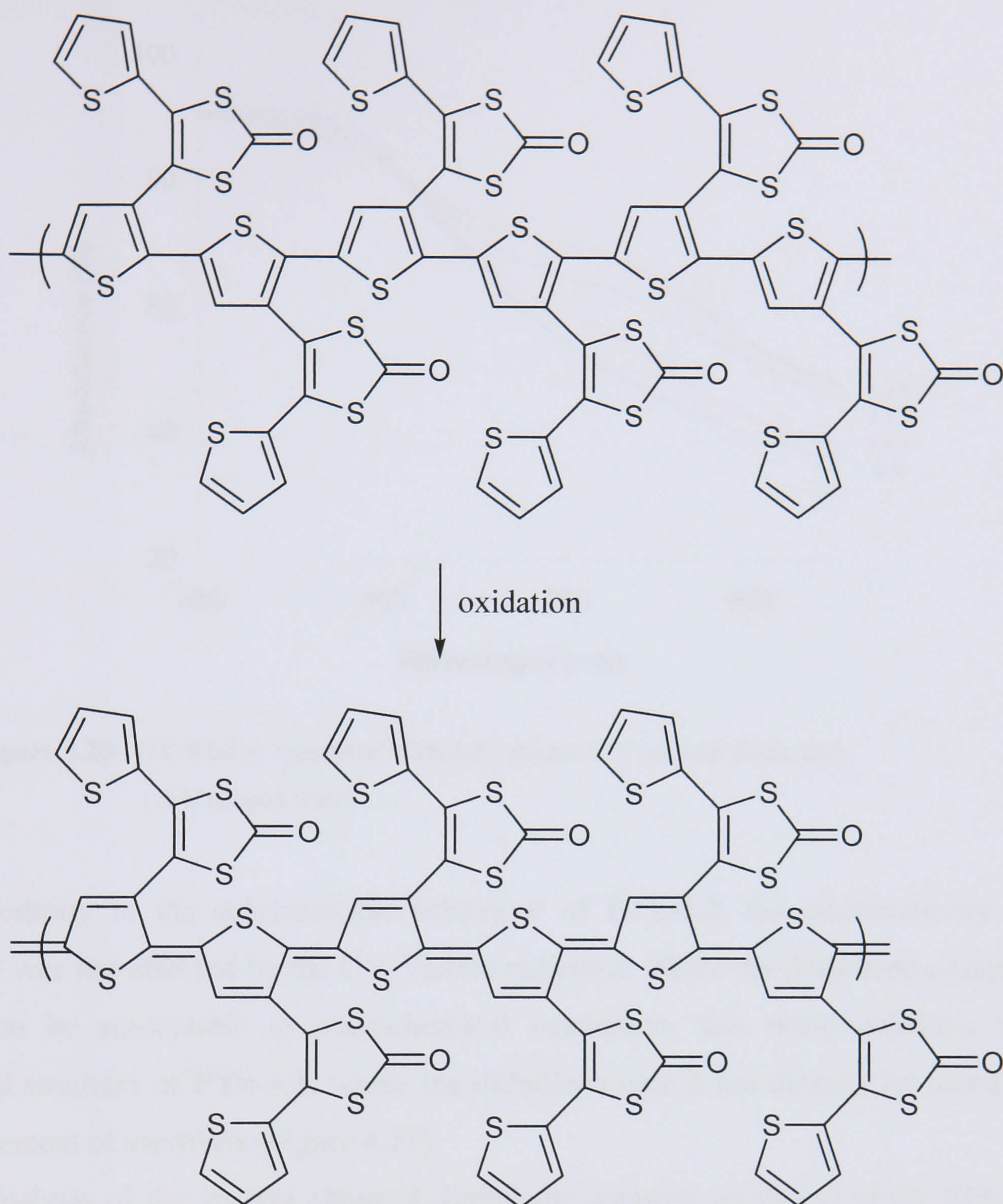


Figure 4.27 - Proposed structure for neutral and oxidised PTh-2,3.

The presence of a large substituent group could induce considerable deviation from coplanarity between adjacent thiophene rings which would lead to a decrease in conductivity.

### UV-Visible Studies

The electrochemical switching of PTh-2,3 between the neutral and oxidised states was investigated by UV-Visible spectroscopy. The *in situ* absorbance spectra recorded at successively higher doping levels are shown in Figure 4.28.



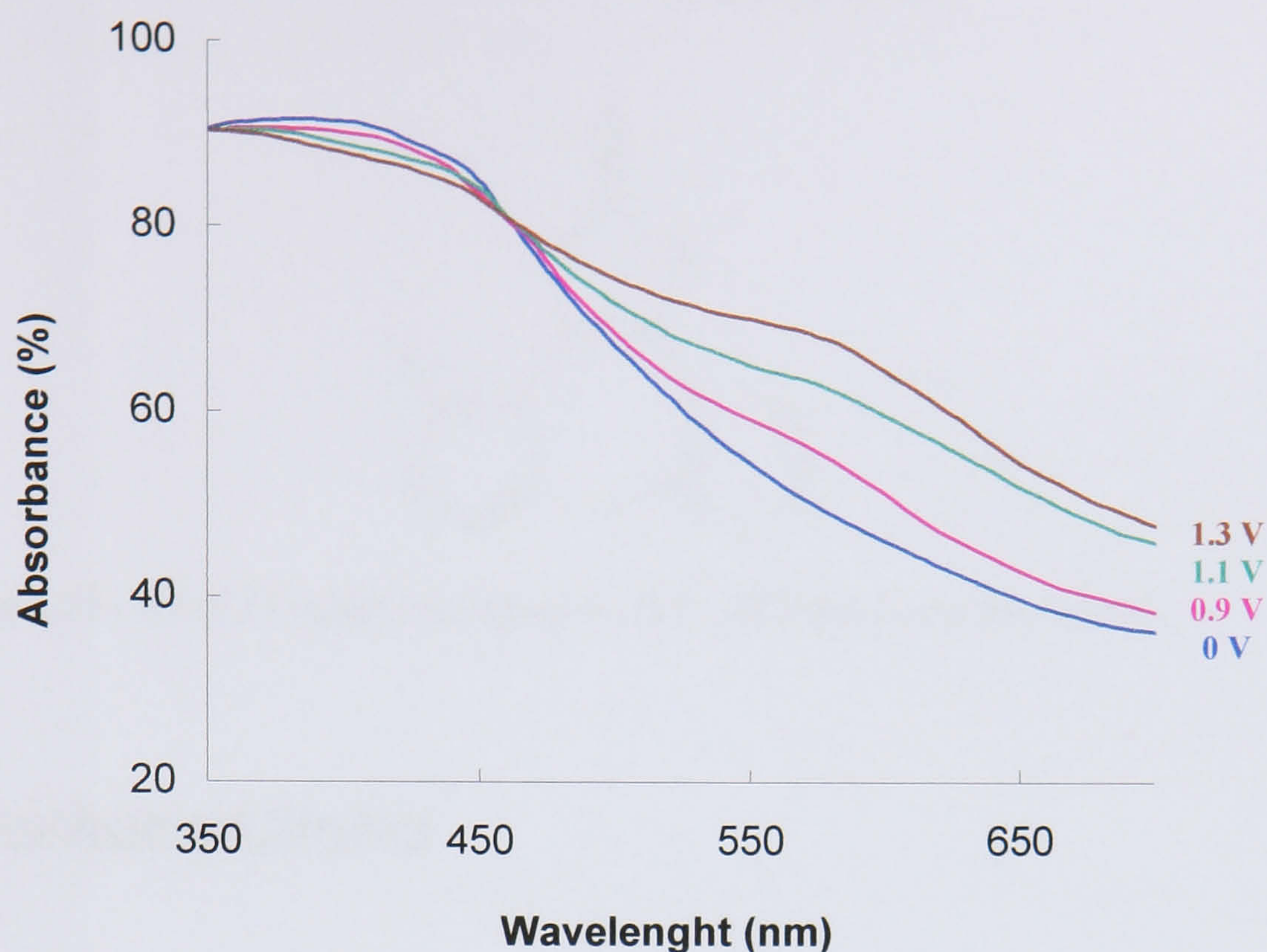


**Figure 4.28** - UV-Visible spectra of **PTh-2,3** between 0 V (neutral film), and 1.3 V (doped film).

Contrary to the spectroscopic behaviour of **PTh-2,2**, the electroactivity of **PTh-2,3** was not affected by the UV-Visible radiation. Since the dithiolene group is known to be susceptible to photochemical irradiation, this result confirms the proposed structure of **PTh-2,3**, where the dithiolene unit is not directly involved in the movement of electrons (Figure 4.27).

Analysis of the spectra obtained during the stepwise oxidation of the film in the range 350 - 700 nm shows a small decrease in the intensity of the broad band centred at 400 nm (assigned to the  $\pi$ - $\pi^*$  transition). The band gap of **PTh-2,3** is estimated to be 2.18 eV from the onset of the absorption of neutral polythiophene. The doping process is accompanied by the appearance of a new broad band at around 585 nm (onset at 1.86 eV) characteristic of the presence of free carriers. The presence of an isosbestic point around 525 nm can be interpreted as a two-phase behaviour of fully doped and completely undoped chains.<sup>52</sup>

In the same way as suggested by the spectroelectrochemical studies of **PTh-3,3** and **PTh2,2**, the presence of two subgap transitions at 1.86 eV (Figure 4.28) and 0.23 eV (revealed by the SNIFTIR spectra presented in Figure 4.24) indicates that bipolarons are the most likely charge carriers formed upon p-doping of **PTh2,3**.



#### 4.3.4 Studies on Thiophene Dithiolenes Th-3,3Me

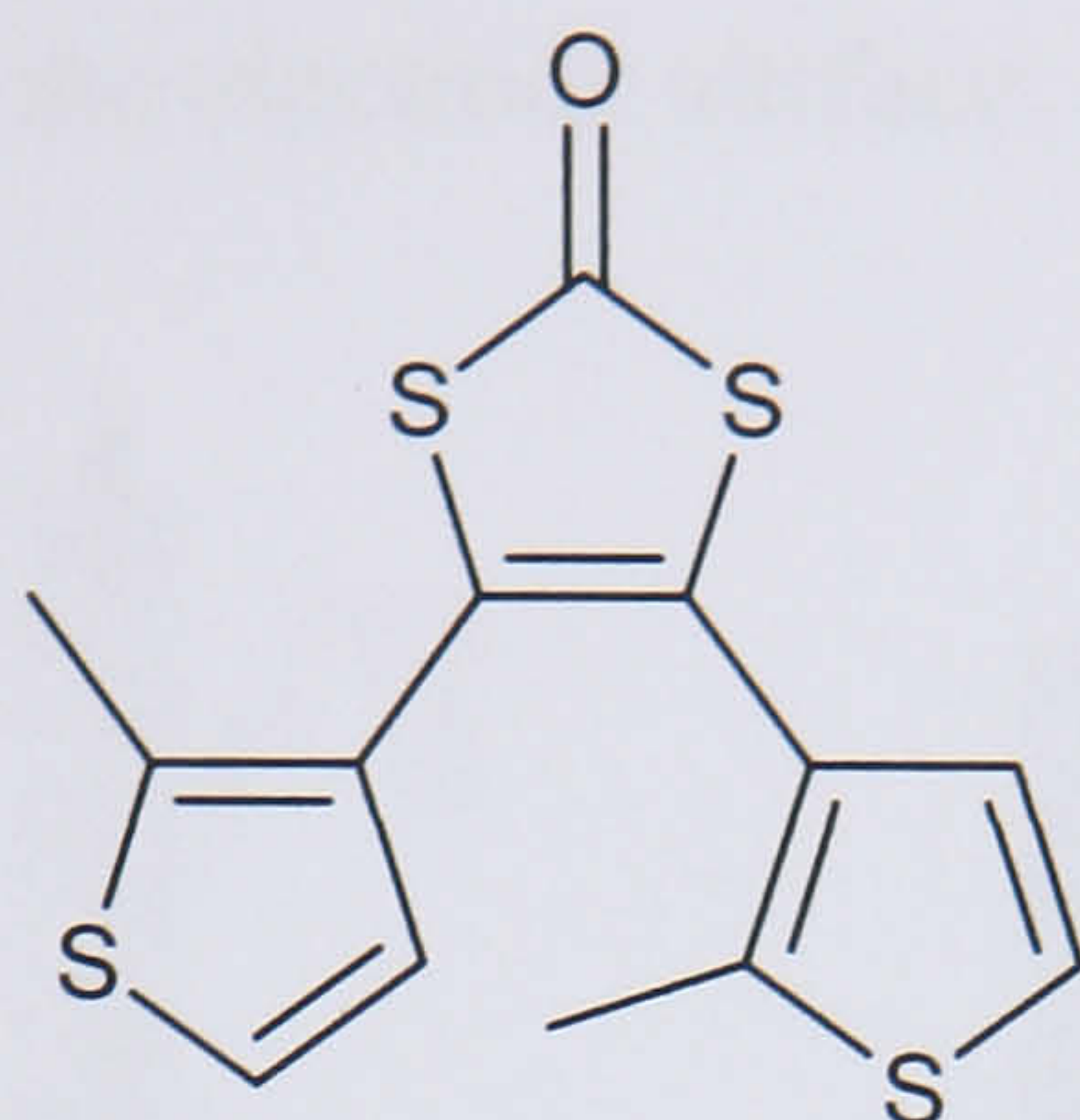


Figure 4.29 - 4,5-di-(5-methyl-thiophen-3-yl)-[1,3]dithiol-2-one **Th-3,3Me**.

#### Electrochemical Studies

As previously suggested, the coupling of **Th-3,3**, **Th-2,2** and **Th-2,3** monomer units occurs essentially through the  $\alpha$ -position. In order to confirm this, the polymerisation of **Th-3,3Me** has been attempted. The presence of the methyl group is expected to obstruct the formation of  $\alpha,\alpha$ -bonding between the thiophene units, thus hindering the development of a polymeric film. Polymerisation through the  $\beta$ -position has been reported, though leading to poor quality films.<sup>43</sup> The electrochemical behaviour of **Th-3,3Me** was investigated by CV as shown in Figure 4.30.

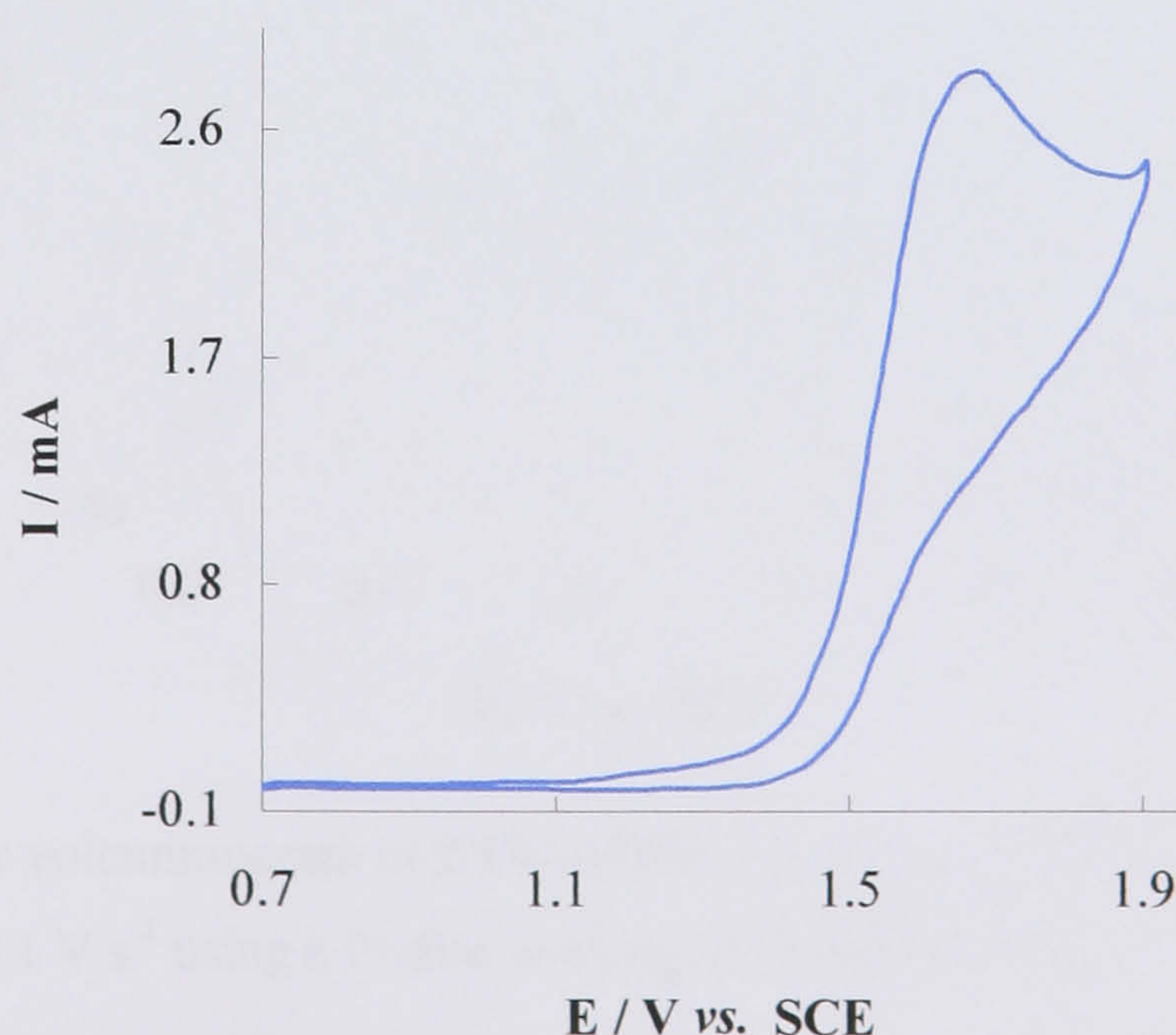


Figure 4.30 - Voltammogram of a **Th-3,3Me** solution ( $0.01 \text{ mol dm}^{-3}$ ) in electrolyte recorded at  $v = 0.1 \text{ V s}^{-1}$ .



As the electrochemical potential was taken above 1.5 V, blue-coloured species (Figure 4.31), normally associated with the cation radical of thiophene<sup>1</sup>, could be observed streaming away from the electrode surface.

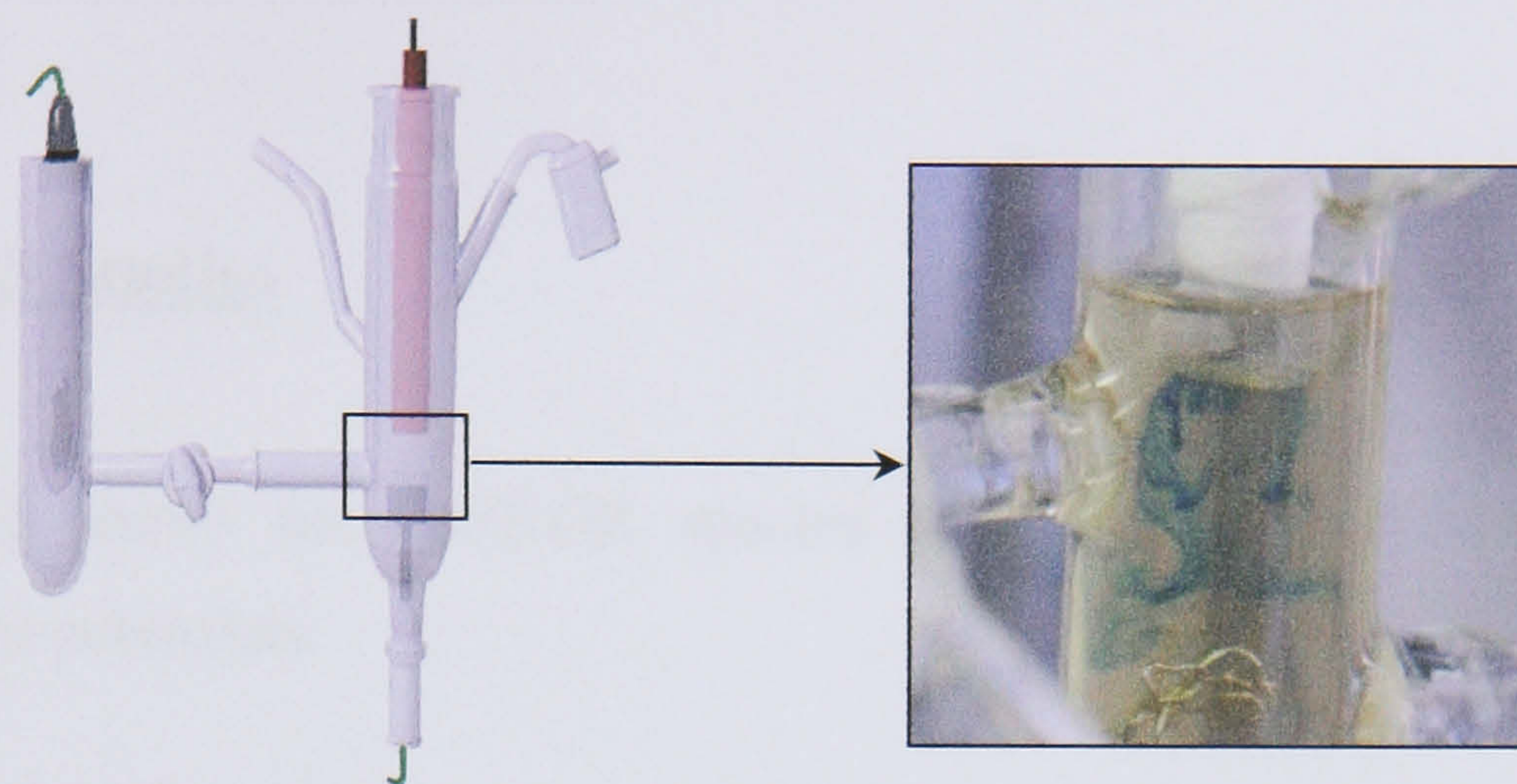


Figure 4.31 - Schematic diagram and photograph of the electrochemical cell.

Polymerisation could only be achieved by prolonged cycling (i.e. 2 h) of the **Th-3,3Me** solution between 0.7 and 1.9 V. The resultant polymer film was investigated in a monomer-free electrolyte solution. Figure 4.32 illustrates the voltammetric response obtained between different potential limits.

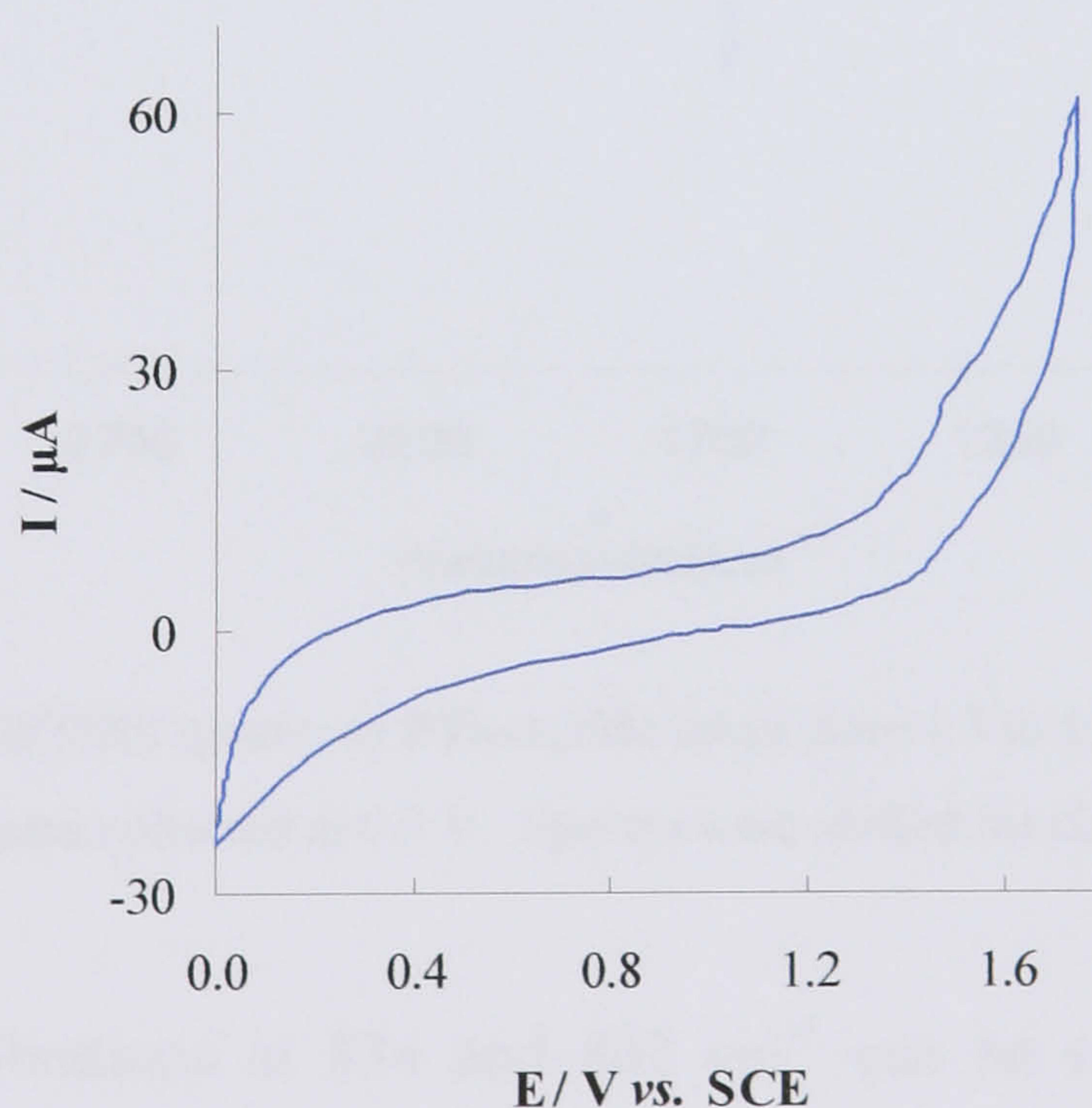


Figure 4.32 - Cyclic voltammogram of **PTh-3,3Me** in monomer free solution recorded at  $\nu = 0.1 \text{ V}\cdot\text{s}^{-1}$  using a Pt disc working electrode ( $0.44 \text{ cm}^2$ ).

The electroactivity of **PTh-3,3Me** is considerably different from the previous studied polythiophene dithiolenes. The oxidation of the polymer occurs at a



relatively high potential ( $E_{\text{ox}} = 1.55 \text{ V}$ ) and no perceptible colour change can be observed upon redox switching. The **PTh-3,3Me** film was found to be much less stable than the other three polythiophene dithiolenes, decomposing after a few potential cycles.

### SNIFTIRS Studies

Figure 4.33 shows the SNIFTIR spectra of **PTh-3,3Me** at progressively increasing positive potentials.

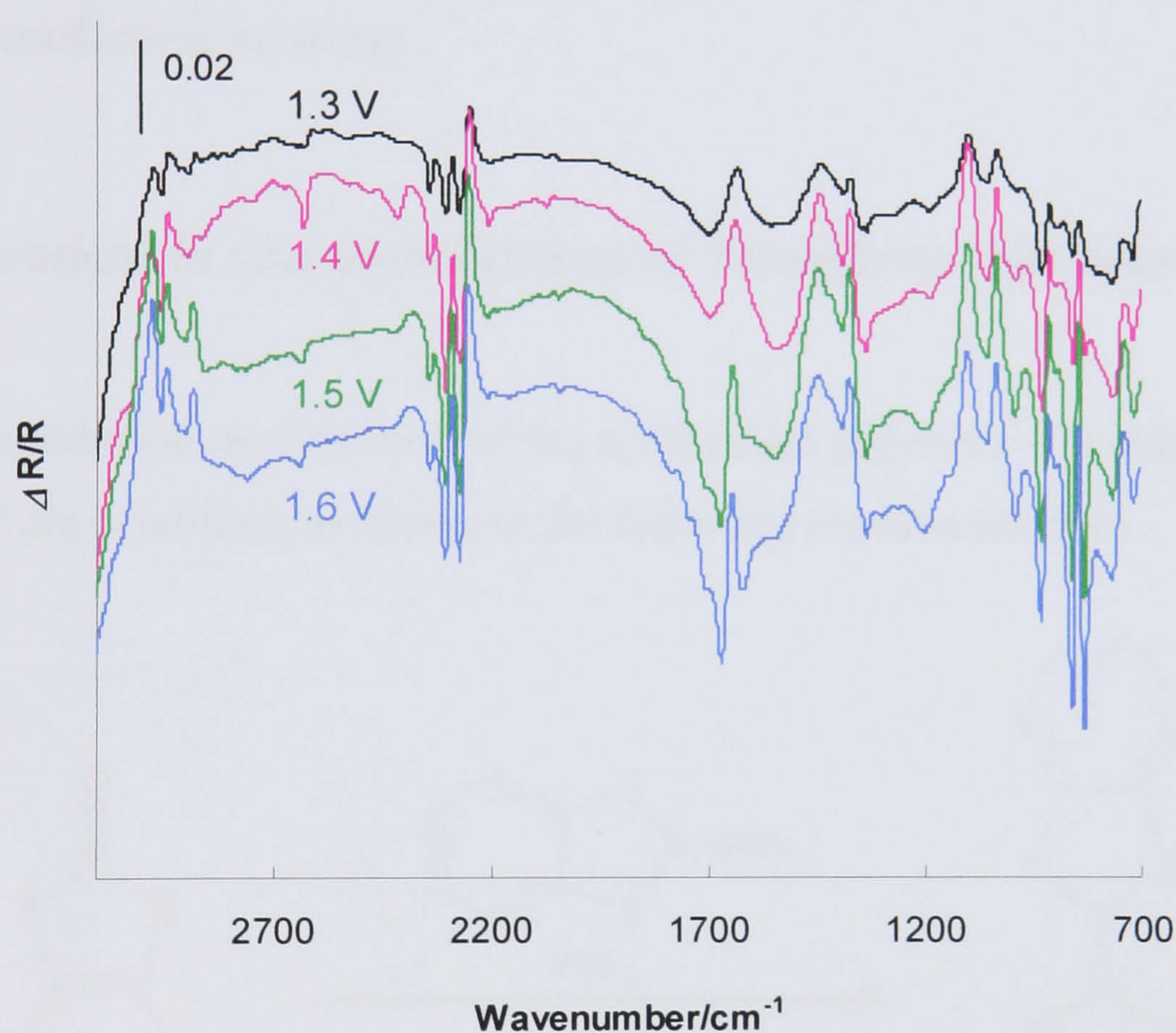


**Figure 4.33** - SNIFTIRS spectra of **PTh-3,3Me** taken from 1.3 to 1.6 V. Reference spectra collected at 0.3 V. Spectra were shifted for clarity.

Strong C-S vibrations at  $834$  and  $862 \text{ cm}^{-1}$  can be seen in the spectra of **PTh-3,3Me**. The  $\text{C}_{\alpha}\text{-H}$  stretching vibration observed at  $715 \text{ cm}^{-1}$  confirms that **Th-3,3Me** monomer units polymerise *via* the  $\beta$ -position. The effect of the oxidation on the strength of the C=O bond is manifested by the emergence of a positive band at  $1648 \text{ cm}^{-1}$  (neutral carbonyl) and an increasing negative peak at  $1705 \text{ cm}^{-1}$  (oxidised carbonyl).



A significant difference between the IR behaviour upon p-doping of **PTh-3,3Me** and the other polythiophene dithiolenes studied lies in the absence of a doping induced broad band assigned to the new electronic subgap transitions. Also, the IRAVs are relatively much weaker and ill-defined, suggesting that much less mobile carriers are being formed as the polymer is oxidised.

In light of the observed electrochemical and spectroelectrochemical response of **PTh-3,3Me** it can be concluded that induced polymerisation through  $\beta$ -position results in a poorly conductive film. This is consistent with the suggestion that the **Th-3,3**, **Th-2,2** and **Th-2,3** monomers polymerise by means of  $\alpha,\alpha$ -coupling, as all the three obtained polymers demonstrate the characteristic IR and UV-Visible features of conducting polymers.

#### 4.3.5 Chemical *in situ* modification of Thiophene Dithiolenes

The solid-state modification of the synthesised polymers was attempted using standard Wittig conditions as shown in the following reaction scheme:

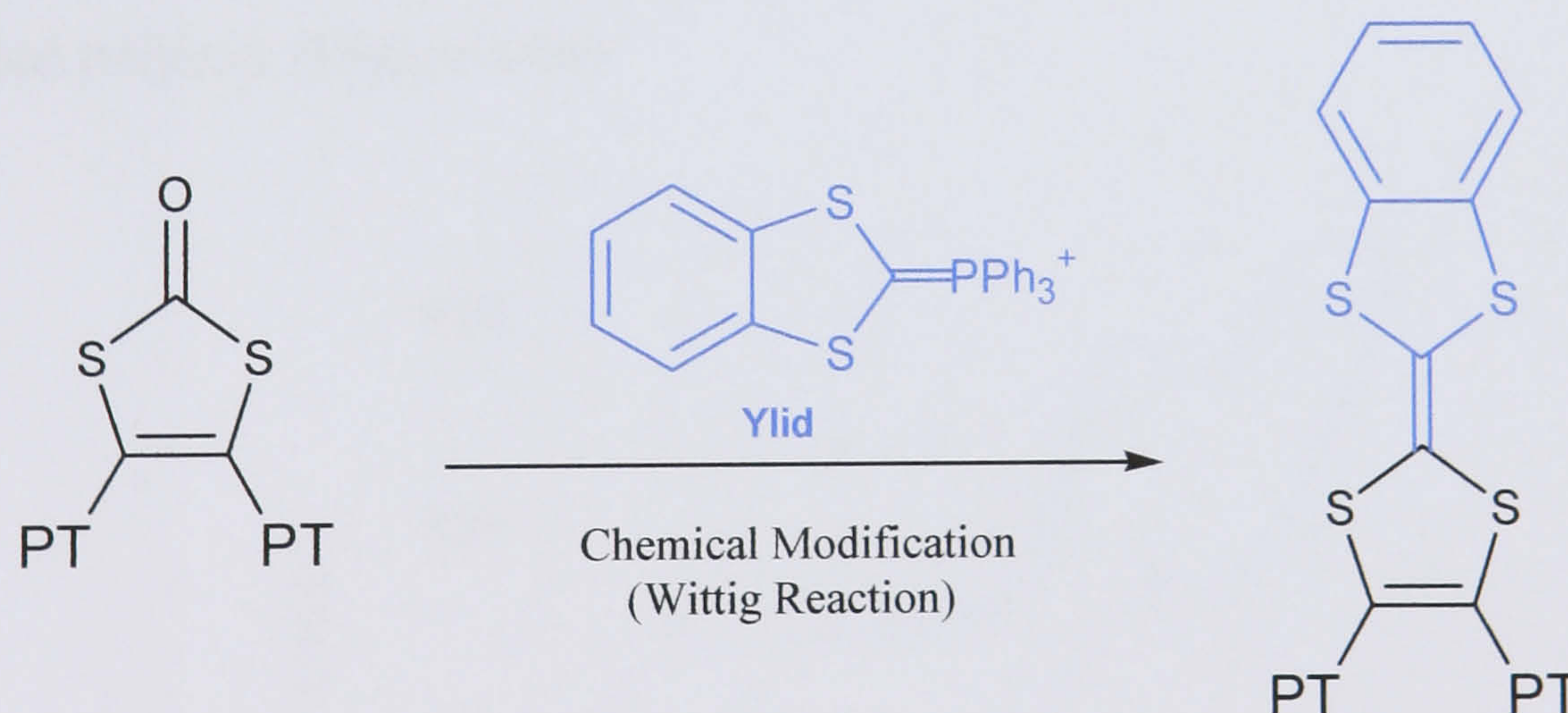


**Figure 4.34** - Reactional scheme for *in situ* modification of the polymer deposited on the electrode surface; PT – polythiophene chain.

A detailed description of the synthetic procedure used has been given in Chapter Two (pages 56 – 58).

Initial efforts to chemically modify the electropolymerised **PTh-3,3**, **PTh-2,2** and **PTh-2,3** were ineffective. Bearing in mind that the electrolyte used during the



electropolymerisation of thiophenes can have a direct influence on the structure of the obtained films a different supporting electrolyte (0.1 M of TBABF<sub>4</sub>, instead of 0.1 M TBAPF<sub>6</sub>, in acetonitrile) was used during the growth of the thiophene dithiolenes. It was envisaged that, as suggested by Marque *et al.*<sup>65</sup>, the presence of a different anion in the growth electrolyte would affect the morphology and electrochemical properties of the polythiophene dithiolenes films enabling their chemical modification. The first outcome of this change in electrolyte was a considerably faster growth of the polythiophene derivatives. The chemical modification of the electropolymerised polythiophene derivatives was then attempted. The Wittig reaction carried out on **PTh-2,3** and **PTh-2,2** was once again ineffective. However, **PTh-3,3** could be successfully modified and the characteristics of the new polymer were investigated by cyclic voltammetry and SNIFTIRS.

### Electrochemical Studies

Figure 4.35 illustrates the voltammogram of the modified **PTh-3,3** film **TTF(PTh-3,3)**, showing considerable differences in comparison with the CV of the unmodified polymer (Figure 4.06)

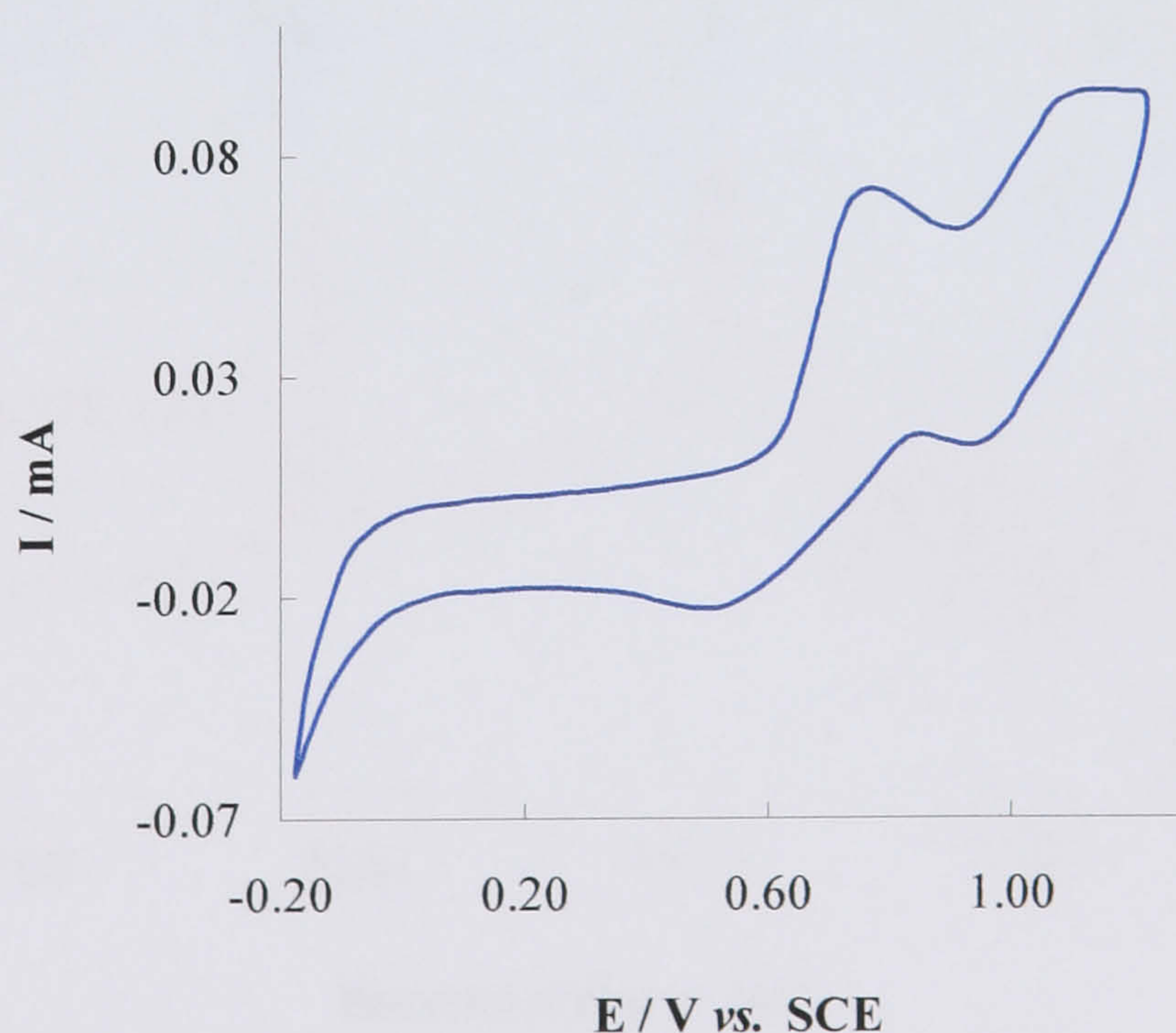


**Figure 4.35** - Cyclic voltammogram of **TTF(PTh-3,3)** in monomer free solution recorded at  $\nu = 0.1 \text{ V}\cdot\text{s}^{-1}$  using a Pt disc working electrode ( $0.44 \text{ cm}^2$ ).



The voltammetric response of **TTF(PTh-3,3)** shows two redox processes ( $E_{\text{ox}}^1 = 0.79 \text{ V} / E_{\text{red}}^1 = 0.51 \text{ V}$  and  $E_{\text{ox}}^2 = 1.12 \text{ V} / E_{\text{red}}^2 = 0.95 \text{ V}$ ), which are characteristic of TTF redox couples. The calculated half wave potentials,  $E_{1/2}^1 = 0.62 \text{ V}$  and  $E_{1/2}^2 = 1.03 \text{ V}$ , are more positive compared to the standard literature potentials for the TTF unit ( $E_{1/2}^1 = 0.34 \text{ V}$  and  $E_{1/2}^2 = 0.71 \text{ V}$ )<sup>4,6,66</sup>, under similar electrochemical conditions. This difference between the half wave potentials of **TTF(PTh-3,3)** and TTF had been expected due to the introduction of substituents onto the TTF unit.<sup>4</sup> The more positive values for the half wave potentials of **TTF(PTh-3,3)** indicate that this is a relatively less strong donor system than TTF.

### SNIFTIRS Studies

The SNIFTIRS spectra of the **TTF(PTh-3,3)** taken upon stepwise oxidation are shown in Figure 4.36 alongside with the SNIFTIR spectrum of **PTh-3,3** at 1.2 V.

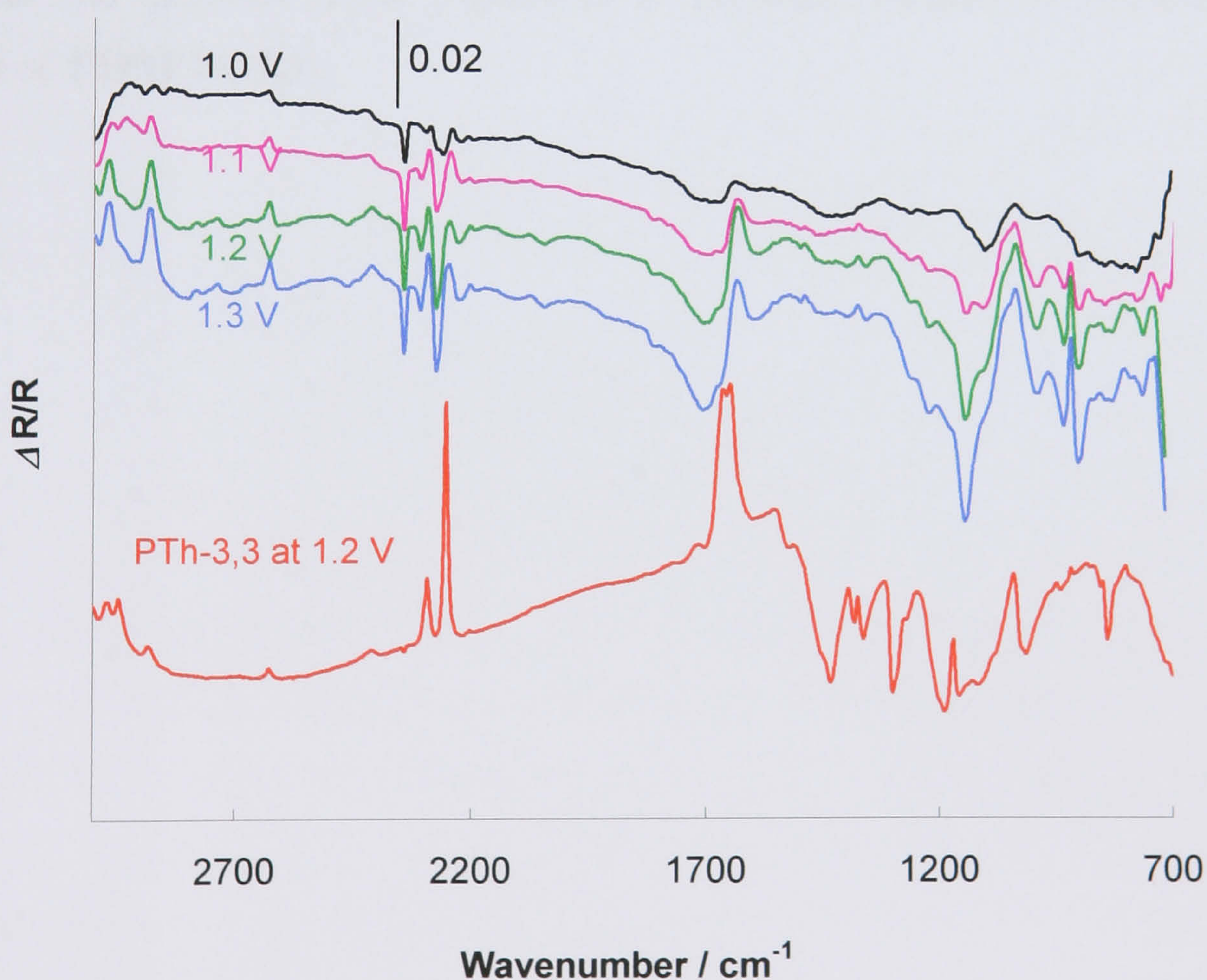


**Figure 4.36** - SNIFTIRS spectra of **TTF(PTh-3,3)** taken from 1.0 to 1.3 V. Reference spectra collected at 0.3 V. Spectra were shifted for clarity.



The spectra shown in Figure 4.36 reveal an apparent decrease in the conductivity level of **PTh-3,3** upon chemical modification, as the most revealing shifts observed for doped conducting polymers (IRAVs and broad absorbance band extending into the near infrared) are absent in the spectrum of the **TTF(PTh-3,3)**.

Bands at 763, 827 and 932  $\text{cm}^{-1}$ , arise from the C-S ring vibrations.<sup>27,67</sup> A positive absorption band at 1040  $\text{cm}^{-1}$ , related to the insertion of the  $\text{BF}_4^-$  into the film is also observed.<sup>28,68</sup>

The presence of peaks at 1673  $\text{cm}^{-1}$  and 1263  $\text{cm}^{-1}$ , assigned to the stretching vibration of the C=C bond in TTFs<sup>34,69</sup> confirms the chemical modification of **PTh-3,3** to **TTF(PTh-3,3)**. Nonetheless, the emergence of a positive band at 1629  $\text{cm}^{-1}$ , associated with a decrease in the strength of the C=O bond upon oxidation, indicates that only partial modification of the polymer has been achieved. A possible explanation for the incomplete modification of **PTh-3,3** is that the Wittig reaction only takes place at the polymer's surface. The existence of two different structural regions (PTh-3,3 / TTF(PTh-3,3)) in the film might also hinder charge transport and therefore cause a decrease in polymer conductivity as seen in the spectra of **TTF(PTh-3,3)**.



## 4.4 Conclusions

Polythiophene dithiolenes have been prepared electrochemically and their properties evaluated by cyclic voltammetry, SNIFTIR and UV-Visible spectroscopy.

The voltammetric investigation of **Th-3,3**, **Th-2,2** and **Th-2,3**, three thiophene dithiolenes that only differ in the substitution pattern on the thiophene ring, showed an irreversible oxidation at roughly the same potential for all the compounds, owing to the formation of radical cations. Cycling to this potential value leads to the deposition of **PTh-3,3**, **PTh-2,2** and **PTh-2,3**. The voltammograms of the electrosynthesised polymers were considerably similar and resembled those of many polythiophenes. It was clear that all three polythiophene dithiolenes could be reversibly (and easily) p-doped but none showed stability towards n-doping. They also exhibited an electrochromic effect with the colour changing from yellow in the neutral state, to black in the oxidised state.

The spectroelectrochemical investigation of these polymers was performed using the same range of potentials as those applied during the characterisation by cyclic voltammetry. The films exhibit comparable IR activity to other conducting polymer systems reported in the literature during p-doping. As expected, the spectra were dominated by the appearance of IRAV bands (due to the selective enhancement of four thiophene ring modes) and by a broad band extending towards the near IR. This band has been attributed to electronic transitions between the valence band and new subgap states formed upon doping. In contrast with the spectroelectrochemical behaviour of the dithienylethylenes reported in Chapter Three, the doping of the polythiophene dithiolenes induces an IR response typical of conducting polymers. Considering that the main structural difference between these two classes of polymers lies in the electron withdrawing 1,3-dithiol-2-one unit, it has been suggested that its presence has the effect of extending the  $\pi$ -conjugated system, therefore allowing a more efficient electron delocalisation along the polymer chains.



The SNIFTIRS spectra also revealed the effect of the doping process on the strength of the C=O bond. Upon oxidation, the positive charge on the carbonyl carbon atom increases which creates a polarised bond resulting in increased bond strength. This phenomenon was evident in the IR spectra that showed a band associated with the carbonyl group being progressively lost and the peak associated with the oxidised polymer becoming increasingly dominant. The absence of the C<sub>α</sub>-H stretching vibration peak was indicative of the presence of α,α-coupling between thiophene rings. Also, the analysis of subtle differences between the SNIFTIR spectra of **PTh-3,3**, **PTh-2,2** and **PTh-2,3**, specifically, the change in reflectivity upon doping, gave an insight into their structures. It is possible that whereas in **PTh-2,2** and **PTh-3,3**, almost all the molecule can participate in the conduction mechanism, in the case of **PTh-2,3**, only one of the thiophene rings is involved in the transport of charge across the polythiophene backbone.

UV-Visible spectroscopy has been used to examine the optical behaviour the polythiophene dithiolenes. The UV-Visible spectra of the neutral polymers exhibited an absorbance band assigned to the π-π\* transition. From the onset of this transition it has been determined that **PTh-3,3**, **PTh-2,2** and **PTh-2,3** have a bandgap of 2.04, 2.30 and 2.18 eV, respectively. Oxidation of the polymer films was accompanied by the appearance of a new broad absorption band characteristic of the presence of free carriers.

Since the electrochemical doping of **PTh-3,3**, **PTh-2,2** and **PTh-2,3**, has triggered the appearance of two new electronic subgap transitions, revealed by UV-Visible spectroscopy and SNIFTIRS, it has been suggested that bipolarons are the most likely charge carriers formed upon p-doping of the polythiophene dithiolenes.

In order to confirm that the bonding of the thiophene dithiolenes occurs through the α- position, the polymerisation of **Th-3,3Me** has been attempted. The presence of the methyl group was expected to obstruct the α,α-bonding between the thiophene units, thus hindering the formation of a polymeric film. Surprisingly, the electrochemical polymerisation of **Th-3,3Me** did occur but through the β-position. The electroactivity of **PTh-3,3Me** was considerably different from the previous studied polythiophene dithiolenes. The oxidation of the polymer took place at a



relatively higher potential and no perceptible colour change could be observed upon redox switching.

The spectroelectrochemical studies on **PTh-3,3Me** showed a polymer with a rather different IR behaviour from the other polythiophene derivatives studied. The absence of a doping induced broad band assigned to new electronic subgap transitions and the appearance of relatively much weaker and ill-defined IRAVs suggests the formation of less mobile carriers upon doping. In light of the observed electrochemical and spectroelectrochemical response of **PTh-3,3Me** it can be concluded that induced polymerisation through  $\beta$ -position results in a poorly conductive film. Consequently, the proposed structures for **PTh-3,3**, **PTh-2,2** and **PTh-2,3**, with monomer units linking through  $\alpha$ - position, must be fairly accurate, as all these three polymers demonstrate the characteristic IR and UV-Visible features of conducting polymers.

The solid-state modification of the synthesised polymers was attempted using standard Wittig conditions. Initial efforts to chemically modify the electropolymerised **PTh-3,3**, **PTh-2,2** and **PTh-2,3** were ineffective. To overcome these difficulties, a new electrolyte was used in the synthesis and study of the thiophene derivatives. It was envisaged that the use of TBABF<sub>4</sub> instead of TBAPF<sub>6</sub> (different anions) could induce the formation of a structurally different polymer susceptible to chemical modification. Even though attempts to chemically modify **PTh-2,3** and **PTh-2,2** remained ineffective, the Wittig reaction was successfully carried out on **PTh-3,3**.

Cyclic voltammetric studies on **TTF(PTh-3,3)** showed the presence of the characteristic tetrathiafulvalene redox couples corresponding to the TTF unit of the modified film. SNIFTIRS data also confirmed the presence of the TTF group (C=C vibrations at 1263 and 1668 cm<sup>-1</sup>). Nevertheless, the emergence of a positive IR band, associated with the decrease in the strength of the C=O bond upon oxidation, indicated that only partial modification of the polymer has been achieved.

Given that, the switch of the growth electrolyte has made possible the chemical modification of **PTh-3,3** it is likely that future improvements, at the experimental level, will eventually lead to the complete chemical modification of the polythiophene dithiolenes.



## 4.5 References

1. A. Charlton, M. Kalaji, P.J. Murphy, S. Salmaso, A.E. Underhill, G. Williams, M.B. Hursthouse and K.M. Abdul Malik, *Synth. Met.*, 95 (1998) 75.
2. L. Huchet, S. Akoudad, J. Roncali and E. Levillain, *Synth. Met.*, 101 (1999) 37.
3. A. Charlton, A. Underhill, G. Williams, M. Kalaji, P.J. Murphy, K.M.A. Malik and M.B. Hursthouse, *J. Org. Chem.*, 62 (1997) 3098.
4. G.O. Williams, Ph.D. Thesis, University of Wales, Bangor (1999).
5. D.L. Coffen, J.Q. Chambers, D.R. Williams, P.E. Garrett and N.D. Canfield, *J. Am. Chem. Soc.*, 93 (1971) 2258.
6. F.B. Kaufman, A.H. Schroeder, E.M. Engler, S.R. Kramer and J.Q. Chambers, *J. Am. Chem. Soc.*, 102 (1980) 483.
7. B.S. Furniss, A.J. Hannaford, P.W.G. Smith and A.R. Tatchell, in "Textbook of Practical Organic Chemistry", Longman, London, (1989).
8. M. Kabasakaloglu, T. Kiyak, H. Toprak and M.L. Aksu, *Appl. Surf. Sci.*, 152 (1999) 115.
9. R.J. Wattman, J. Bargon and A.F. Diaz, *J. Phys. Chem.*, 87 (1983) 1459.
10. G. Tourillon and F. Garnier, *J. Electroanal. Chem.*, 161 (1984) 51.
11. C. Jerome, C. Maertens, M. Mertens, R. Jerome, C. Quattrocchi, R. Lazzaroni and J.L. Bredas, *Synth. Met.*, 83 (1996) 103.
12. P. Camurlu, A. Cirpan and L. Toppare, *Mat. Chem. Phys.*, 92 (2005) 413.
13. C.J. Walsh, T. Sooksimuang and B.K. Mandal, *Macromolecules*, 32 (1999) 2397.
14. B. Sankaran and J.R. Reynolds, *Macromolecules*, 30 (1997) 2582.
15. M.R. Fernandes, J.R. Garcia, M.S. Schultz and F.C. Nart, *Thin Solid Films*, 474 (2005) 279.
16. A. Patil, A.J. Heeger and F. Wudl, *Chem. Rev.*, 88 (1988) 183.
17. P.R. Somani and S. Radhakrishnan, *Mat. Chem. Phys.*, 77 (2003) 117.
18. H.S. Nalwa, ed., "Handbook of organic conductive molecules and polymers – Conductive polymers: Spectroscopy and Physical Properties". Vol. 3. J. Wiley & Sons Ltd., UK, (1997).



19. B. Ballarin, F. Costanzo, F. Mori, A. Mucci, L. Pigani, L. Schenetti, R. Seeber, D. Tonelli and C. Zanardi, *Electrochim. Acta*, 46 (2001) 881.
20. S. Hotta, S. Rughooputh, A.J. Heeger and F. Wudl, *Macromolecules*, 20 (1987) 212.
21. C. Ehrendorfer, A. Karpfen, P. Bauerle, H. Neugebauer and A. Neckel, *J. Mol. Struc.*, 298 (1993) 65.
22. J.T. Lopez Navarrete, V. Hernandez, J. Casado, L. Favaretto and G. Distefano, *Synth. Met.*, 101 (1999) 590.
23. L.M.H. Groenewoud, G.H.M. Engbers, R. White and J. Feijen, *Synth. Met.*, 125 (2001) 429.
24. A. Berlin and G. Zotti, *Synth. Met.*, 106 (1999) 197.
25. J.R. Reynolds, J.P. Ruiz, A.D. Child, K. Nayak and D.S. Marynick, *Macromolecules*, 24 (1991) 678.
26. J. Casado, H.E. Katz, V. Hernandez and J.T. Lopez Navarrete, *Vibrational Spectroscopy*, 30 (2002) 175.
27. C. Kvarnstrom, H. Neugebauer, S. Blomquist, H.J. Ahonen, J. Kankare and A. Ivaska, *Electrochim. Acta*, 44 (1999) 2739.
28. M. Kofranek, T. Kovar, H. Lischka and A. Karpfen, *J. Molec. Struc.: THEOC.*, 259 (1992) 181.
29. M. Pohjakallio, G. Sundholm and P. Talonen, *J. Electroanal. Chem.*, 401 (1996) 191.
30. C. Ehrendorfer, H. Neugebauer, A. Neckel and P. Bauerle, *Synth. Met.*, 55 (1993) 493.
31. G. Tourillon and F. Garnier, *J. Electroanal. Chem.*, 135 (1982) 173.
32. G. Louarn, J.-Y. Mevellec, J.P. Buisson and S. Lefrant, *Synth. Met.*, 55 (1993) 587.
33. J.T. Lopez Navarrete, J. Casado, H. Muguruma, S. Hotta and V. Hernandez, *J. Mol. Struc.*, 521 (2000) 239.
34. R. Bozio, I. Zanon, A. Girlando and C. Pecile, *J. Phys. Chem.*, 71 (1979) 2282.
35. D. Kumar, *Synth. Met.*, 114 (2000) 369.
36. M. Pohjakallio, G. Sundholm and P. Talonen, *J. Electroanal. Chem.*, 406 (1996) 165.



37. B. Rasch and W. Vielstich, *J. Electroanal. Chem.*, 370 (1994) 109.
38. P.A. Christensen, A. Hamnett, A.R. Hillman, M.J. Swann and S.J. Higgins. *J. Chem. Soc. Faraday Trans.*, 88 (1992) 595.
39. W. Hayes, F.L. Pratt, K.S. Wong, K. Kaneto and K. Yoshino, *J. Phys. C: Solid State Phys.*, 18 (1985) 555.
40. H.S. Nalwa, ed., "Handbook of organic conductive molecules and polymers – Conductive polymers: Synthesis and electrical properties", Vol. 2, J. Wiley & Sons Ltd., UK, (1997).
41. P.A. Christensen, A. Hamnett and D.C. Read, *Electrochim. Acta*, 39 (1994) 187.
42. G. Tourillon and F. Garnier, *J. Electrochem. Soc.*, 130 (1983) 2042.
43. H.S.O. Chan and S.C. Ng, *Prog. Polym. Sci.*, 23 (1998) 1167.
44. E. Lankinen, G. Sundholm, P. Talonen, T. Laitinen and T. Saario, *J. Electroanal. Chem.*, 447 (1998) 135.
45. R. Beyer, M. Kalaji, G. Kingscote-Burton, P.J. Murphy, V.M.S.C. Pereira, D.M. Taylor and G.O. Williams, *Synth. Met.*, 92 (1998) 25.
46. U. Schlick, F. Teichert and M. Hanack, *Synth. Met.*, 92 (1998) 75.
47. J. Roncali, *Chem. Rev.*, 97 (1997) 173.
48. P.J. Skabara, I.M. Serebryakov, D.M. Roberts, I.F. Perepichka, S.J. Coles and M.B. Hursthouse, *J. Org. Chem.*, 64 (1999) 6418.
49. E. Lankinen, M. Pohjakallio, G. Sundholm, P. Talonen, T. Laitinen and T. Saario, *J. Electroanal. Chem.*, 437 (1997) 167.
50. M.J. Nowak, S.D.D.V. Rughooputh, S. Hotta and A.J. Heeger, *Macromolecules*, 20 (1987) 965.
51. M. Onoda, T. Iwasa, T. Kawai and K. Yoshino, *J. Phys. D: Appl. Phys.*, 24 (1991) 2076.
52. E.E. Havinga and C.M.J. Mutsaers, *Chem. Mater.*, 8 (1996) 769.
53. B. Dias, E. Giroto, R. Matos, M. Santos, M. Paoli and W. Gazotti, *J. Braz. Chem. Soc.*, 16 (2005) 733.
54. Y. Furukawa, *J. Phys. Chem.*, 100 (1996) 15644.
55. C. Carlberg, X. Chen and O. Inganäs, *Solid State Ionics*. 85 (1996) 73.
56. H. Neugebauer, *J. Electroanal. Chem.*, 563 (2004) 153.
57. D.N. Tito, Ph.D. Thesis, University of Wales, Bangor (2005).



58. V.W. Jones and M. Kalaji, *J. Electroanal. Chem.*, 395 (1995) 323.
59. Y. Martinez, R. Hernandez, M. Kalaji, O.P. Marquez and J. Marquez, *J. Electroanal. Chem.*, 563 (2004) 145.
60. J. Foley, C. Korzeniewski and S. Pons, *Can. J. Chem.*, 66 (1987) 201.
61. A.M. Celli, D. Donati, F. Ponticelli, S.J. Roberts-Bleming, M. Kalaji and P.J. Murphy, *Org. Lett.*, 3 (2001) 3573.
62. S.J. Roberts-Bleming, G.L. Davies, M. Kalaji, P.J. Murphy, A.M. Celli, D. Donati and F. Ponticelli, *J. Org. Chem.*, 68 (2003) 7115.
63. T.A. Skotheim, ed., "Handbook of Conducting Polymers", Vol. 1, Marcel Dekker Inc., New York, (1986).
64. M.R. Andersson, M. Berggren, G. Gustafson, T. Hjertberg, O. Inganas and O. Wennerstrom, *Synth. Met.*, 71 (1995) 2183.
65. P. Marque, J. Roncali and F. Garnier, *J. Electroanal. Chem.*, 218 (1987) 107.
66. G. Zotti, S. Zecchin, G. Schiavon, A. Berlin, L. Huchet and J. Roncali, *J. Electroanal. Chem.*, 504 (2001) 64.
67. A.K. Bakhshi, *Mat. Sci. Eng. C*, 3 (1995) 249.
68. K. Gurunathan, A.V. Murugan, R. Marimuthu, U.P. Mulik and D.P. Amalnerkar, *Mat. Chem. Phys.*, 61 (1999) 173.
69. M. Meneghetti, R. Bozio, I. Zanon, C. Pecile and C. Ricotta, *J. Phys. Chem.*, 80 (1983) 6210.



## **Chapter 5**

# **Studies on Nickel**

## **Dithiolenes**



## 5.1 Introduction

Continuing the studies in the area of thiophene derivatives, the electrochemical and spectroelectrochemical properties of new nickel dithiolenes have been investigated. The aim of this research was to attempt the incorporation of transition metal complexes into conjugated organic polymers. Previous investigations in this field have received considerable attention as they offer the prospect of novel conducting, magnetic, and catalytic materials<sup>1,2</sup>. Dithiolenes are attractive building blocks for such polymeric systems because of their aromaticity, and ease of reduction of the aromatic system.

Figures 5.01 – 5.02 show the structure of the nickel dithiolenes analysed in this project.

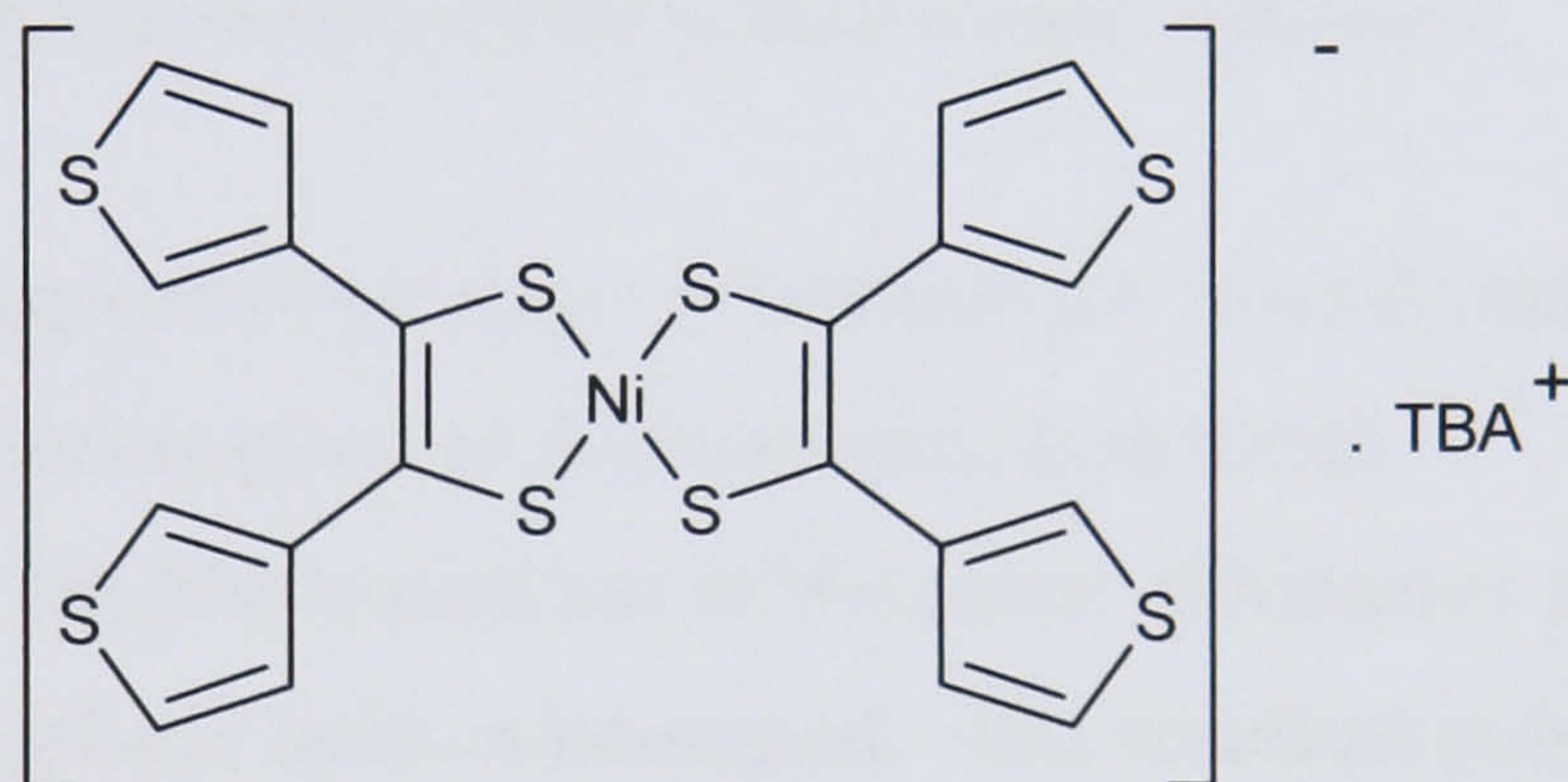


**Figure 5.01** - Structure of bis[1,2-di(3-thienyl)-1,2-ethenedithiolenes] nickel tetrafluoroborate,  $\text{Ni}(\text{Th-3,3})_2$ .

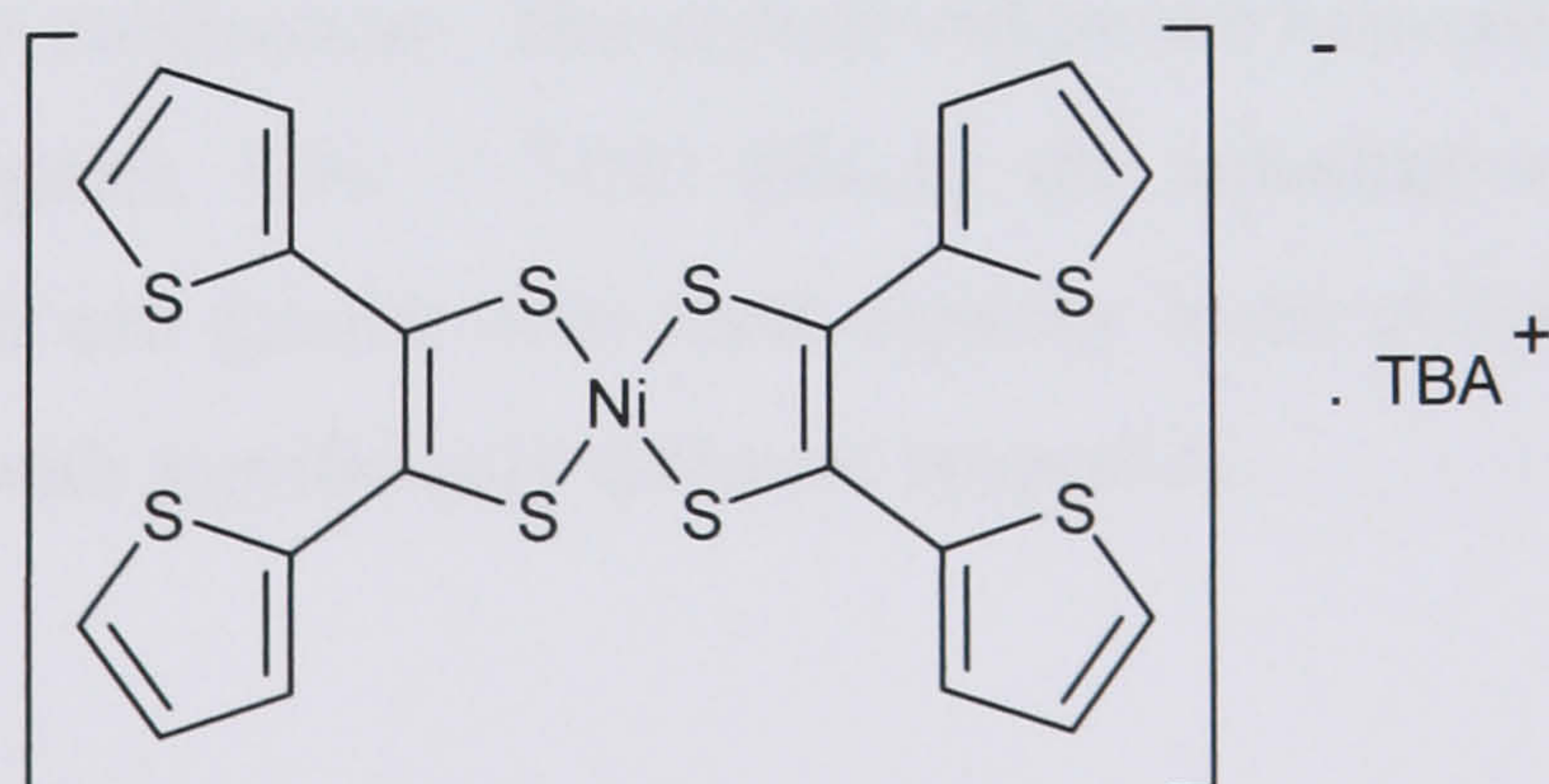


**Figure 5.02** - Structure of bis[1,2-di(2-thienyl)-1,2-ethenedithiolenes] nickel tetrafluoroborate  $\text{Ni}(\text{Th-2,2})_2$ .



The neutral nickel dithiolenes are known to have low solubility in acetonitrile<sup>3</sup>, and therefore, the electrochemical studies were carried out on the tetrabutylammonium salts instead.

The extensive conjugation exhibited by nickel dithiolenes and the electron donating effect of the peripheral thiophenes makes them central units in the research towards the development of molecular conductors.<sup>4-7</sup> One of the unique properties of metal dithiolenes is their ability to exist in several clearly defined oxidation states as represented in Figure 5.03.<sup>8-12</sup>

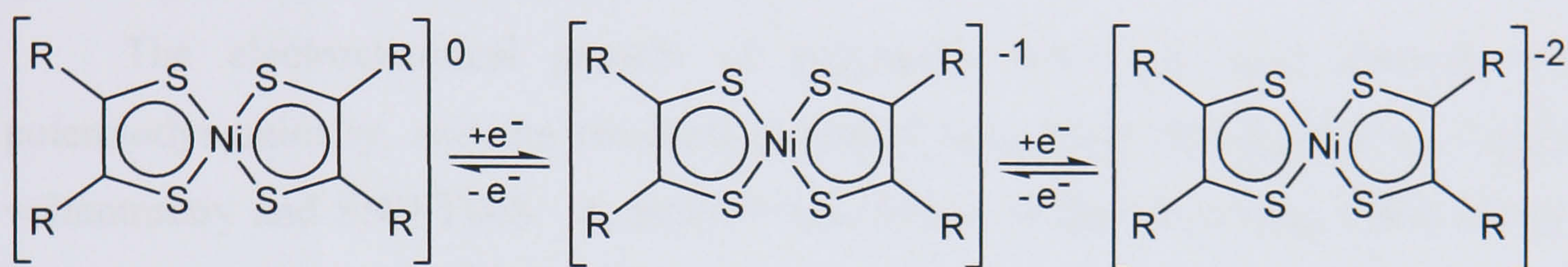


**Figure 5.03** - The interconvertible oxidation states of metal dithiolenes.

The reversible one-electron transfer between the neutral and anionic species can be achieved by either chemical or electrochemical methods.<sup>10,13</sup>

In this Chapter, the polymerisation of the metal dithiolenes shown in Figures 5.01 - 5.02 *via* the thiophene units is attempted. The resultant polythiophene chain would have incorporated into its structure a nickel dithiolenes centre. This may prove to be advantageous in the control of the electronic properties of the synthesised polymeric film, by improving its structural regularity or even providing an alternative pathway for conduction. The central difference between the investigated nickel complexes (Figures 5.01 - 5.02) lies in the substitution pattern of the thiophene rings, which can greatly alter their capacity to be polymerised and may also lead to polymers with significantly different properties.



## 5.2 Experimental

The electrochemistry of  $\text{Ni(Th-3,3)}_2$  and  $\text{Ni(Th-2,2)}_2$  was investigated by cyclic voltammetry, using a monomer solution of  $0.0002 \text{ mol dm}^{-3}$  in supporting electrolyte ( $0.1 \text{ M TBAPF}_6 / \text{MeCN}$ ). The experiments were performed in a three-electrode glass cell using a platinum disc as the working electrode (electrode area =  $0.44 \text{ cm}^2$ ), a platinum foil as the counter electrode, and a  $\text{Ag/Ag}^+$  reference electrode ( $+ 0.32 \text{ V vs. SCE}$ ). All potentials values presented in this Chapter are quoted against the saturated calomel electrode.

The electrochemical growth of polymeric films has been carried out potentiodynamically, and the resultant polymers have been investigated by cyclic voltammetry and SNIFTIRS. A detailed description of the procedures followed for the voltammetric and spectroscopic measurements can be found in Chapter Two.



## 5.3 Results and Discussion

### 5.3.1 Studies on Nickel Dithiolene $\text{Ni}(\text{Th-3,3})_2$

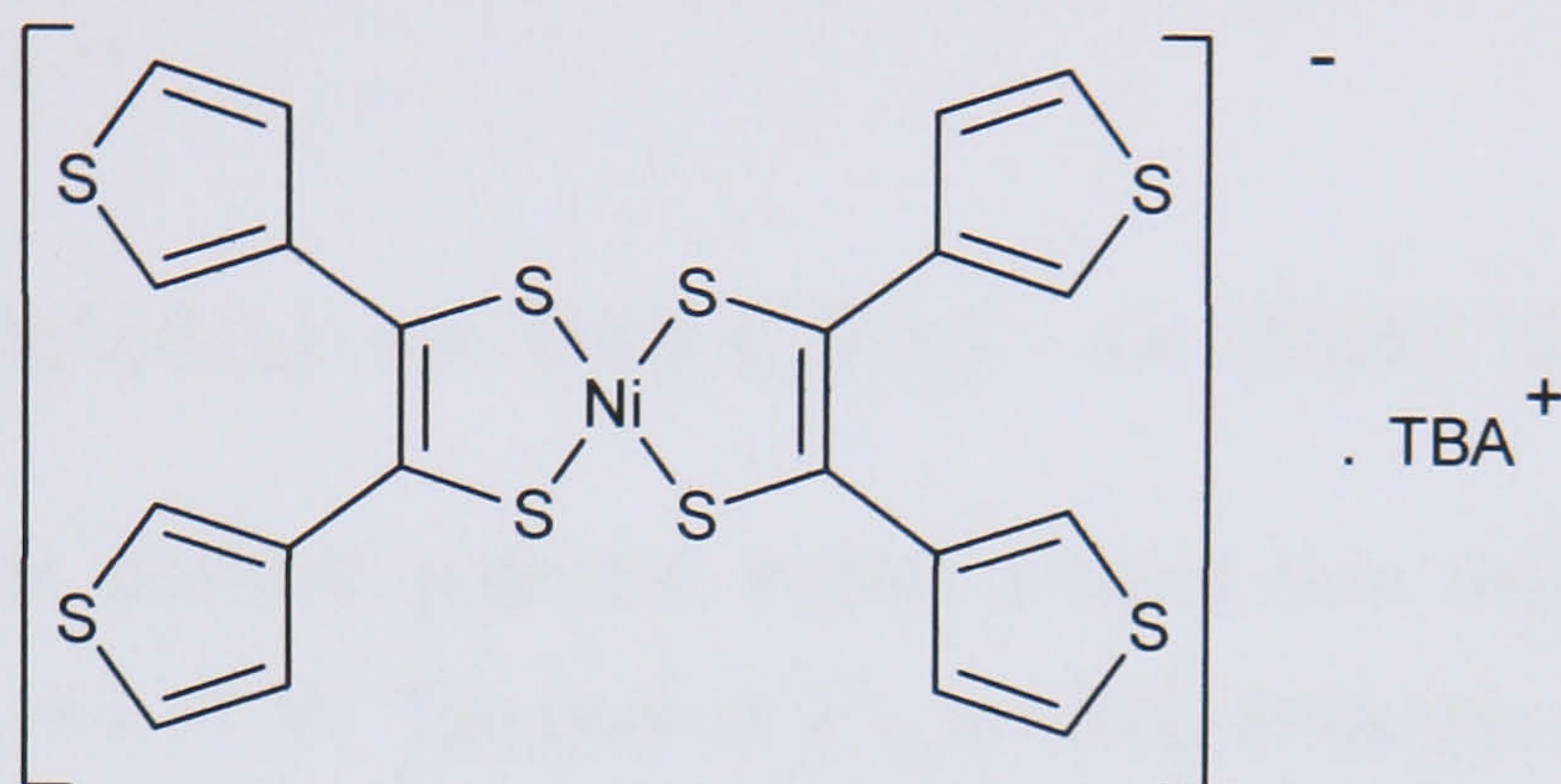


Figure 5.04 - Structure of bis[1,2-di(3-thienyl)-1,2-ethenedithiolene] nickel tetrafluoroborate  $\text{Ni}(\text{Th-3,3})_2$ .

### Electrochemical Studies

The electrochemical behaviour of  $\text{Ni}(\text{Th-3,3})_2$  was investigated by CV. The voltammetric responses obtained when the potential was cycled between -1 V and increasing positive values are shown in Figure 5.05.

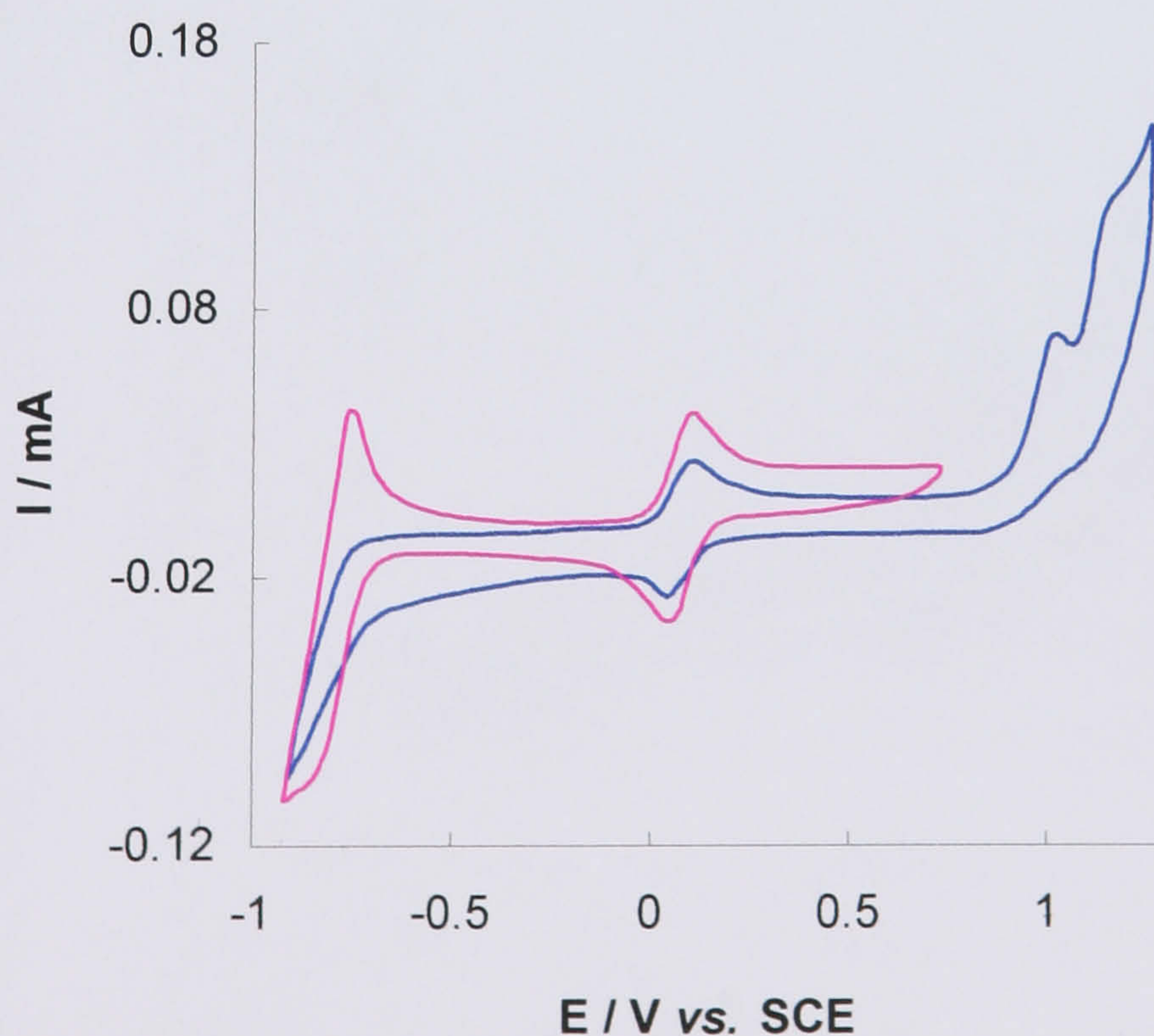


Figure 5.05 - Voltammogram of a  $\text{Ni}(\text{Th-3,3})_2$  solution ( $0.0002 \text{ mol dm}^{-3}$ ) in electrolyte recorded at  $\nu = 0.1 \text{ V s}^{-1}$ .



The cyclic voltammograms show two reversible or quasi-reversible one electron redox processes at  $E_{\text{ox}}^1 = -0.74$  V,  $E_{\text{red}}^1 = -0.83$  V ( $E_{1/2}^1 = -0.79$  V) and  $E_{\text{ox}}^2 = 0.09$  V,  $E_{\text{red}}^2 = 0.04$  V ( $E_{1/2}^2 = 0.07$  V). By analogy with the electrochemical behaviour reported for many dithiolene complexes these can be assigned to the sequential interchange between the neutral, anionic and dianionic states of the nickel dithiolene centre.<sup>3,7,9,14-17</sup>



Cycling towards positive potential values reveals two oxidation peaks at  $E_{\text{ox}}^3 = 1.04$  V and  $E_{\text{ox}}^4 = 1.17$  V. The peak at  $E_{\text{ox}}^3$  is likely to be due to the formation of the cationic state in the dithiolene unit.<sup>3,10,18</sup> Figure 5.05 shows that polymer oxidation above this potential has an irreversible effect on the dithiolene ligand, hampering the formation of the dianionic state. The increase in the electrochemical potential up to  $E_{\text{ox}}^4$  leads to the deposition of a polymer on the electrode surface, and therefore this peak can be assigned to the oxidation of the thiophene units to radical cations.

Polymerisation of  $\text{Ni}(\text{Th-3,3})_2$  was achieved by potential cycling between 0.2 V and 1.3 V as shown in Figure 5.06.

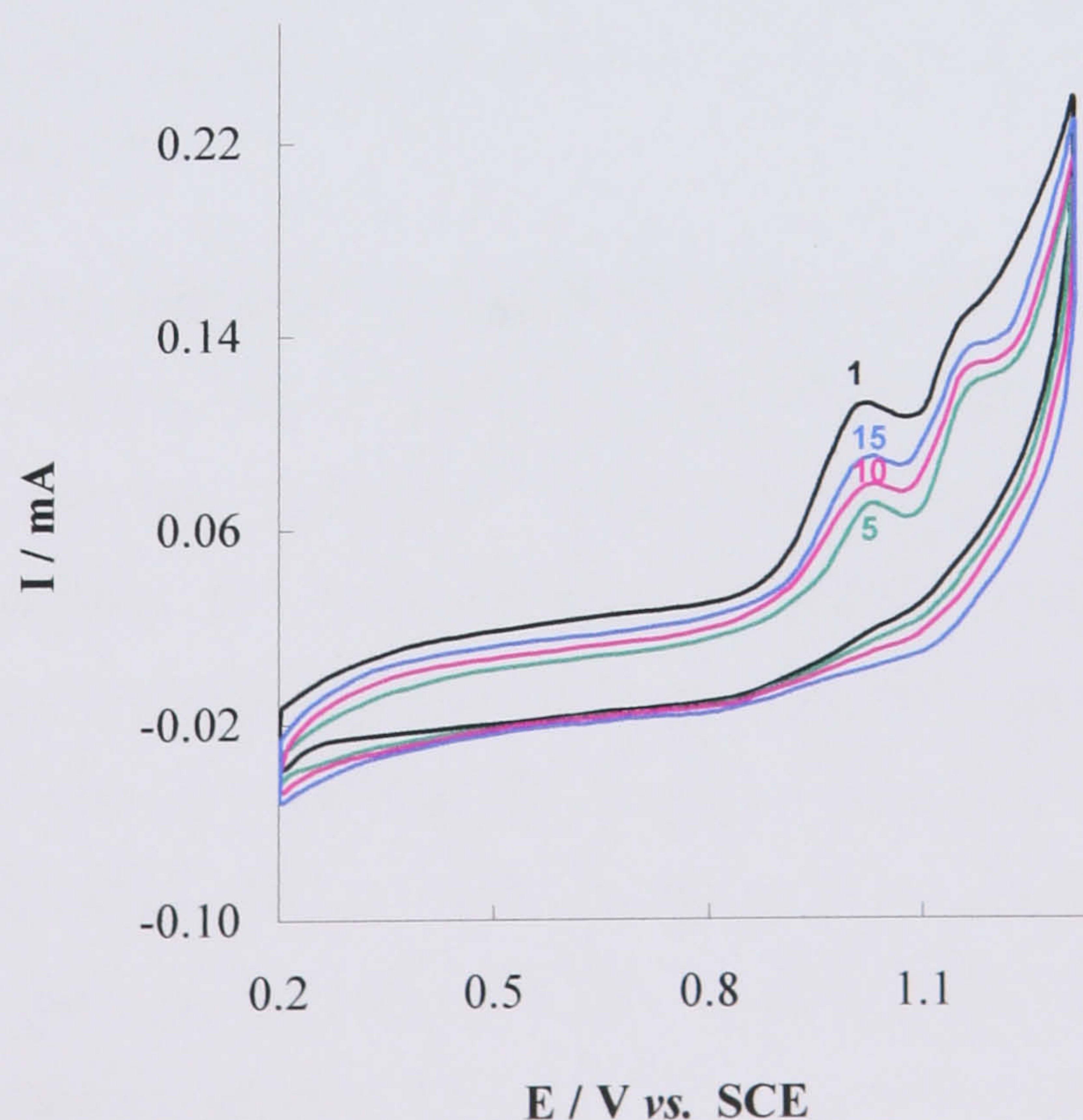


**Figure 5.06** - Voltammograms of the polymerisation of  $\text{Ni}(\text{Th-3,3})_2$  recorded at  $\nu = 0.1$  V s<sup>-1</sup>. (1<sup>st</sup>, 5<sup>th</sup>, 10<sup>th</sup> and 15<sup>th</sup> cycles).



The observed increase in peak currents from the fifth cycle is characteristic of most electropolymerisation processes and indicates the continuous growth of material on the electrode.<sup>19,20</sup>

The electroactivity of the polymerised yellow **polyNi(Th-3,3)<sub>2</sub>** film was investigated using cyclic voltammetry in a monomer-free electrolyte solution. The obtained voltammogram is shown in the Figure 5.07.

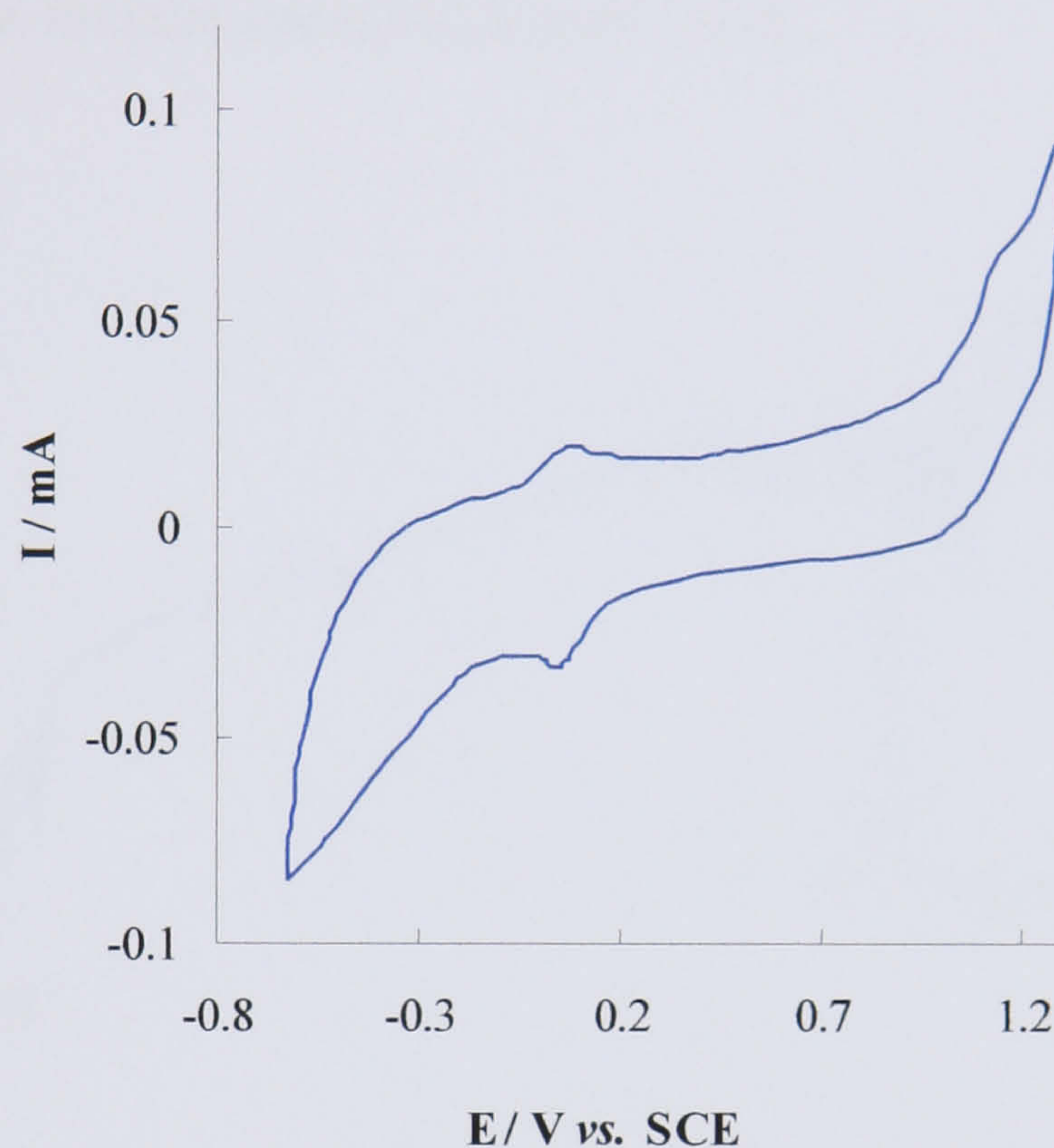


**Figure 5.07** - Cyclic voltammogram of **polyNi(Th-3,3)<sub>2</sub>** in monomer free solution (0.1 M TBAPF<sub>6</sub>/ MeCN) recorded at  $\nu = 0.1 \text{ V s}^{-1}$  using a Pt disc working electrode (0.44 cm<sup>2</sup>).

The voltammetric response of **polyNi(Th-3,3)<sub>2</sub>** reveals a redox couple at  $E_{\text{ox}} = 0.07 \text{ V} / E_{\text{red}} = 0.04 \text{ V}$  ( $E_{1/2} = 0.06 \text{ V}$ ). The small peak separation, 30 mV, suggests a relatively fast rate of electron transfer, characteristic of surface bound species.<sup>21,22</sup> This confirms the immobilisation of an active redox couple at the electrode surface. By comparison with the electrochemical behaviour of **Ni(Th-3,3)<sub>2</sub>** in solution, this redox process can be attributed to the interchange between the  $-1/0$  states of the nickel dithiolene centre, which indicates that the incorporation of the metal complex into the polymer has occurred. The cyclic voltammogram of **polyNi(Th-3,3)<sub>2</sub>** also shows a second peak at  $E_{\text{ox}} = 1.17 \text{ V}$  that can be assigned to the oxidation of the polythiophene backbone chain.<sup>23</sup>



### SNIFTIRS Studies

The spectroelectrochemical investigation of **polyNi(Th-3,3)<sub>2</sub>** was carried out in a monomer-free electrolyte solution and using the same range of potentials as those applied during the characterisation of the film by CV. In order to assign the IR peaks present in the SNIFTIRS spectra of **polyNi(Th-3,3)<sub>2</sub>**, the FTIR spectrum of the neutral **Ni(Th-3,3)<sub>2</sub>** was initially recorded (Figure 5.08).

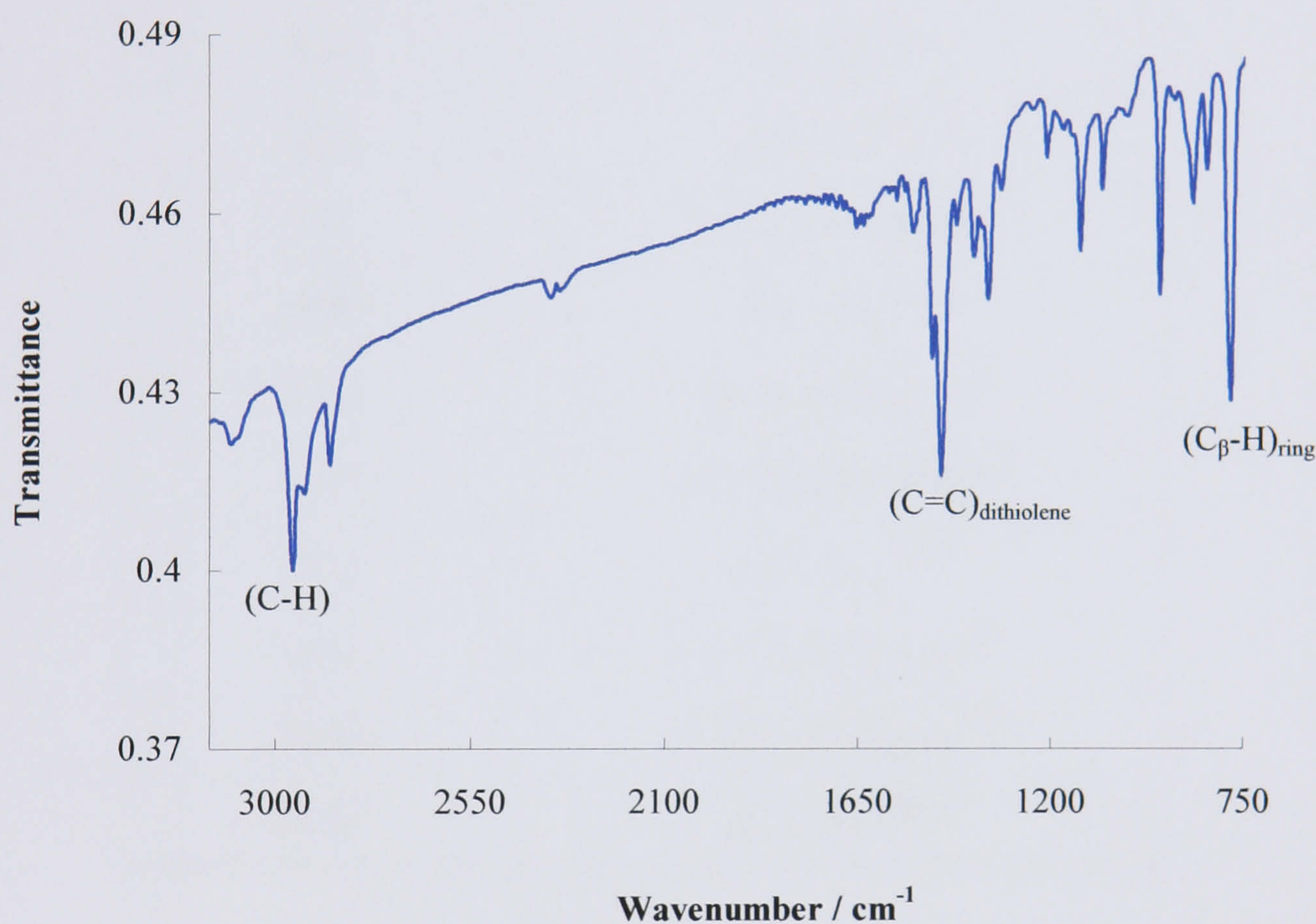


**Figure 5.0.8** - Infrared spectrum of neutral **Ni(Th-3,3)<sub>2</sub>** in KBr disc pellet.

The FTIR spectrum of **Ni(Th-3,3)<sub>2</sub>** displays several IR absorption bands related with the thiophene and dithiolene units. Peaks at 836 and 869  $\text{cm}^{-1}$  are assigned to C-S symmetric and asymmetric stretching vibrations of the thiophene rings.<sup>24,25</sup> The  $\text{C}_\alpha\text{-H}$  vibration and  $\text{C}_\beta\text{-H}$  out-of-plane deformation are observed at 3101 and 779  $\text{cm}^{-1}$ , respectively.<sup>26,27</sup> The C=C stretching vibrations of the dithiolene group can be found at 1456 and 1346  $\text{cm}^{-1}$ .<sup>28,29</sup> Smaller peaks at 1132 and 945  $\text{cm}^{-1}$  are due to the C=S and C-S vibrations of the dithiolene unit.<sup>5,30</sup>



A summary of the main IR bands for  $\text{Ni}(\text{Th-3,3})_2$  and their assignment is presented in the Table 5.01 ( $\nu$  – stretching,  $\delta$  - in-plane deformation,  $\gamma$  - out-of-plane deformation,  $s$  – symmetric and  $as$  – asymmetric).

**Table 5.01** - FTIR bands frequency assignments for  $\text{Ni}(\text{Th-3,3})_2$ .

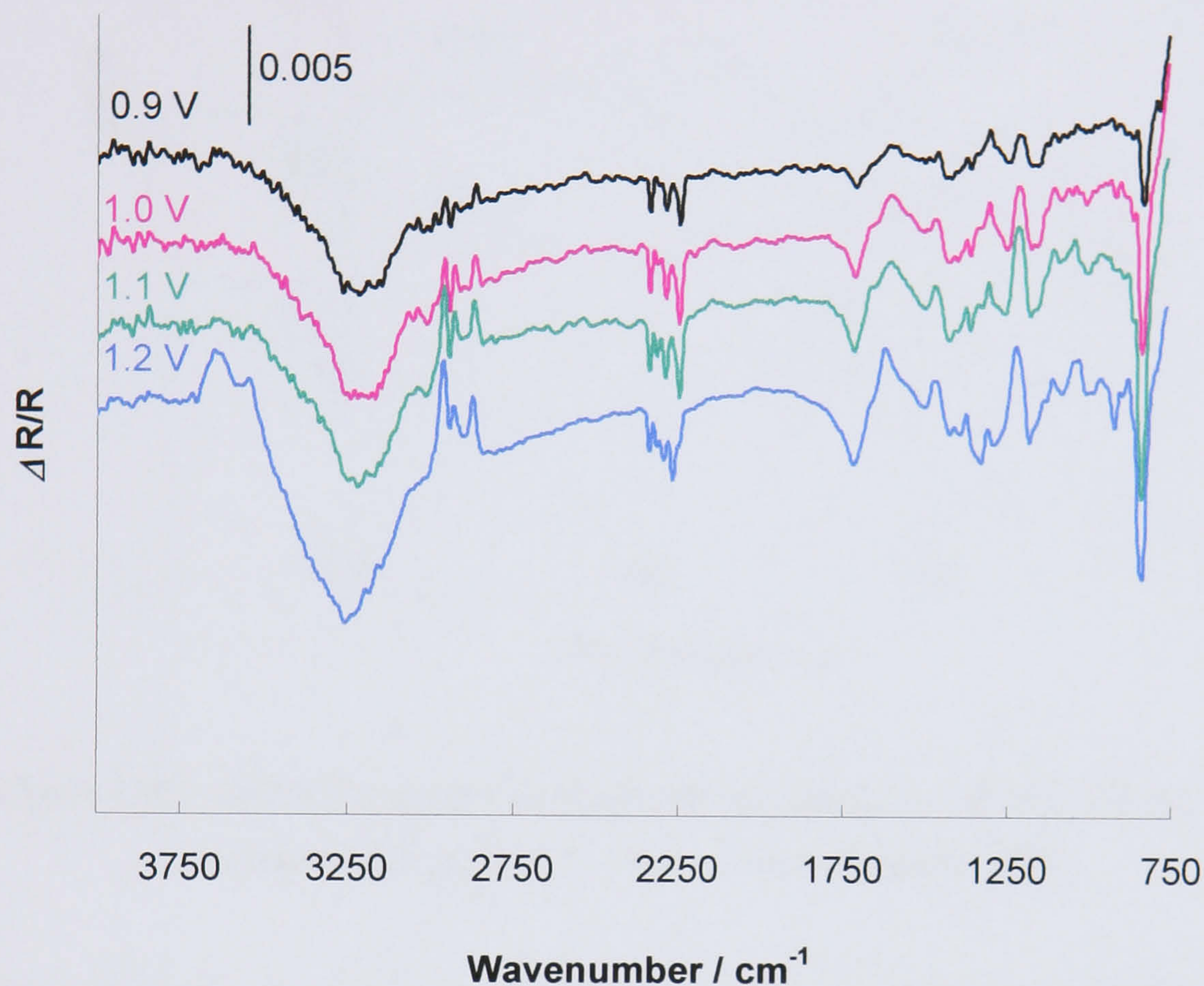
FTIR Band ( $\text{cm}^{-1}$ )	Band assignment
778	$\gamma(\text{C}_\beta\text{-H})^{27,31,32}$
836	$\nu_s(\text{C-S})^{20,24}$
869	$\nu_a(\text{C-S})^{25,33,34}$
945	$\nu(\text{C-S})\text{dithiolene}^{30}$
1080	$\delta(\text{C}_\alpha\text{-H})^{35,36}$
1132	$\nu(\text{C-S})\text{dithiolene}^5$
1346	$\nu(\text{C=C})\text{dithiolene}^{8,11}$
1378	$\nu(\text{C-C})_{\text{ring}}^{37,38}$
1456	$\nu(\text{C=C})\text{dithiolene}^{8,39}$
2958	$\nu(\text{C-H})\text{dithiolene}^{5,40}$
3101	$\nu(\text{C}_\alpha\text{-H})^{36,41,42}$

Figure 5.09 illustrates the SNIFTIRS spectra of  $\text{polyNi}(\text{Th-3,3})_2$  between 4000 and 750  $\text{cm}^{-1}$ , collected at successively higher potentials and normalised to the reference spectrum recorded at 0.3 V. The spectra show an increase in the intensity of the IR absorbance peaks as the polymer is oxidised from 0.9 to 1.2 V. Solvent bands are seen centred at 3200 and 2300  $\text{cm}^{-1}$ .<sup>20,43</sup> The sharp peak at 847  $\text{cm}^{-1}$ , is due to the incorporation of hexafluorophosphate ions<sup>44</sup> balancing the positive charge formed on the  $\text{polyNi}(\text{Th-3,3})_2$  film by the oxidation process.

The spectroelectrochemical response of  $\text{polyNi}(\text{Th-3,3})_2$  upon oxidation seems to miss some of the characteristics features usually found in IR spectra of polythiophenes (i.e. IRAV bands and broad absorbance band in the near infrared) implying that the conductivity level in  $\text{polyNi}(\text{Th-3,3})_2$  is rather limited.



The absence of IR peaks assigned to the  $C_{\alpha}$ -H bond and the presence  $C_{\beta}$ -H out-of-plane deformation at  $795\text{ cm}^{-1}$  suggests that, as previously concluded for the other polythiophene derivatives investigated, the coupling of thiophene units occurs primarily through the  $\alpha$ -positions.



**Figure 5.09** - SNIFTIRS spectra of  $\text{polyNi(Th-3,3)}_2$  taken from 0.9 to 1.2 V.

Reference spectra collected at 0.3 V. Spectra were shifted for clarity.

The symmetric  $C=C$  stretching vibration of the thiophene ring can be seen at  $1511\text{ cm}^{-1}$ .<sup>20,35,45</sup> SNIFTIRS peaks at  $1400/1337$ ,  $1193$  and  $933\text{ cm}^{-1}$  can be assigned to the stretching vibration of the  $C=C$ ,  $C-S$  and  $C-S$  bonds present in the dithiolenic unit, correspondingly.<sup>5,8,30</sup> The vibrations of the  $Ni-C$  bond occur below the detected spectral range, (at  $465$  and  $435\text{ cm}^{-1}$ )<sup>15</sup> and therefore cannot be seen in the SNIFTIRS spectra.

Careful analysis of the SNIFTIRS of  $\text{polyNi(Th-3,3)}_2$  upon reduction (Figure 5.10) reveals the shifting of the  $C=C$  dithiolenic vibrations to higher wavenumbers (from  $1400$  to  $1442\text{ cm}^{-1}$  and from  $1337$  to  $1375\text{ cm}^{-1}$ ). At the same time, a decrease in the  $C-S$  stretching frequency of the dithiolenic centre from  $933$  to  $897\text{ cm}^{-1}$  is also observed. In addition, the  $C-S$  vibration at  $1193\text{ cm}^{-1}$  considerably loses its intensity as the polymer is reduced.



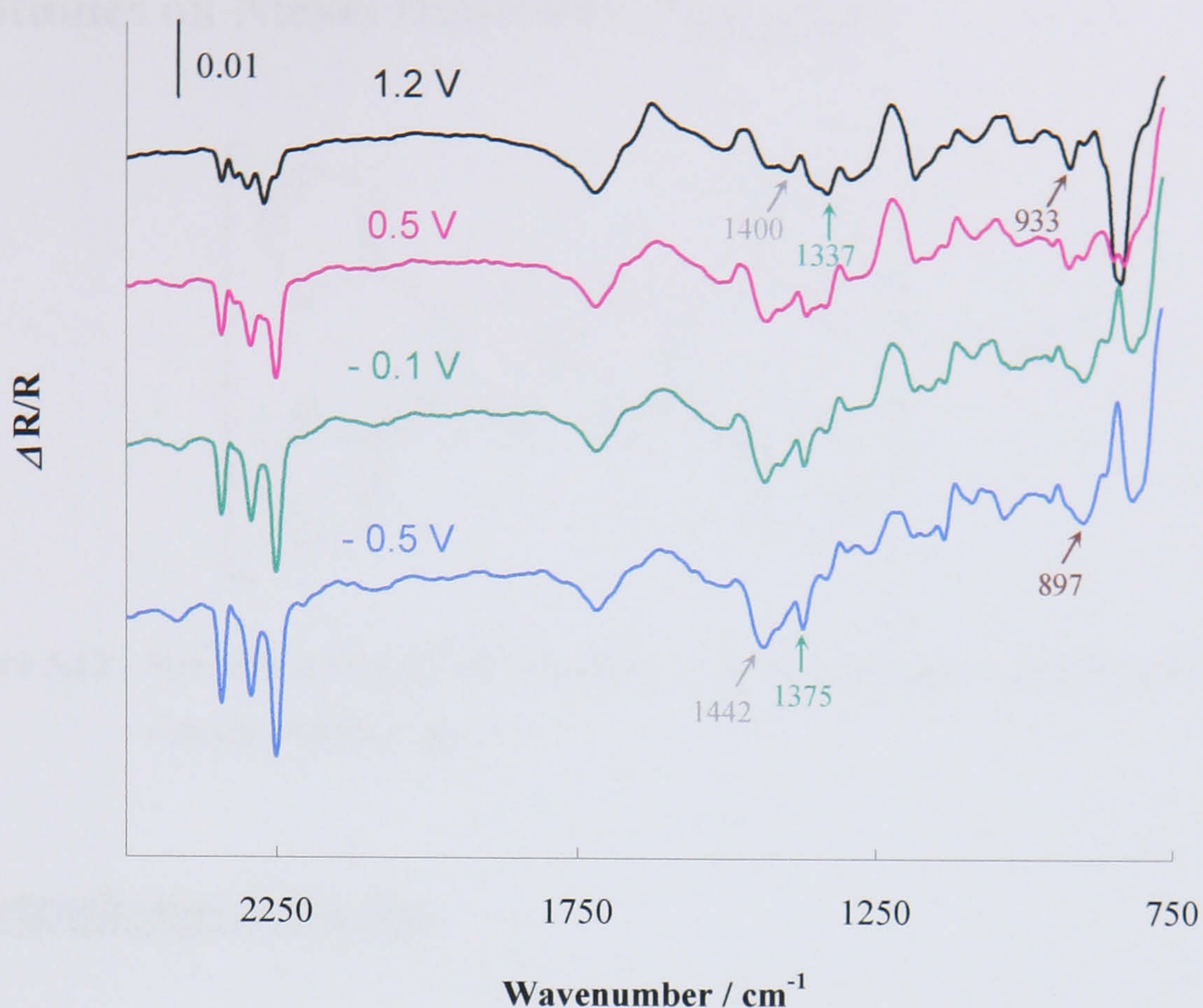


**Figure 5.10** - SNIFTIRS spectra of  $\text{polyNi(Th-3,3)}_2$  between 2300 and 750  $\text{cm}^{-1}$ . Reference spectra collected at 0.3 V. Spectra were shifted for clarity.

Similar shifts have been reported for a vast number of metal dithiolenes and are an indication that the dithiolene ligands assume a dithiolate character upon reduction.<sup>6,11,15,28</sup> This is consistent with dithiolene complexes possessing both a dithioketone and dithiolate behaviour.

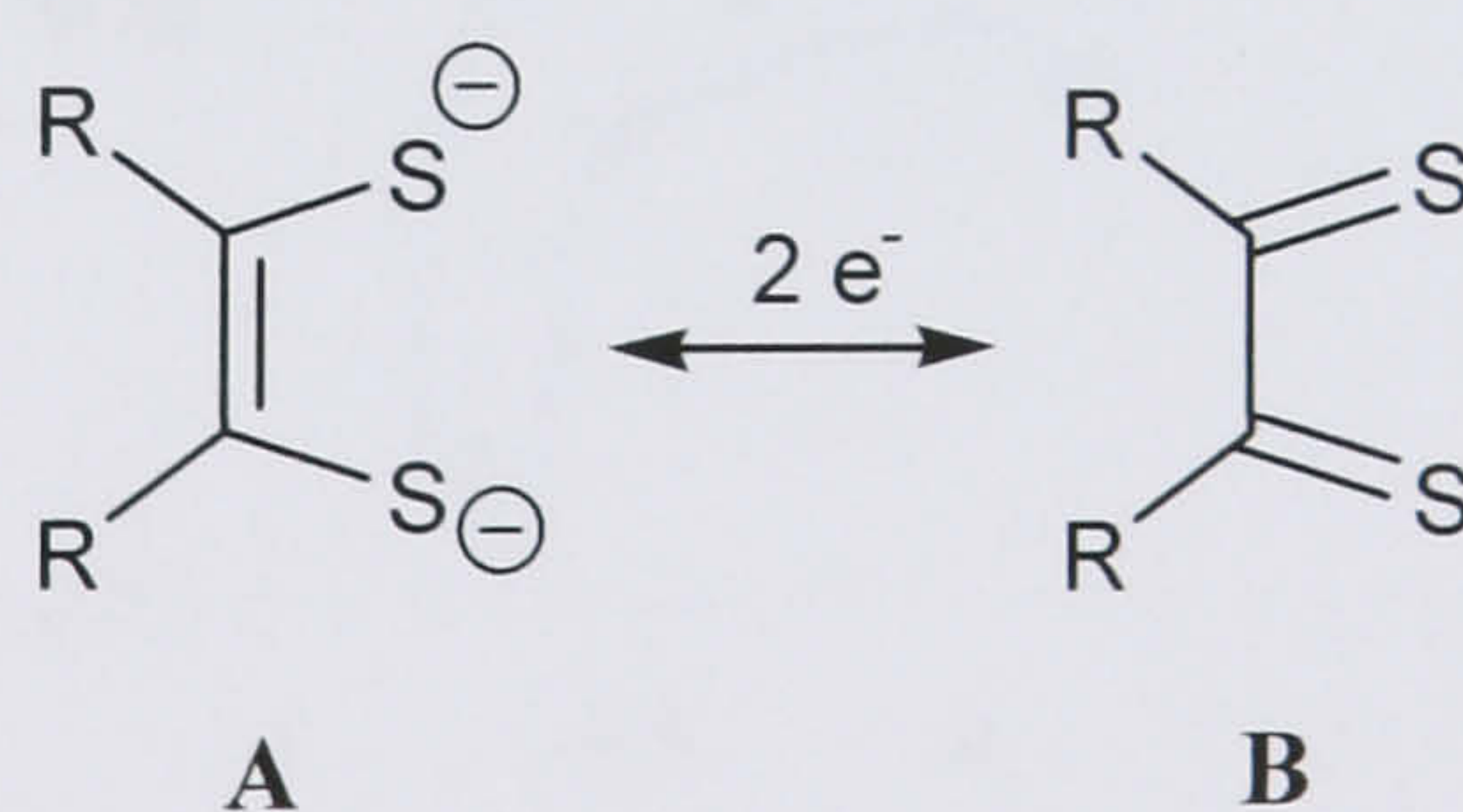


**Figure 5.11** - Resonance structures of the A - dinegative dithiolate and B - neutral dithioketone forms.

Figure 5.10 also shows that upon reduction, there is a progressive increase in the intensity of the positive band at 847  $\text{cm}^{-1}$ , representing the expulsion of  $\text{PF}_6^-$  anions from the  $\text{polyNi(Th-3,3)}_2$ , as the polymer is electrochemically reduced.



### 5.3.2 Studies on Nickel Dithiolene $\text{Ni}(\text{Th-2,2})_2$

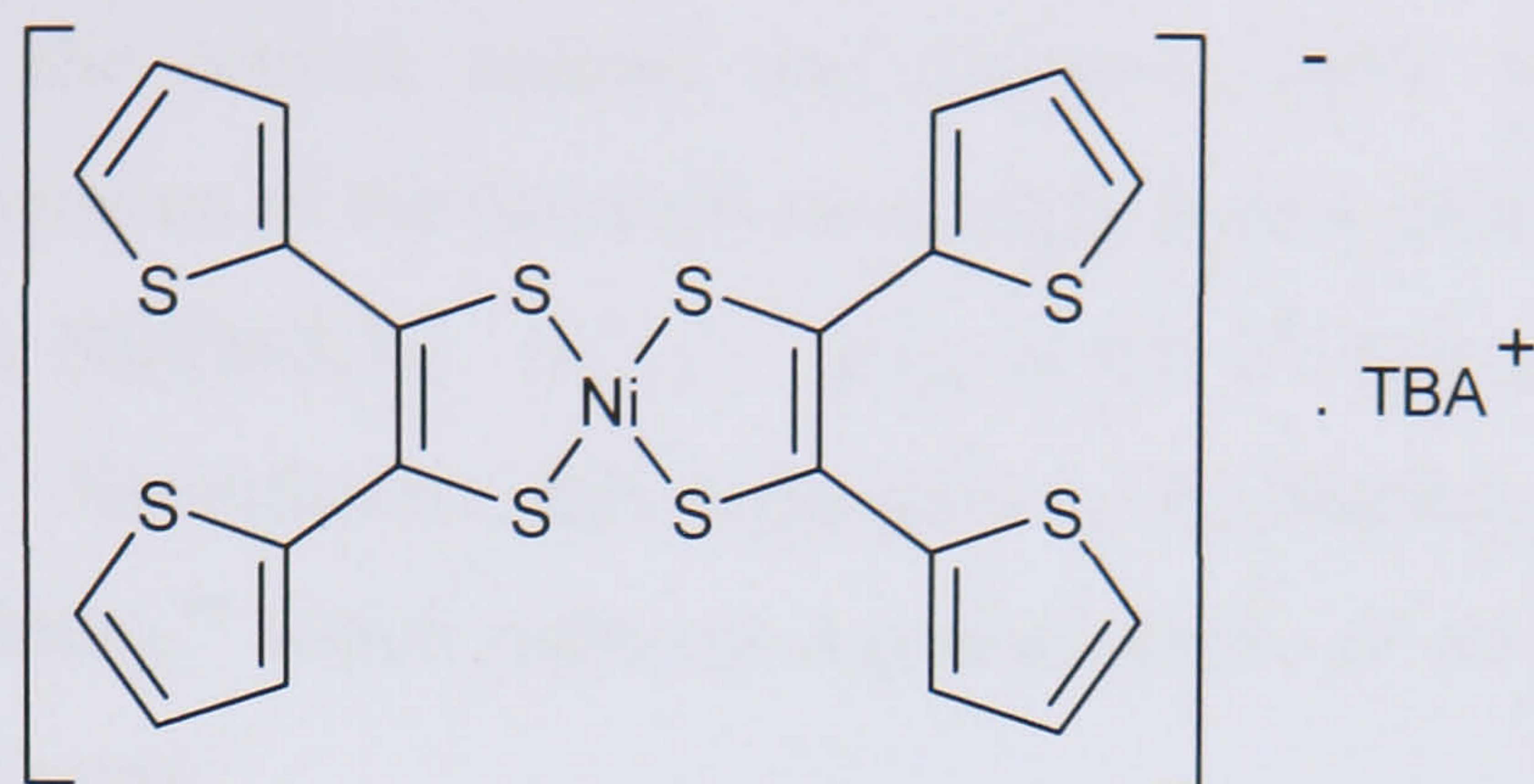


**Figure 5.12** - Structure of bis[1,2-di(2-thienyl)-1,2-ethenedithiolene] nickel tetrafluoroborate  $\text{Ni}(\text{Th-2,2})_2$ .

#### Electrochemical Studies

The voltammetric response of a solution of  $\text{Ni}(\text{Th-2,2})_2$  in supporting electrolyte (0.1 M TBAPF<sub>6</sub>/ MeCN) is shown in Figure 5.13.

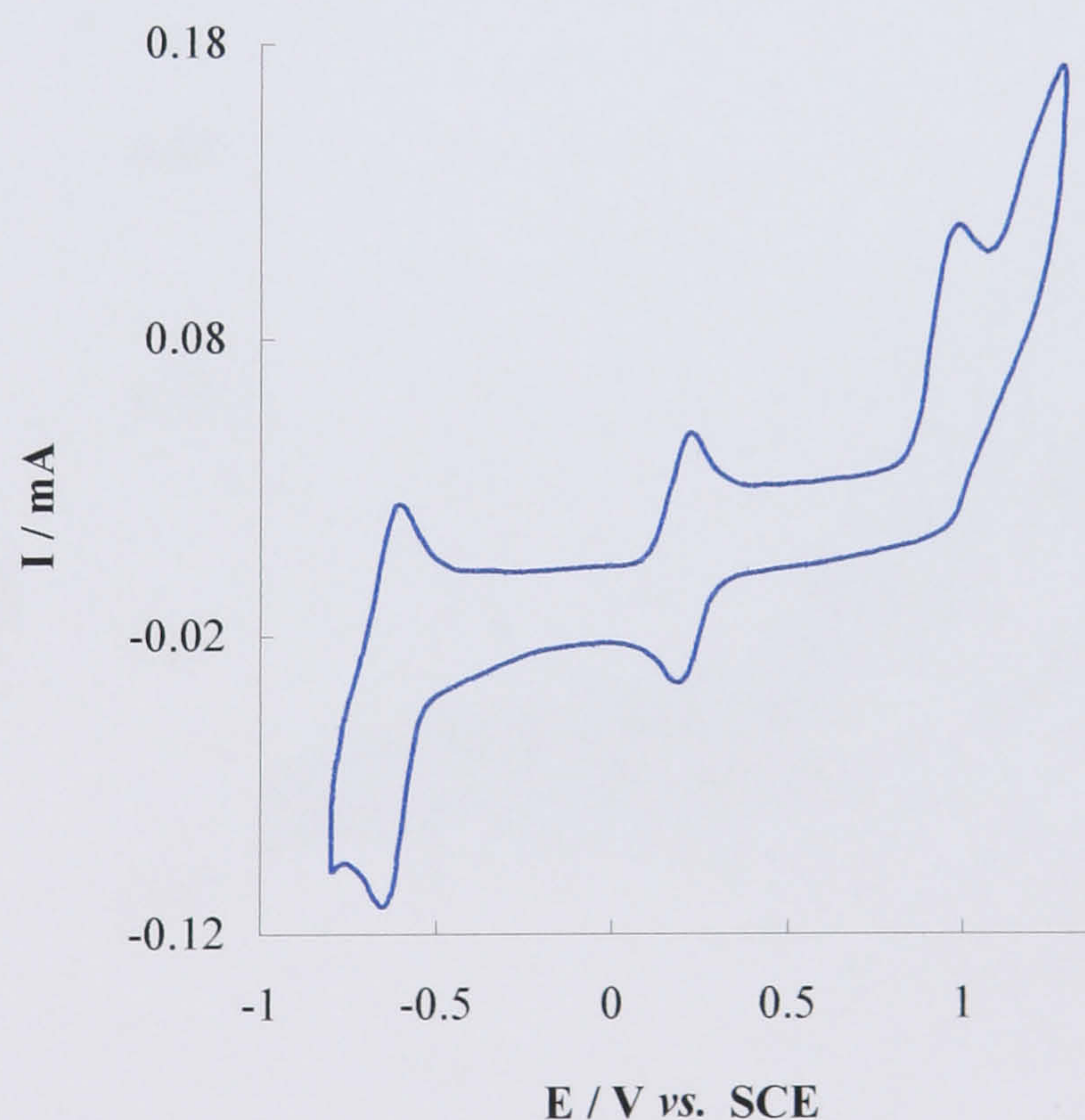


**Figure 5.13** - Voltammogram of a  $\text{Ni}(\text{Th-2,2})_2$  solution (0.0002 mol dm<sup>-3</sup>) in electrolyte recorded at  $\nu = 0.1 \text{ V s}^{-1}$ .

The electrochemical behaviour of  $\text{Ni}(\text{Th-2,2})_2$  has some similarities with the cyclic voltammogram of  $\text{Ni}(\text{Th-3,3})_2$  in that it shows two reversible or quasi-



reversible one electron redox processes at  $E_{\text{ox}}^1 = -0.59$  V,  $E_{\text{red}}^1 = -0.64$  V ( $E_{1/2}^1 = -0.62$  V) and  $E_{\text{ox}}^2 = 0.23$  V,  $E_{\text{red}}^2 = 0.19$  V ( $E_{1/2}^2 = 0.21$  V) assigned to the interchange between the neutral, anionic and dianionic states of the dithiolene centre.<sup>3,7,14,16</sup> The separation of the two half-wave redox potentials for **Ni(Th-2,2)<sub>2</sub>** is much the same as in **Ni(Th-3,3)<sub>2</sub>** ( $E_{1/2}^1 - E_{1/2}^2 \approx 0.8$  V) and comparable with analogous systems.<sup>8,9</sup> Nevertheless, this separation is significantly larger than the one reported for **Ni(dmit)<sub>2</sub>**<sup>46</sup> which indicates a poorer ability of these complexes to delocalise the added charge.

The cyclic voltammogram also reveals two oxidation peaks at  $E_{\text{ox}}^3 = 0.99$  V and  $E_{\text{ox}}^4 = 1.23$  V. The first peak is due to the formation of the cationic state in the dithiolene sites and the second can be assigned to the oxidation of the thiophene units to radical cations.

Electropolymerisation of **Ni(Th-2,2)<sub>2</sub>** was achieved by potential cycling between 0.2 and 1.3 V, as shown in Figure 5.14. The gradual increase in the current intensity upon consecutive cycles indicates a continuous growth of material on the electrode surface.

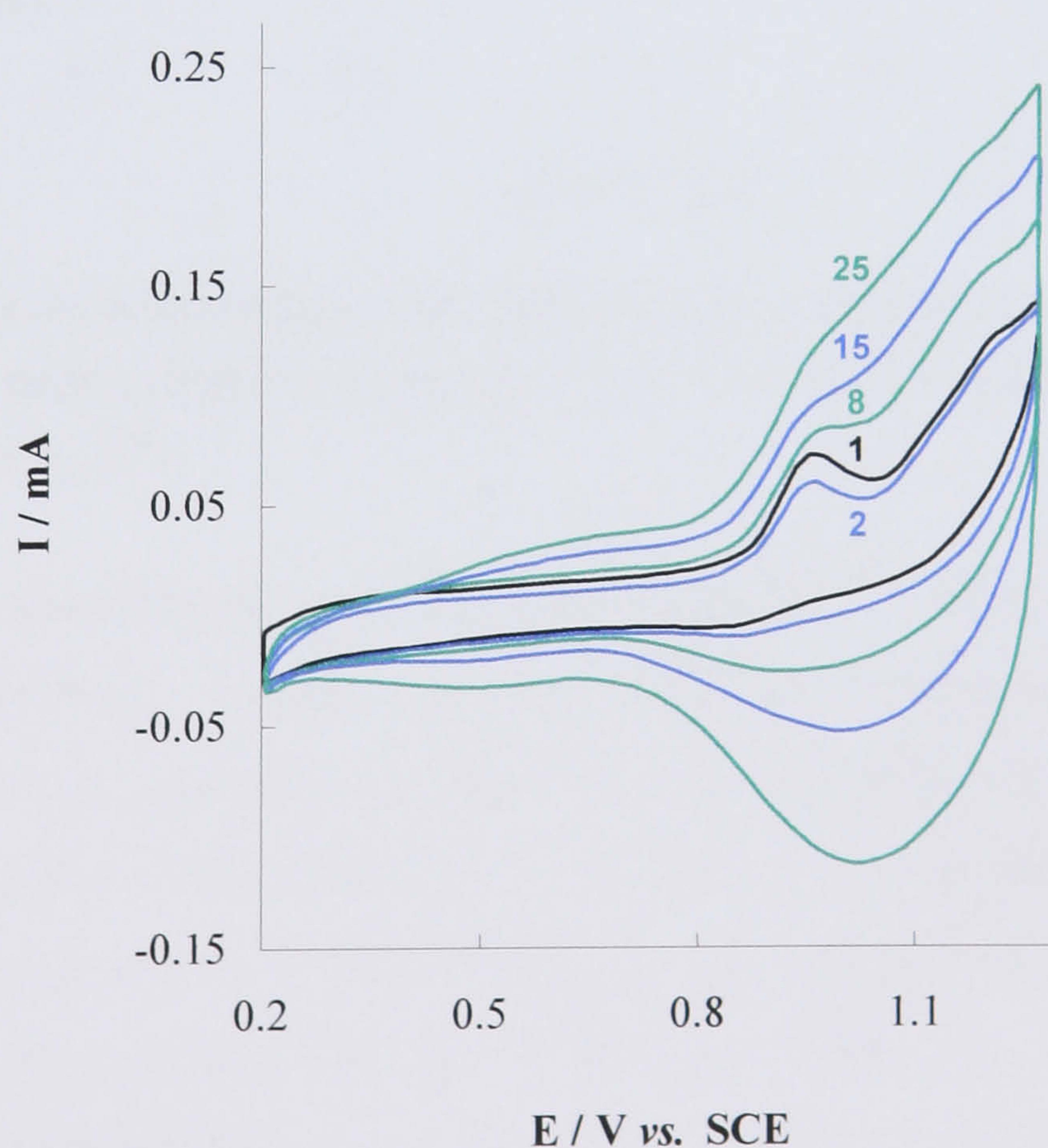


**Figure 5.14** - Voltammograms of the polymerisation of **Ni(Th-2,2)<sub>2</sub>** recorded at  $\nu = 0.1$  V s<sup>-1</sup>. (1<sup>st</sup>, 2<sup>nd</sup>, 8<sup>th</sup>, 15<sup>th</sup> and 25<sup>th</sup> cycles).



The electroactivity of the polymerised red **polyNi(Th-2,2)<sub>2</sub>** film was investigated by CV in a monomer-free electrolyte solution (Figure 5.15).

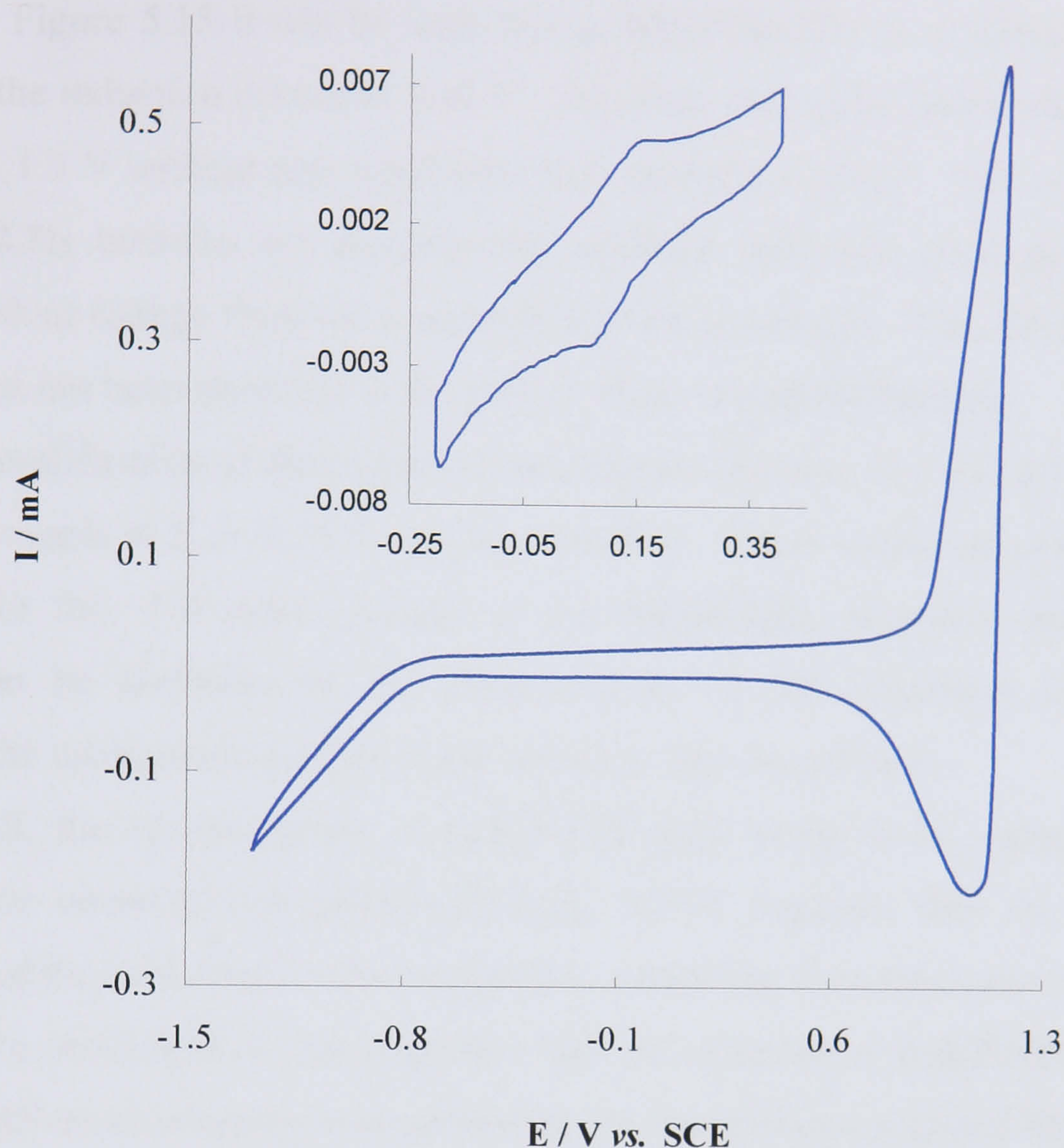


**Figure 5.15** - Cyclic voltammogram of **polyNi(Th-2,2)<sub>2</sub>** in monomer free solution 0.1 M TBAPF<sub>6</sub>/ MeCN) recorded at  $\nu = 0.1 \text{ V s}^{-1}$  using a Pt disc working electrode (0.44 cm<sup>2</sup>).

The cyclic voltammogram presented in Figure 5.15 resembles that of many polythiophene derivatives, namely, the polythiophene dithiolenes analysed in Chapter Four. This is a quite different result from the one described by Kean *et al.*<sup>7</sup> for the neutral complex obtained by chemical oxidation of **Ni(Th-2,2)<sub>2</sub>**. In those studies, the voltammogram of the polymer formed upon electropolymerisation of the neutral nickel dithiolenes complex clearly showed three redox waves assigned to the electroactivity of the nickel dithiolenes centre. Such contrasting electroactivity can be explained by the different oxidation state of the monomeric neutral nickel complex used by Kean *et al.* in comparison with the monomer **Ni(Th-2,2)<sub>2</sub>** analysed in this Thesis. Also, that research group carried out the polymerisation of the neutral



dithiolene complex under a distinct setup of experimental conditions (i.e. different supporting electrolyte) which might have had an influence in the structure and properties of the resultant polymer.

From Figure 5.15 it can be seen that **polyNi(Th-2,2)<sub>2</sub>** is oxidised at around 1.05 V and the reduction occurs at 0.94 V. The film was cycled repeatedly between the -1.4 and 1.3 V without any significant loss of electroactivity. The switching of **polyNi(Th-2,2)<sub>2</sub>** between the reduced and oxidised state was accompanied by a reversible colour change from red (reduced) to black (oxidised). This electrochromic behaviour has not been observed in the yellow films of **polyNi(Th-3,3)<sub>2</sub>**.

The amplification of the above voltammogram between -0.2 and 0.4 V reveals a reversible couple at  $E_{\text{ox}} = 0.14$  V and  $E_{\text{red}} = 0.08$  V. These values are similar to the ones seen for the -1/0 redox process of the **Ni(Th-2,2)<sub>2</sub>** monomer solution and therefore can be attributed to the electroactivity of the dithiolene unit, hence confirming the incorporation of the metal complex into the polymer.

Overall, the electroactivity of **polyNi(Th-2,2)<sub>2</sub>** seems to be rather different from the one observed for **polyNi(Th-3,3)<sub>2</sub>** which suggests that the mode of substitution of the thiophene units considerably affects the final structures of the two polymers. To shed light on the properties and the structure of **polyNi(Th-2,2)<sub>2</sub>**, *in situ* SNIFTIRS measurements were performed on an electropolymerised film.

### SNIFTIRS Studies

The spectroelectrochemical investigation of **polyNi(Th-2,2)<sub>2</sub>** was carried out employing a monomer-free electrolyte solution and using the same range of potentials as those applied during the characterisation of the film by cyclic voltammetry. Figure 5.16 shows the acquired SNIFTIRS spectra collected at successively higher potentials and normalised to the reference spectrum taken at 0.3 V.



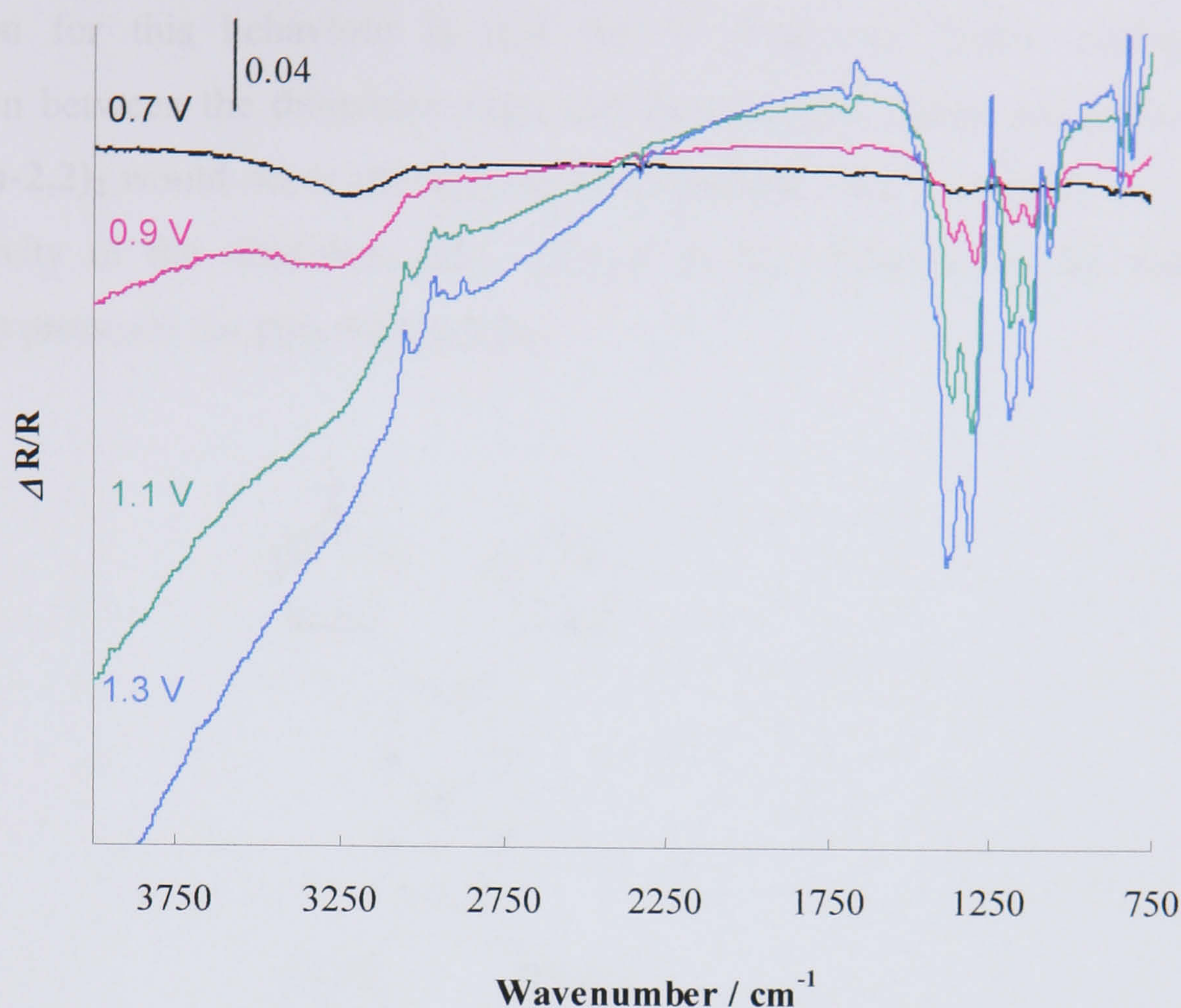


**Figure 5.16** - SNIFTIRS spectra of **polyNi(Th-2,2)<sub>2</sub>** taken from 0.8 to 1.4 V. Reference spectra collected at 0.3 V.

Analysis of the spectra between  $800\text{ cm}^{-1}$  and  $1600\text{ cm}^{-1}$  shows the presence of Infra Red Active Bands characteristic of conducting polymers such as polythiophenes.<sup>47,48</sup> These bands arise from the coupling of the quinoid-type vibrations of the polymer backbone and become increasingly dominant as the film is oxidised.<sup>49,50</sup> A very broad absorbance, attributed to the electronic transition between the valence band and the lowest polaron or bipolaron state<sup>51</sup>, is observed extending from about  $2500\text{ cm}^{-1}$  out into the near-IR. Small peaks at  $867$  and  $833\text{ cm}^{-1}$  can be assigned to the symmetric and asymmetric stretching vibrations of the C-S bonds of the thiophene rings.<sup>20,34,52</sup>

The absence of the spectroelectrochemical response characteristic of the electroactivity of the dithiolenes unit (which has been previously observed for **polyNi(Th-3,3)<sub>2</sub>**) suggests that the aromaticity of the dithiolenes centre has been disrupted. The voltammetric data appear to confirm this given that the charge involved in the redox process assigned to the dithiolenes unit is significantly smaller than the one related with the oxidation of the polythiophene chain. A possible



explanation for this behaviour is that the Ni dithiolene centre mediates the conjugation between the thiophene rings and therefore the charge delocalisation in **polyNi(Th-2,2)<sub>2</sub>** would occur through the Ni dithiolene sites, disrupting the normal electroactivity of the dithiolene unit. Based on this information, the following structure is proposed for **polyNi(Th-2,2)<sub>2</sub>**.

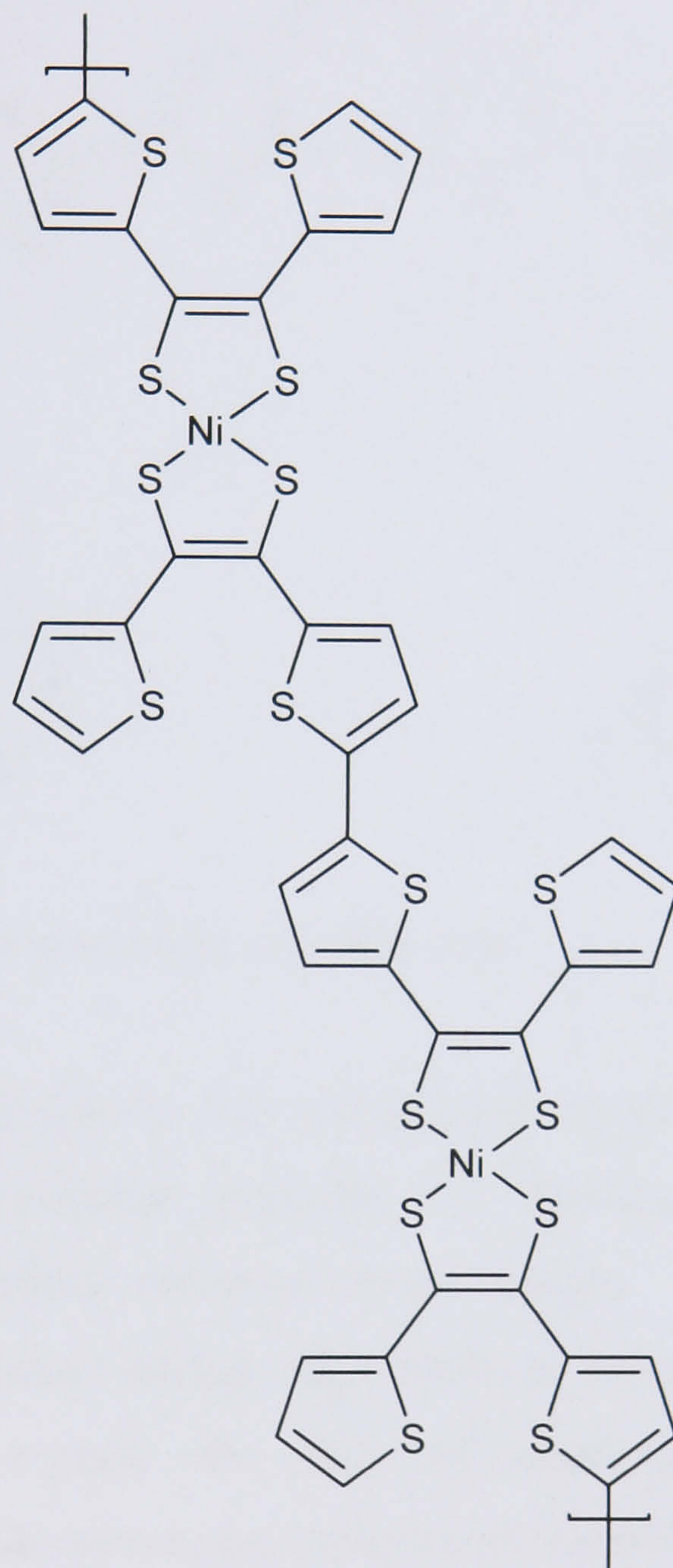


**Figure 5.17** - Proposed structure for **polyNi(Th-2,2)<sub>2</sub>**.

In contrast with the results obtained for **polyNi(Th-2,2)<sub>2</sub>**, the electroactivity of the nickel dithiolene centre in **polyNi(Th-3,3)<sub>2</sub>** is clearly evident in the voltammetric and spectroscopic data. This indicates that in this film, the nickel dithiolene sites are electronically isolated, preserving the aromaticity of the dithiolene system. The proposed structure for **polyNi(Th-3,3)<sub>2</sub>** is shown in Figure 5.18.



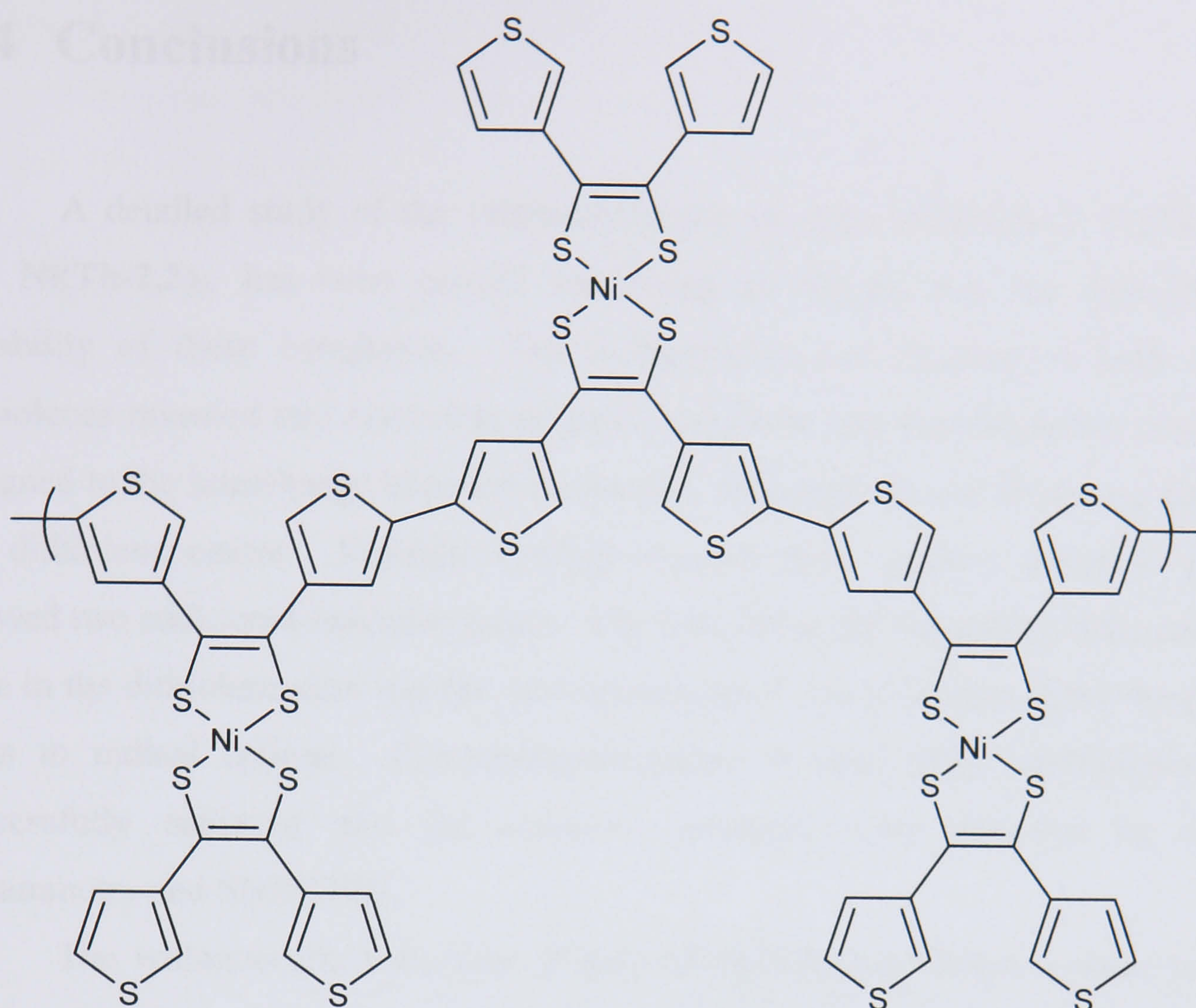


Figure 5.18 - Proposed structure for  $\text{polyNi(Th-3,3)}_2$ .

Polymerisation through the four peripheral thiophene rings in  $\text{Ni(Th-3,3)}_2$ , each one with two  $\alpha$ -positions available for bonding, can produce a highly crosslinked polymer without extended linear chains. The formation of such extremely irregular structure, arising from multiple coupling combinations of the thiophene units, can explain the lack of conductivity observed for the  $\text{polyNi(Th-3,3)}_2$  films. Moreover, the presence of a sterically bulky side group like the nickel dithiolenic centre could have a detrimental influence in the conjugation length which would lead to a poorly conductive polythiophene.



## 5.4 Conclusions

A detailed study of the electrochemistry of metal dithiolenes, **Ni(Th-3,3)<sub>2</sub>** and **Ni(Th-2,2)<sub>2</sub>**, has been carried out giving an insight into the film-forming capability of these complexes. The voltammetric investigation of both nickel dithiolenes revealed two reversible or quasi-reversible one electron redox processes assigned to the interchange between the neutral, monoanionic and dianionic states of the dithiolenes centre. Potential cycling towards more positive potential values showed two additional oxidation peaks. The first due to the formation of the cationic state in the dithiolenes sites and the second assigned to the oxidation of the thiophene units to radical cations. Electropolymerisation of both nickel dithiolenes was successfully achieved and the resultant polymers were analysed by cyclic voltammetry and SNIFTIRS.

The voltammetric behaviour of **polyNi(Th-3,3)<sub>2</sub>** has shown a redox couple attributed to the  $-1/0$  process, hence confirming the incorporation of the metal complex into the polymer. The electroactivity of the polythiophene backbone chain could be observed at higher potential values. The spectroscopic studies revealed a polymer without the characteristic IR features of conducting polymers suggesting that the conductivity level in **polyNi(Th-3,3)<sub>2</sub>** is rather limited. The electrochemical reduction of **polyNi(Th-3,3)<sub>2</sub>** was accompanied by an increase in the infra-red frequency (blue shift) associated with the C=C bonds of the dithiolenes unit, and a decrease in the frequency (red shift) related with the C-S dithiolenes bonds. Similar shifts have been reported for a vast number of metal dithiolenes, and reflect the fact that the dithiolenes ligands assume a dithiolate character upon reduction.

The electrochemistry of **polyNi(Th-2,2)<sub>2</sub>** resembled that of many polythiophenes with the switching between the doped and undoped states being accompanied by a reversible colour change, from red (reduced film) to black (oxidised film). Detailed study of the electroactivity of **polyNi(Th-2,2)<sub>2</sub>** revealed a reversible redox couple attributed to the  $-1/0$  redox process of the dithiolenes sites. This result indicates the capability to incorporate the nickel complex into a polythiophene film. The spectroelectrochemical behaviour of **polyNi(Th-2,2)<sub>2</sub>** was investigated by SNIFTIRS exhibiting comparable IR activity to other conducting



polythiophenes reported in the literature during p-doping. The spectra were dominated by the appearance of IRAV bands and by a broad band extending towards the near IR. The absence of the characteristic dithiolenic IR response suggests that the aromaticity of the dithiolenic centre has been disrupted. This is confirmed by the data collected from the CV measurements in which the electronic response of the dithiolenic sites was shown to be almost irrelevant when compared with the large charges involved in the oxidation and reduction of the thiophene units.

Taking this information into account it has been suggested that the two electropolymerised polymers, **polyNi(Th-3,3)<sub>2</sub>** and **polyNi(Th-2,2)<sub>2</sub>**, should have a reasonably different structure. In the case of **polyNi(Th-2,2)<sub>2</sub>**, the nickel dithiolenic centre mediates the conjugation between the thiophene rings and therefore the charge delocalisation would occur through the Ni dithiolenic sites, disrupting the typical electroactivity of the dithiolenic unit. For **polyNi(Th-3,3)<sub>2</sub>** films, the nickel dithiolenic sites are electronically isolated, preserving the aromaticity of the dithiolenic system. It is then concluded that the polymerisation of **Ni(Th-2,2)<sub>2</sub>**, with 2-substituted thiophenes, requires the meta-bis-1,2-dithiolenic complex to be incorporated into the polymer backbone, whereas polymerisation of the 3-substituted isomer **Ni(Th-3,3)<sub>2</sub>**, allows a polythiophene chain to be formed with the metal complex attached as a side chain. Therefore, the different substitution pattern of the thiophene rings in **Ni(Th-3,3)<sub>2</sub>** and **Ni(Th-2,2)<sub>2</sub>** leads to polymeric films with distinctly different properties.



## 5.5 References

1. P.I. Clemenson, *Coord. Chem. Rev.*, 106 (1990) 171.
2. R.M. Olk, B. Olk, W. Dietzsch, R. Kirmse and E. Hoyer, *Coord. Chem. Rev.*, 117 (1992) 99.
3. C.L. Kean, D.O. Miller and P.G. Pickup, *J. Mater. Chem.*, 12 (2002) 2949.
4. A. Kobayashi, H. Tanaka, M. Kumasaki, H. Torii, B. Narymbetov and T. Adachi, *J. Am. Chem. Soc.*, 121 (1999) 10763.
5. G.N. Schrauzer and V.P. Mayweg, *J. Am. Chem. Soc.*, 87 (1965) 3585.
6. R. Kato, *Chem. Rev.*, 104 (2004) 5319.
7. C.L. Kean and P.G. Pickup, *Chem. Commu.*, (2001) 815.
8. J.A. McCleverty, *Prog. Inorg. Chem.*, 10 (1968) 49.
9. Y. Ji, J.-L. Zuo, L. Chen, Y.-Q. Tian, Y. Song, Y.-Z. Li and X.-Z. You, *J. Phys. Chem. Solids*, 66 (2005) 207.
10. A. Charlton, Ph.D. thesis, University of Wales, Bangor (1994).
11. C.W. Schlapfer and K. Nakamoto, *Inorg. Chem.*, 14 (1975) 1338.
12. U.T. Mueller-Wexerhoff, B. Vance and D. Yoon, *Tetrahedron*, 47 (1991) 909.
13. N. Robertson and L. Cronin, *Coord. Chem. Rev.*, 227 (2002) 93.
14. G. A. Bowmaker, P. D. W. Boyd and G.K. Campbell, *Inorg. Chem.*, 22 (1982) 1208.
15. B.S. Lim, D.V. Fomitchhev and R.H. Holm, *Inorg. Chem.*, 40 (2001) 4257.
16. F. Bigoli, P. Cassoux, P. Deplano, M.L. Mercuri, M.A. Pellinghelli, G. Pintus, A. Serpe and E.F. Trogu, *J. Chem. Soc., Dalton Trans.*, (2000) 4639
17. W.E. Geiger, *Inorg. Chem.*, 12 (2001) 136.
18. F. Bigoli, P. Deplano, F. A. Devillanova, J. R. Ferraro, V. Lippolis. P. J. Lukes, M. Mercuri, M. Pellinghelli, E. F. Trogu and J. M. Williams, *Inorg. Chem.*, 36 (1997) 1218.
19. C. Jerome, C. Maertens, M. Mertens, R. Jerome, C. Quattrocchi, R. Lazzaroni and J.L. Bredas, *Synth. Met.*, 83 (1996) 103.
20. C. Kvarnstrom, H. Neugebauer, S. Blomquist, H.J. Ahonen, J. Kankare and A. Ivaska, *Electrochim. Acta*, 44 (1999) 2739.



21. D. Pletcher, R. Greff, R. Peat, L. M. Peter and J. Robinson, in "Instrumental Methods in Electrochemistry", Halsted Press, Southampton, (1985).
22. W. Kwan, L. Atanasoska and L. Miller, *Langmuir*, 7 (1991) 1419.
23. C. Pozo-Gonzalo, R. Berridge, P. J. Skabara, E. Cerrada, M. Laguna, S. J. Coles and M.B. Hursthouse, *Chem. Commu.*, (2002) 2408.
24. A. Charlton, M. Kalaji, P.J. Murphy, S. Salmaso, A.E. Underhill, G. Williams, M.B. Hursthouse and K.M. Abdul Malik, *Synth. Met.*, 95 (1998) 75.
25. J.T. Lopez Navarrete, V. Hernandez, J. Casado, L. Favaretto and G. Distefano, *Synth. Met.*, 101 (1999) 590.
26. M. Gerard, A. Chaubey and B.D. Malhotra, *Biosens. Bioelec.*, 17 (2002) 345.
27. G. Tourillon and F. Garnier, *J. Electroanal. Chem.*, 135 (1982) 173.
28. S. Curreli, P. Deplano, C. Faulmann, A. Ienco, C. Mealli, M. L. Mercuri, L. Pilia, G. Pintus, A. Serpe, and E. F. Trogu, *Inorg. Chem.*, 43 (2004) 5069.
29. C. Lauterbach and J. Fabian, *J. Inorg. Chem.*, (1999) 1995.
30. K.I. Pokhodnya, C. Faulmann, I. Malfant, R. Andreu-Solano, P. Cassoux, A. Mlayah, D. Smirnov and J. Leotin, *Synth. Met.*, 103 (1999) 2016.
31. J.R. Reynolds, J.P. Ruiz, A.D. Child, K. Nayak and D.S. Marynick, *Macromolecules*, 24 (1991) 678.
32. A. Berlin and G. Zotti, *Synth. Met.*, 106 (1999) 197.
33. M. Pomerantz, Y. Cheng, R.K. Kasim and R.L. Elsenbaumer, *Synth. Met.*, 85 (1997) 1235.
34. J. Casado, H.E. Katz, V. Hernandez and J.T. Lopez Navarrete, *Vibrational Spectroscopy*, 30 (2002) 175.
35. C. Ehrendorfer, H. Neugebauer, A. Neckel and P. Bauerle, *Synth. Met.*, 55 (1993) 493.
36. M. Pohjakallio, G. Sundholm and P. Talonen, *J. Electroanal. Chem.*, 401 (1996) 191.
37. P. Camurlu, A. Cirpan and L. Toppare, *Mat. Chem. Phys.*, 92 (2005) 413.
38. G. Louarn, J.-Y. Mevellec, J.P. Buisson and S. Lefrant, *Synth. Met.*, 55 (1993) 587.
39. P. Deplano, L. Marchio, M.L. Mercuri, L. Pilia, A. Serpe and E.F. Trogu, *Polyhedron*, 22 (2003) 2175.



40. S. Liu, Y. Liu and D. Zhu, *Synth. Met.*, 89 (1997) 187.
41. L.M.H. Groenewoud, G.H.M. Engbers, R. White and J. Feijen, *Synth. Met.*, 125 (2001) 429.
42. B. Rasch and W. Vielstich, *J. Electroanal. Chem.*, 370 (1994) 109.
43. D.N. Tito, Ph.D. Thesis, University of Wales, Bangor (2005).
44. R. Beyer, M. Kalaji, G. Kingscote-Burton, P.J. Murphy, V.M.S.C. Pereira, D.M. Taylor and G.O. Williams, *Synth. Met.*, 92 (1998) 25.
45. G.O. Williams, Ph.D. Thesis, University of Wales, Bangor (1999).
46. M. Mulder, J.G. Haasnoot, D.J. Stufkens, L. Tjeng, H. Lin, C. Chen and J. Reedijk, *Eur. J. Inorg. Chem.*, 12 (2002) 3083.
47. P. Christensen, A. Hamnett, A. Hillman, M.J. Swann and S.J. Higgins, *J. Chem. Soc. Faraday Trans.*, 89 (1993) 921.
48. P.A. Christensen, A. Hamnett, A.R. Hillman, M.J. Swann and S.J. Higgins, *J. Chem. Soc. Faraday Trans.*, 88 (1992) 595.
49. H. Neugebauer, *J. Electroanal. Chem.*, 563 (2004) 153.
50. H. Neugebauer, G. Nauer, A. Neckel, G. Tourillon, F. Garnier and P. Lang, *J. Phys. Chem.*, 88 (1984) 652.
51. G. Tourillon and F. Garnier, *J. Electrochem. Soc.*, 130 (1983) 2042.
52. M. Pohjakallio, G. Sundholm and P. Talonen, *J. Electroanal. Chem.*, 406 (1996) 165.



**Chapter 6**

**Conclusions**

**and**

**Further Work**



The study and polymerisation of a variety of thiophene derivatives (dithienylethylenes, thiophene dithiolenes and nickel dithiolenes) was attempted. The new electrosynthesised polymers were examined electrochemically and using *in situ* spectroscopic techniques.

The voltammetric behaviour of the conjugated polymers obtained from the polymerisation of dithienylethylenes **DTE-cis** and **DTE-trans** suggested the formation of polarons and bipolarons upon oxidation. The spectral data obtained from the SNIFTIRS investigations on **PDTE-cis** and **PDTE-trans** lacked the characteristic IR features of conductive polymers and for this reason it was concluded that only limited conduction could be accomplished by electrochemical doping.

In order to improve the electrical properties of these polymers, iodine was used as a chemical p-doping agent. The chemical doping of **PDTE-trans** and **PDTE-cis** produced a shift in the reduction peak potential towards a more negative value indicating that an increased stability of the p-doped state had been achieved. The **PDTE-trans** isomer exhibited significantly different spectroelectrochemical behaviour after I<sub>2</sub> doping displaying similar IR characteristics to that of conductive polythiophenes. Such response might have been caused by the occurrence of changes in the polymer morphology produced by the introduction of charged species. In contrast with the SNIFTIRS response of I<sub>2</sub> doped **PDTE-trans**, the chemical doping of **PDTE-cis** did not prompt the appearance of the typical IR features of conducting polymers.

Based on the information obtained by SNIFTIRS it was concluded that the ethylene linkage should be involved in the charge transport mechanism across the polymer chains in **PDTE-cis** but not in **PDTE-trans**. Therefore, it was proposed that the charge movement in **PDTE-trans** occurs through the polythiophene backbone whereas **PDTE-cis** exhibits a charge-transfer mechanism similar to that of polyacetylene.

Four different thiophene dithiolenes, **Th-3,3**, **Th-2,2**, **Th-2,3** and **Th-3,3Me** were investigated in this Thesis. The voltammograms of the electrosynthesised polymers **PTh-3,3**, **PTh-2,2** and **PTh-2,3** were very similar and resembled those of many polythiophenes. It was clear that all three polythiophene dithiolenes were



reversibly (and easily) p-doped but none showed stability towards n-doping. They also exhibited an electrochromic effect with the colour changing from yellow in the neutral state, to black in the oxidised state. SNIFTIRS analysis of these polymeric films revealed an IR activity comparable to other conducting polymer systems reported in the literature during p-doping. This was a rather different result from the one obtained for the dithienylethylenes, **PDTE-cis** and **PDTE-trans**, which suggests that the presence of the electron withdrawing 1,3-dithiol-2-one unit can lead to the formation of a planar polymeric system where the two thiophenes adopt a restricted *cis*-conformation, allowing a more efficient electron delocalisation along the polymer chains.

Analysis of subtle differences between the SNIFTIRS spectra of **PTh-3,3**, **PTh-2,2** and **PTh-2,3**, specifically, the absence of the C<sub>α</sub>-H stretching vibration peak and the change in reflectivity upon doping, gave an insight into their structures. It was concluded that polymerisation occurred through the α-positions and that while in **PTh-2,2** and **PTh-3,3**, almost all the molecule participates in the conduction mechanism, in the case of **PTh-2,3**, only one of the thiophene rings is involved in the transport of charge across the polythiophene backbone.

The UV-Visible spectra of the neutral polymers exhibited an absorbance band assigned to the π-π\* transition. From the onset of this transition it was determined that **PTh-3,3**, **PTh-2,2** and **PTh-2,3** have a bandgap of 2.04, 2.30 and 2.18 eV, respectively. Oxidation of the polymer films was accompanied by the appearance of a new broad absorption band characteristic of the presence of free carriers. Since the electrochemical doping of these polymers triggered the appearance of two new electronic subgap transitions, revealed by UV-Visible spectroscopy and SNIFTIRS, it was proposed that bipolarons are the most likely charge carriers formed upon p-doping of the polythiophene dithiolenes.

The electrochemical polymerisation of **Th-3,3Me** has been carried out with the bonding between thiophene units occurring *via* the β-position. The electroactivity of **PTh-3,3Me** was considerably different from that of other polythiophene dithiolenes studied; the oxidation of the polymer took place at a relatively higher potential and no perceptible colour change was observed upon redox switching. The spectroelectrochemical studies on **PTh-3,3Me** revealed a



polymer without the characteristic IR features of conducting polymers and therefore it was concluded that induced polymerisation through  $\beta$ -position results in a poorly conductive film.

Following the electropolymerisation and analysis of the resultant polythiophene dithiolenes, the chemical solid-state modification of these polymers was attempted. The *in situ* Wittig reaction was successfully carried out on **PTh-3,3** producing the new TTF derivatised polythiophene, **TTF(PTh-3,3)**. Cyclic voltammetric studies on this polymer showed the presence of the characteristic tetrathiafulvalene redox couples corresponding to the TTF unit of the modified film. This was later confirmed by the SNIFTIRS data that also revealed the presence of C=O bond suggesting that only partial modification of the polymer had been achieved.

With the aim of incorporating transition metal complexes into conjugated organic polymers, the polymerisation of the nickel dithiolenes **Ni(Th-3,3)<sub>2</sub>** and **Ni(Th-2,2)<sub>2</sub>**, was carried out. The cyclic voltammogram of the monomeric nickel dithiolenes revealed two reversible or quasi-reversible one electron redox processes assigned to the interchange between the neutral, monoanionic and dianionic states of the dithiolenes. Electropolymerisation was successfully achieved and the resultant polymers were analysed by CV and SNIFTIRS.

The CV investigation on **polyNi(Th-3,3)<sub>2</sub>** showed a redox couple attributed to the electrochemistry of the nickel dithiolenes centre, confirming the incorporation of the metal complex into the polymer. Spectroscopic studies on this polymer revealed the characteristic IR features of metal dithiolenes complexes with the dithiolenes ligands assuming a dithiolate character upon reduction.

The electrochemistry of **polyNi(Th-2,2)<sub>2</sub>** resembled that of many polythiophenes with the switching between the doped and undoped states being accompanied by a reversible colour change, from red (reduced film) to black (oxidised film). A detailed study of the electroactivity of **polyNi(Th-2,2)<sub>2</sub>** also revealed a reversible redox couple attributed to the  $-1/0$  redox process of the dithiolenes sites. The spectroelectrochemical behaviour observed for **polyNi(Th-2,2)<sub>2</sub>** was comparable to the IR activity of conducting polythiophenes. The absence of the



characteristic dithiolene IR response suggested that the aromaticity of the dithiolene centre had been disrupted.

Considering this information it was suggested that the two electropolymerised polymers, **polyNi(Th-3,3)<sub>2</sub>** and **polyNi(Th-2,2)<sub>2</sub>**, should have a reasonably different structure. In the case of **polyNi(Th-2,2)<sub>2</sub>**, the nickel dithiolene centre mediates the conjugation between the thiophene rings and therefore charge delocalisation occurs through the Ni dithiolene sites, disrupting the typical electroactivity of the dithiolene unit. For **polyNi(Th-3,3)<sub>2</sub>** films, the nickel dithiolene sites seem to be electronically isolated, preserving the aromaticity of the dithiolene system. Therefore, the polymerisation of **Ni(Th-2,2)<sub>2</sub>**, with 2-substituted thiophenes, requires the meta-bis-1,2-dithiolene complex to be incorporated into the polymer backbone, whereas polymerisation of the 3-substituted isomer **Ni(Th-3,3)<sub>2</sub>**, allows a polythiophene chain to be formed with the metal complex attached as a side chain.

A summary of the main results and conclusions obtained for each thiophene derivative investigated in this project is presented in Table 6.01.

**Table 6.01** – Main results and conclusions obtained for each thiophene derivative.

Thiophene	Polymerisation	Conducting Polymer	Electrochromic Effect	Bandgap (ev)
DTE-cis	✓	✗	✗	-
DTE-trans	✓	✓ <sup>**</sup>	✗	-
Th-3,3	✓	✓	✓	2.04
Th-2,2	✓	✓	✓	2.30
Th-2,3	✓	✓	✓	2.18
Th-3,3Me	✓ <sup>*</sup>	✗	✗	-
Ni(Th-3,3) <sub>2</sub>	✓	✗	✗	-
Ni(Th-2,2) <sub>2</sub>	✓	✓	✓	-

\* Polymerisation achieved only after prolonged cycling.

\*\* Polymer with conductive characteristics only after doping with iodine.



In conclusion the study of a range of polythiophene derivatives with structures based on dithienylethylene has provided an insight into the influence different functionalities on their electrochemical and spectroelectrochemical properties. Moreover, by means of a rigorous investigation it was possible to suggest a chemical structure for the electrosynthesised polymers. Nevertheless, further work would be required to fully understand the electrical/optical properties and to confirm the proposed structures for these polythiophenes dithiolenes. It would be also vital to establish the relation between structure and conductivity in these types of electronic materials.

Microscopic techniques such as scanning electron microscopy (SEM) or atomic force microscopy (AFM) could provide important information on the morphological characteristics of the electrosynthesised polymer films. Scanning tunneling microscopy (STM), which is designed to be able to measure the tunneling current between a sample substrate and a probe, could be used to determine film thickness and film conductivity. Computational studies could be carried out in order to obtain reliable information about the molecular structure and properties not only for neutral systems but also for ionised molecules. The use of all these techniques should provide enough data to confirm the structure of the electrochemically polymerised polythiophene derivatives.

The polydithienylethylene **PDTE-trans** studied in this project showed an increase in conductivity upon iodine doping. Therefore, it would be interesting to further investigate the effect of chemical doping in the other thiophene derivatives (thiophene dithiolenes and nickel dithiolenes). Also, given that, the switch of the growth electrolyte has made possible the chemical modification of **PTh-3,3** it is likely that future improvements, at the experimental level, could eventually lead to the complete chemical modification of the polythiophene dithiolenes. Further research in the use of *in situ* modifications would be of interest since this method can give access to new polymers with tailored properties.